Roles of the Epigenetic Modifier EZH2 in Melanoma

Dissertation

zur

Erlangung der naturwissenschaftlichen Doktorwürde

(Dr. sc. nat.)

vorgelegt der

Mathematisch-naturwissenschaftlichen Fakultät

der

Universität Zürich

von

Daniel Kaspar Zingg

von Zürich ZH

Promotionskomitee

Prof. Dr. Lukas Sommer (Vorsitz / Leitung der Dissertation)

Prof. Dr. Konrad Basler

Prof. Dr. Gerhard Christofori

Zürich, 2015

Acknowledgements

I would like to express my gratitude to the following persons:

Prof. Dr. Lukas Sommer,
for giving me the opportunity to conduct my doctorate in his research group. You have been a tremendous mentor during this long journey. You have provided a very motivating and enjoyable scientific environment, which has taught independence and has promoted innovative ideas.

Prof. Dr. Konrad Basler and Prof. Dr. Gerhard Christofori,
for accepting to be members of my PhD committee, for co-reviewing my PhD thesis, and for the scientific inputs during my doctorate.

All the members of the Sommer Lab,
for contributing to an excellent scientific spirit and for being extraordinary friends over the last five years. Without you guys, my doctorate would have been barely as much fun as it was!

Dr. Olga Shakhova,
for the competent supervision during my doctorate.

Nicole Bachelin and Monika Jenny,
for being a great administrative team. You have always been supportive, whether it concerned administrative issues as much as moral encouragement, such as offering Prosecco on a New Year's Eve afternoon in the Lab.

Prof. Dr. Reinhard Dummer and Dr. Phil Cheng,
for the extensive scientific advice concerning the clinical facet of melanoma and, Phil, for being a great friend.

Prof. Dr. Raffaella Santoro and Sandra Frommel,
for their tremendous help in performing ChIP on melanoma samples.

Prof. Dr. Onur Boyman, Dr. Rodney A. Rosalia, and Natalia Arenas-Ramirez,
for the stimulating collaboration on and the insights into immunoediting in melanoma.

My family,
especially my parents, Sabina Zingg-Trieb and Ulrich Zingg, for their encouraging and open-minded support and sympathy throughout my doctorate.

Steffi,
for being with and caring about me during my doctorate. You have brought the invaluable counterbalance into my science-driven life. Thank you!

Table of contents

Table of figures and tables

1. Summary

The epigenetic modifier EZH2 is a methyltransferase that obstructs gene expression through trimethylation of lysine 27 in histone 3. While EZH2 function is critical for developmental processes and homeostasis of several adult tissues, aberrant EZH2 activity has been connected to a variety of cancers. Likewise, in cutaneous melanoma, a deadly skin cancer arising from melanocytes, EZH2 levels are elevated and correlate with reduced patient survival. However, evidence for functional roles of EZH2 in the course of melanoma formation and progression remain poor. In my PhD thesis, I reveal central roles of EZH2 in promoting growth and especially metastasis of cutaneous melanoma.

In a transgenic mouse model of cutaneous melanoma, conditional *Ezh2* ablation counteracted growth of skin tumors without affecting homeostasis of physiological melanocytes and benign, nevus-like hyperplasia. Importantly, whether *Ezh2* was ablated before or after the onset of cutaneous melanomagenesis, emergence of distant metastases was completely prevented. Likewise, treatment of melanoma-bearing mice with the preclinical EZH2 inhibitor GSK503 virtually abolished metastases formation, resulting in prolonged survival. In support, EZH2 inactivation in human and murine melanoma cells suppressed EMT and cell motility, which are both prerequisites for metastasis.

Furthermore, interference with EZH2 activity in human melanoma cells allowed the identification of novel EZH2 target genes using transcriptome and methylated histone enrichment analyses. In a cohort of melanoma patients, high expression of these genes correlated with prolonged survival. In contrast, silencing of EZH2 targets promoted either melanoma cell proliferation or metastases *in vivo*, while a third group of target genes facilitated immunogenicity. These findings establish this set of EZH2 target genes as a functionally diverse set of tumor suppressors.

Cutaneous melanoma is a cancer with a prominent phenotypic plasticity involving metastatic spread and expeditious resistance to therapy. EZH2 acts as a central node in driving melanoma growth, metastatic progression, and immunoediting through dynamic repression of distinct tumor suppressors. Therefore, targeted EZH2 inhibition might represent a highly promising strategy to interfere with these aspects of melanomagenesis, potentially locking tumor plasticity and augmenting therapeutic responses.

2. Zusammenfassung

Der epigenetische Modifikator EZH2 ist eine Methyltransferase, welche durch die Methylierung von Lysin 27 des Histon-Proteins 3 die Expression von Genen unterdrückt. EZH2 hat die Aufgabe, verschiedene Prozesse während der Embryonalentwicklung sowie die Homöostase von adultem Gewebe zu steuern. Fehlfunktionen von EZH2 können dementsprechend zur Entstehung von Krebs beitragen. Das maligne Melanom, auch schwarzer Hautkrebs genannt, entwickelt sich aus Hautpigmentzellen. In dieser Krebserkrankung ist EZH2 häufig hochreguliert, wobei die erhöhte Expression mit einer verkürzten Lebenserwartung von Melanompatienten korreliert. Jedoch wurde bis heute nicht nachgewiesen, ob EZH2 direkt die Entstehung des Melanoms beeinflusst. In meiner Dissertation zeige ich auf, dass die genunterdrückende Funktion von EZH2 wesentlich zur Entstehung sowie zur Metastasierung des Melanoms beiträgt.

Um das maligne Melanom in angemessener Weise zu studieren, verwendete ich transgene Mäuse, welche im Verlauf ihres Lebens schwarzen Hautkrebs entwickeln. Die Entfernung des *Ezh2*-Gens aus dem Genom dieser Mäuse verhinderte die Entstehung maligner Tumoren. Jedoch beeinflusste diese *Ezh2*-Gendeletion die Homöostase von physiologischen Hautpigmentzellen und gutartigen Naevuszellen nicht. Massgeblich war aber, dass die *Ezh2*-Deletion die Metastasen-Bildung in bereits an Melanomen erkrankten Mäusen verhinderte. Basierend auf diesen Erkenntnissen behandelte ich melanomkranke Mäuse mit einem pharmakologischen Hemmstoff, welcher die Aktivität von EZH2 unterdrückt. Dies verhinderte die Entstehung von Metastasen und verlängerte die Lebensdauer der Tiere. Zudem konnte ich aufzeigen, dass die Unterdrückung von EZH2 die Motilität von Melanomzellen beeinflusst. Eine erhöhte Motilität wird mit dem Abwandern von Krebszellen von Primärtumoren und dem Kolonisieren von inneren Organen, sprich der Metastasierung, in Verbindung gebracht.

Des Weiteren analysierte ich, welche Gene EZH2 während der Melanomentstehung unterdrückt. Interessanterweise korrelierte eine Hochregulierung dieser Gene wiederum mit einer positiven Prognose für Melanompatienten. Zudem zeigten funktionelle Experimente, dass diese Gene unterschiedliche Vorgänge während der Melanomentstehung beeinträchtigen. Während eine Gruppe von Genen das

Wachstum der Tumoren unterband, behinderten andere Gene die Motilität von Melanomzellen und dementsprechend die Metastasierung im Tiermodell. Ein dritter Satz von Genen aktivierte Immunzellen, welche die Melanomzellen angriffen.

Das maligne Melanom ist eine Krebsart, die sich optimal an äussere, sich verändernde Gegebenheiten anpassen kann. Diese Plastizität trägt zu der Metastasierung wie auch zur Resistenzbildung gegenüber Krebstherapien bei. Meine Ergebnisse verdeutlichen, dass EZH2 die Plastizität des Melanoms durch dynamische Unterdrückung von Genen mit unterschiedlichsten anti-tumoralen Funktionen steuert. Deshalb stellt die Hemmung von EZH2 mit neuartigen Substanzen eine vielversprechende, zukünftige Melanomtherapie dar, möglicherweise als Ergänzung für bereits bestehende Therapien.

3. Introduction

3.1. Epigenetic mechanisms

During embryogenesis, programs of gene expression promote development and specification of different organs and tissues. These programs are initiated by distinct sets of transcription factors (Reik, 2007). Conceivably, re-expression of key embryonic stem cell (ESC) transcription factors in fibroblasts can result in reprogrammed ES-like cells. However, this process is relatively inefficient, partly due to silencing of POU domain class 5 transcription factor 1 (*Pou5f1*), one of the ESC transcription factors, through DNA methylation of its endogenous promoter (Epsztejn-Litman et al., 2008; Feldman et al., 2006; Takahashi and Yamanaka, 2006). Thus, changes in gene expression are not only driven by transcription factors, but also accompanied or even caused by chemical alterations, such as methylation of DNA, one of the so-called epigenetic modifications. The term "epigenetics" is defined as all meiotically and mitotically heritable changes in gene expression that are not coded in the DNA sequence (Holliday, 1987). Among the mechanisms used to initiate and sustain epigenetic regulation, we find DNA methylation and post-translational modifications of histone tails (Reik, 2007).

3.1.1. DNA methylation

DNA is methylated on cytosine residues in cytosine-guanine dinucleotides (CpG). ~80% of all CpGs are methylated, and DNA methylation represses transcription in a manner that depends on the location and density of the methyl-CpGs relative to a gene promoter. Stretches of CpGs are referred to as CpG islands and are present in promoter regions of ~60% of the loci of vertebrate genomes. In contrast to isolated CpGs, CpG islands remain mostly unmethylated, except during development, where a few key loci become stably silent through corresponding CpG island methylation. During murine embryogenesis, global CpG methylation levels decline rapidly after zygosis to ~30% of typical somatic levels, but *de novo* methylation restores normal levels by the time point of implantation (Bird, 2002; Reik, 2007). The essence of dynamic DNA de- and re-methylation during development becomes apparent with the

resulting embryonic lethality upon knockout of the *de novo* DNA methyltransferases 3a and 3b (*Dnmt3a*/*b*) (Hsieh, 1999; Okano et al., 1999; 1998). In contrast, ESC self-renewal is independent of Dnmt3a/b function (Tsumura et al., 2006). During embryogenesis, Dnmt3a/b silences pluripotency genes including *Pou5f1* to induce lineage specifications (Feldman et al., 2006). Along serial somatic cell divisions, DNA methylation patterns are then maintained by Dnmt1 (Pradhan et al., 1999). Maintenance of these patterns is as essential as *de novo* methylation of genes, highlighted by embryonic lethality upon *Dnmt1* deletion (Li et al., 1992). In most cancers, global CpG methylation levels are reduced in comparison to their normal tissue counterparts (Greger et al., 1989; Weber et al., 2005). Comparably, in a murine carcinoma model, methylation decreases during progression from benign neoplasia to malignant tumors (Fraga et al., 2004), while Dnmt1 attenuation in adult mice promotes various cancers (Eden et al., 2003; Gaudet et al., 2003). Acquired hypomethylation might sustain chromosomal instability through relieved mitotic recombination and activation of transposons, thus contributing to tumorigenesis (Bestor, 2005; Eden et al., 2003; Karpf and Matsui, 2005). In contrast, hypermethylation of CpG islands in promoter regions of various tumor suppressors is a major event in promoting cancer (Herman and Baylin, 2003). However, different cancer types usually acquire distinct hypermethylomes (Costello et al., 2000; Esteller et al., 2001a; Esteller, 2007). Interestingly, CpG island methylation-mediated silencing frequently functions as secondary hit in cooperation with an already-present mono-allelic genetic loss of a tumor suppressor resulting in homozygous abrogation (Esteller et al., 2001b). As a potential strategy to target cancer, forced re-expression of aberrantly silenced genes through chemical compounds preventing CpG methylation has been emphasized (Herman and Baylin, 2003). 5-azanucleosides, such as azacitidine (Celgene) and decitabine (Janssen-Cilag), are cytidine analogues that are incorporated into DNA and covalently bind DNMTs resulting in demethylation (Jones and Taylor, 1980). These molecules have substantial clinical activity in patients with myelodysplastic syndrome (Fenaux et al., 2009) and might accordingly be considered for further hematopoietic and solid malignancies (Azad et al., 2013).

3.1.2. Post-translational histone modifications

Apart from DNA methylation, chromatin density determines DNA accessibility. Chromatin, the physiological form of the eukaryotic genome, is a polymer of DNA and histone (H) proteins.

Hierarchical chromatin structure dynamically changes during fundamental cellular processes, such as DNA replication, recombination, transcription, repair, and chromosome segregation. Chromatin structures can be broadly divided into the loose euchromatin and the dense heterochromatin. However, site-specific DNA access mostly depends on local nucleosome repositioning (Elgin and Workman, 2000). The nucleosome is the repeating core unit of chromatin built of an octamer of canonical histone proteins (2 of each: H2A, H2B, H3, H4) wrapped with 146 base pairs of DNA (Luger et al., 1997; Richmond and Davey, 2003). Apart from canonical histones, diverse histone variants confer unique functions within the chromatin template, thus increasing chromatin complexity and contributing to key developmental processes as much as tumorigenesis (Vardabasso et al., 2014). Histones are post-translationally modified, mostly at their N-terminal tails. The great diversity of modifications includes acetylation (ac), methylation (me), sumoylation, and ubiquitination (ub) at lysines (K), methylation at arginines, and phosphorylation (P) at serines and threonines (Figure 1).

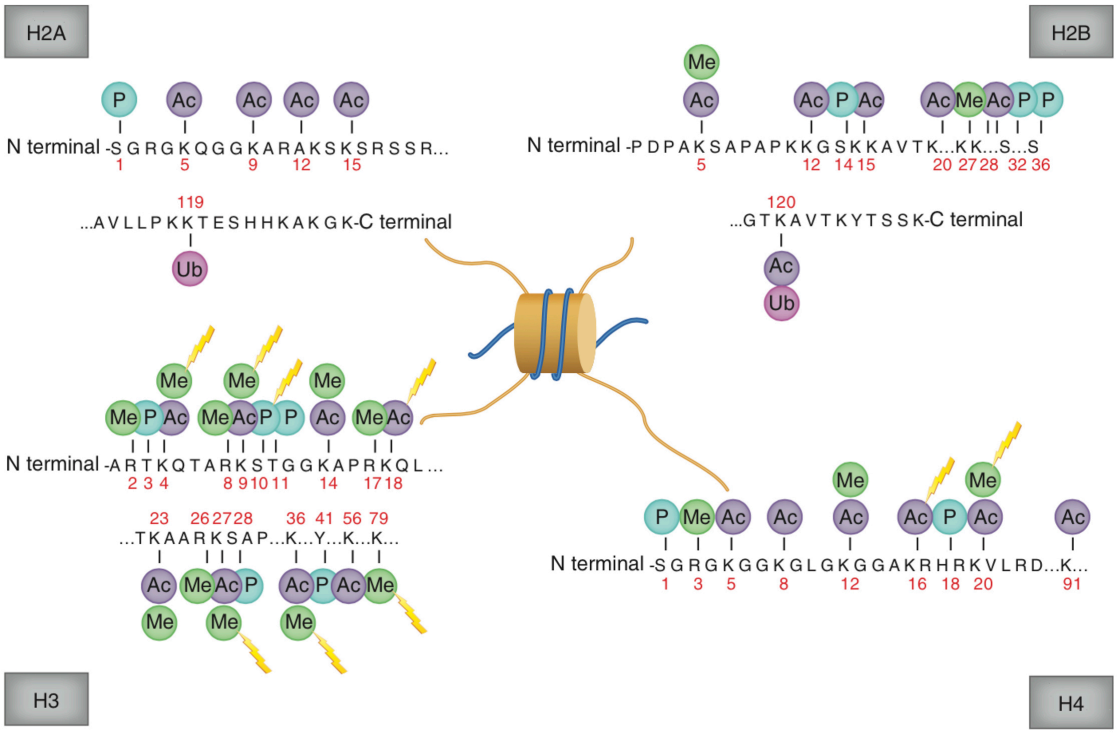

Figure 1 | Post-translational histone modifications in normal and cancerous cells. Histones can undergo diverse post-translational modifications mainly along their protruding N-terminal tails, but also within their C-terminal regions. In the right combination and translated by the appropriate effectors, this histone modification code establishes the global and local chromatin density, which ultimately determines gene expression. Disruption of these normal patterns results in aberrant gene expression, which may contribute to cancer. “Yellow flash”, histone modifications known to be conductive to cancer. Ac, acetylation; Me, methylation; H, histone; P, phosphorylation; Ub, ubiquitination (adapted from: Rodríguez-Paredes and Esteller, 2011).

Depending on the position of the corresponding amino acid in the histone tail, a given modification might either facilitate or suppress DNA access. For instance, trimethylation of K27 in histone 3 (H3K27me3) prevents DNA access through chromatin compaction, while H3K4me3 maintains an open chromatin structure. Similarly, H3K9me3 is a repressive mark, while H3K9ac induces DNA accessibility. Thus, the composition of such modifications at a given nucleosome ultimately defines accessibility of the nearby DNA sequence (Huang et al., 2014; Kouzarides, 2007). Dynamic addition and removal of post-translational modifications is catalyzed by two groups of enzymes termed writers and erasers, respectively (Jenuwein and Allis, 2001). A third group of proteins interprets the histone modification code and are referred to as readers (Musselman et al., 2012) (Figure 2). Proper organization of DNA into chromatin through the according histone modification code and its interpretation is essential for the integrity of lineage specifications during development and tissue homeostasis in the adult including maintenance of cell identities. Hence, misplacement and misinterpretation of the code can likely result in developmental defects and cancer (Laugesen and Helin, 2014) (Figure 1).

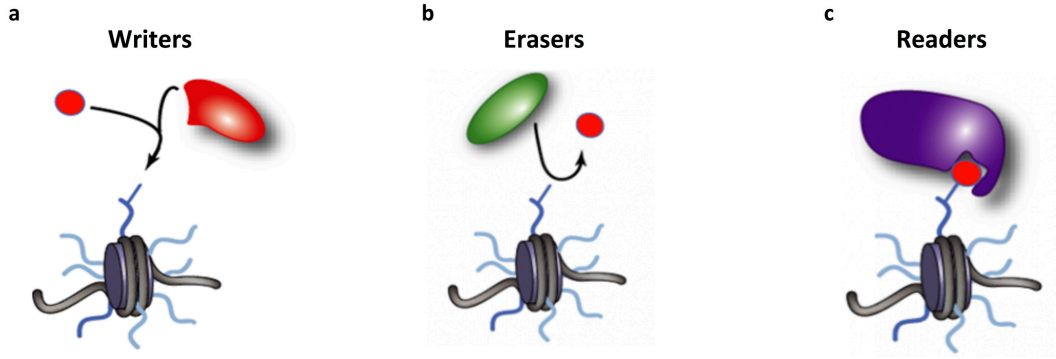

Figure 2 | Histone modification readers, erasers, and writers. (**a**, **b**) Addition of post-translational histone modifications is catalyzed by enzymes termed writers (**a**), while erasers (**b**) remove histone modifications. (**c**) A third group of proteins interprets the histone modification code, referred to as readers (adapted from: Constellation Pharmaceuticals, http://www.constellationpharma.com/research-development/).

3.1.3. Histone deacetylases

Histone deacetylases (HDAC) are enzymes that remove acetyl groups from various lysines in histone tails. Although HDACs by themselves do not display exquisite lysine specificity, they often operate in large protein complexes, which confer their lysine specificity. Acetylation predominantly confers open chromatin, thus HDAC activity results in more condensed chromatin leading to repression of gene

transcription (Kelly and Cowley, 2013). HDACs play crucial roles during development. ESC self-renewal is dependent on Hdac1 function (Dovey et al., 2010; Lagger et al., 2002). Comparably, *Hdac1* and *Hdac2* knockout is embryonically lethal (Lagger et al., 2002; Montgomery et al., 2007). Interestingly, interference with Hdac activity in various tissues leads to a visible phenotype, only when *Hdac1* and *Hdac2* are simultaneously depleted, indicating a partial functional redundancy between these homologs (Kelly and Cowley, 2013). Among many target genes, HDACs suppress cell cycle inhibitors in ESCs (Lagger et al., 2002; Yamaguchi et al., 2010). Accordingly, HDAC inactivation interferes with growth of a variety of cancer cells (Rosato et al., 2003; Senese et al., 2007). Therefore, targeted HDAC inhibition has been proposed as a strategy to counteract tumorigenesis (Azad et al., 2013), and two HDAC inhibitors, vorinostat (Merck) and romidepsin (Celgene), have demonstrated profound clinical responses in cutaneous T-cell lymphoma patients (Duvic et al., 2007; Lane and Chabner, 2009; Whittaker et al., 2010). Interestingly, upon exposure of tumor cells to chemotherapy, HDAC inhibition prevents emergence of resistant sub-clones, while chemotherapy-tolerant cells regain sensitivity through HDAC inhibition (Sharma et al., 2010). This highlights the significance of epigenetic regulation for tumor plasticity.

3.1.4. Histone methyltransferases

Histone methyltransferases catalyze methylation of lysines and commonly contain a suppressor of variegation 3-9 - enhancer of zeste - trithorax (SET) domain, which represents their catalytic subunit. For instance, suppressor of variegation 3-9 H1 (SUV39H1) and enhancer of zeste homolog 2 (EZH2) sustain H3K9me3 and H3K27me3, respectively, which are both repressive marks (Mohan et al., 2012; Rea et al., 2000). ESCs mostly contain euchromatin. During differentiation, however, Suv39h1 promotes chromatin compaction through H3K9me3, which then recruits Dnmt3a/b to stably silence pluripotency genes, such as *Pou5f1* (Elgin and Workman, 2000; Epsztejn-Litman et al., 2008; Feldman et al., 2006; Lehnertz et al., 2003; Maison et al., 2002; Peters et al., 2001). Likewise, SET domain bifurcated 1 (SETDB1), another H3K9 methyltransferase, maintains ESC differentiation (Bilodeau et al., 2009) and is amplified in diverse cancers, thus inducing aberrant H3K9me3-mediated silencing of tumor suppressor genes (Ceol et al., 2011). Interestingly, depletion of *Suv39h1* increases H3K27me3 at genomic sites usually covered

by H3K9me3. This underscores the plasticity of chromatin architecture and the partial redundancy between different histone modifications (Peters et al., 2001; 2003).

3.1.4.1. EZH2 function in ESCs

In contrast to H3K9me3, the repressive H3K27me3 modification is mostly present in open chromatin of ESCs and declines during differentiation. Accordingly, H3K9me3 and H3K27me3 are mutually exclusive marks at a given locus. Besides H3K27me3, H3K9ac and H3K4me3, both marks indicative of active transcription, are abundant in ESCs. In this cellular context, H3K27me3 allows repression of lineage commitment genes, while H3K9ac and H3K4me3 ensure pluripotency gene expression (Azuara et al., 2006; Bernstein et al., 2006; Krejcí et al., 2009; Lindroth et al., 2008; Meshorer et al., 2006; Mikkelsen et al., 2007; Pan et al., 2007; Xie et al., 2013). H3K27me3 is maintained by polycomb repressive complex 2 (PRC2), which is composed of, among others, embryonic ectoderm development (EED), suppressor of zeste 12 (SUZ12), and the catalytic unit EZH2 (Figure 3).

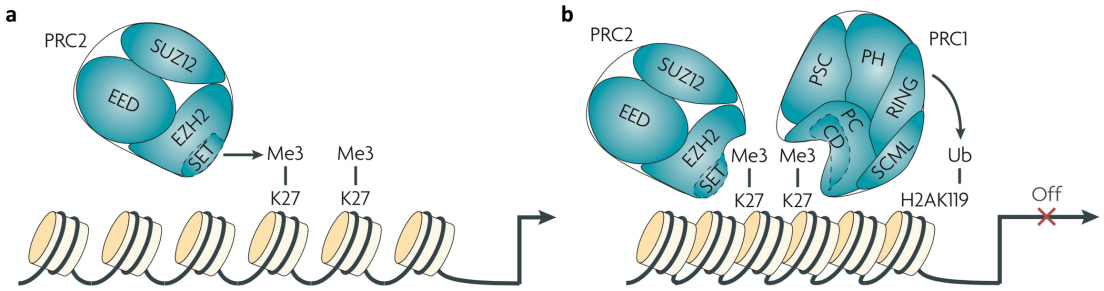

Figure 3 | Members and function of PRC2. (**a**) The PRC2 complex contains EZH2, EED, and SUZ12, while EZH2 catalyzes H3K27 trimethylation. The SET domain of EZH2 confers this activity. (**b**) H3K27me3 then induces a cascade of events including recruitment of PRC1, which mediates ubiquitination of H2A-K119. This histone mark is thought of inducing chromatin compaction, thus repressing transcription. EED, embryonic ectoderm development; EZH2, enhancer of zeste homolog 2; H2A-K119, histone 2A lysine 119; H3K27, histone 3 lysine 27; PRC, polycomb repressive complex; SET, suppressor of variegation 3-9 - enhancer of zeste - trithorax; SUZ12, suppressor of zeste 12 (adapted from: Bracken and Helin, 2009).

Ablation of any of the PRC2 members results in dampened H3K27me3, thus EZH2 can be catalytically active only in conjunction with all PRC2 members (Cao and Zhang, 2004; Cao et al., 2002; Ciferri et al., 2012; Czermin et al., 2002; Kuzmichev et al., 2002; Müller et al., 2002). Surprisingly, despite de-repression of lineage commitment genes, ESCs can be isolated from *Ezh2*$^{-/-}$, *Eed*$^{-/-}$, and *Suz12*$^{-/-}$ blastocysts, and pluripotency of these ESC cultures does not seem to be majorly affected, likely due to

maintained expression of stemness genes. However, PRC2-dysfunctional ESCs are more prone to differentiate spontaneously and incapable of giving rise to cells of all germ layers *in vitro* (Boyer et al., 2006; Chamberlain et al., 2008; Lee et al., 2006; Pasini et al., 2007; Shen et al., 2008). Likewise, deletion of *Ezh2*, *Eed*, or *Suz12* is embryonically lethal around gastrulation, thus PRC2 activity *in vivo* is absolutely required for early lineage specifications (Faust et al., 1998; 1995; O'Carroll et al., 2001; Pasini et al., 2004).

3.1.4.2. EZH2 function in development and tissue homeostasis

According to its function in ESCs, PRC2 is also regulating lineage-specific stem cell maintenance versus differentiation in both development and adult tissue homeostasis (Laugesen and Helin, 2014). For instance, depletion of *Ezh2* in fetal hematopoietic stem cells (HSC) impairs self-renewal resulting in perinatal anemia, while adult HSCs are not immediately affected by loss of *Ezh2* (Mochizuki-Kashio et al., 2011). However, exhaustion of HSCs in aged mice is counteracted by *Ezh2* overexpression (Kamminga et al., 2006). In contrast, deletion of the Ezh2 homolog *Ezh1* is not affecting fetal HSCs, but interferes with adult HSC maintenance (Hidalgo et al., 2012). Thus, PRC2 operates through EZH2 and EZH1, respectively, to differentially regulate fetal liver hematopoiesis and maintenance of the adult HSC compartment in the bone marrow. Besides HSC maintenance, PRC2 is also required for lymphopoiesis (Hidalgo et al., 2012; Mochizuki-Kashio et al., 2011). *Ezh2* knockout impairs early stages of B-cell differentiation and homing of B-cells to germinal centers (Béguelin et al., 2013; Caganova et al., 2013; Su et al., 2003; Velichutina et al., 2010), while *Ezh2* is required for proper differentiation of T-helper cells (Tumes et al., 2013). Apart from the hematopoietic system, the skin and the central nervous system (CNS) represent hierarchically structured organs with self-renewing stem cells giving rise to differentiating progeny (Hsu and Fuchs, 2012). Conceivably, epigenetic mechanisms are likely to also regulate homeostasis of these organs. Indeed, ablation of *Ezh2* affects self-renewal of neonatal basal skin progenitors, however, without apparent consequence for skin integrity. Ezh2 expression declines in adult skin progenitors at the expense of elevated Ezh1, resembling the Ezh2-Ezh1 interplay in HSCs (Ezhkova et al., 2009). Hence, an *Ezh1 Ezh2* double knockout severely compromises hair follicle and skin homeostasis with progressive degeneration of these tissues (Ezhkova et al., 2011). This also includes a restriction in fate determination towards lineage-committed Merkel cells, a progeny of basal skin progenitors (Bardot et al., 2013). Comparably, CNS-specific depletion of *Ezh2* during embryogenesis alters cortical neurogenesis by shifting neural progenitor self-renewal towards basal progenitor

differentiation (Pereira et al., 2010), while the *in vitro* differentiation potential and maintenance of neural stem cells (NSC) is Ezh2 dependent. *Ezh2* overexpression skews NSC differentiation towards astrogenesis (Sher et al., 2012; 2008; Sparmann et al., 2013). During cortical development, PRC2 activity is similarly required for the neurogenic-astrogenic competence switch of neural progenitors (Hirabayashi et al., 2009), and changes in PRC2 activity during corticogenesis might be fine-tuned by microRNAs (miR) (Neo et al., 2014b). Importantly, Ezh2 does not only govern CNS development, but is also required for adult neurogenesis. Deletion of *Ezh2* in NSCs of adult mice interferes with hippocampal NSC activation and neuron production, resulting in learning and memory disabilities (Zhang et al., 2014a). Interestingly, germline mutations in *EZH2* predispose to Weaver syndrome, a congenital disorder composed of craniofacial malformations as well as intellectual disabilities (Gibson et al., 2012; Tatton-Brown et al., 2011; 2013). The latter might reflect mutated *EZH2*-provoked NSC dysfunction, in analogy to the *Ezh2* knockout-induced behavioral phenotype in mice (Zhang et al., 2014a).

3.1.4.3. EZH2 function in hematopoietic malignancies

In accordance to germline *EZH2* mutations causing Weaver syndrome, somatic functional mutations in epigenetic modifiers might conceivably facilitate tumorigenesis. Indeed, mutations in epigenetic regulators including PRC2 members are frequently occurring in diverse cancers (Roy et al., 2014). For instance, ~20% of non-Hodgkin lymphoma patients (e.g. follicular, large B-cell, or high-grade B-cell lymphomas) as well as T-cell acute lymphoblastic leukemia (T-ALL) and acute myeloid leukemia (AML) patients harbor tumor-specific *EZH2* mutations, in which case *EZH2* mutational status usually correlates with poor patient prognosis (Abdel-Wahab et al., 2011; Bödör et al., 2011; 2013; Capello et al., 2011; Ernst et al., 2010; Grossmann et al., 2011; Guglielmelli et al., 2011; Lohr et al., 2012; Makishima et al., 2010; Morin et al., 2010; 2011; Nikoloski et al., 2010; Okosun et al., 2014; Ryan et al., 2011; Wang et al., 2013b; Zhang et al., 2012b). Furthermore, several highly recurrent mutations, such as $EZH2^{Y646C/F/H/N/S}$, $EZH2^{A682G}$, and $EZH2^{A692V}$, affect the SET domain of EZH2 and confer increased catalytic activity, resulting in aberrant H3K27me3 (Majer et al., 2012; McCabe et al., 2012a; Ott et al., 2014; Ryan et al., 2011; Sneeringer et al., 2010; Wigle et al., 2011; Yap et al., 2011) (Figure 4a, b).

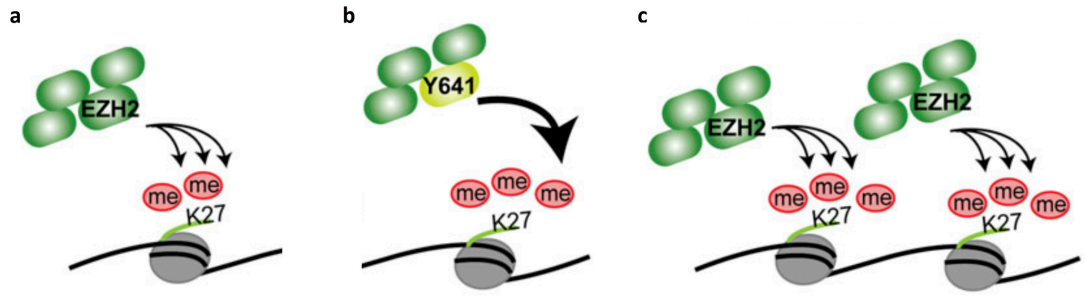

Figure 4 | Both *EZH2* mutations and EZH2 overexpression propagate aberrant H3K27me3. (**a**) $EZH2^{WT}$ displays high efficiency to catalyze H3K27me1 and H3K27me2, but only marginal catalytic activity for H3K27me3. (**b**) In contrast, PRC2 bearing mutated EZH2, such as $EZH2^{Y641N}$, has greatly enhanced capacity for H3K27me3. (**c**) Similarly, increased expression of $EZH2^{WT}$ leads to higher overall H3K27me3 levels, presumably due to a net increase in assembled PRC2 complexes. Thus, both *EZH2* mutations and EZH2 overexpression may propagate aberrant H3K27me3-dependent gene silencing potentially contributing to tumorigenesis. WT, wild type (adapted from: O'Meara and Simon, 2012).

Accordingly, overexpression of wild type (wt) *Ezh2* and $Ezh2^{Y646N/F}$ in murine HSCs and germinal center B-cells promotes neoplastic transformation reminiscent of myeloproliferative disease and lymphoma, respectively, while *Ezh2* depletion prevents AML and lymphoma formation (Berg et al., 2014; Béguelin et al., 2013; Caganova et al., 2013; Herrera-Merchan et al., 2012; Shi et al., 2013; Tanaka et al., 2012; Velichutina et al., 2010). These findings establish EZH2 as an oncogenic driver of hematopoietic malignancies and have prompted the development of small molecules interfering with its methyltransferase activity. Specific EZH2 inhibitors including GSK126, GSK343, and GSK503 (Figure 5) (GlaxoSmithKline; Béguelin et al., 2013; McCabe et al., 2012b; Verma et al., 2012), EPZ-5687 and EPZ-6438 (Epizyme; Knutson et al., 2013; 2012), EI1 (Novartis; Qi et al., 2012), UNC1999 (Sigma-Aldrich; Konze et al., 2013), and "compound 3" (Constellation Pharmaceuticals; Garapaty-Rao et al., 2013) sterically hinder the SET domain of $EZH2^{WT}$ and mutant EZH2, which results in reduced H3K27me3 and de-repression of genes with tumor suppressor potentials. These compounds induce apoptosis and cell cycle arrest *in vitro*, and counteract lymphoma and leukemia progression in transplantation models (Béguelin et al., 2013; Caganova et al., 2013; Garapaty-Rao et al., 2013; Knutson et al., 2012; Konze et al., 2013; McCabe et al., 2012b; Qi et al., 2012; Xu et al., 2015a). Comparably, GSK503 abrogates $Ezh2^{Y646N}$-induced murine germinal center B-cell neoplasia (Béguelin et al., 2013). Thus, EZH2 inhibition represents a strategy with high potential to target hematopoietic malignancies and is currently clinically verified in phase I studies (GSK126, NCT02082977; EPZ-6438, NCT01897571).

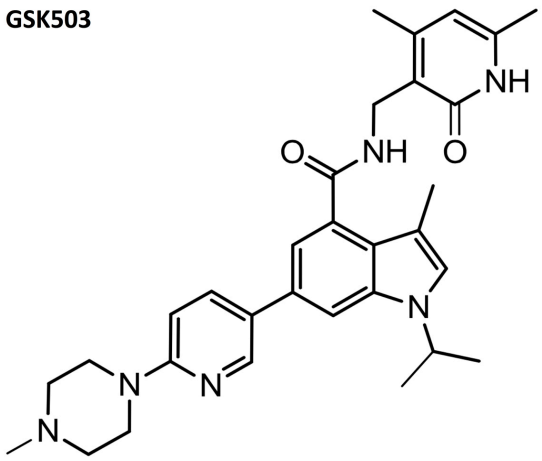

Figure 5 | Chemical structure of GSK503. GSK503 is an EZH2 methyltransferase-inhibiting compound with similar potency for $EZH2^{WT}$ and mutant EZH2 (Ki^{app} = 3–27nM). Importantly, GSK503 is more than 200-fold selective over EZH1 (Ki^{app} = 636nM) and more than 4'000-fold selective over other histone methyltransferases. GSK503 displays favorable pharmacokinetics in mice, thus represents an optimal tool for *in vivo* experiments (adapted from: Béguelin et al., 2013).

3.1.4.4. EZH2 function in solid cancers

As originally identified in breast and prostate cancer (Bracken et al., 2003; Kleer et al., 2003; Varambally et al., 2002), *EZH2* has been found, apart from being mutated, amplified or overexpressed in most cancers (Figure 4a, c), with a good correlation between high EZH2 expression levels and poor disease outcome. In many tissues as much as in the corresponding malignancies, EZH2 sustains stem cell identity and proliferation by transcriptional repression of senescence and differentiation genes (Laugesen and Helin, 2014). For instance, *EZH2* depletion attenuates stemness features of glioblastoma cells (de Vries et al., 2015; Kim et al., 2013; 2015; Orzan et al., 2011; Suvà et al., 2009), akin to the role of PRC2 in propagating neural stem cells (Hirabayashi et al., 2009; Pereira et al., 2010; Sher et al., 2008). Likewise, in normal and cancerous breast epithelial cells, PRC2 induces stemness features, while *in vivo*, ectopic *Ezh2* expression initializes hyperplasia in murine mammary glands (Chang et al., 2011; Gonzalez et al., 2009; 2014; Iliopoulos et al., 2010; Kleer et al., 2003; Li et al., 2009). Interestingly, PRC2 not only promotes breast carcinoma growth, but is also a major regulator of a process referred to as epithelial to mesenchymal transition (EMT) (Iliopoulos et al., 2010; Tiwari et al., 2013), the initial step in a course of events required for tumor cell dissemination and distant metastasis (Tam and Weinberg, 2013). In a mouse model of prostate cancer, *Ezh2* ablation similarly interferes with EMT and metastatic progression (Min et al., 2010). *Suz12*-deficient ESCs show an increased expression of E-cadherin (*Cdh1*), a major adhesion molecule of epithelial cells, while in breast, prostate, lung, colon, and pancreatic cancer cells,

PRC2 epigenetically silences *CDH1*, thus initializing EMT (Cao et al., 2008; Herranz et al., 2008; Iliopoulos et al., 2010; Oktyabri et al., 2014; Tiwari et al., 2013). Most importantly, *SUZ12* and *EZH2* depletion in breast, pancreatic, and ovarian cancer cell xenotransplants has been shown to prevent tumor relapse after chemotherapy, thus PRC2-mediated gene silencing confers adaptive chemoresistance (Hu et al., 2010; Iliopoulos et al., 2010; Ougolkov et al., 2008). Hence, beyond regulating tumor growth in similar ways as propagating normal tissue homeostasis, aberrant PRC2 activity could be held responsible for tumor plasticity resulting in EMT, metastasis, and resistance to chemotherapy (Tam and Weinberg, 2013) (Figure 6).

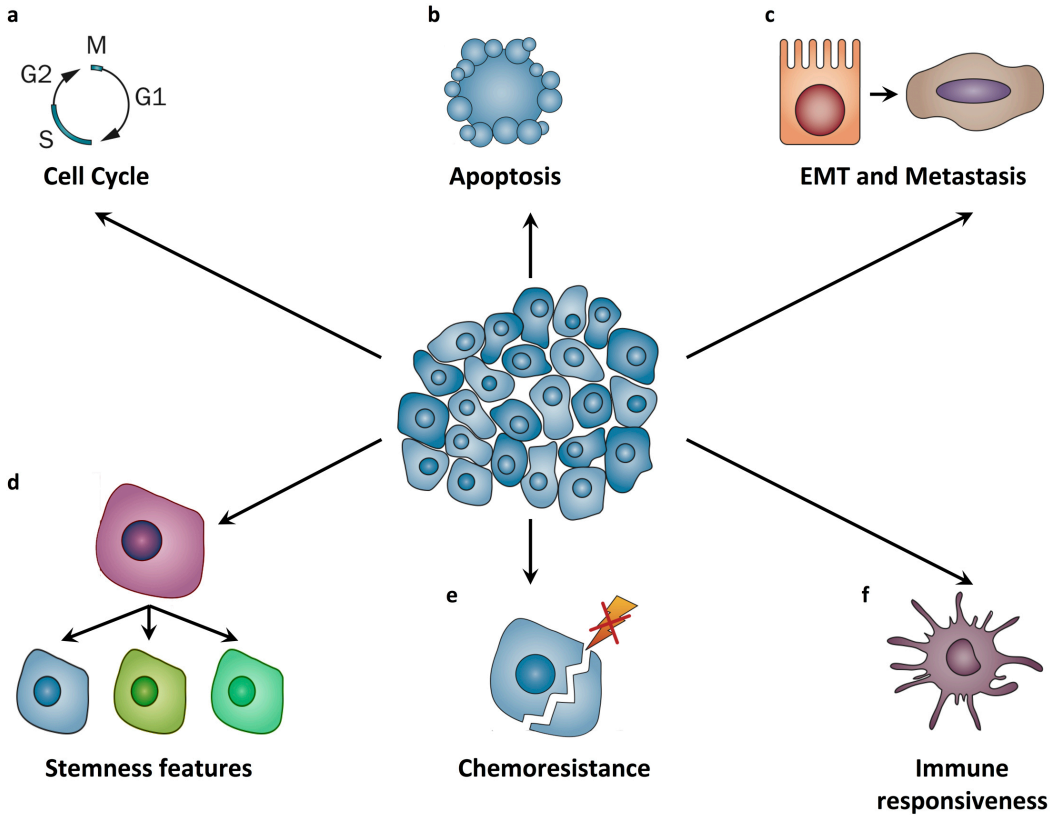

Figure 6 | Epigenetic miss-regulation contributes to diverse aspects of tumorigenesis. In the course of tumorigenesis, aberrant epigenetic regulation contributes to distinct processes favorable for cancer progression. Epigenetic modifiers have been shown to propagate cell cycle (**a**), suppress apoptosis (**b**), drive EMT resulting in metastasis (**c**), sustain tumor stemness (**d**), establish chemoresistance (**e**), and attenuate immune responsiveness (**f**). Accordingly, in various cancers, EZH2 promotes tumor progression and plasticity through silencing of tumor suppressors, such as cell cycle inhibitors, epithelial adhesion molecules, and differentiation genes. Consequently, an effective way in counteracting tumor progression and plasticity might be comprised of targeting epigenetic modifiers, such as EZH2 (adapted from: Azad et al., 2013).

A growing body of evidence suggests that EZH2, apart from canonically silencing genes through H3K27me3, mediates tumorigenesis by non-canonical mechanisms. Protein kinase B (AKT) can phosphorylate EZH2 at serine 21. Phospho-EZH2, in return, methylates signal transducer and activator of transcription 3 (STAT3), and methylated STAT3 promotes stemness features of glioblastoma (Kim et al., 2013). In prostate cancer, phospho-EZH2 similarly activates transcription in a PRC2-independent manner (Xu et al., 2012), while in breast cancer, EZH2 non-canonically regulates gene transcription through interaction with nuclear factor kappa-B (NF-κB) or β-catenin (CTNNB1) (Lee et al., 2011; Shi et al., 2007). Nevertheless, independently of the modality of EZH2-sustained oncogenesis, inhibition of the catalytic SET domain, the central node of EZH2 function, likely interferes with distinct aspects of solid cancer formation (Figure 6). Indeed, EZH2 inhibitors that have proven valid in lymphoma show promising features in preclinical models of diverse solid cancers (Amatangelo et al., 2013; Ferraro et al., 2014; Kim et al., 2013; Knutson et al., 2013; Liu et al., 2015; Zingg et al., 2015), thus might conceivably be considered for tumor entities beyond lymphoma.

3.1.5. Histone demethylases

A biological alternative to gain-of-function mutations in *EZH2*, a variety of cancers including AML, T-ALL, bladder cancer, and medulloblastoma harbor somatic loss-of-function mutations in ubiquitously transcribed tetratricopeptide repeat on chromosome X (*UTX*) (Gui et al., 2011; Jones et al., 2012; Pugh et al., 2012; Robinson et al., 2012; van Haaften et al., 2009), an H3K27me3 demethylase regulating diverse developmental processes (Van der Meulen et al., 2014). For instance, UTX emerges as a *bona fide* tumor suppressor in T-ALL. In mice, *Utx* deletion promotes leukemia and results in increased H3K27me3. Thus, the net output of *UTX* loss is reminiscent of increased EZH2 activity, which is supported by an increased sensitivity of *UTX*-deficient leukemia to EZH2 inhibitors (Van der Meulen et al., 2015). In contrast to *UTX* loss, H3K9me3 demethylases Jumonji domain 2 A, B, and C (*JMJD2A*/*B*/*C*) are frequently overexpressed in cancer (Young and Hendzel, 2013). *Jmjd2c* knockout prevents embryonic development beyond 4-cell-stage (Wang et al., 2010a), whereas increased JMJD2 activity in cancer affects de-repression of tumor promoters including pluripotency genes, resulting in enhanced tumor growth and stemness (Young and Hendzel, 2013). For instance, *JMJD2C* is amplified in breast cancer, and *its* silencing interferes with self-renewal capacity *in vitro* (Liu et al., 2009). Accordingly, a novel

pan-JMJD inhibitor counteracts breast carcinoma in mice, thus representing a possible therapeutic tool (Wang et al., 2013a). Yet another family of histone demethylases, Jumonji and ARID domain-containing protein 1A, B, C, and D (JARID1A/B/C/D), are able to erase the open chromatin mark H3K4me3, which enables gene repression, for instance through PRC2 (Benevolenskaya, 2007). Jarid1a/b represses differentiation of ESCs (Christensen et al., 2007; Lin et al., 2011), while *JARID1A/B* is highly expressed in breast and prostate cancer (Blair et al., 2011). *Jarid1b* knockout affects mammary gland development in mice and *JARID1B* depletion attenuates growth of human breast carcinoma cells (Catchpole et al., 2011). Comparably, *Jarid1a* deletion in thyroid and pituitary cancer-prone mice mitigates tumorigenesis (Lin et al., 2011). Furthermore, acquired chemotolerance in lung carcinoma cells is JARID1A dependent (Sharma et al., 2010). Therefore, JARID1 inactivation with a novel inhibitor (Sayegh et al., 2013) represents a possible strategy to target cancers and especially associated chemoresistance.

3.1.6. Histone modification readers

The histone modification landscape is perceived by epigenetic readers. These recruit various components of the nuclear signaling network to chromatin including transcription factors and RNA polymerases, thus mediating chromatin accessibility and gene expression. Reader proteins contain diverse domains allowing the recognition of specific histone modifications. For example, the domains WD40 and chromodomain recognize H3K27me3 and H3K9me3, respectively, while double chromodomain detects H3K4me3. In contrast, bromodomain recognizes various acetylated lysines (Musselman et al., 2012). For instance, EED contains WD40 repeats, which allows its recognition of H3K27me3 and, through recruitment of EZH2, the induction of H3K27 methylation on neighboring nucleosomes (Margueron et al., 2009; Xu et al., 2010). Similarly, heterochromatin protein 1 (HP1) contains a chromodomain, allowing the protein to recognize H3K9me3 and subsequently recruit DNMTs to induce stable gene silencing (Bannister et al., 2001; Feldman et al., 2006; Lehnertz et al., 2003). As histone acetylation mostly represents an open chromatin mark, bromodomain-containing readers frequently facilitate transcription (Filippakopoulos et al., 2012). For example, bromodomain-containing protein 4 (BRD4) is a critical mediator of transcriptional elongation (Yang et al., 2005). Furthermore, in contrast to transcription factors, BRD4 remains bound to transcriptionally active chromatin sites during mitosis, thus inheriting global transcriptional patterns (Dey et al., 2009). In murine and human ESCs, BRD4

regulates expression of pluripotency genes (Di Micco et al., 2014; Horne et al., 2014; Liu et al., 2014; Wu et al., 2015), while a *Brd4* knockout prevents embryogenesis beyond blastocyst stage (Houzelstein et al., 2002). In squamous cell carcinoma, *BRD4* is recurrently a component of chromosomal translocation, resulting in BRD4-driven epithelial differentiation blockade and tumor growth (French et al., 2001; 2003; 2008). Similarly, aberrant activity of bromodomain and extra terminal (BET) family members (BRD2, BRD3, and BRD4) promotes leukemia and multiple myeloma, partly through transcriptional activation of V-myc avian myelocytomatosis viral oncogene homolog (*MYC*), an oncogene overexpressed in a plethora of cancers (Dawson et al., 2011; Delmore et al., 2011). Therefore, small molecules sterically hindering BET family members have been developed, among which are JQ1 (Filippakopoulos et al., 2010) and I-BET151/762 (GlaxoSmithKline; Dawson et al., 2011; Nicodeme et al., 2010). Such inhibitors prevent BET members from recognizing transcription-starting sites and especially distal enhancers. This results in suppression of oncogenes, such as *C-MYC* or *N-MYC*, and remarkable anti-tumor effects in a wide set of preclinical cancer models including AML (Dawson et al., 2011), T-ALL (Knoechel et al., 2014; Ott et al., 2012; Roderick et al., 2014), lymphoma (Chapuy et al., 2013; Trabucco et al., 2015), multiple myeloma (Delmore et al., 2011; Lovén et al., 2013), squamous cell carcinoma (Filippakopoulos et al., 2010), prostate cancer (Asangani et al., 2014; Wyce et al., 2013a), lung cancer (Shimamura et al., 2013), Merkel cell carcinoma (Shao et al., 2014), glioblastoma (Cheng et al., 2013; De Raedt et al., 2014; Pastori et al., 2014), medulloblastoma (Bandopadhayay et al., 2014; Henssen et al., 2013; Venkataraman et al., 2014), neuroblastoma (De Raedt et al., 2014; Puissant et al., 2013; Wyce et al., 2013b), malignant peripheral nerve sheath tumors (De Raedt et al., 2014; Patel et al., 2014), and cutaneous melanoma (De Raedt et al., 2014; Gallagher et al., 2014a; 2014b; Segura et al., 2013). Thus, BET bromodomain inhibition represents a highly promising strategy to target various malignancies and is currently clinically verified in several phase I studies (AML, NCT01713582, NCT02158858, NCT02308761; lymphoma, NCT01949883; multiple myeloma, NCT02157636; glioblastoma, NCT02296476; various solid cancers, NCT02259114, NCT01987362, NCT01587703).

3.2. The neural crest and its derivatives

3.2.1. The embryonic neural crest

Originally identified in the developing chick embryo (His, 1868), the neural crest (NC) has later been defined as a transient cell population in the vertebrate embryo that emerges from the neural plate border and gives rise to a wide range of derivatives (Sauka-Spengler and Bronner, 2010). During neurulation, NC specification becomes apparent between the neural plate and its adjacent ectoderm, and after neural tube closure, NC cells localize to the dorsal neural tube. NC specification is driven by extracellular cues, such as ligands of the wingless/integrated (Wnt), bone morphogenic protein (Bmp), and fibroblast growth factor (Fgf) families. The intracellular signaling cascades induce a transcriptional network including v-ets avian erythroblastosis virus E26 oncogene homolog 1 (*Ets1*), forkhead box D3 (*Foxd3*), snail family zinc finger 1 and 2 (*Snai1*, *Snai2*), sex determining region Y-box 9 and 10 (*Sox9*, *Sox10*), twist family bHLH transcription factor 1 (*Twist1*), and zinc finger E-box binding homeobox 1 (*Zeb1*) (Betancur et al., 2010; Bronner and Ledouarin, 2012; Nelms and Labosky, 2010; Sauka-Spengler and Bronner, 2010). NC cells then delaminate from the dorsal neural tube through EMT and extensively migrate to distant locations. The same transcriptional network that is involved in NC specification also triggers the EMT. These transcription factors induce an EMT-typical program including expression of type-II cadherins, down regulation of tight junctions, loss of apico-basal polarity, and expression of matrix metalloproteases (MMP). The migration of NC cells to distinct target sites is established through a variety of signaling inputs, such as Wnts, ephrins, and semaphorins, but also Fgfs, platelet-derived growth factors (Pdgf), and vascular endothelial growth factor (Vegf). These signaling cascades are thought of commonly activating small rat sarcoma (Ras) homolog (Rho)-GTPases, key regulators of cell motility (Nelms and Labosky, 2010; Strobl-Mazzulla and Bronner, 2012a; Theveneau and Mayor, 2012). During this course of events, the NC differentiates into a plethora of cell types, such as neurons and glial cells of the peripheral nervous system (sensory, sympathetic, and parasympathetic), medullar cells of the adrenal gland, calcitonin-producing cells of the thyroid gland, adipocytes, mesenchymal cells (osteocytes, chondrocytes, myofibroblasts, and smooth muscle cells), and melanocytes (Figure 7a). However, fates of NC cells are dependent on the rostral-caudal level of emigration. For instance, the NC emigrating rostral to somite 7 gives rise to the peripheral nervous system and melanocytes of the trunk,

while NC cells emigrating caudal to somite 4 have broader fates including mesenchymal specification required for craniofacial structures (Dupin and Sommer, 2012; Sauka-Spengler and Bronner, 2010).

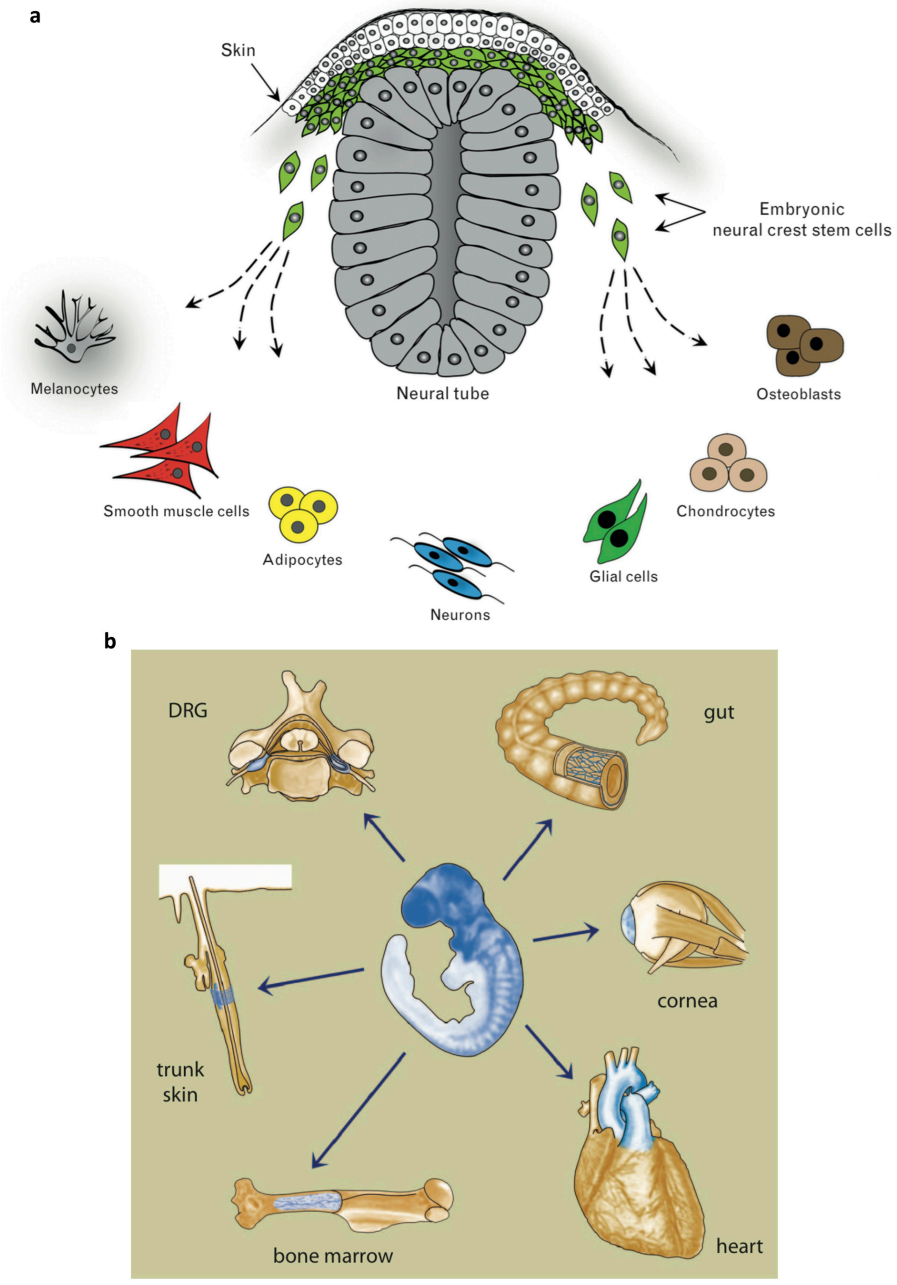

Figure 7 | Embryonic NCSC progeny and NCSC locations in adult tissues. (**a**) Embryonic NCSCs emerge from the neural plate border and, after extensive migration, give rise to a wide range of derivatives including neurons, glial cells, melanocytes, smooth muscle cells, osteoblasts, chondrocytes, and adipocytes. (**b**) In the adult organism, self-renewing NCSCs reside at post-migratory locations of the embryonic NC. These adult NCSCs have a capacity and differentiation potential resembling those of NCSCs during embryonic development. NCSCs have been described in diverse tissues and organs, such as DRG, gut, cornea, heart, bone marrow, and skin. DRG, dorsal root ganglia; NC, neural crest; NCSC, NC stem cell (adapted from: Shakhova, 2014; Shakhova and Sommer, 2010).

3.2.2. Neural crest stem cells

While the NC gives rise to different progeny *in vivo* (Dupin and Sommer, 2012; Sauka-Spengler and Bronner, 2010), NC cells maintain the potential to differentiate into a variety of cell types *in vitro*, depending on the combination of instructive growth factors applied to the NC culture (Shakhova and Sommer, 2010). Importantly, NC cells can also be sustained in an undifferentiated state using a combinatorial application of Wnt and Bmp (Kléber et al., 2005). Due to this self-renewal capacity and the broad *in vitro* potential, NC cells were originally defined as multipotent stem cells, using first avian (Baroffio et al., 1991; Sieber-Blum and Cohen, 1980) and later rodent NC cultures (Stemple and Anderson, 1992). Likewise, the NC was described to be a stem cell population *in vivo* using single cell labeling in chicks (Bronner-Fraser and Fraser, 1989; Frank and Sanes, 1991), while NC cells have been associated with stem cell attributes in mouse embryos using targeted activation of a reporter gene (Jiang et al., 2000) and manipulation of NC-relevant transcriptional pathways, such as Sox10 (Kim et al., 2003; Paratore et al., 2002), Wnt (Hari et al., 2002; Lee et al., 2004), and transforming growth factor beta (Tgfβ) (Wurdak et al., 2005). Recently, the murine embryonic NC was proven to be a multipotent NC stem cell (NCSC) population both before and after delamination from the neural tube by harnessing multicolor-based *in vivo* fate-mapping (Baggiolini et al., 2015). Although it was assumed that the multipotent NCSC population is a transient appearance during embryogenesis, it has only recently become evident that multipotent and self-renewing NCSCs reside at post-migratory locations of the embryonic NC and persist into adulthood (Dupin and Sommer, 2012). To this day, NCSCs have been identified, among others, in dorsal root ganglia (Bixby et al., 2002; Hagedorn et al., 1999; Nagoshi et al., 2008), sciatic nerves (Morrison et al., 1999), the gut (Bixby et al., 2002; Kruger et al., 2002), the heart (Tomita et al., 2005), the cornea (Yoshida et al., 2006), teeth (Janebodin et al., 2011), the bone marrow (Nagoshi et al., 2008), and the skin (Nagoshi et al., 2008; Sieber-Blum et al., 2004; Wong et al., 2006) (Figure 7b). Because of their broad accessibility and potential, adult NCSCs might be a potential source for cell and tissue replacement therapies. In fact, skin-derived NCSCs have already been applied in nerve (McKenzie et al., 2006), spinal cord (Biernaskie et al., 2007; Sieber-Blum et al., 2006), and bone injury models (Lavoie et al., 2009).

3.2.3. The melanocytic lineage

Historically demonstrated with transplantation experiments of embryonic mouse tissue into the coelom of chick embryos (Mayer, 1973; Rawles, 1947), it is nowadays well established that melanocytes originate from the NC (Figure 7a). In the mouse embryo, NCSCs specify towards a melanoblastic fate early after delamination from the neural tube, while shortly migrating towards and then pausing in the so-called Migration Staging Area (MSA). Subsequently, melanoblasts migrate extensively on the dorsolateral pathway before invading the epidermis, where they fully differentiate into epidermal melanocytes or populate forming hair follicles. Apart from the skin, NC-derived melanoblasts also populate the uvea of the eye, the heart, the inner ear, and the leptomeninges (Pavan and Raible, 2012; Sommer, 2011). Recently, glial progenitors were shown to possess the potential of differentiating into melanocytes, representing an alternative source of pigment-producing cells during development and potentially during regenerative processes of the skin (Adameyko et al., 2009; 2012). Indeed, adult NCSCs associated with the endings of hair follicle-wrapping nerves contribute to the wound healing process of murine skin (Johnston et al., 2013). Although whether or not these cells also have the capacity of producing melanocytes remains unclear. In humans, the precise developmental origin of melanocytes remains a challenging question to address. However, human ESCs were recently successfully differentiated into NCSCs and further into pigmented melanocytes, demonstrating, at least *in vitro*, the potential of human NCSCs to give rise to the melanocytic lineage (Mica et al., 2013).

3.2.4. Adult melanocyte biology

Mature melanocytes are melanin-producing cells and responsible for pigmentation of skin and hair. Melanocytes deliver their melanin content to neighboring keratinocytes through melanosomes, either at the basal lamina of the epidermis, or in the hair matrix (bulb) of hair follicles (Figure 8). Pigment accumulation in keratinocytes allows protection of hairless skin from exposure to sunlight-induced ultraviolet (UV) damage. However, in hair coat-covered areas, epidermal melanocytes are frequently absent, since pigmented hair is a sufficient protection from UV radiation (Lin and Fisher, 2007). In agreement, epidermal inter-follicular melanocytes are completely absent in murine adult trunk skin (Hirobe, 1984). During mouse development, trunk skin melanoblasts solely populate hair follicles. They either migrate into the forming hair bulb, where they fully differentiate into pigment-producing

melanocytes, or they reside in the bulge (Nishimura et al., 2002a). Importantly, the hair follicle bulge is the concomitant stem cell niche for epidermal stem cells (Cotsarelis et al., 1990). During subsequent hair cycles, melanoblasts in the bulge self-renew and give rise to differentiating melanocytes to re-pigment newly growing hairs. Therefore, melanoblasts in the bulge have been defined as melanocyte stem cells (MSC) (Nishimura et al., 2002a) (Figure 8).

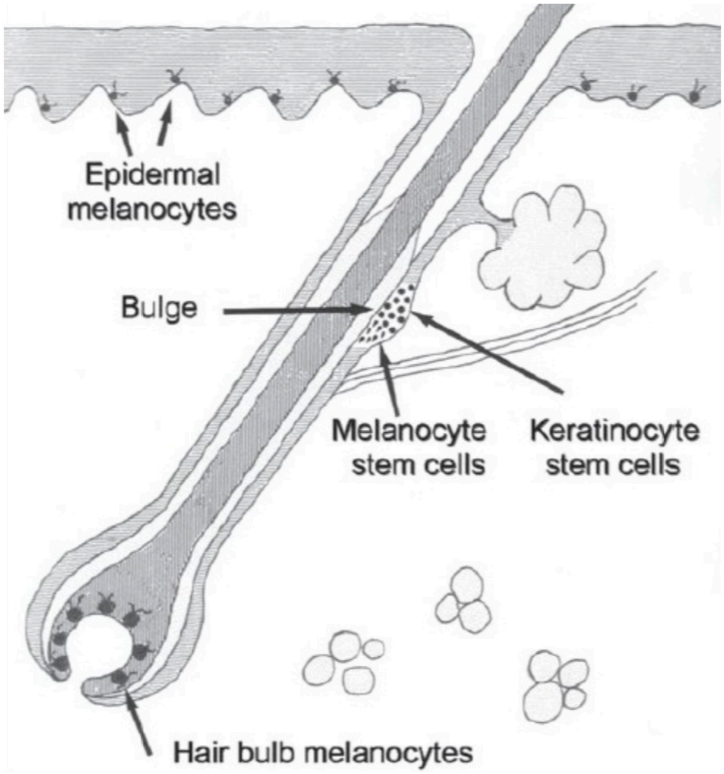

Figure 8 | Melanocyte locations in human hair-bearing skin. Human melanocytes are located either at the basal lamina of the epidermis or in the bulb of hair follicles, while murine trunk skin lacks interfollicular, epidermal melanocytes. A growing hair follicle is fueled with epithelial cells and melanocytes, which originate from epithelial (keratinocyte) stem cells and MSCs, respectively. These cell populations represent a stem cell reservoir that resides in the bulge area, the permanent niche of the hair follicle throughout the hair cycle. Accordingly, dysfunctions affecting either MSC homeostasis or bulge integrity result in hair graying, due to the lack of pigment-producing melanocytes in the subsequent hair cycles. MSC, melanocyte stem cell (adapted from: Falabella, 2009).

In human skin, amelanotic melanoblasts residing in hair follicle bulges were described (Staricco, 1963), thus representing a potential reservoir to replenish the epidermis and hair follicles with melanocytes. In support, local de-pigmentation of human skin, induced through ionizing irradiation, is usually supplemented with pigment-producing melanocytes starting from the orifices of hair follicles (Cui et al., 1991; Ortonne et al., 1980). Interestingly, UV irradiation of murine trunk skin similarly induces

migration of MSCs into hair follicle-neighboring epidermis and subsequent differentiation into melanin-producing melanocytes in order to provide UV-protection (Chou et al., 2013). It is supposable that murine MSCs and amelanotic melanoblasts in human hair follicles are the corresponding cell population, although a formal proof is still missing. Further, it remains to be clarified, whether MSCs and NCSCs in the adult murine skin represent the same cell population.

3.2.5. Melanocyte-relevant transcription factors and signaling pathways

Interestingly, transcription factors and signaling pathways, critical to early NC specification and NCSC function, are still highly relevant for melanoblast development and adult MSC homeostasis.

3.2.5.1. FOXD3 and SOX9

For instance, the transcription factor Foxd3 is required for NC specification and early NCSC maintenance (Teng et al., 2008). However, during melanoblast specification Foxd3 is downregulated. *In ovo*, silencing of *Foxd3* in early NC cells induces dorsolateral migration, while *Foxd3* overexpression prevents melanocyte development (Kos et al., 2001). In agreement, overexpression of the NC specifiers *Sox9* and *Snai2* in early NC cells similarly represses melanocytic fate in favor of ventrally migrating NC cells (Nitzan et al., 2013). Likewise, Sox9 is dispensable for adult murine melanocyte homeostasis (Shakhova et al., 2015).

3.2.5.2. SOX10

In contrast, Sox10 is required for the embryonic NC as much as throughout the melanocytic lineage. Sox10 is expressed in NC cells upon delamination from the neural tube and highly relevant for NCSC survival, differentiation, and migration (Bondurand et al., 1998; Britsch et al., 2001; Kapur, 1999; Kim et al., 2003; Paratore et al., 2001; 2002; Southard-Smith et al., 1998). Especially extensive dorsolateral migration of melanoblasts is affected by aberrations affecting *Sox10*. This frequently results in a congenital melanocyte-free belly spot reminiscent of the human Waardenburg syndrome (Aoki et al., 2003; Britsch et al., 2001; Pingault et al., 1998; Potterf et al., 2001; Southard-Smith et al., 1998). Sox10 remains expressed in murine post-migratory melanoblasts (Osawa et al., 2005) and SOX10 is similarly detectable in human neonatal epidermal melanocytes (Cook et al., 2003). In murine adult hair follicles,

Sox10 function is essential for bulge-associated MSC homeostasis as much as retention of differentiated melanocytes in the bulb (Harris et al., 2013; Shakhova et al., 2015).

3.2.5.3. PAX3 and MITF

Sox10 drives embryonic melanoblast specification and melanocyte maintenance through an interplay with the transcription factors paired box 3 (Pax3) and microphthalmia-associated transcription factor (Mitf). Pax3 is expressed during NC specification, NC delamination, melanoblast development, and required for MSC homeostasis (Kubic et al., 2008; Lang et al., 2005). The synergistic function of Sox10 and Pax3 becomes apparent in the co-activation of *Mitf* transcription (Bondurand et al., 2000; Potterf et al., 2000). Mitf itself is referred to as master regulator of the melanocytic lineage (Steingrimsson et al., 2004). Mitf is first expressed in NC cells in the MSA, thus initializing melanoblast specification (Opdecamp et al., 1997). Sox10, Pax3, and Mitf then co-regulate expression of melanogenesis-relevant genes including dopachrome tautomerase (*Dct*), melan-A (*Mlana*), premelanosome protein (*Pmel*), tyrosinase (*Tyr*), and tyrosinase-related protein 1 (*Tyrp1*). Highlighting the essence of Mitf for melanocyte development, disruption of the *Mitf* locus leads to a complete absence of melanocytes in adult mice (Steingrimsson et al., 2004), while in humans, genetic alterations affecting *PAX3* or *MITF* loci, similar to alterations in *SOX10*, result in Waardenburg syndromes (Pingault et al., 2010).

3.2.5.4. WNT signaling

Among critical signaling cues controlling NC development are WNTs. These ligands bind to frizzled receptor, which induces an intracellular signaling cascade that leads to the translocation of CTNNB1 to the nucleus, thus regulating transcriptional responses (Cadigan and Liu, 2006). Wnts are crucial for NC specification (Ikeya et al., 1997; Saint-Jeannet et al., 1997) and, in combination with Bmp, for NCSC maintenance (Kléber et al., 2005), while interference with Ctnnb1 function prevents fate acquisitions of NCSCs, such as craniofacial structures, sensory neurons, and melanocytes (Brault et al., 2001; Hari et al., 2002). In avian and zebrafish NC, Wnts induce melanocytic differentiation (Dorsky et al., 1998; Jin et al., 2001), while in the murine migratory NC, expression of a stabilized form of *Ctnnb1* promotes melanocyte formation at the expense of other fates (Hari et al., 2012). Interestingly, expression of similarly stabilized *Ctnnb1* in specified melanoblasts rather leads to a decreased melanocyte number possibly due to diminished migratory capacity (Gallagher et al., 2013). Ctnnb1 mediates *Mitf* transcription, thus inducing melanoblast specification (Takeda et al., 2000; Widlund et al., 2002). However, excessive Mitf levels also trigger senescence while preventing migration of melanoblasts.

Therefore, stabilized Ctnnb1 might over-induce *Mitf* and, therefore, interfere with dorsolateral migration of melanoblasts resulting in the reported pigmentation defect (Gallagher et al., 2013; Steingrimsson et al., 2004). In murine adult hair follicles, stabilized Ctnnb1 induces ectopic MSC proliferation and differentiation in the bulge, possibly due to aberrant *Mitf* induction. Likewise, MSC activation upon hair cycle initiation or UV irradiation is Wnt signaling dependent, such as *Ctnnb1*-deficient MSCs remain quiescent (Rabbani et al., 2011; Yamada et al., 2013).

3.2.5.5. TGFβ signaling

Another relevant signaling cue for NC development is TGFβ, which binds to TGFβ receptor 2 (TGFBR2), thus inducing an intracellular signaling cascade through phosphorylation of mothers against decapentaplegic homologs 2 and 3 (SMAD2/3). Phosphorylated SMAD2/3 then form a complex with SMAD4, translocate to the nucleus, and ultimately regulate transcriptional responses (Moustakas and Heldin, 2009). Upon exposure to Tgfβ, NCSCs differentiate towards neuronal lineages or smooth muscle cells, depending on the culture conditions (Hagedorn et al., 1999; 2000; Shah et al., 1996), while interference with Tgfbr2 function in the NC mostly prevents mesenchymal fate acquisition crucial for craniofacial structures and smooth muscle cells contributing to the outflow tract of the heart (Ito et al., 2003; Wurdak et al., 2005). Interestingly, specification of NCSCs towards mesenchymal progenitors is driven through Tgfβ-mediated repression of *Sox10* and re-expression of *Sox9* (John et al., 2011), which has previously been highlighted as an essential specifier for NC-derived mesenchyme (Akiyama et al., 2004; 2002; Mori-Akiyama et al., 2003). If Tgfβ-mediated *Sox10* repression was a common trait throughout NC development, an involvement of Tgfβ signaling in melanoblast biology would be surprising, since Sox10 function is essential for the melanocytic lineage (Harris et al., 2013; Shakhova et al., 2015). However, it was reported that adult MSCs have slightly reduced Sox10 levels compared to differentiated melanocytes (Osawa et al., 2005; Sharov et al., 2005). Simultaneously, Tgfβ is secreted by epidermal stem cells of the bulge (Tanimura et al., 2011; Tumbar et al., 2004). Remarkably, Tgfβ signaling is required for quiescence of MSCs. Depletion of *Tgfbr2* induces premature differentiation of MSCs, thus the bulge provides a functional niche for MSC homeostasis (Nishimura et al., 2010; Tanimura et al., 2011). Similarly, *Smad4* deletion mitigates MSC homeostasis resulting in hair graying (Zingg and Tuncer, in preparation). Whether Tgfβ-mediated quiescence of MSCs functions through temporal repression of *Sox10* and possibly increased Sox9 expression, remains to be clarified.

3.2.6. Congenital neurocristopathies

During embryonic development, abnormal specification, migration, differentiation, or survival of NC cells frequently leads to congenital organ and tissue dysplasia with diverse clinopathological features (Etchevers et al., 2006).

3.2.6.1. Waardenburg syndromes and Hirschsprung disease

For instance, as described above, genetic aberrations affecting *SOX10*, *PAX3*, or *MITF* loci regularly cause Waardenburg syndromes. These genes are especially relevant for melanoblast specification, migration, and survival. Therefore, the clinopathological features of these syndromes are, among others, pigmentary abnormalities of the skin as well as hearing disabilities due to absence of inner ear melanocytes (Pingault et al., 2010). Dependent on the type of *SOX10* mutations, maintenance of NC-derived enteric nervous system (ENS) precursors is similarly impaired, resulting in precocious differentiation and, therefore, aganglionosis of the most distal gut, commonly known as Hirschsprung disease (McKeown et al., 2013; Paratore et al., 2002; Pingault et al., 1998; Southard-Smith et al., 1998). Comparably, endothelins are ligands that are required for proper migration and differentiation of both melanoblasts and ENS precursors (Baynash et al., 1994; Hosoda et al., 1994). Therefore, mutations affecting endothelins or its receptors can cause a Waardenburg syndrome partly consisting of Hirschsprung disease (McKeown et al., 2013; Pingault et al., 2010).

3.2.6.2. DiGeorge syndrome

In contrast, interference with signaling pathways responsible for mesenchymal fate of the NC, such as Tgfβ signaling, potentially results in craniofacial and cardiovascular defects reminiscent of the congenital DiGeorge syndrome (Ito et al., 2003; Wurdak et al., 2005; 2006). In mice, Tgfβ signaling controls expression of v-crk sarcoma virus CT10 oncogene homolog (avian)-like (*Crkl*) (Wurdak et al., 2005). Interestingly, the chromosomal region flanking *CRKL* is frequently deleted in DiGeorge patients (Driscoll et al., 1992; Scambler et al., 1991). In accordance, deletion of *Crkl* in mice, causes a phenotype again similar to the human DiGeorge syndrome (Guris et al., 2001).

3.2.6.3. Giant congenital nevus

Yet another neurocristopathy is giant congenital nevus, a dermal benign hyperplasia of melanocytic cells that arises during embryonic melanoblast migration towards the epidermis. Formation of these nevi is driven by *in utero*-acquired gain-of-function mutations predominantly in the *NRAS* locus (e.g. $NRAS^{Q61K}$), resulting in permanent stimulation of mitogen-activated kinase (MAPK) signaling (Bauer et al., 2007; Charbel et al., 2014; Kinsler et al., 2013; Lyon, 2010) (Figure 11). Due to the constitutive activation of oncogenic NRAS and the large increase in melanocytic cells, congenital nevus patients have an increased risk of developing malignant melanoma (Lyon, 2010), a cancer arising from melanocytes (3.3. Melanoma). Accordingly, expression of the $N\text{-}Ras^{Q61K}$ oncogene in the melanocytic lineage of mice promotes dermal melanocytic hyperplasia followed by occasional melanomagenesis (Ackermann et al., 2005; Shakhova et al., 2012). Interestingly, *Sox10*-haploinsufficient mice are devoid of $N\text{-}Ras^{Q61K}$-driven hyperplasia, thus highlighting the requirement of Sox10 for the establishment of congenital nevi (Shakhova et al., 2012), in analogy to its relevance for NCSCs and melanocytes (Aoki et al., 2003; Harris et al., 2013; Kim et al., 2003; Paratore et al., 2001; 2002; Potterf et al., 2001; Shakhova et al., 2015).

3.2.7. Acquired neurocristopathies

Apart from congenital neurocristopathies, a variety of acquired pathologies including cancers arise from NC-derived cell types. Malignancies can, for example, arise from peripheral and cranial nerves (e.g. peripheral nerve sheath tumors), the sympathetic nervous system (e.g. neuroblastoma), or the melanocytic lineage (e.g. melanoma, which will be discussed in detail in chapter (3.3. Melanoma)) (Dundr and Ehrmann, 2012).

3.2.7.1. Peripheral nerve sheath tumors

Malignant peripheral nerve sheath tumors (MPNST) are the most common malignant mesenchymal tumors of soft tissue. In about 50%, MPNSTs emerge *de novo* from NC-derived Schwann cell precursors of peripheral or cranial nerves. In the remaining cases, neurofibromatosis type 1, a benign syndrome affecting Schwann cells, progresses into MPNSTs (Carroll, 2012; Joseph et al., 2008; Mrugala et al., 2005). A gene of importance for the peripheral glial lineage is neurofibromin 1 (*NF1*), which inhibits MAPK signaling through dephosphorylation of RAS proteins (Carroll, 2012; Wrabetz et al., 1995)

(Figure 11). Neurofibromatosis type 1 patients usually harbor aberrations in both *NF1* loci (Legius et al., 1993; Messiaen et al., 2000; Viskochil et al., 1990; Wallace et al., 1990), which increases MAPK signaling, thus promoting the disease (Basu et al., 1992). Accumulation of further driver mutations in distinct loci, such as cyclin-dependent kinase inhibitor 2a (*CDKN2A*) or transformation-related protein 53 (*TRP53*), then promotes MPNSTs (Holtkamp et al., 2007; Kourea et al., 1999; Nielsen et al., 1999). In agreement, ablation of *Nf1* in mice induces a phenotype comparable to neurofibromatosis type 1 and, in combination with *Trp53* or *Cdkn2a* deficiency, promotes MPNSTs (Cichowski et al., 1999; Joseph et al., 2008; Mayes et al., 2011; Vogel et al., 1999; Wu et al., 2008). Untransformed peripheral glia is Sox10 positive, while *Sox9* is repressed (Betancur et al., 2010; Sauka-Spengler and Bronner, 2010). However, progression of benign neurofibroma into MPNSTs is associated with a gradual increase in SOX9 and concomitant loss of SOX10 (Carbonnelle-Puscian et al., 2011; De Raedt et al., 2014; Lévy et al., 2004; Miller et al., 2009; 2006; Nonaka et al., 2008). Thus, processes driving MPNSTs might be reminiscent of embryonic NC development, namely differentiation of Sox10-positive NCSCs towards Sox9-expressing mesenchymal progenitors (John et al., 2011). In support of this, neurofibroma progression has been associated with EMT (Arima et al., 2010), while human MPNSTs frequently harbor mesenchymal components (Ducatman and Scheithauer, 1984).

3.2.7.2. Neuroblastoma

Neuroblastoma is the most common solid extracranial childhood tumor, and often appears within the first year of life (Heck et al., 2009). Neuroblastoma is a cancer frequently emerging from ganglia of the sympathetic nervous system including the adrenal medulla (Cheung and Dyer, 2013). During embryogenesis, NCSCs specify towards sympathoadrenal precursors, which then give rise to sympathetic ganglia including the adrenal medulla (Anderson and Axel, 1986; Anderson et al., 1991). A key transcription factor regulating these specification and differentiation processes is paired-like homeobox 2b (Phox2b). In familial and sporadic neuroblastoma, *PHOX2B* locus often appears to be disturbed (Raabe et al., 2008; Trochet et al., 2004; 2005; van Limpt et al., 2004). Interestingly, in mice harboring *Phox2b* mutations, Sox10 aberrantly remains expressed in autonomic ganglia, pointing towards miss-specified cells with characteristics of NCSCs or glial progenitors (Nagashimada et al., 2012). SOX10 is also upregulated in human neuroblastoma samples (Gershon et al., 2005). However, it remains to be investigated, whether SOX10 promotes neuroblastoma through propagation of an undifferentiated NCSC-like status.

3.3. Melanoma

3.3.1. Clinopathological classification of human melanoma

Melanoma is defined as the cancer arising from the melanocytic lineage (Gray-Schopfer et al., 2007), which originates during embryonic development from the NC (3.2.3. The melanocytic lineage). However, dependent on the subtype of melanocytes and the acquired driver mutations, different classes of melanocytic pathologies arise. The vast majority (95%) of melanomas are derived from melanocytes residing at the basal lamina of the epidermis, thus referred to as cutaneous melanoma. Rarely, melanoma arises from mucosal (1.3%) or uveal (3.7%) melanocytes (Chang et al., 1998; McLaughlin et al., 2005) (Figure 9).

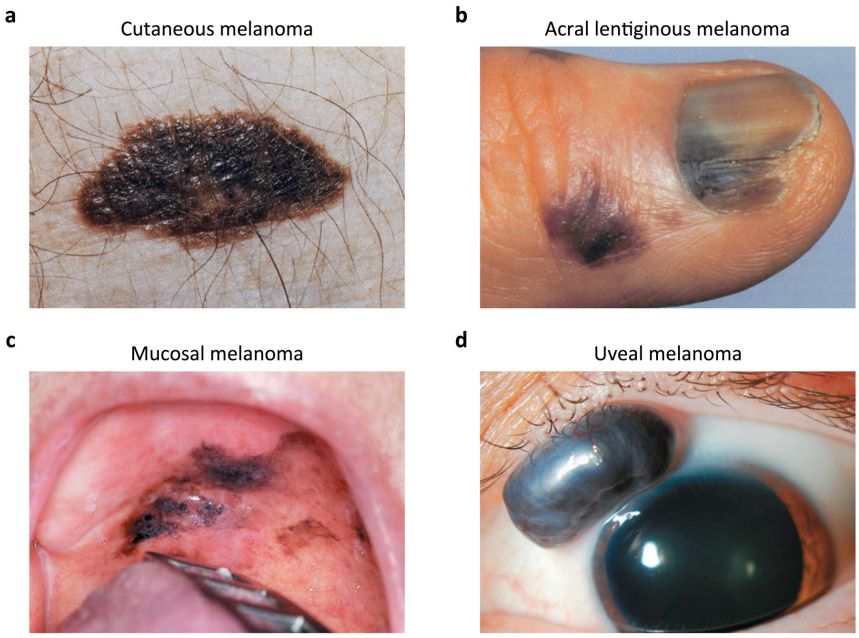

Figure 9 | Clinopathological classifications of human malignant melanomas. (**a**, **b**) Subtypes of malignant melanoma include cutaneous melanoma (**a**) and acral lentiginous melanoma (**b**), which originate from cutaneous melanocytes located in hear-bearing skin and acral hairless skin, respectively. (**c**, **d**) Furthermore, melanoma can arise from mucosal and uveal melanocytes resulting in mucosal (**c**) and uveal melanoma (**d**) (adapted from: Benoist and van Looij, 2013; Koh, 1991; Vavvas and Brodowska, 2009).

3.3.1.1. Cutaneous melanoma

Cutaneous melanoma will be discussed below (paragraphs 3.3.2. – 3.3.7.) (Figure 9a).

3.3.1.2. Mucosal melanoma

Mucosal melanocytes are found at the basal lamina of squamous epithelium of mucous tissues, such as in the oral and the sinonasal cavity, the rectum, and the vagina (Mihajlovic et al., 2012) (Figure 9c). Mucosal melanoma is frequently driven by activating mutations in stem cell factor receptor (*KIT*) or through amplification of the *KIT* locus (Garrido and Bastian, 2010). KIT is a receptor tyrosine kinase (RTK) that signals, among others, through MAPK pathway (Vidwans et al., 2011) (Figure 11). During murine embryonic development, Kit signaling is required for survival and migration of melanoblasts, while differentiation of adult MSCs is dependent on functional Kit (Nishikawa et al., 1991; Nishimura et al., 2002a; Wehrle-Haller and Weston, 1995). It remains to be investigated, whether oncogenic mutations in *Kit* are sufficient to induce mucosal melanoma in mice.

3.3.1.3. Uveal melanoma

Melanocytes in the uvea of the eye (e.g. the iris) produce pigment in order to protect the eye from UV damage, though, in contrast to cutaneous melanocytes, without transferring the pigment to neighboring cells (Hu, 2000) (Figure 9d). Oncogenic mutations inducing a transformation of uveal melanocytes are often found in loci of the guanine nucleotide binding protein (G-protein) q polypeptide (*GNAQ*) or the G-protein alpha 11 (*GNA11*) (Van Raamsdonk et al., 2009; 2010). Both G-proteins similarly activate MAPK pathway (Vidwans et al., 2011) (Figure 11). Indeed, *Gnaq* or *Gna11* transgenes bearing the human activating mutations are sufficient to transform murine melanocytes into cells giving rise to metastatic melanoma in recipient mice (Van Raamsdonk et al., 2009; 2010), thus confirming *GNAQ* and *GNA11* as melanoma drivers. Interestingly, homozygous knockout of *Gnaq* and *Gna11* results in embryos with cardiovascular and craniofacial defects (Offermanns et al., 1998), highlighting these G-proteins as potential players during cranial NC-derived mesenchyme and, presumably, uveal melanoblast development.

3.3.1.4. Acral lentiginous melanoma

Acral lentiginous melanoma is a subclass of cutaneous melanoma. However, cutaneous melanocytes giving rise to acral melanoma are located at hairless acral locations of the skin, namely the palms, the soles, and underneath nails (Piliang, 2011) (Figure 9b). Similar to mucosal melanoma, activating alterations affecting the *KIT* locus are often found in acral melanoma (Garrido and Bastian, 2010) (Figure 11). Acral lentiginous melanoma, as much as mucosal and uveal melanoma, arises at areas of the body with little exposure to sunlight. Indeed, the UV-induced mutational burden is negligible in these

melanomas in great contrast to cutaneous melanoma of hair-bearing skin. In agreement, drivers of acral and mucosal melanoma are frequently activated through large scale chromosomal rearrangements rather than UV-induced point mutations (Furney et al., 2012; 2013; 2014).

3.3.2. Cutaneous melanoma epidemiology and risk factors

5% of all new cancer cases registered in the United States in 2013 were estimated to be cutaneous malignant melanoma events. Over the last decades, cutaneous melanoma incidence rates have increased yearly about 2.5% in males and 3.9% in females. Thus, cutaneous melanoma is the most rapidly escalating cancer. Men are more susceptible to develop cutaneous melanoma than women (Curado et al., 2007; Siegel et al., 2013). Apart from gender, a number of risk factors are associated with melanoma susceptibility. For instance, skin, hair, and eye color correlate with melanoma risk, such as persons with fair skin or red hair are more prone to develop melanoma. Familial melanoma history is another risk factor, mostly due to inactivating germ line mutations in the *CDKN2A* locus (Gandini et al., 2005c; Goldstein and Tucker, 2001). Presence of cutaneous nevi, benign melanocytic lesions with the potential to progress into malignant melanoma, also implies an increased risk (Gandini et al., 2005a). The highest risk, however, comes from repetitive exposure to sunlight or UV light (e.g. tanning bench), especially when causing actinic dermatitis (Gandini et al., 2005b). Indeed, melanoma-susceptible mice exposed to UV irradiation show a considerably shortened melanoma-free survival (Viros et al., 2014), highlighting UV radiation as a leading cause and, therefore, sunlight exposure as a major risk for development of cutaneous melanoma.

3.3.3. Pathogenesis of cutaneous melanoma

UV light is divided into three components, UVA (400nm – 320nm), UVB (320nm – 290nm), and UVC (290nm – 200nm). UVC is mostly absorbed by the ozone layer of the atmosphere, while 10% of UVB and 95% of UVA reach the surface of earth (Garibyan and Fisher, 2010). Upon penetration of the skin, UVB and UVA are absorbed by photosensitive molecules. UVB is directly absorbed by DNA, which itself is photosensitive. Photochemical reactions then induce cyclobutane pyrimidine dimers, which are usually corrected through the DNA damage machinery. However, incorrect repair frequently induces

C→T and CC→TT transition mutations (Cadet et al., 2005). In contrary, upon absorption, UVA rather generates reactive oxygen species causing oxidative DNA damage, and miss-repair mostly induces G→T transversions and G→A transitions (Besaratinia and Pfeifer, 2006). In human melanocytes, accumulation of such somatic mutations in loci of critical growth regulatory genes can induce proliferation while suppressing apoptosis (Rudolph et al., 1998). These neoplastic lesions either remain benign, commonly referred to as nevi, or progress into malignant melanoma (Figure 10). Nevi can be restricted to the epidermis (junctional nevus), the dermis (dermal nevus), or overlap both (compound nevus) (Gray-Schopfer et al., 2007). Nevi typically remain at a certain size for decades without progressing into malignant melanoma through a phenomenon known as oncogene-induced senescence (Michaloglou et al., 2005; Serrano et al., 1997). Only further acquired mutations in tumor-suppressing senescence genes, such as *CDKN2A*, phosphatase and tensin homolog (*PTEN*), or *TRP53* allow benign nevi cells to acquire dysplastic features and eventually to progress into malignancy (Box and Terzian, 2008; Sharpless and Chin, 2003; Wu et al., 2003). Accordingly, mice harboring dermal, nevus-like, melanocytic hyperplasia efficiently develop malignant melanoma only when *Cdkn2a*, *Pten*, or *Trp53* is depleted (Ackermann et al., 2005; Dankort et al., 2009; Dhomen et al., 2009; Gembarska et al., 2012; Goel et al., 2009).

Although presence of nevi implies an increased risk of developing melanoma (Gandini et al., 2005a), about 70% of melanomas develop in normal skin devoid of nevi, and less than half of the nevi associated with melanomas are dysplastic. Further, nevus-associated melanomas have a similar prognosis as *de novo*-developing melanomas (Bevona et al., 2003; Lin et al., 2015). Therefore, presence of multiple nevi might rather represent a symptom of an underlying genetic predisposition or a measure for frequent UV exposure, while malignant melanomas regularly arise *de novo* from transformed melanocytes, and not, as previously proposed (Clark et al., 1984), in a serial manner from senescent nevi (Figure 10). The Clark model of melanoma progression further suggests that malignant melanoma cells first spread radially in the epidermis (melanoma *in situ*, Clark's clinical stage I), before starting to grow vertically to invade the dermis (Clark's clinical stage II). Only upon dermal invasion, melanoma cells intravasate into the blood or lymph circulation and eventually disseminate to lymph nodes (Clark's clinical stage III) and to distant organs (Clark's clinical stage IV) (Balch et al., 2001; Clark et al., 1984) (Figure 10). Indeed, primary melanoma thickness represents the most important prognostic factor for patients. 5-year survival rate is highly decreased for patients bearing vertically growing lesions that reach reticular dermis or subcutis (Breslow depth > 4mm) in comparison to patients with melanoma *in situ* (Balch et al., 2001; Breslow,

1970). Accordingly, metastatic spread to sentinel lymph nodes correlates with Breslow depth of primary melanomas (Cadili and Dabbs, 2010).

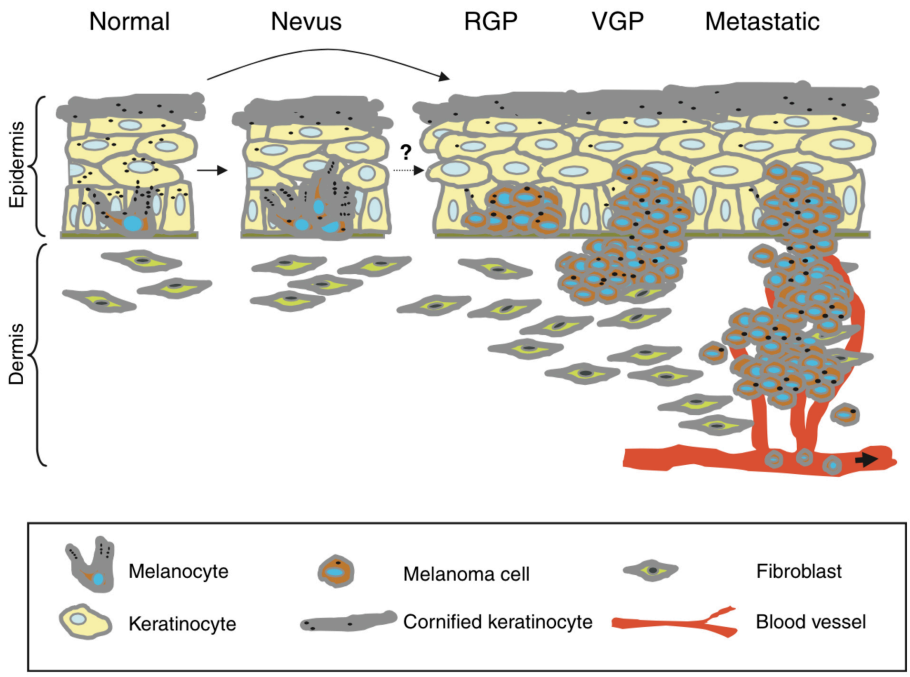

Figure 10 | The Clark model for melanoma progression. According to the Clark model for melanoma progression, an epidermal melanocyte first undergoes a neoplastic transformation, which gives rise to a benign nevus. Most nevi remain benign. Rarely, a nevus progresses into malignant metastatic melanoma through a series of events. These include radial tumor expansion followed by vertical invasion into the dermis and metastasis to distant organs. However, not every melanoma closely follows the Clark's course of events. A melanocyte may directly progress into a malignant tumor. Furthermore, metastases arising from both benign nevi and radially growing melanomas have been observed. RGB, radial growth phase; VGB, vertical growth phase (adapted from: Gaggioli and Sahai, 2007).

However, not all melanomas closely follow Clark's course of events. Some stage I melanomas directly metastasize bypassing a vertical growth phase (Haqq et al., 2005; Lomuto et al., 2004; Taran and Heenan, 2001), and circulating tumor cells have been measured in the peripheral blood of patients with radially growing melanoma (Brownbridge et al., 2001). Similarly, even benign nevus cells have been detected in lymph nodes (Ridolfi et al., 1977; Shenoy et al., 1987). This implies an adoption of disseminating features much prior to the progression into an advanced primary melanoma. In accordance, for a considerable number of metastatic melanoma patients (3.2%), a primary cutaneous tumor is untraceable (Kamposioras et al., 2011). However, these "melanomas of unknown primary" share a UV-typical mutational signature, suggesting an origin from UV-exposed cutaneous melanocytes

(Dutton-Regester et al., 2013). Thus, transformed melanocytes of early neoplasia regularly achieve the potential to disseminate throughout the body and to grow at distant sites. This exceptional metastatic capacity appears reminiscent of the excessive migratory behavior of the NC, the embryonic origin of melanocytes (3.2. The neural crest and its derivatives). Indeed, multiple transcription factors and signaling pathways known to regulate NCSC and melanocyte development have been connected to melanomagenesis and metastasis and will be discussed below (3.3.6. Cutaneous melanoma-relevant transcription factors and signaling pathways; 3.3.7. NCSC features in cutaneous melanoma). The aggressive metastasizing nature of melanoma becomes apparent in severely reduced 5-year patient survival once distant metastases are present (4%) in comparison to stage I and II patients (84%) (Curado et al., 2007; Siegel et al., 2013), which stresses the importance of especially investigating mechanisms involved in metastatic spread of cutaneous melanoma.

3.3.4. Molecular pathogenesis: oncogenic drivers of cutaneous melanoma

The series of events from neoplastic proliferation of melanocytes in the epidermis to distant metastasis is usually initiated through the acquirement of driver mutations in loci of proto-oncogenes. The most prevalent melanoma-driving signal transduction pathway is the MAPK pathway, such as the majority of nevi and melanomas (~95%) harbor activity-enhancing oncogenic alterations in loci of MAPK members (Hodis et al., 2012; Krauthammer et al., 2012; Sullivan and Flaherty, 2013; Vidwans et al., 2011). Canonical MAPK signaling is initialized through RTKs (e.g. KIT), which activate RAS (HRAS, KRAS, NRAS), a membrane-bound GTPase. The intracellular MAPK cascade then functions through sequential phosphorylation of each kinase, such as RAS phosphorylates v-Raf murine sarcoma viral oncogene homologs (ARAF, BRAF, CRAF), RAF phosphorylates mitogen-activated protein kinase kinase (MEK), and MEK phosphorylates mitogen-activated protein kinase (ERK). ERK translocates to the nucleus and interacts with transcription factors to regulate key cellular events, such as survival and proliferation (Sullivan and Flaherty, 2013; Vidwans et al., 2011) (Figure 11).

3.3.4.1. Activating alterations affecting the *BRAF* locus

A majority of cutaneous melanomas (~60%) and most acquired nevi (~80%) harbor activating *BRAF* mutations, particularly the $BRAF^{V600E}$ point mutation (Curtin et al., 2005; Davies et al., 2002; Hodis et

al., 2012; Krauthammer et al., 2012; Omholt et al., 2003; Pollock et al., 2003) (Figure 11). The V600E amino acid substitution allows BRAF to bypass the inhibitory effects of negative feedback regulation by ERK, thus $BRAF^{V600E}$ remains constantly active conferring its oncogenic function (Davies et al., 2002; Wan et al., 2004; Wellbrock et al., 2004). In line with these findings, the kinase domain of BRAF has been reported to be fused in frame to N-terminal partners through genomic rearrangements, thus depleting the auto-inhibitory N-terminal domain of BRAF and resulting in an enhanced kinase activity similar to $BRAF^{V600E}$ (Botton et al., 2013). The uniform appearance of $BRAF^{V600E}$ in early melanomas and benign nevi suggests that the acquirement of $BRAF^{V600E}$ is a clonal, key-driving event in melanomagenesis (Omholt et al., 2003; Pollock et al., 2003; Yeh et al., 2013).

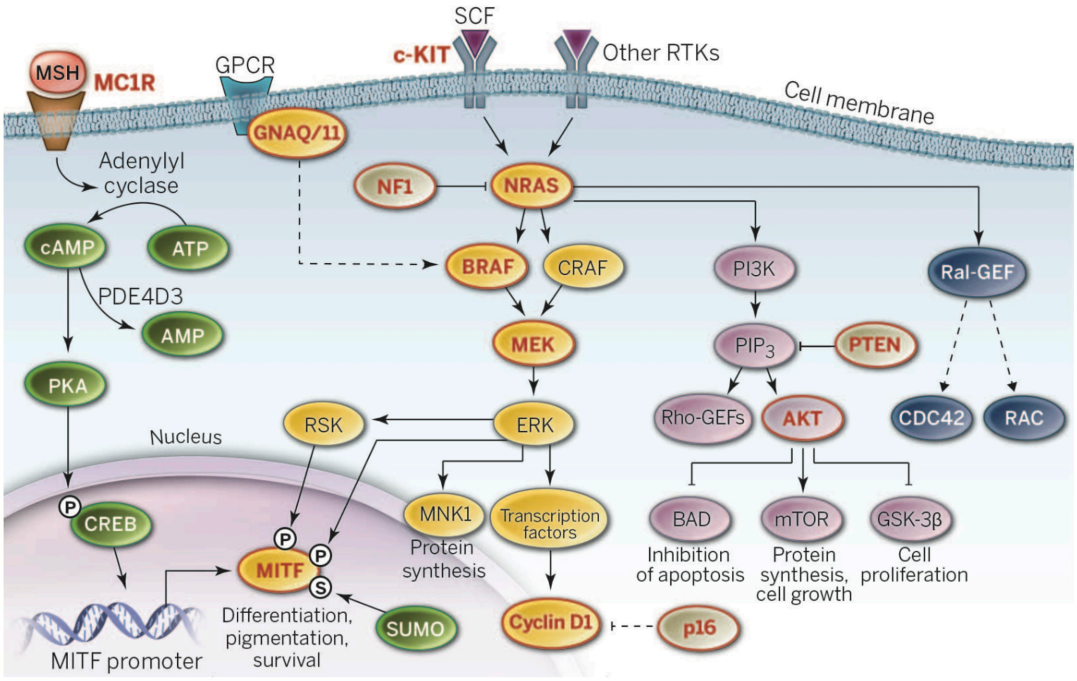

Figure 11 | Relevant signaling pathways in malignant melanoma. RTKs activate RAS family members, which signal through effector proteins, such as RAF kinases. RAF further activates a signaling cascade including MEK and ERK. Apart from MAPK, RAS also activates PI3K, which signals through AKT and mTOR. In the vast majority of cutaneous melanomas, MAPK signaling is constitutively active. Most frequent are oncogenic mutations affecting either *BRAF* (~60%) or *NRAS* (~20%). Furthermore, activating mutations affect *HRAS* and *KRAS* (~2%), *CRAF* and *MEK* (~1%), *KIT* (~6%), and *GNAQ* / *GNA11* (~2%). *KIT* alterations mostly appear in mucosal and acral lentiginous melanomas, while *GNAQ* / *GNA11* mutations are typical for uveal melanoma. Simultaneously inactivating alterations in *CDKN2A* (p16) (~85%), *PTEN* (~70%), and *NF1* (~4%) are frequent. Notably, *NF1* loss is a major cause of neurofibromatosis, a syndrome arising from peripheral glia or nerves that frequently progresses into MPNSTs. MITF is the master transcriptional regulator of melanocytes and *MITF* overexpression has been linked to melanoma growth. In contrast, MITF reduction promotes invasion and metastatic progression of melanoma. MPNST, malignant peripheral nerve sheath tumor; RTK, receptor tyrosine kinase (adapted from: Lo and Fisher, 2014).

Indeed, expression of $BRAF^{V600E}$ is sufficient to transform immortalized melanocytes into tumorigenic cells (Wellbrock et al., 2004), and expression of $B\text{-}Raf^{V600E}$ in the melanocytic lineage of adult mice induces dermal hyperplasia reminiscent of human nevi (Dankort et al., 2009; Dhomen et al., 2009; Goel et al., 2009). In agreement with oncogenic $BRAF^{V600E}$-provoked senescence (Michaloglou et al., 2005), $B\text{-}Raf^{V600E}$-induced murine nevi mostly remain benign. Only upon loss of tumor suppressors, such as *Cdkn2a*, *Pten*, or *Trp53*, dermal hyperplasia consistently progresses to metastatic melanoma (Dankort et al., 2009; Dhomen et al., 2009; Goel et al., 2009), confirming somatic acquirement of $BRAF^{V600E}$ as initial melanoma-driving event.

3.3.4.2. Activating alterations affecting the *NRAS* locus

Besides $BRAF^{V600E}$, activating *NRAS* point mutations (mostly $NRAS^{Q61K/L/R}$, few $NRAS^{G12D/V}$) are recurrent in melanoma (~20%) and predominant in congenital nevi (~80%), but mostly absent in acquired nevi (Albino et al., 1984; Bauer et al., 2007; Charbel et al., 2014; Curtin et al., 2005; Hodis et al., 2012; Kinsler et al., 2013; Krauthammer et al., 2012; Omholt et al., 2003). Notably, the majority of familial melanoma patients (~95%) harbor $NRAS^{Q61K/R}$ (Eskandarpour et al., 2003). According point mutations in the *NRAS* homologs *HRAS* and *KRAS* are also recurrent in melanoma (~2%) and in Spitz nevi (Bastian et al., 2000; Hodis et al., 2012; Krauthammer et al., 2012; Milagre et al., 2010) (Figure 11). The Q61K/L/R amino acid substitutions lock RAS into a GTP-bound, activated conformation, whereas G12D/V substitutions render RAS insensitive to GTP-dephosphorylating mechanisms, both allowing RAS to constantly signal through MAPK (Buhrman et al., 2007; Der et al., 1986; Krengel et al., 1990). $NRAS^{Q61K/L/R}$ has been found throughout all stages of melanoma progression including benign congenital nevi indicating that $NRAS^{Q61K/L/R}$ might be an early melanoma driver comparable to $BRAF^{V600E}$ (Bauer et al., 2007; Charbel et al., 2014; Kinsler et al., 2013; Omholt et al., 2003; 2002). Indeed, mutant *HRAS*, *KRAS*, and *NRAS* transform immortalized melanocytes into tumor-forming cells (Whitwam et al., 2007). Accordingly, $H\text{-}Ras^{G12V}$, $K\text{-}Ras^{G12V}$, $N\text{-}Ras^{G12D}$, and $N\text{-}Ras^{Q61K}$ promote dermal hyperplasia in mice and, upon depletion of *Cdkn2a* or *Trp53*, metastasizing melanoma (Ackermann et al., 2005; Bardeesy et al., 2001; Chin et al., 1997; 1999; Gembarska et al., 2012; Huijbers et al., 2006; Milagre et al., 2010; Pedersen et al., 2013), establishing somatic acquirement of oncogenic *RAS* mutations as initial melanoma-driving event.

Apart from mutant *BRAF* (~60%), *NRAS* (~20%), and *HRAS* / *KRAS* (~2%), activating mutations in *CRAF* and *MEK* (~1%), *KIT* (~6%), and *GNAQ* / *GNA11* (~2%) as well as inactivating alterations affecting *NF1* (~4%) occur in diverse melanoma subtypes (Garrido and Bastian, 2010; Hodis et al., 2012; Krauthammer et al., 2012; Van Raamsdonk et al., 2009; 2010). In sum, about 95% of all malignant melanomas present enhanced MAPK signaling, emphasizing targeted MAPK inhibition as a valid strategy for melanoma therapy (Sullivan and Flaherty, 2013; Vidwans et al., 2011) (Figure 11).

3.3.5. Molecular pathogenesis: tumor suppressors in cutaneous melanoma

MAPK signaling-enhancing mutations allow a first expansion of transformed melanocytes. However, these hyperplastic cells usually senesce *in vitro* and *in vivo*, while malignant progression requires loss of tumor suppressors (Ackermann et al., 2005; Dankort et al., 2009; Dhomen et al., 2009; Gembarska et al., 2012; Goel et al., 2009; Michaloglou et al., 2005; Serrano et al., 1997).

3.3.5.1. *CDKN2A* as tumor suppressor

For instance, loss-of-function alterations affecting the *CDKN2A* locus frequently occur in melanoma (~60%) as much as in a plethora of different cancers, and the promoter of *CDKN2A* is methylated in a considerable amount of melanomas (~20%), resulting in repression of *CDKN2A* transcription. Therefore, the proteins encoded by *CDKN2A*, p14 and p16, are absent in more than 85% of malignant melanomas (Hodis et al., 2012; Jonsson et al., 2010; Kamb et al., 1994; Krauthammer et al., 2012; Nobori et al., 1994; Venza et al., 2015). p16 is an inhibitor of cyclin-dependent kinase 4 (CDK4), itself promoting G1- to S-phase cell cycle progression (Sharpless and Chin, 2003). Interestingly, *CDK4* appears to be amplified in melanoma (Hodis et al., 2012; Krauthammer et al., 2012; Muthusamy et al., 2006) (Figure 11). Loss of p16 (and CDK4 upregulation) impedes a potential DNA miss match-induced cell cycle arrest, which leads to genomic instability and eventually results in malignancy (Sharpless and Chin, 2003). This becomes apparent in formation of diverse tumors in *Cdkn2a* knockout mice (Serrano et al., 1996). In human melanocytes, depletion of *CDKN2A* is sufficient to overcome $BRAF^{V600E}$- and $HRAS^{G12V}$-induced senescence (Michaloglou et al., 2005; Serrano et al., 1997), while inactivation of *Cdkn2a* in melanocytic hyperplasia-harboring mice promotes melanomagenesis (Ackermann et al., 2005;

Bardeesy et al., 2001; Chin et al., 1997; Dhomen et al., 2009; Goel et al., 2009; Huijbers et al., 2006), establishing *CDKN2A* as a major tumor suppressor in melanoma.

3.3.5.2. *PTEN* as tumor suppressor

Comparable to *CDKN2A*, a considerable number of melanomas (~70%) harbor inactivating alterations or DNA methylation-mediated silencing of the *PTEN* locus (Guldberg et al., 1997; Hodis et al., 2012; Krauthammer et al., 2012; Madhunapantula and Robertson, 2009; Tsao et al., 1998; Zhou et al., 2000). PTEN dephosphorylates, thus inactivates, phosphatidylinositol (3,4,5)-trisphosphate (PIP_3), which is a cue of the phosphoinositide 3-kinase (PI3K) pathway. RTKs activate PI3K, which phosphorylates PIP_2 to PIP_3. PIP_3 then triggers activation of AKT, a regulator of key cellular processes including proliferation and survival. AKT confers its roles, among others, through activation of mechanistic target to rapamycin (mTOR) (Madhunapantula and Robertson, 2009; Wu et al., 2003) (Figure 11). Accordingly, copy gains spanning *AKT3* and activating point mutations in *AKT3* have been reported in melanoma (Davies et al., 2008; Stahl et al., 2004). Therefore, loss of *PTEN* (and AKT3 upregulation) allows constant PI3K signaling contributing to malignancy, which becomes apparent in formation of diverse neoplasms in mice lacking a *Pten* allele (Di Cristofano et al., 1998; Podsypanina et al., 1999). Interestingly, *PTEN* alterations strongly correlate with $BRAF^{V600E}$ mutations, while PTEN inactivation and *NRAS* mutations are mutually exclusive, presumably because mutant NRAS, besides MAPK, also activates PI3K signaling (Goel et al., 2006; Hodis et al., 2012; Krauthammer et al., 2012; Tsao et al., 2000; 2004; Vidwans et al., 2011) (Figure 11). Accordingly, inactivation of *Pten* promotes melanomagenesis in mice with $B\text{-}Raf^{V600E}$-induced hyperplasia (Dankort et al., 2009), establishing *PTEN* as an important tumor suppressor in $BRAF^{V600E}$ melanoma.

3.3.5.3. *TRP53* as tumor suppressor

Various signals activate TRP53, such as DNA damage and oncogenic, genotoxic, and oxidative stress, which leads to the induction of pro-apoptotic, cell cycle-regulative, or senescence genes. Therefore, during tumor evolution, this selective pressure results in depletion of *TRP53* in most cancers (Box and Terzian, 2008; Vousden and Prives, 2009). In contrast, deleterious *TRP53* alterations only appear in a relatively small cohort of melanomas (~20%). Interestingly, mutations affecting *TRP53* in cutaneous melanoma show UV-typical patterns (Hocker and Tsao, 2007; Hodis et al., 2012; Krauthammer et al., 2012), and UV irradiation of mice induces loss-of-function mutations in *Trp53* resulting in accelerated melanoma formation (Viros et al., 2014). Apart from mutational burden, loss of TRP53-upstream

activators, such as p14 (encoded by *CDKN2A*), is a frequent event in human melanoma (3.3.5.1. *CDKN2A* as a tumor suppressor). Similarly, TRP53 inhibitors, such as the E3 ubiquitin-protein ligases mouse double minute homologs (MDM2, MDM4), are regularly upregulated in malignant melanoma (Gembarska et al., 2012; Marine and Jochemsen, 2005; Muthusamy et al., 2006; Polsky et al., 2001). In melanoma-prone mice, overexpression of *Mdm4* significantly accelerates tumor development, while *Mdm4* depletion is sufficient to prevent melanomagenesis (Gembarska et al., 2012; Terzian et al., 2010). Similarly, depletion of *Trp53* enhances melanocyte transformation *in vitro* and tumorigenesis in mouse models of melanoma (Bardeesy et al., 2001; Gembarska et al., 2012; Goel et al., 2009; Serrano et al., 1997). Thus, TRP53 inactivation through various mechanisms is a key event during melanomagenesis.

3.3.6. Transcription factors and signaling pathways relevant for cutaneous melanoma

Gain of oncogenic driver mutations and loss of tumor suppressors represents key events for melanoma induction. Apart from these essential genetic aberrations, a plethora of transcription factors and signaling pathways known to regulate NCSC and melanocyte development are also involved in further promoting melanoma formation and metastatic progression.

3.3.6.1. SOX10 and SOX9

For instance, the transcription factor SOX10 is not only relevant for NCSC maintenance and adult melanocyte homeostasis (3.2.5.2. SOX10), but also plays pivotal roles in melanomagenesis. SOX10 is highly expressed in cells of nevi and malignant melanomas (Agnarsdóttir et al., 2010; Bakos et al., 2010; Flammiger et al., 2009; Mohamed et al., 2013; Nonaka et al., 2008; Shakhova et al., 2012; Shin et al., 2012), while Sox10 levels are increased in the melanocytic lineage of melanoma-developing mice in comparison to melanocytes of *wt* animals (Shakhova et al., 2012). Depletion of *SOX10* in human melanoma cells induces apoptosis and cell cycle arrest, and *Sox10* haploinsufficiency counteracts melanoma formation in mice (Cronin et al., 2013; Graf et al., 2014; Shakhova et al., 2012). Interestingly, *SOX10* silencing in melanoma cells results, apart from interfering with cell cycle and survival, in induction of a mesenchymal gene network including *SOX9* (Shakhova et al., 2012; 2015). This appears highly reminiscent of the Sox10-Sox9 interplay during mesectodermal fate acquisition of the NC (John et al., 2011). In melanoma, upregulation of such mesenchymal genes might reflect acquirement of EMT-typical features including increased cell motility and metastasis formation. Indeed, melanoma cell lines

with an intrinsic capacity of invading extra cellular matrix (ECM)-mimicking collagen layers have low SOX10 levels and express more SOX9 than cell lines devoid of this capacity (Cheng et al., 2015; Shakhova et al., 2015), while *SOX9* overexpression in invasion-poor cells decreases SOX10 and induces invasive capacity. Comparably, after intravenous (i.v.) transplantation into mice, murine B16-F1 melanoma cells with a negligible metastasizing potential only form lung nodules following overexpression of *Sox9* (Cheng et al., 2015). In melanoma-developing mice, *Sox9* ablation rescues *Sox10* deficiency-induced tumor regression resulting in normal melanoma growth (Shakhova et al., 2015). These findings suggest a reciprocal action in between SOX10 and SOX9. Indeed, SOX10 and SOX9 transcriptionally repress each other in an antagonistic manner (Cheng et al., 2015; Shakhova et al., 2015). Likely, the differential expression of SOX10 and SOX9 allows a given melanoma to tightly regulate growth versus dissemination and metastasis. In melanoma-harboring mice, temporal Sox10 reduction might, therefore, induce dissemination of melanoma cells from primary tumor sites resulting in colonization of distant organs, while *Sox9* depletion might suffice to prevent metastasis.

3.3.6.2. MITF

Comparably to Sox10 function, Mitf is highly relevant for melanocyte biology (3.2.5.3. PAX3 and MITF), and increasing evidence connects MITF to melanomagenesis. MITF is expressed in a majority of melanomas (Agnarsdóttir et al., 2012; King et al., 1999; Nazarian et al., 2010b; O'Reilly et al., 2001; Shakhova et al., 2012), while point mutations affecting *MITF* are substantial and frequently elevate MITF activity (Cronin et al., 2009). For instance, $MITF^{E318K}$ results in altered transcriptional activity of MITF and predisposes to familial and sporadic melanoma development (Bertolotto et al., 2011; Yokoyama et al., 2011). Comparably, the chromosomal region harboring *MITF* is amplified in a subset of melanomas (~20%), while elevated MITF levels, in synergy with activated MAPK signaling, promote growth of melanoma cells (Du et al., 2004; Garraway et al., 2005; Hodis et al., 2012; Stark and Hayward, 2007) (Figure 11). However, distant metastases show a reduced frequency in MITF positivity (Nazarian et al., 2010b; Shakhova et al., 2012), and advanced melanoma lesions harbor melanocytic subpopulations completely devoid of MITF (Goodall et al., 2008). Furthermore, reduced MITF levels correlate with increased invasive capacity of melanoma cells (Hoek et al., 2008; 2006). This indicates a possible role of MITF loss in promoting metastasis, in analogy to the low SOX10 / high SOX9-associated invasive behavior of melanoma cells (Cheng et al., 2015; Shakhova et al., 2015). Indeed, *MITF* silencing in human melanoma cell cultures results in diminished growth but increases invasion in collagen layers

(Carreira et al., 2006; Hoek et al., 2008), while depletion of *Mitf* in murine B16-F10 melanoma cells enhances metastatic potential after i.v. transplantation (Cheli et al., 2012). Likely, during melanoma growth and metastasis, temporal *MITF* repression follows the dynamic SOX10-SOX9 interplay, given that *MITF* is a direct transcriptional target of SOX10 (Bondurand et al., 2000; Potterf et al., 2000). Alternatively, it was proposed that MITF reduction upon gain of invasive capacity might be triggered through a PAX3-driven genetic program that antagonizes MITF (Eccles et al., 2013). PAX3 itself is expressed in nevi and malignant melanomas (Gershon et al., 2005; He et al., 2010), and *PAX3* silencing enhances MITF expression *in vitro* (He et al., 2011). However, this appears conflicting in the frame of MITF-PAX3 synergistic roles in co-regulating embryonic melanoblast specification and melanocyte homeostasis (Steingrimsson et al., 2004). Independently of the cause for differential MITF expression along melanomagenesis, an MITF level-elevating chemical compound was demonstrated to be sufficient to prevent melanoma metastases in mice (Sáez-Ayala et al., 2013). However, given the role of MITF in promoting melanoma growth (Du et al., 2004; Garraway et al., 2005), such MITF-enhancing treatments had to be implicitly combined with anti-proliferation therapeutics in order to circumvent adverse clinical outcome.

3.3.6.3. WNT signaling

WNT signaling controls melanoblast specification as much as adult MSC homeostasis (3.2.5.4 WNT signaling). Likewise, WNT signaling has pivotal roles in melanomagenesis. In human nevi and primary melanoma, CTNNB1 is frequently expressed (Bachmann et al., 2005; Kageshita et al., 2001; Maelandsmo et al., 2003; Omholt et al., 2001). Functionally, CTNNB1 is involved in, among others, activating *MITF* (Damsky et al., 2011; Widlund et al., 2002) and suppressing *CDKN2A* (Delmas et al., 2007), thus overcoming oncogene-induced senescence and promoting melanoma growth. Accordingly, melanoma-prone mice expressing stabilized *Ctnnb1* show decreased tumor-free survival, while *Ctnnb1* depletion delays melanoma formation (Damsky et al., 2011; Delmas et al., 2007; Gallagher et al., 2013). However, high CTNNB1 levels in human melanoma correlate with good patient prognosis (Bachmann et al., 2005; Chien et al., 2009; Gould Rothberg et al., 2009), while expression and especially nuclear localization of CTNNB1 is reduced in metastases (Bachmann et al., 2005; Kageshita et al., 2001; Maelandsmo et al., 2003). Furthermore, intrinsically low CTNNB1 levels correlate with increased invasive capacity of melanoma cells, and *CTNNB1* silencing reduces MITF and induces invasion in collagen layers (Arozarena et al., 2011). Thus, WNT signaling is required for melanoma growth, but the

pathway is down-regulated to suppress melanocytic genes including *MITF*, allowing dissemination and metastasis. Indeed, *Ctnnb1* depletion in melanoma-developing mice promotes formation of amelanotic tumors devoid of Mitf. Against expectation, these mice do not present increased metastasis formation, albeit animals were not specifically screened for occurrence of unpigmented nodules (Damsky et al., 2011). Contrariwise, expression of the stabilized *Ctnnb1* allele in both *B-Raf*^{V600E} *Pten*-deficient and *N-Ras*^{Q61K} mice not only promotes primary tumors, but also metastasis (Damsky et al., 2011; Gallagher et al., 2013). This is unexpected in the frame of stabilized Ctnnb1-induced *Mitf* expression, since high MITF levels rather connect to melanoma growth including a more differentiated / pigmented tumor status. However, stabilized Ctnnb1 might differentially regulate target genes beyond *Mitf* that would be responsible for driving metastasis. Indeed, stabilized Ctnnb1 activates protein peptidyl-prolyl cis/trans isomerase NIMA-interacting 1 (*Pin1*), which enhances PI3K pathway through regulation of AKT (Damsky et al., 2011; Liao et al., 2009). In the frame of already active PI3K due to *Pten* loss (Damsky et al., 2011) or N-Ras^{Q61K}-PI3K axis (Gallagher et al., 2013), Pin1-induced additional enhancement of PI3K signaling might overwrite the Mitf-dependent melanoma growth program and promote metastasis. In contrast, upon stabilized *Ctnnb1* expression, melanoma-prone *B-Raf*^{V600E} mice with intact *Pten* (no enhanced PI3K signaling) develop highly differentiated melanomas devoid of metastasis (Damsky et al., 2011). Therefore, in a PI3K pathway-dependent melanoma, WNT signaling might promote metastatic progression, whereas in a PI3K-independent context, temporal reduction of WNT signaling might support melanoma metastasis.

3.3.6.4. TGFβ signaling

In normal epithelial, endothelial, and hematopoietic cells, TGFβ functions as powerful tumor suppressor in prohibiting uncontrolled proliferation. Along tumorigenesis, however, differential transcriptional responses to TGFβ signaling convert TGFβ from a tumor suppressor to a promoter of tumor growth and especially tumor stemness, metastasis, and chemoresistance (Oshimori et al., 2015; Tian et al., 2011; Xu et al., 2015b). Accordingly, TGFβ suppresses proliferation of untransformed human melanocytes (Krasagakis et al., 1999; Rodeck et al., 1994; 1999), and Tgfβ signaling is required for quiescence of MSCs *in vivo* (Nishimura et al., 2010; Tanimura et al., 2011). In contrast, melanoma-derived cell cultures are resistant to TGFβ-induced senescence (Krasagakis et al., 1999; Rodeck et al., 1994; 1999). However, exposure of melanoma cells to TGFβ induces an EMT through activation of EMT transcription factors, such as *SNAI1*, *TWIST1*, and GLI family zinc finger 2 (*GLI2*) (Alexaki et al., 2010;

Javelaud et al., 2011; Menon et al., 2013), as well as novel metastatic progression genes, such as TGFβ-Induced (*TGFBI*) (Lauden et al., 2014). Simultaneously, TGFβ exposure suppresses *MITF* (Hoek et al., 2006; Javelaud et al., 2011; Pierrat et al., 2012; Schlegel et al., 2015). TGFβ-induced EMT in melanoma appears reminiscent of TGFβ-dependent mesectodermal specification of the embryonic NC (John et al., 2011). Whether this induction of EMT also similarly functions through *SOX10* suppression and *SOX9* expression, remains to be clarified. *In vitro*, TGFβ-induced EMT is associated with invasion of melanoma cells in collagen layers (Alexaki et al., 2010; Mohammad et al., 2011; Qu et al., 2014; Schlegel et al., 2015), while in mice, interference with SMAD2/3 activity prevents outgrowth of i.v. transplanted melanoma cells at distant sites (Divito et al., 2010; Javelaud et al., 2005; 2007; Mohammad et al., 2011). Similarly, in melanoma-developing mice, *Smad4* depletion efficiently counteracts melanomagenesis, while depletion of the inhibitory *Smad7* enhances Smad2/3 activation and accelerates melanoma cell dissemination from primary tumor sites, resulting in distant metastases. However, deletion of *Tgfbr2* has no effect on metastatic melanoma progression (Zingg and Tuncer, in preparation). Thus, activated Smad2/3-Smad4 axis is essential for melanoma metastasis. *In vivo*, Tgfβ, which signals through Tgfbr2, might however not be the major *in situ* promoter of Smad2/3 activation. Other signaling cues, such as activin A (INHBA) or nodal growth differentiation factor (NODAL), can activate SMAD2/3, although through different receptors than TGFBR2 (Moustakas and Heldin, 2009). Indeed, NODAL expression in melanoma correlates with an aggressive metastasizing phenotype (Postovit et al., 2008; Seftor et al., 2014; Topczewska et al., 2006; Yu et al., 2010). Comparably, in B16-F10 cells, Nodal induces *Snai1*-dependent EMT including increased invasive capacity, and upon subcutaneous (s.c.) transplantation, inhibition of Nodal signaling diminishes metastasis to distant organs (Fang et al., 2013). Therefore, TGFβ has the potential to promote melanoma EMT *in vitro*, while NODAL might be the *in situ* ligand responsible for melanoma dissemination and metastasis formation *in vivo*.

3.3.7. NCSC features in cutaneous melanoma

Malignant cutaneous melanoma is a highly heterogeneous cancer. Intratumoral heterogeneity becomes apparent on a genomic level (Anaka et al., 2013; Ennen et al., 2014; Shi et al., 2012a), but also by phenotypic appearance. Apart from expressing melanocytic markers, melanomas are often composed of cells displaying neuronal, glial, smooth muscle-like, chondrocytic, and adipocytic features (Banerjee and

Eyden, 2008; Civenni et al., 2011; Cruz et al., 2003; Laga and Murphy, 2010; Mete et al., 2010; Parente et al., 2013). This heterogeneity resembles the plethora of derivatives, which arise from the NC during embryogenesis (3.2.1. The embryonic neural crest). Therefore, it has been proposed that during tumorigenesis transformed melanocytes reacquire embryonic NCSC-resembling features, allowing these cells to diverge into heterotypic NC-like progeny. Indeed, cellular melanoma subpopulations have been identified that express stem cell markers. Functionally, these subpopulations also show cancer stem cell-like behaviors, which include high self-renewal capacity *in vitro* and enhanced tumor initiation potential upon xenotransplantation (Beck and Blanpain, 2013; Kreso and Dick, 2014).

3.3.7.1. Cluster of differentiation 271 as NCSC-like melanoma stem cell marker

For instance, the low-affinity nerve growth factor receptor cluster of differentiation 271 (CD271) labels embryonic and adult NCSCs (Bixby et al., 2002; Hagedorn et al., 1999; Kruger et al., 2002; Morrison et al., 1999; Nagoshi et al., 2008; Stemple and Anderson, 1992; Wong et al., 2006). In contrast, melanocytes do not express CD271 (Wilson et al., 2004). However, malignant melanomas retrieve positivity for CD271 in variable degrees, and CD271 positivity correlates with poor patient prognosis and disease progression (Boiko et al., 2010; Chesa et al., 1988; Civenni et al., 2011; Innominato et al., 2001; Iwamoto et al., 2001). These CD271-expressing cells are frequently devoid of melanocyte differentiation markers including MITF, pointing towards an undifferentiated subpopulation with possible stem cell features (Boiko et al., 2010). Indeed, tumor-initiating cells capable of recapitulating the phenotypic heterogeneity observed in melanoma are mostly present in the CD271-positive tumor fraction (Boiko et al., 2010; Civenni et al., 2011), while *CD271* depletion prevents melanoma initiation (Redmer et al., 2014). Therefore, CD271-positive cells might represent a melanoma subpopulation with NCSC characteristics that sustains melanoma initiation, heterogeneity, malignancy, and presumably plasticity including metastasis.

3.3.7.2. Melanoma stem cell markers beyond CD271

Apart from CD271, various stem cell markers have been identified in melanoma. The ESC pluripotency factor *SOX2* (Avilion et al., 2003; Ivanova et al., 2006) is heterogeneously re-expressed in melanoma and functionally involved in maintaining tumor initiation and in promoting melanoma cell invasion *in vitro* (Girouard et al., 2012; Laga et al., 2010; 2011; Santini et al., 2014). Interestingly, GLI2 promotes *SOX2* re-expression (Santini et al., 2014; 2012), while *MITF* is suppressed by SOX2 (Adameyko et al., 2012; Cimadamore et al., 2012), thus establishing a melanoma stemness network likely promoting EMT and

metastasis. Apart from transcription factors, both cell surface receptors CD20 and CD133, previously associated with B-cells including B-cell malignancies (Okroj et al., 2013) and HSCs (Bauer et al., 2008), respectively, define melanoma subpopulations with stem cell propensities (Fang et al., 2005; Monzani et al., 2007). Furthermore, expression of multi-drug resistance genes, such as ATP-binding cassette sub-family B members (*ABCB1/5*) or aldehyde dehydrogenase (*ALDH*), correlates with melanoma progression, and positive cells show melanoma-initiating stemness properties (Boonyaratanakornkit et al., 2010; Chartrain et al., 2012; Frank et al., 2005; Keshet et al., 2008; Luo et al., 2012b; Schatton et al., 2008; Setia et al., 2012). This highlights the likely emergence of stem cell-like subpopulations during exposure to melanoma therapeutics eventually resulting in acquired resistance and disease relapse.

3.4. Melanoma therapies

To this day, the most effective treatment for primary melanoma remains surgical excision. Similarly, sentinel lymph node biopsy followed by complete excision of affected lymph nodes enhances perspectives for patients. Even stage IV melanoma patients with oligometastatic disease show some benefit from radical tumor removal (Sosman et al., 2011; Testori et al., 2009). Besides surgery, treatment of metastatic melanoma patients has been limited to decarbazine, a DNA-alkylating chemotherapeutic agent (Eggermont and Kirkwood, 2004), or local radiotherapy, mostly to target non-resectable lesions, such as cerebral metastases (Fife et al., 2004; Testori et al., 2009). However, the ineffectiveness of these approaches becomes evidently apparent in stage IV patient's median survival of 6 to 9 months, whereas only 4% of these patients surviving beyond 5 years (Curado et al., 2007; Eggermont et al., 2014; Siegel et al., 2013). This reflects the great need for novel melanoma therapies. Recently, the landscape of melanoma therapeutics has changed spectacularly with two distinct therapeutic advancements in the areas of oncogene-targeted therapy and immunomodulation, both of which show significant survival benefits for metastatic melanoma patients (Eggermont et al., 2014; Lo and Fisher, 2014) (Figure 12).

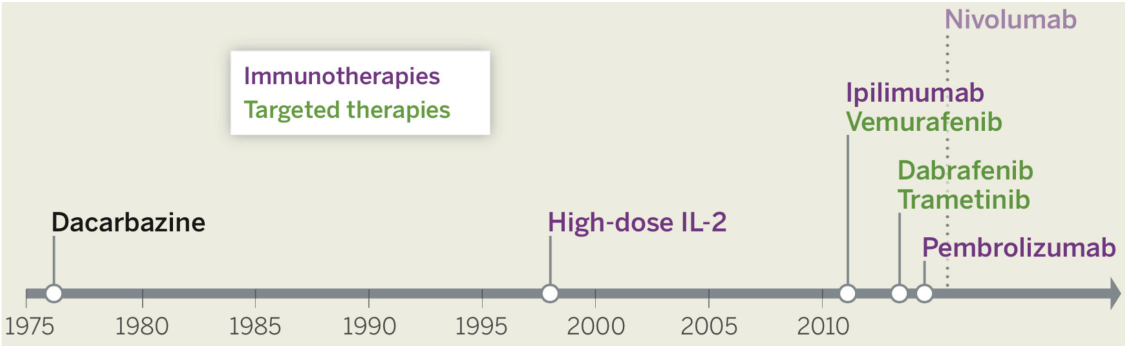

Figure 12 | Timeline of FDA-approved melanoma therapeutics. Between 1976 and 2011, decarbazine chemotherapy and high-dose IL-2 were the only FDA-approved melanoma therapeutics. Recently, the landscape of melanoma therapeutics has changed spectacularly. The novel therapeutics include MAPK signaling inhibitors and immune checkpoint blockade agents. Vemurafenib (Roche) and dabrafenib (GlaxoSmithKline) target $BRAF^{V600E}$ and were FDA-approved in 2011 and 2013, respectively. Trametinib (GlaxoSmithKline) targets MEK and its approval took place in 2013. These MAPK-inactivating drugs have profound clinical activity. However, melanoma patients frequently develop resistances resulting in progressive disease. Ipilimumab (Bristol-Myers Squibb) is a CTLA4-blocking antibody, which was FDA-approved in 2011. Pembrolizumab (Merck) and nivolumab (Bristol-Myers Squibb) are both antibodies targeting PD-1 and were approved by FDA in September and December 2014, respectively. These immune checkpoint blockade antibodies show surpassing clinical responses with tolerable side effects. Importantly, in a considerable fraction of patients, stable disease persists long after treatment discontinuation. FDA, US food and drug administration (adapted from: Lo and Fisher, 2014).

3.4.1. BRAF^{V600E}-targeting and MEK-targeting therapeutics

The identification of *BRAF^{V600E}* in a majority of melanomas and in a variety of different cancers (Davies et al., 2002; Tiacci et al., 2011) prompted intensive efforts to develop chemical compounds inhibiting RAF kinase activity. However, first-generation pan-RAF inhibitors turned out to be clinically ineffective at the maximal tolerable dose, which was defined by harsh side effects, likely due to systemic inhibition of all RAF homologs as well as PDGF and VEGF receptors (PDGFR, VEGFR) (Sullivan and Flaherty, 2013). In contrast, PLX4032 (vemurafenib, Roche) was the first RAF inhibitor with highly increased selectivity towards BRAF^{V600E} over BRAF^{WT}, ARAF, and CRAF, resulting in efficient counteraction of melanoma growth *in vitro*, in xenografts, and in patients (Bollag et al., 2010; Sala et al., 2008; Yang et al., 2010). To this day, vemurafenib and a similar BRAF^{V600E} inhibitor, GSK2118436 (dabrafenib, GlaxoSmithKline), have shown unprecedented clinical activity in melanoma patients with mutant *BRAF* (Chapman et al., 2011; Flaherty et al., 2010; Hauschild et al., 2012) (Figure 12). In order to block MAPK signaling downstream of BRAF, efforts have also led to the development of MEK inhibitors, such as GSK1120212 (trametinib, GlaxoSmithKline; Gilmartin et al., 2011) and MEK162 (Novartis; Ascierto et al., 2013). These inhibitors also demonstrate clinical benefits for *BRAF^{V600E}* melanoma patients, albeit with lower response rates than vemurafenib and dabrafenib (Ascierto et al., 2013; Flaherty et al., 2012b) (Figure 12). Importantly, vemurafenib and dabrafenib efficiently inhibit MAPK signaling only in *BRAF*-mutant melanoma, while *BRAF^{WT}* melanomas including *RAS*-mutated tumors paradoxically upregulate MAPK signaling upon RAF inhibition. Mutant RAS does not signal through BRAF, but through CRAF, which is negligibly sensitive to BRAF^{V600E}-targeting drugs. Moreover, drug-bound BRAF^{WT} serves as a scaffold in recruiting CRAF to RAS, thus enhancing MAPK signaling through CRAF (Hatzivassiliou et al., 2010; Heidorn et al., 2010; Poulikakos et al., 2010). This phenomenon becomes apparent in highly increased tumor and metastases formation in melanoma-prone *K-Ras^{G12D}* mice, either upon genetic alteration of *B-Raf*, thus mimicking drug-bound BRAF, or upon vemurafenib treatment (Heidorn et al., 2010; Pedersen et al., 2014; Sanchez-Laorden et al., 2014). Comparably, vemurafenib treatment of *BRAF^{V600E}*-mutant melanoma patients occasionally stimulates proliferation and dysplastic features of before-benign nevi. These nevi usually turn out to be *BRAF^{WT}* and *NRAS^{Q61K}*-positive, pointing towards the paradoxical MAPK stimulation (Zimmer et al., 2012). MEK inhibition represents an alternative strategy to target MAPK-activated, but *BRAF^{WT}* melanomas (e.g. *NRAS^{Q61K}*). However, MEK inhibitors

have shown only partial efficacy in *BRAF*^{WT} melanomas (Sullivan and Flaherty, 2013), possibly due to the ability of RAS to signal through diverse pathways aside of MAPK (Kwong et al., 2012).

3.4.2. MAPK-dependent mechanisms in MAPK inhibitor resistance

Although anti-melanoma effects of RAF and MEK inhibitors are considerable, intrinsic and mostly acquired resistances limit the therapeutic benefits of these approaches (Ascierto et al., 2013; Flaherty et al., 2010; 2012b; Sosman et al., 2012). Concomitant treatments with RAF and MEK inhibitors have further improved clinical benefits for *BRAF*-mutant melanoma patients, and have been thought of minimizing acquired resistances. However, patients show progressive disease even under these combo treatments (Flaherty et al., 2012a; Larkin et al., 2014; Long et al., 2014; Robert et al., 2015a). Resistance frequently results from re-established MAPK signaling, which is acquired through various mechanisms (Figure 13). Genetic alterations lead to *BRAF* splicing variants and amplification (Poulikakos et al., 2011; Shi et al., 2014; Van Allen et al., 2014) (Figure 13e), *de novo* mutations in *RAS*, *MEK*, or *ERK* loci (Emery et al., 2009; Goetz et al., 2014; Nazarian et al., 2010a; Shi et al., 2014; Van Allen et al., 2014; Wagle et al., 2011) (Figure 13b-d), and *NF1* loss (Maertens et al., 2013; Van Allen et al., 2014; Whittaker et al., 2013) (Figure 13f). Besides genetic MAPK signaling reactivation, altered expression of MAPK pathway members frequently occurs during resistance, such as RTK (e.g. epithelial growth factor receptor (EGFR), FGF receptor (FGFR), or PDGFR) upregulation (Girotti et al., 2013; Lito et al., 2012; Nazarian et al., 2010a; Sun et al., 2014; Wilson et al., 2012; Yadav et al., 2012) (Figure 13h, i), enhanced expression of *BRAF, CRAF*, or *NRAS* (Johannessen et al., 2010; Montagut et al., 2008; Nazarian et al., 2010a; Shi et al., 2012b) (Figure 13g), and increased BRAF dimerization (Poulikakos et al., 2011; Rajakulendran et al., 2009). All these mechanisms allow the tumor to circumvent BRAF^{V600E} and MEK inhibition, or even to take advantage of it (e.g. upon *de novo NRAS*^{Q61K}), comparable to paradoxical MAPK enhancement upon BRAF inhibition in *NRAS*-mutant melanomas (Hatzivassiliou et al., 2010; Heidorn et al., 2010; Nazarian et al., 2010a; Poulikakos et al., 2010; Sanchez-Laorden et al., 2014). To successfully counteract resistance to BRAF or MEK inhibition, it has been proposed to vertically target MAPK pathway with ERK inhibitors, possibly in combination with MEK inhibitors (Morris et al., 2013; Rebecca et al., 2014; Van Allen et al., 2014; Wong et al., 2014). However, apart from MAPK signaling re-enhancement, a plethora of MAPK-independent resistance mechanisms to MAPK-targeted therapy

have been uncovered, which postulates only limited success for future combinatorial treatments solely targeting canonical MAPK pathway.

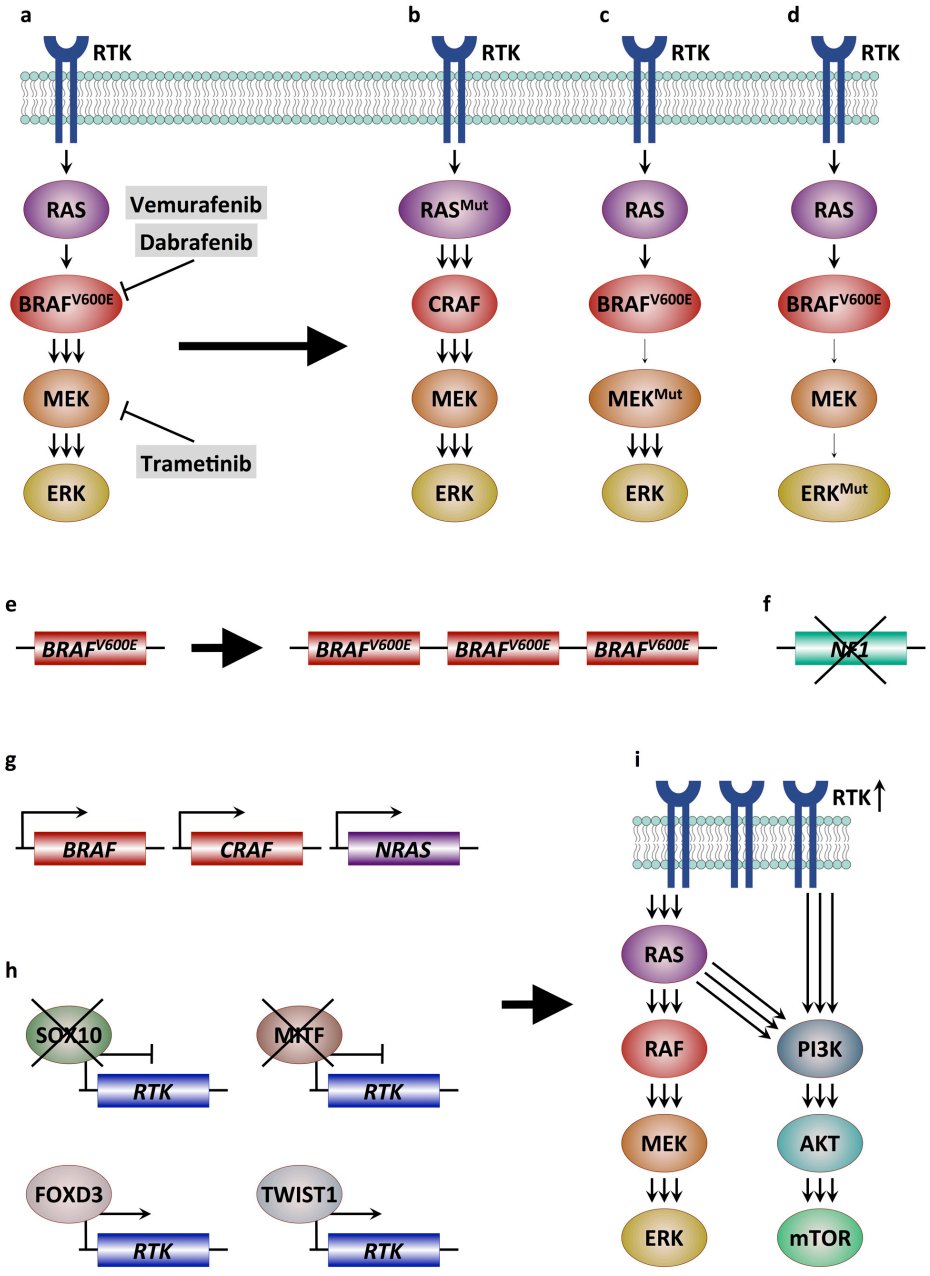

Figure 13 | Mechanisms of resistance to MAPK-targeting therapeutics. (**a**) Clinical activities of vemurafenib, dabrafenib, and trametinib are considerable. However, intrinsic and mostly acquired resistances limit the therapeutic benefits of these agents. (**b - d**) Acquired oncogenic mutations in *NRAS*, *MEK*, or *ERK* are sufficient to restore MAPK signaling. (**e**, **f**) Similarly, $BRAF^{V600E}$ amplifications as well as loss of *NF1* alleles re-establish MAPK pathway. Besides genetic aberrances, adaptive gene expression, likely due to epigenetic rewiring, contributes to resistance. (**g**) Increased expression of *BRAF*, *CRAF*, or *NRAS* counteracts MAPK blockade. (**h**, **i**) Furthermore, upregulation of RTKs, such as AXL, EGFR, FGFR, HGFR, IGFR, KIT, and PDGFR, enhances signaling through MAPK and PI3K pathways. This RTK induction is partly due to downregulation of SOX10 and MITF and a simultaneous upregulation of FOXD3 and TWIST1. Mut, mutant.

3.4.3. MAPK-independent mechanisms in MAPK inhibitor resistance

3.4.3.1. PI3K signaling-dependent resistance

For instance, increased PI3K signaling through either loss of *PTEN* (3.3.5.2. *PTEN* as tumor suppressor) or increased RTK (e.g. EGFR, hepatocyte growth factor receptor (HGFR), or insulin-like growth factor receptor (IGFR)) activity is sufficient to bypass MAPK inhibition (Girotti et al., 2013; Lito et al., 2012; Paraiso et al., 2011; Shi et al., 2014; Straussman et al., 2012; Van Allen et al., 2014; Villanueva et al., 2010; Wilson et al., 2012; Xing et al., 2012) (Figure 13h, i). Furthermore, TGFβ and NODAL activate AKT in melanoma cells, thus SMAD2/3 signaling might also contribute to acquired MAPK resistance by stimulating PI3K pathway (Fang et al., 2013; Qu et al., 2014; Schlegel et al., 2015). To counteract resistance to MAPK inhibitors, several compounds targeting PI3K pathway have been emphasized as potential strategies for melanoma therapy. These inhibitors target PI3K signaling at different nodes, such as RTKs, PI3K, AKT, or mTOR, and are currently being tested in clinics (Deng et al., 2012; Gopal et al., 2010; 2014; Lasithiotakis et al., 2008; Lassen et al., 2014; Roberts et al., 2012; Sarker et al., 2015; Schneider et al., 2014; Shi et al., 2014; 2011; Straussman et al., 2012; Tolcher et al., 2015; Van Allen et al., 2014; Wang et al., 2015).

3.4.3.2. CDK4-dependent resistance

Besides PI3K pathway, a functional screen identified CDK4 as a node potentially involved in resistance to MAPK-targeted therapy (Kwong et al., 2012). In *RAS*-mutant melanoma, loss of *CDKN2A* or *CDK4* amplification frequently increases melanoma progression (3.3.5.1. *CDKN2A* as tumor suppressor). Indeed, concomitant application of MEK and CDK4 inhibitors overcomes innate resistance of *Ras*-mutant murine melanoma cells to Mek inhibition, resulting in tumor regression in xenograft models (Kwong et al., 2012), while a CDK4 inhibitor counteracts acquired vemurafenib resistance in $BRAF^{V600E}$ melanoma xenotransplants (Yadav et al., 2014).

3.4.3.3. SOX10-dependent and MITF-dependent resistance

Acquired resistance to vemurafenib or dabrafenib is accompanied by *SOX10* (Sun et al., 2014) and *MITF* suppression (Konieczkowski et al., 2014; Müller et al., 2014). SOX10 itself represses *EGFR* and *PDGFR* loci. Hence, downregulation of SOX10 induces expression of these RTKs, which confers resistance to MAPK inhibition (Figure 13h). Depletion of *SOX10* also induces *TGFBR2* expression, and activated TGFβ signaling further enhances upregulation of RTKs (Sun et al., 2014). Silencing of *MITF* similarly

promotes expression of RTKs, such as *EGFR*, *PDGFR*, and TYR-protein kinase receptor UFO (*AXL*), that signal through MAPK, thus reactivating the pathway (Johannessen et al., 2013; Konieczkowski et al., 2014; Müller et al., 2014; Sensi et al., 2011) (Figure 13h). Interestingly, SOX10 / SOX9 and MITF transcriptional programs, which regulate melanoma growth versus invasion and metastasis, seem similarly involved in driving drug resistance. Indeed, *AXL* expression also induces invasion of melanoma cells (Tai et al., 2008), and therapy-resistant cells show increased ability to invade and metastasize (Sanchez-Laorden et al., 2014; Wang et al., 2015). Whether SOX9 is involved in *SOX10-MITF* suppression-dependent resistance to MAPK-targeted therapy, and whether this promotes melanoma dissemination and metastasis *in vivo*, remains to be deciphered.

3.4.3.4. Stemness-related resistance

In contrast to repression of melanocyte lineage commitment genes, NC specifier / EMT genes (Betancur et al., 2010; Nelms and Labosky, 2010) are re-expressed during MAPK inhibitor resistance. In embryonic NC, *Foxd3* is silenced upon melanoblast specification (3.2.5.1. FOXD3 and SOX9), and FOXD3 remains mostly absent in melanoma. However, vemurafenib exposure promotes *FOXD3* expression in melanoma cells. FOXD3 transcriptionally activates RTKs including *EGFR*, *HGFR*, *IGFR*, and *PDGFR*, which confer resistance through enhanced MAPK and PI3K signaling (Figure 13h), while *FOXD3* silencing sensitizes cells to MAPK inhibitors (Abel and Aplin, 2010; Abel et al., 2013; Basile et al., 2012). The embryonic NC mesectoderm specifier and EMT gene *TWIST1* (Füchtbauer, 1995; Stoetzel et al., 1995) similarly mediates resistance to MAPK inhibition (Menon et al., 2013) (Figure 13h). Interestingly, expression of *TWIST1* and *ZEB1*, another NC / EMT gene (Cacheux et al., 2001), also drives EMT and metastasis in malignant melanoma, accompanied by TGFβ signaling induction and by *SOX10* and *MITF* suppression (Caramel et al., 2013; Denecker et al., 2014; Weiss et al., 2012). ZEB1 has been linked to chemoresistance in glioblastoma and lung cancer models (Fang et al., 2014; Ren et al., 2013; Siebzehnrubl et al., 2013) and might be conceivably involved in acquiring resistances to therapies in cutaneous melanoma. Accordingly, the NCSC and melanoma stemness marker CD271 does not only mark melanoma-sustaining subpopulations, but CD271-positive cells are more abundant in biopsies of vemurafenib-treated melanoma patients. Indeed, CD271-positivity is greatly enriched in melanoma cells during vemurafenib exposure, and these drug-tolerant cells have an increased melanoma-initiating capacity upon xenotransplantation (Menon et al., 2014). Thus, in cutaneous melanoma, akin transcriptional programs propagate NCSC-like stemness, EMT, and drug resistance. This reflects

melanoma plasticity and emphasizes the complicacy but potentially also the opportunities in successfully medicating melanoma.

3.4.4. Immunotherapies

The plethora of genetic and epigenetic alterations that are typical for all cancers provide a diverse set of antigens used by the immune system to distinguish tumor cells from their normal counterparts. Upon activation through exposure to these antigens, cytotoxic T-lymphocytes (CTL) infiltrate tumors and ultimately destroy such antigen-positive cancer cells through the release of perforin and granzymes (Schatton et al., 2014). Indeed, improved melanoma patient survival correlates with an increased number of tumor-infiltrating T-cells (Azimi et al., 2012; Erdag et al., 2012). However, these T-cell responses become ineffective because of immunosuppressive and -adaptive processes occurring at the tumor sites. Therefore, to combat melanoma more effectively, diverse strategies have focused on reinforcing quantity and efficacy of tumor-infiltrating CTLs (Schatton et al., 2014).

3.4.4.1. Interleukin 2-based therapies

Interleukin 2 (IL2) is a potent cytokine that stimulates proliferation and maturation of T-cells (Boyman and Sprent, 2012). Therefore, IL2 has been applied as immunotherapeutic agent, and high-dose IL2 immunotherapy resulted in considerable long-term survival of some melanoma patients (Figure 12). However, these promising features fade out in the face of the severe adverse side effects caused by IL2 (Atkins et al., 1999; Margolin et al., 1989). IL2 toxicity is provoked by stimulation of endothelial cells resulting in a vascular leak syndrome (Krieg et al., 2010). Furthermore, IL2 also stimulates regulatory T-cells (Treg) responsible for immunotolerance, thus partially canceling the anti-tumorigenic effects of CTLs. IL2 binds to 2 different receptor subunits, comprised of CD25, which is present on Tregs and endothelial cells, and CD122, which is expressed on CTLs (Boyman and Sprent, 2012). In order to scavenge IL2 binding towards CD122, selective antibodies blocking the CD25 binding site on IL2 have been developed. Complexes of IL2 and such antibodies (IL2-Cx) efficiently stimulate CTLs without affecting Tregs and endothelial cells (Figure 14). Administration of IL2-Cx substantially counteracts B16-F10 melanoma *in vivo* without any of the side effects observed upon treatment with IL2 (Boyman et al., 2006; Krieg et al., 2010; Levin et al., 2012; Létourneau et al., 2010). Therefore, IL2-Cx-based therapeutics might herald a second generation of more promising IL2 therapies.

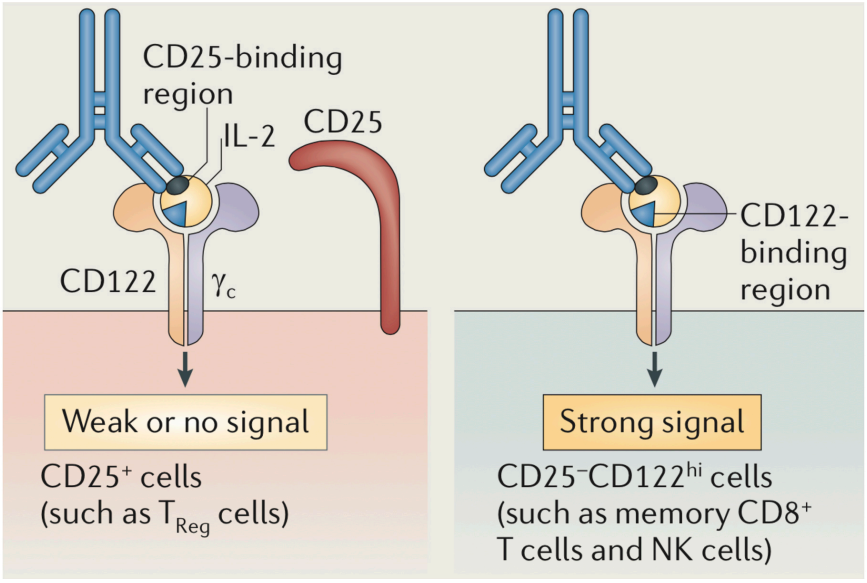

Figure 14 | IL2-Cx mediates a selective stimulation of CTLs. IL2 promotes proliferation and maturation of T-cells as well as a variety of further immune and non-immune cells, which is the cause for IL2 toxicity during high dose IL2 immunotherapy. To scavenge this pan-activation effect towards CTLs, an antibody was developed that blocks the CD25-binding site on IL2. CD25 is expressed on lung endothelial cells and Tregs, but is absent on CTLs and NK cells. Complexes of IL2 and such anti-IL2 antibodies (IL2-Cx) efficiently activate CTLs and NK cells through CD122 without stimulating Tregs and lung endothelium. Thus, IL2-Cx might represent a potent immunotherapeutic that strongly activates CTLs but minimizes the harsh side effects seen during IL2 therapy. CTL, cytotoxic T-lymphocyte; IL2, interleukin 2; NK, natural killer; Treg, regulatory T-cell (adapted from: Boyman and Sprent, 2012).

3.4.4.2. Adoptive T-cell transfer-based therapies

Apart from boosting the endogenous T-cell pool *in vivo* through systemic IL2 administration, tumor-infiltrating CTLs have been isolated from excised lesions and expanded *ex vivo*. This enriched population of CTLs is then re-administered to patients, possibly in combination with IL2 treatment (Restifo et al., 2012). These approaches show durable responses in ~50% of stage IV melanoma patients (Besser et al., 2010; Itzhaki et al., 2011; Rosenberg et al., 2011). Interestingly, in melanoma animal models and patients, such *ex vivo*-enriched CTLs frequently target antigens derived from melanocyte-specific proteins, such as DCT, MLANA, PMEL, or TYR (Bloom et al., 1997; Dudley et al., 2002; Overwijk et al., 1998; Yee et al., 2002). This prompted the development of protocols to genetically engineer CTLs prior to implantation, allowing retroviral expression of T-cell receptors with high affinity against such antigens presented by the patient's melanoma cells (Restifo et al., 2012). Adoptive transfer of genetically engineered CTLs has demonstrated success in counteracting metastatic melanoma (Morgan et al., 2006). However, such personalized treatments are limited by their expenses, as much as biosafety and ethical concerns. Furthermore, tumors are able to escape from CTL-based therapies using a

variety of mechanisms (Restifo et al., 2012). Melanoma sub-clones deficient of target antigens, antigen-presenting major histocompatibility complex class 1 (MHC-I) molecules, or components of the antigen-processing machinery have been isolated from patients that had undergone IL2 therapy or adoptive T-cell transfer (Garrido et al., 2010; Jäger et al., 1997; Khong et al., 2004; Restifo et al., 1996). Similarly, in mice, transplantation of Pmel-targeting CTLs promotes silencing of *Pmel* in growing B16-F10 melanomas (Wang et al., 2005). Notably, transplantation of such CTLs into a transgenic mouse model of melanoma first induces tumor regression followed by a relapse associated with melanoma dedifferentiation including *Dct*, *Mlana*, and *Pmel* silencing and *Cd271* induction (Landsberg et al., 2010; 2012). Furthermore, various immunosuppressive and simultaneously inflammation-promoting mechanisms, induced by secretion of IL6, TGFβ, and tumor necrosis factor alpha (TNFα), abrogate CTL function in the melanoma microenvironment, thus sustain immune evasion. (Baitsch et al., 2011; Gorelik and Flavell, 2001; Landsberg et al., 2012; Meyer et al., 2011; Soudja et al., 2010). Interestingly, these mechanisms not only promote immune escape, but also stimulate EMT and metastasis (Bald et al., 2014; Landsberg et al., 2012; Toh et al., 2011). Thus, malignant melanoma takes advantage of similar strategies, namely dedifferentiation, achieving NCSC-like stemness features, and EMT, to acquire resistances against MAPK-targeted therapies and to escape immunosurveillance.

3.4.4.3. Immune checkpoint blockade as therapeutic approaches

Besides immune evasion and immunosuppression, melanoma also coopts certain immune checkpoint pathways as a mechanism of immune resistance, in particular against tumor-infiltrating CTLs. Immune checkpoints are regulatory pathways hardwired into the immune system that are crucial for preventing autoimmunity and modulating the duration and amplitude of physiological immune responses in order to mitigate collateral tissue damage. For instance, CTL antigen 4 (CTLA4) is expressed on CTLs and dampens activation of these cells through binding to CD80 or CD86, which are present on antigen-presenting cells and tumor cells (Pardoll, 2012) (Figure 15). The essence of CTLA4 for immune response regulation becomes apparent as a result of early lethality of *Ctla4* knockout mice due to systemic immune hyperactivation (Tivol et al., 1995; Waterhouse et al., 1995). Surprisingly, temporal Ctla4 blockade with an antibody is passably tolerated by tumor-bearing mice, and leads to a significant anti-tumor response (Leach et al., 1996). Therefore, fully humanized anti-CTLA4 antibodies (α-CTLA4) have been developed, such as MDX-010 (ipilimumab, Bristol-Myers Squibb; Lipson and Drake, 2011). Ipilimumab has shown great clinical responses in melanoma patients, especially by increasing survival

beyond 2 years by ~15%. However, ipilimumab temporally promotes considerable side effects, likely due to autoimmune activity (Hodi et al., 2010; Prieto et al., 2012; Robert et al., 2011) (Figure 12). Besides CTLA4, programmed cell death 1 (PD-1), which is present on CTLs, and its ligand (PD-L1), expressed on antigen-presenting cells and tumor cells, are important negative checkpoint regulators (Pardoll, 2012) (Figure 15). PD-L1 is frequently upregulated in human melanoma (Dong et al., 2002; Madore et al., 2014; Tumeh et al., 2014), while *Pd-L1* overexpression in murine B16-F10 melanoma inhibits CTL-mediated anti-tumor responses (Blank et al., 2004). The mild *Pd-1* knockout phenotype in mice (Nishimura et al., 1999) has prompted the development of anti-PD-1 antibodies, such as BMS-936558 (nivolumab, Bristol-Myers Squibb; Wang et al., 2014). In melanoma patients, nivolumab has shown surpassing clinical responses with minor side effects. Importantly, response status is usually maintained long after treatment discontinuation (Robert et al., 2015b; Topalian et al., 2012; 2014) (Figure 12). Currently, anti-PD-L1 antibodies are clinically evaluated and show performances comparable to nivolumab (Brahmer et al., 2012; Herbst et al., 2014). If checkpoint blockade served only to temporally reverse inhibition of CTLs in the melanoma microenvironment, tumors would be expected to re-engage these mechanisms and progress after drug discontinuation. Instead, the persistence of stable disease in a considerable fraction of patients following ipilimumab or nivolumab discontinuation suggests that an effective melanoma-selective immune memory response may have been established, similar to immune memory against specific infectious organisms after antigen exposure (Allie et al., 2011). Besides long-term responders, a notable number of melanoma patients is intrinsically resistant to checkpoint blockade therapies, for instance due to a complete lack of tumor-infiltrating CTLs or absence of PD-L1 on the tumor cells (Herbst et al., 2014; Kelderman et al., 2014; Madore et al., 2014; Tumeh et al., 2014). It remains to be studied, whether in a subset of melanoma patients, in analogy to adoptive CTL transfer, checkpoint blockade might also trigger adaptive immune evasion and local immunosuppression resulting in relapse.

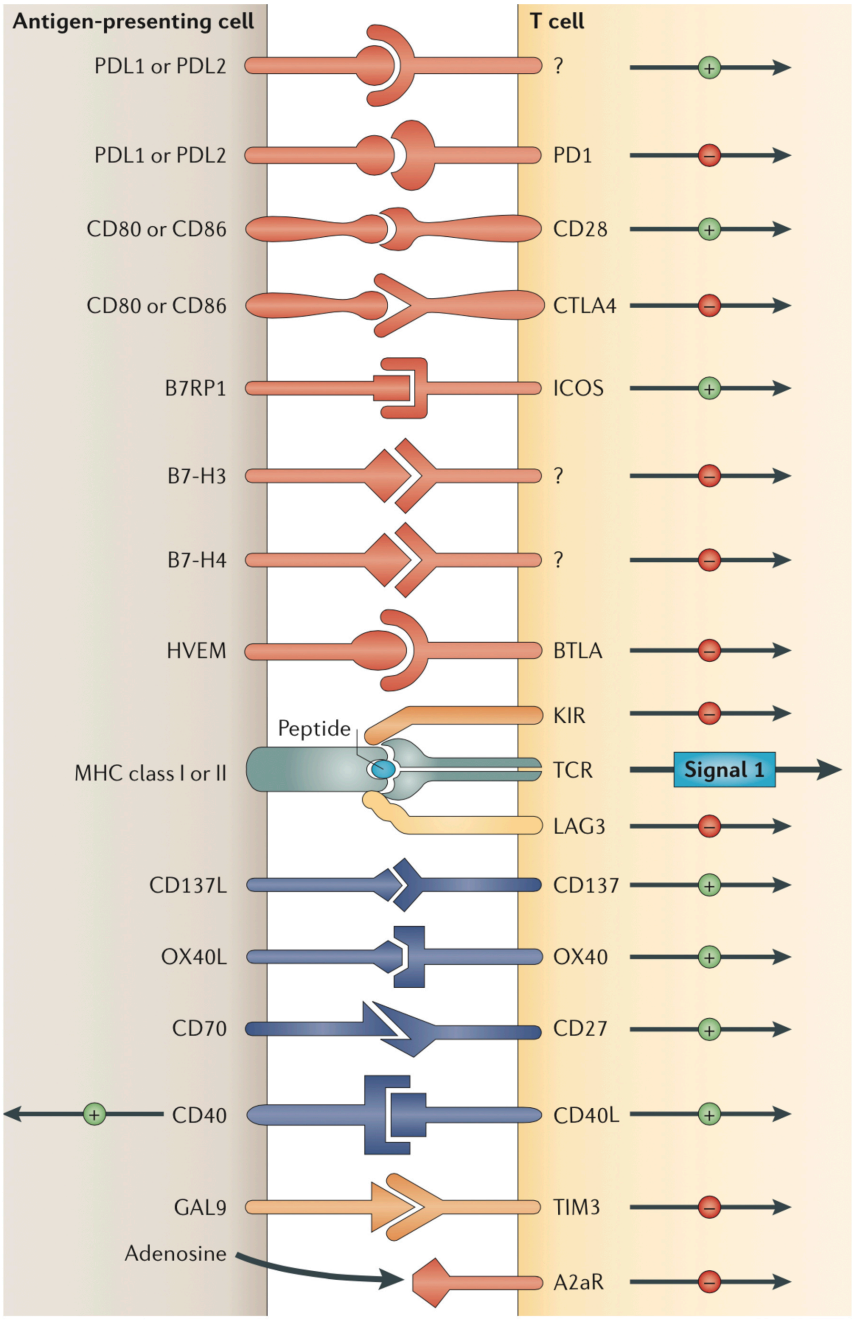

Figure 15 | CTL-stimulatory and CTL-inhibitory immune checkpoints. The primary signal activating CTLs is antigen presentation through peptide-MHC molecule complexes, which are present on antigen-presenting cells including tumor cells and bind TCRs on CTLs. This occurs either at the initiation of CTL responses in lymph nodes or in peripheral tissues, such as tumors, to sustain effector responses. Furthermore, a plethora of ligand–receptor interactions between CTLs and antigen-presenting cells tightly regulates the CTL response to antigen. For instance, CD40, CD70, CD80, CD86, and OX40L co-stimulate CTLs through binding to CD40L, CD27, CD28, and OX40, respectively. Activated CTLs then upregulate CTLA4, which also binds CD80 / CD86. Signaling through CTLA4, however, confines CTL response. An immune checkpoint that similarly dampens CTL response is binding of PD-L1 to PD-1. Cancers including melanoma coopt these immune checkpoint pathways as a mechanism of immune resistance. Tumor cells frequently downregulate MHC-I as much as checkpoint activators, while upregulating checkpoint inhibitors. CD, cluster of differentiation; CTLA4; CTL antigen 4; MHC, major histocompatibility complex; PD, programmed cell death; TCR, T-cell receptor (adapted from: Pardoll, 2012).

3.5. Epigenetic regulation of the NC and cutaneous melanoma

3.5.1. Epigenetic regulation during NC development

According to epigenetic modifiers regulating development, homeostasis, and cancer of various tissues (3.1. Epigenetics), epigenetic mechanisms are likewise participating in neural crest development and formation of neurocristopathies (Table 1). In human ESCs, *DNMT3B* loss promotes upregulation of NCSC genes including *FOXD3*, *SNAI2*, *SOX10*, and *CD271* (Martins-Taylor et al., 2012). Similarly, upon neural tube closure in the chick embryo, both Dnmt3a and Dnmt3b silences neuroepithelial genes, such as *Sox2* and *Sox3*, which induces expression of the NC specifiers *Foxd3*, *Snai2*, *Sox9*, and *Sox10* (Hu et al., 2014; 2012). In synergy, *Jmjd2a* is required for demethylation of the H3K9me3 repressive mark at the promoters of *Snai2* and *Sox10*, thus promoting expression of these NC specifiers (Strobl-Mazzulla et al., 2010). However, during EMT of the cranial NC, Dnmt3b re-induces silencing of *Sox10*, allowing the formation of Sox10-negative mesenchymal progenitors (Hu et al., 2014). EMT itself is promoted through Hdac and PRC2 activity. Hdacs and Ezh2 form a complex with Snai2 to repress the promoter of the epithelial adhesion molecules cadherin 6B (*Cad6b*) and *Cdh1*, respectively, thus inducing EMT (Coles et al., 2007; Strobl-Mazzulla and Bronner, 2012b; Tien et al., 2015).

After NC delamination in zebrafish larvae, hdac1 activity is required for *foxd3* repression, which induces *mitf* and melanoblast specification (Ignatius et al., 2008). In murine trunk NCSCs, Hdac1 and Hdac2 promote Sox10 expression, while *Hdac1/2* deletion attenuates NC specification towards Sox10-positive peripheral glia and maintenance of Schwann cells (Chen et al., 2011; Jacob et al., 2011; 2014). Interestingly, in cranial NC of zebrafish larvae, hdac1 activity promotes, rather than melanogenesis, specification of sox9-positive mesenchymal progenitors and subsequent mesectodermal differentiation (Ignatius et al., 2013). In contrast, different Hdac homologues than Hdac1/2 seem to induce murine NC-derived mesectoderm. Hdac3 is required for NC differentiation towards smooth muscle cells contributing to the outflow tract of the heart (Singh et al., 2011), while *Hdac8* ablation interferes with skull morphogenesis (Haberland et al., 2009). Comparably, mesectodermal differentiation of NC-derived mesenchymal progenitors depends on gene repression mediated by Ezh2. Importantly, apart from cartilage and bone formation, *Ezh2* deletion affects neither NCSC proliferation nor differentiation of the trunk NC (Schwarz et al., 2014). Notably, in differentiated peripheral glia, PRC2 activity is again required for Schwann cell maturation and proper axon myelination (Heinen et al., 2012).

Table 1 | Roles of epigenetic modifiers during NC development and in neurocristopathies.

Tissue / Disease	DNMT3A/B	HDACs	JMJD2 / JARID1 / SETDB1	PRC2
NC specification	Repress *Sox2/3* → induction of *Foxd3*, *Snai2*, *Sox9/10*	n.a.	Jmjd2a de-represses *Snai2*, *Sox10*	n.a.
NC EMT	n.a.	Repress *Cad6b* → EMT induction	n.a.	Represses *Cdh1* → EMT induction
NCSCs	Repress *Sox10* → cranial NCSCs	n.a.	n.a.	Not relevant
Melanoblast specification	n.a.	Repress *Foxd3* → *Sox10*, *Mitf* induction	n.a.	Not relevant
Glia specification	n.a.	Induce *Sox10* → glia induction / maintenance	n.a.	Required for Schwann cell maturation
Craniofacial / Mesenchymal specification	n.a.	Required for smooth muscle cells / skull morphogenesis	n.a.	Required for skull morphogenesis
Waardenburg syndromes	n.a.	n.a.	n.a.	Ezh2 might repress *Sox10*, *Pax3*
DiGeorge syndrome	n.a.	n.a.	n.a.	n.a.
Weaver syndrome	*DNMT3A* mutations → craniofacial anomalies	n.a.	n.a.	*EZH2* mutations → craniofacial anomalies
ICF syndrome	*DNMT3B* mutations → craniofacial anomalies	n.a.	n.a.	n.a.
MPNSTs	n.a.	n.a.	n.a.	*SUZ12*, *EED* loss-of-function mutations → tumor progression
Neuroblastoma	Promote drug resistance	Promote tumor growth / stemness	n.a.	EZH2 overexpression → tumor progression
Melanoma	Repress *CDKN2A*, *PTEN*, *SOX9* → tumor growth	Promote tumor growth	*SETDB1* amplification JARID1 activity → growth / stemness	$EZH2^{Y641N}$ / EZH2 overexpression → growth / metastasis

EMT, epithelial to mesenchymal transition; ICF, immunodeficiency - centromeric instability - facial anomalies; MPNST, malignant peripheral nerve sheath tumor; n.a., not available; NC, neural crest; NCSC, NC stem cell.

3.5.2. Epigenetic regulation of neurocristopathies

Epigenetic modifiers do not only regulate neural crest development, but equiprobably contribute to neurocristopathies (Table 1). For instance, Weaver syndrome patients harbor germline *EZH2* mutations, which are likely deleterious for EZH2 function. The Weaver syndrome partly consists of craniofacial malformations (Gibson et al., 2012; Tatton-Brown et al., 2011; 2013). These anomalies are presumably due to attenuated EZH2 function during cranial NC development, in accordance with the murine *Ezh2* knockout phenotype (Schwarz et al., 2014). Comparably, recurrent mutations in *DNMT3A* are associated with an overgrowth disorder that includes facial dysmorphism similar to the Weaver syndrome (Tatton-Brown et al., 2014), while *DNMT3B* germline mutations are a cause for the immunodeficiency - centromeric instability - facial anomalies (ICF) syndrome (Hansen et al., 1999). Interestingly, mice harboring such *Dnmt3b* mutations show developmental defects reminiscent of the ICF syndrome (Ueda et al., 2006). The DNMT3A/B-related craniofacial malformations likely originate from aberrant NC development, as observed in *Dnmt3a/b*-depleted mice (Hu et al., 2012; 2014). Attenuation of adipocyte enhancer binding protein 2 (*Aebp2*) results in mice with a phenotype resembling Waardenburg syndromes. Interestingly, Aebp2 and Ezh2 co-maintain H3K27me3 at promoters of *Sox10* and *Pax3* (Kim et al., 2011a), genes previously implicated in Waardenburg syndromes and Hirschsprung disease (3.2.6.1. Waardenburg syndromes and Hirschsprung disease). Thus, their aberrant epigenetic regulation might contribute to this congenital disorder.

Along with its roles in congenital syndromes, epigenetic dysregulation also contributes to NC-derived cancers (Table 1). In most malignancies, increased PRC2 activity promotes tumorigenesis (3.1.4.3. EZH2 function in hematopoietic malignancies; 3.1.4.4. EZH2 function in solid cancers). Likewise, elevated EZH2 levels confer poor prognosis in neuroblastoma patients, and aberrant EZH2 function sustains neuroblastoma formation through repression of a diverse set of tumor suppressors (Wang et al., 2012). In great contrast, somatic mutations affecting either *SUZ12* or *EED* are recurrent in MPNSTs, result in abrogated PRC2 function, and are promoting the progression of *NF1* loss-induced neurofibroma to MPNSTs. Mutational loss of PRC2 activity enforces de-repression of diverse NC specifier / EMT genes including *ETS1*, *SOX9*, and *ZEB1* (De Raedt et al., 2014; Lee et al., 2014; Zhang et al., 2014b). In the context of neurofibroma, these genes might have oncogenic attributes, which would explain the counterintuitive appearance of PRC2 to conduct tumor suppressive activities. Besides epigenetic modifiers, epigenetic readers also contribute to NC-derived malignancies. In mice, *Brd4* deletion

interferes with progression of neurofibroma to MPNSTs, and BET bromodomain inhibitors induce MPNST regression in xenotransplantation models. BRD4 actively stimulates transcription of the anti-apoptosis gene B-cell leukemia/lymphoma 2 (*BCL2*) as well as the NC specifier / EMT genes *ETS1*, *SOX9*, and *ZEB1*, which are already disposed to transcription in the context of *SUZ12* or *EED* loss. This reflects a remarkable interplay between genetic PRC2 inactivation and aberrant BRD4 activity driving MPNSTs (De Raedt et al., 2014; Patel et al., 2014). In neuroblastoma, however, BET bromodomain inhibitors promote tumor regression by attenuating expression of the *N-MYC* oncogene rather than through a PRC2-dependent mechanism (Puissant et al., 2013; Wyce et al., 2013b).

3.5.3. Epigenetic regulation of cutaneous melanoma

During cutaneous melanomagenesis, similarly as in neuroblastoma and MPNSTs, BRD4 propagates transcription of pro-tumorigenic genes including *BCL2*, *MYC*, and *NF-κB*, while BET bromodomain inhibitors impede melanoma growth *in vitro* and upon xenotransplantation (De Raedt et al., 2014; Gallagher et al., 2014a; 2014b; Segura et al., 2013). Beyond BRD4-mediated transcriptional activation, a variety of epigenetic modifiers contribute to melanoma initiation, progression, and plasticity.

3.5.3.1. Aberrant function of DNMTs in melanoma

For instance, DNMT3A/B expression is elevated in malignant melanoma in comparison to benign lesions and further increases with metastatic progression. Likewise, high DNMT3B levels correlate with reduced patient survival (Molognoni et al., 2011; Nguyen et al., 2011), while *Dnmt3a* deletion counteracts B16-F10 melanoma growth (Deng et al., 2009). Comparably, CpG island methylation-induced silencing of a substantial number of tumor suppressor genes, such as *CDKN2A* or *PTEN*, has been identified in malignant melanoma biopsies (Bonazzi et al., 2011; Conway et al., 2011; Jonsson et al., 2010; Schinke et al., 2010; Venza et al., 2015; Zhou et al., 2000), and high density of promoter methylation correlates with poor prognosis for melanoma patients (Sigalotti et al., 2014). These findings, at first sight, emphasize DNMT inhibition as a possible anti-melanoma treatment. Indeed, exposure of melanoma cells to decitabine promotes de-repression of tumor suppressors including *CDKN2A* and apoptosis-inducing Fas cell surface death receptor (*FAS*) promoting a growth arrest and apoptosis. Furthermore, cells upregulate melanocyte differentiation genes, such as *MITF* and *DCT*, underlining the induced senescence phenotype (Alcazar et al., 2012; Molognoni et al., 2011). However, apart from

growth, melanoma plasticity is also controlled by DNMTs. In melanoma cells, decitabine triggers *SOX9* promoter demethylation leading to SOX9 expression, thus the dynamic SOX10-SOX9 interplay observed during melanoma progression appears to be epigenetically regulated (Alcazar et al., 2012; Cheng et al., 2015). Importantly, also acquired resistance to MAPK inhibitors includes epigenetic dynamics. During vemurafenib exposure, the promoter CpGs of *EGFR* are demethylated, allowing melanoma to upregulate EGFR and to re-establish MAPK and PI3K signaling, while decitabine accordingly releases *EGFR* repression (Wang et al., 2015). Since *Sox9* overexpression enhances metastasis formation in B16-F10 melanoma (Cheng et al., 2015) and *EGFR* de-repression confers resistance to vemurafenib (Wang et al., 2015), DNMT inhibition as potential melanoma therapy seems precarious at second sight.

3.5.3.2. Aberrant function of histone modifiers in melanoma

Besides aberrant DNMT function, the locus of the H3K9 methyltransferase *SETDB1* is recurrently amplified in melanoma leading to high SETDB1 expression. SETDB1 aberrantly represses tumor suppressors, such as *CDKN2A*. Accordingly, overexpression of both *setdb1* and *suv39h1*, another H3K9 methyltransferase, accelerates tumorigenesis in a zebrafish model of melanoma (Ceol et al., 2011; Kostaki et al., 2014; Miura et al., 2014). Forced expression of the H3K4me3 demethylase *JARID1B* in human melanoma cells entails a cell cycle arrest through a gain in repressive histone marks at cell cycle-promoting loci (Roesch et al., 2006; 2008). Paradoxically, in malignant melanoma, JARID1B-expressing cells are more abundant than in nevi (Kuźbicki et al., 2013; Roesch et al., 2005). These JARID1B-positive subpopulations are indeed cycling slowly compared to the tumor bulk. However, increased expression of JARID1B also confers stemness features to melanoma cells. JARID1B-positive cells show enhanced self-renewal potential *in vitro* and propagate tumor initiation upon xenotransplantation. Intriguingly, *JARID1B* deletion leads to *in vitro* exhaustion of melanoma cells and diminishes continuous xenotransplant growth and metastatic progression (Roesch et al., 2010). Remarkably, JARID1A/B-positive cells are highly resistant to chemotherapy and vemurafenib (Roesch et al., 2013; Sharma et al., 2010; Yuan et al., 2013). During exposure to vemurafenib, melanoma cells upregulate JARID1B along with stemness markers, such as CD271, while ablation of *JARID1B* interferes with CD271 enrichment and prevents the acquirement of resistance to MAPK inhibition (Menon et al., 2014). Thus, during melanomagenesis, epigenetic rewiring is responsible for tumor growth as much as plasticity resulting in NCSC-like stemness, metastasis formation, and resistance to therapies (Figure 6).

3.5.3.3. EZH2 and melanomagenesis

Comparably to JARID1B, the expression of EZH2 mRNA and protein is incrementally increased in biopsies from benign nevi to metastatic melanoma (Asangani et al., 2012; Fan et al., 2011; Kampilafkos et al., 2015; McHugh et al., 2007). Accordingly, global H3K27me3 is enriched in human melanoma cells in comparison to nevus cells and melanocytes (Mologhoni et al., 2011). Besides high EZH2 expression, a considerable number of melanomas also harbor mutations in *EZH2*, some of which are the gain-of-function $EZH2^{Y646C/F/H/N/S}$ mutations (Alexandrov et al., 2013; Harms et al., 2014; Hodis et al., 2012; Krauthammer et al., 2012). According to *in silico* predictions, most of these non-synonymous *EZH2* mutations are thought of altering the activity of EZH2 (Tiffen et al., 2015). As observed in a variety of cancers (3.1.4.3. EZH2 function in hematopoietic malignancies; 3.1.4.4. EZH2 function in solid cancers), high EZH2 levels correlate with poor melanoma patient survival (Asangani et al., 2012; Bachmann et al., 2006). Strong EZH2 expression in melanoma biopsies is further associated with an increased proliferative index of the corresponding samples (Bachmann et al., 2006), while *EZH2* depletion in melanoma cells promotes a cell cycle arrest and interferes with growth upon xenotransplantation (Fan et al., 2011; Luo et al., 2012a; 2013). However, apart from regulating growth, EZH2 function also appears to be important for invasion in collagen layers. *EZH2* ablation reduces the invasive capacity of cutaneous and uveal melanoma cells (Chen et al., 2013; Luo et al., 2012a; 2013). Likewise, EZH2 expression is increased at the invasive front of human melanomas (Kampilafkos et al., 2015), *Ezh2* deletion lowers cell motility in s.c. growing B16-F10 tumors, and, upon i.v. transplantation, *Ezh2*-deficient B16-F10 cells have reduced lung colonization potential (Manning et al., 2014; Tiwari et al., 2013).

3.6. Accurately investigating the roles of EZH2 during melanomagenesis

To this day, studies investigating the roles of EZH2 in cutaneous melanoma have only been of correlative nature or have been gathered by means of *in vitro* culture and melanoma cell transplantation assays. Furthermore, no study has so far defined possible EZH2 target genes (ETG) that would accurately explain the distinct phenotypes observed upon *EZH2* inactivation (3.5.3.3. EZH2 and melanomagenesis). It is now widely accepted that tumorigenesis is, apart from cancer cell-intrinsic aberrations, propagated through bidirectional interactions of tumor cells with diverse stromal compartments, such as the immune system, vasculature, cancer-associated fibroblasts, as well as distant organs upon metastatic colonization (Hanahan and Weinberg, 2011; Quail and Joyce, 2013). Importantly, this dynamic interference of a growing neoplasm with its microenvironment seems to depend on plastic reshaping of the epigenetic landscape (Azad et al., 2013; Tam and Weinberg, 2013) (Figure 6). Therefore, investigating the relevance of a given (epigenetic) player for various aspects of tumorigenesis is best achieved in physiological cancer models with undisturbed microenvironments, rather than in *ex vivo* culture systems of cancer cells or upon heterotopic transplantation of tumor cells into immunocompromised mice.

Transgenic *N-Ras*^{Q61K}-expressing and *Cdkn2a*-deficient mice display dermal hyperplasia reminiscent of human congenital nevi and consistently develop metastatic melanoma within 6 months of age (Ackermann et al., 2005; Shakhova et al., 2012). Hence, this murine model represents an ideal tool to explore the significance of Ezh2-mediated gene repression for melanoma initiation, growth, metastatic progression, and the interplay of the melanoma compartment with stroma. Moreover, integration of global gene expression analyses, chromatin immunoprecipitation (ChIP) data, and functional experiments will faithfully allow the definition of melanoma-relevant ETGs. Consequently, these findings will deepen our understanding on the mode of EZH2-facilitated melanomagenesis and might set the stage to combat this deadly disease more effectively.

4. Results

4.1. My contributions to published articles and manuscripts in preparation

4.1.1. Roles of NC development-relevant factors during melanomagenesis

Given the close relationship between the embryonic NC and melanoma (chapters 3.2. – 3.4.), a major research focus of the Sommer Lab has been on deciphering putative roles of NC development-relevant transcription factors and signaling pathways in the formation and metastatic progression of melanoma. In the course of my doctorate, I contributed to and initiated several projects investigating these questions:

Firstly, I helped unraveling the antagonistic roles of SOX10 and SOX9 in melanoma initiation and metastasis. I performed a majority of the *in vitro* experiments deciphering the cellular and molecular functions of SOX10 in melanoma cells (Shakhova et al., 2012). Secondly, I contributed to the characterization of the SOX10-SOX9 interplay by analyzing cell cycle progression and apoptosis in the context of *SOX10* and *SOX9* depletion (Cheng et al., 2015; Shakhova et al., 2015). I also performed the B16-F1 i.v. transplantation assays demonstrating the *in vivo* potential of Sox9 in promoting lung metastasis (Cheng et al., 2015). Finally, I initialized and guided a project deciphering the roles of Tgfβ signaling in murine melanoma formation and especially metastasis. Therefore, I established a colony of melanoma-prone mice bearing either $Smad7^{lox/lox}$ or $Tgfbr2^{lox/lox}$, which allowed *in vivo* manipulation of Tgfβ signaling in the context of melanomagenesis. Phenotypes have been analyzed in close collaboration with E. Tuncer, and results will soon be prepared for publication (Zingg and Tuncer, in preparation).

Shakhova, O., **Zingg**, **D.**, Schaefer, S.M., Hari, L., Civenni, G., Blunschi, J., Claudinot, S., Okoniewski, M., Beermann, F., Mihic-Probst, D., Moch, H., Wegner, M., Dummer, R., Barrandon, Y., Cinelli, P., and Sommer, L. (2012). Sox10 promotes the formation and maintenance of giant congenital naevi and melanoma. Nat. Cell. Biol. *14*, 882–890.

Shakhova, O., Cheng, P., Mishra, P.J., **Zingg**, **D.**, Schaefer, S.M., Debbache, J., Häusel, J., Matter, C., Guo, T., Davis, S., Meltzer, P., Mihic-Probst, D., Moch, H., Wegner, M., Merlino, G., Levesque, M.P., Dummer, R., Santoro, R., Cinelli, P., and Sommer, L. (2015). Antagonistic cross-regulation between Sox9 and Sox10 controls an anti-tumorigenic program in melanoma. PLoS Genet. *11*, e1004877.

Cheng, P.F., Shahkova, O., Widmer, D.S., Eichhoff, O.M., **Zingg**, **D.**, Frommel, S.C., Belloni, B., Raaijmakers, M.M., Goldinger, S.M., Santoro, R., Hemmi, S., Hoek, K.S., Sommer, L., Dummer, R., and Levesque, M.P. (2015). Methylation-dependent SOX9 expression mediates invasion in human melanoma cells and is a negative prognostic factor in advanced melanoma. Genome Biol. *16*, 3016.

Zingg, **D.**, Tuncer, E., and Sommer, L. (2015). Tgfβ signaling promotes melanoma metastasis *in vivo*. In preparation.

4.1.2. Roles of the epigenetic modifier EZH2 in melanomagenesis

Besides transcription factors and signaling pathways, epigenetic rewiring likely contributes to distinct aspects of melanomagenesis. Therefore, in the main project of my doctorate, I focused on the roles of the epigenetic modifier EZH2 during melanoma initiation and progression. These results are illustrated in my PhD thesis (4.2. Roles of EZH2 in melanoma formation and metastatic progression) and were recently accepted for publication (Zingg et al., 2015). I conducted the majority of these experiments and analyzed most of these data, with a number of exceptions, in which experiments and data analyses were performed in collaboration as follows: western blots with S. M. Schaefer and J. Debbache, immunofluorescence with E. Tuncer, qPCRs with J. Haeusel, ChIP with S. C. Frommel, and TCGA analyses with P. Cheng. EZH2 mutagenesis was done by J. Debbache and i.v. injections were conducted by N. Arenas-Ramirez.

Zingg, **D.**, Debbache, J., Schaefer, S.M., Tuncer, E., Frommel, S.C., Cheng, P., Arenas-Ramirez, N., Haeusel, J., Zhang, Y., Bonalli, M., McCabe, M.T., Creasy, C.L., Levesque, M.P., Boyman, O., Santoro, R., Shakhova, O., Dummer, R., and Sommer, L. (2015). The epigenetic modifier EZH2 controls melanoma growth and metastasis through silencing of distinct tumour suppressors. Nat. Commun. *6*, 6051.

4.1.3. Roles of the epigenetic modifier EZH2 in immunoediting

Among the identified ETGs, I found *CD40* to be of particular interest. CD40 is a positive immune checkpoint regulator. This prompted me to establish a collaboration with the Boyman Lab to decipher the putative role of EZH2-medited epigenetic repression in immunoediting. The so far acquired results are also illustrated in my PhD thesis (4.3. Roles of EZH2 in melanoma immunoediting) and are currently prepared for publication (Zingg, Arenas-Ramirez, and Rosalia, in preparation). In the frame of this collaboration, both labs contributed equally to the tumor allografting experiments. I performed most of the *in vitro* assays and tumor initiation experiments, whereas immunological analyses were done by N. Arenas-Ramirez and R. A. Rosalia.

Zingg, **D.**, Arenas-Ramirez, N., Rosalia, R.A., Haeusel, J., Boyman, O., and Sommer, L. (2015). Inhibition of the epigenetic modifier EZH2 synergizes with immunotherapy in abrogating melanoma formation. In preparation.

4.2. Roles of EZH2 in melanoma formation and metastatic progression

4.2.1. EZH2 is highly expressed in samples of human and murine melanoma

Previously, high EZH2 expression has been described in biopsies of malignant melanoma in comparison to benign nevi (3.5.3.3. EZH2 and melanomagenesis). To address whether changes in EZH2 expression affect cells of the melanocytic lineage rather than stromal cells in the tumor tissue, I performed co-staining of human cutaneous melanoma sections for EZH2 in combination with SOX10 or MART1-HMB45 (MLANA and PMEL), all markers for the melanocytic lineage (Busam et al., 1998; Gown et al., 1986; Harris et al., 2013; Shakhova et al., 2012; 2015). In agreement with previous studies (Asangani et al., 2012; Fan et al., 2011; Kampilafkos et al., 2015; McHugh et al., 2007), human primary melanomas and metastases displayed high EZH2 expression in cells of the melanocytic lineage compared to epidermal melanocytes and dermal nevus cells (Figure 16a; Table 2). To study the function of Ezh2 in an *in vivo* context of melanoma development, I took advantage of a mouse model of cutaneous melanoma. Overexpression of the *N-Ras*^{Q61K} oncogene under the control of the *Tyr* promoter (*Tyr::N-Ras*^{Q61K}) drives formation of dermal hyperplasia reminiscent of human congenital nevi and, in combination with loss of *Cdkn2a* (hereafter referred to as *Ink4a*$^{-/-}$), results in melanoma formation with a high penetrance (>90%) at around 6 months of age. Furthermore, *Tyr::N-Ras*^{Q61K} *Ink4a*$^{-/-}$ animals consistently develop lymph node and distant metastases in organs typically affected in stage IV melanoma patients, such as the liver, the lung, and the brain. Therefore, this murine melanoma model mimics the human disease accurately (Ackermann et al., 2005; Shakhova et al., 2012). Similar to human patients, Ezh2 protein was strongly expressed in Sox10-positive cells of murine skin melanoma and distant metastases. In contrast, Sox10-expressing cells in hair follicle bulbs, the physiological location of melanocytes in murine trunk skin (3.2.4. Adult melanocyte biology), and in dermal hyperplasia only showed marginal Ezh2 expression (Figure 16b), consistent with the human data.

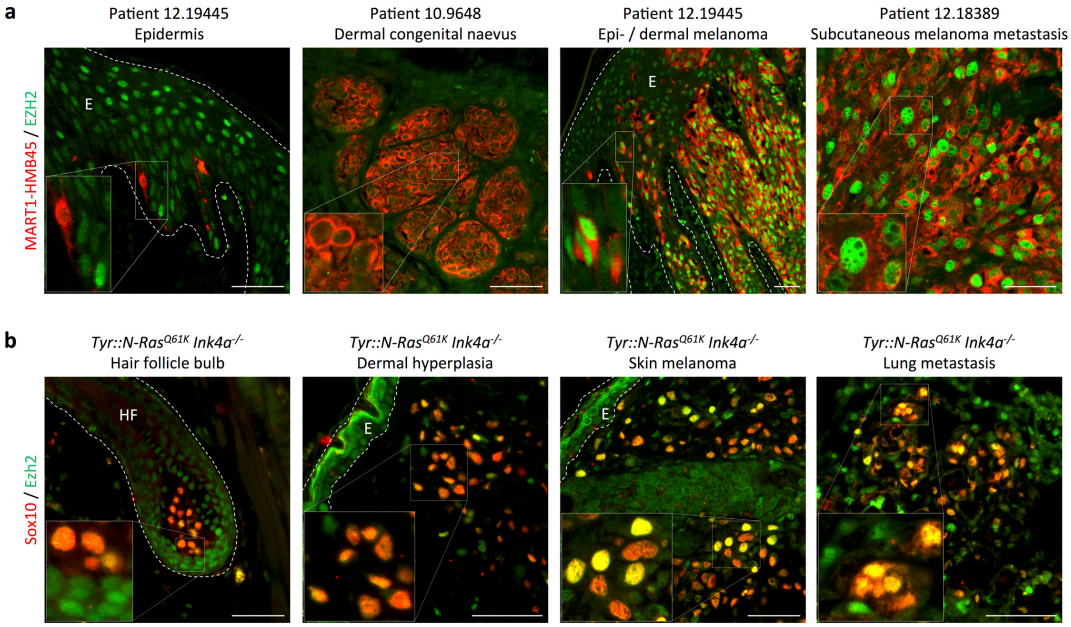

Figure 16 | EZH2 protein is upregulated in human and murine melanoma. (**a**) Immunofluorescent staining for HMB45-MART1 and EZH2 on human epidermis, dermal congenital nevus, primary melanoma, and subcutaneous melanoma metastasis sections from biopsies described in (**Table 2**). (**b**) Immunofluorescent staining for Sox10 and Ezh2 on skin and lung sections of melanoma-developing *Tyr::N-Ras*^{Q61K} *Ink4a*$^{-/-}$ mice. E, epidermis; HF, hair follicle. Scale bars, 50µm.

Table 2 | Clinical data corresponding to human nevus and melanoma biopsies.

Patient ID	Sex	Age	AJCC	Nevus / Melanoma type	*BRAF**	*NRAS**	MART1	HMB45	EZH2 high
12.9648	M	48	0	Dermal nevus	n.d.	n.d.	+	-	no
12.9648	M	48	I	Epidermal melanoma	n.d.	n.d.	+	+	yes
12.6190	F	61	0	Dermal nevus	V600E	--	+	-	no
10.9640	M	36	0	Congenital nevus	--	Q61K	+	-	no
12.13497	M	76	II	Epidermal melanoma	V600E	--	+	+	yes
12.19445	M	55	IIIA	Epi- / dermal melanoma	--	Q61K	+	+	yes
12.18389	F	65	IV	Subcutaneous metastasis	V600E	--	+	+	yes
12.14437	F	n.a.	IIIC	Subcutaneous metastasis	--	Q61R	+	+	yes
12.21491	F	84	IIIB	Subcutaneous metastasis	--	Q61R	+	+	yes

Immunohistochemical staining for MART1 (MLANA) and HMB45 (PMEL) was used to distinguish benign from malignant melanoma lesions (Busam et al., 1998; Gown et al., 1986). AJCC, American Joint Committee on Cancer; F, female; M, male; n.a., not available; n.d., not defined.

4.2.2. Increased EZH2 expression is linked to poor melanoma patient survival

To study the significance of high EZH2 expression for the survival of cutaneous melanoma patients, I established an EZH2 high and an EZH2 low patient group based on RNAseq and clinical data from The Cancer Genome Atlas (TCGA, http://cancergenome.nih.gov/). These groups did not display obvious differences with respect to clinically relevant factors including *BRAF* and *NRAS* mutations (Figure 17a).

However, patients of the EZH2 high group showed a significantly shorter overall survival as compared to those of the EZH2 low group (Figure 17b). Intriguingly, primary melanoma and lymph node metastases patients (stage I – III) of the EZH2 high group developed distant metastases (stage IV) significantly faster than EZH2 low-expressing stage I – III patients (Figure 17c), implying a potential role of EZH2 in metastatic spread of melanoma.

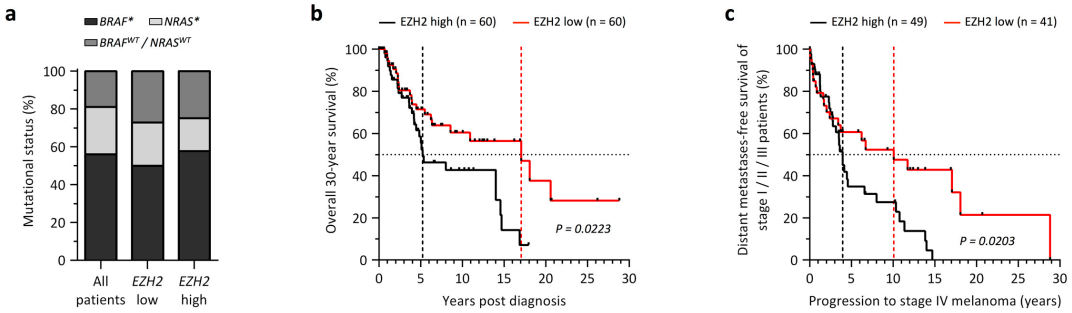

Figure 17 | High EZH2 mRNA expression correlates with adverse patient survival. (**a**) *BRAF* and *NRAS* mutational status of melanoma specimens included in EZH2 TCGA analysis. All patients, n = 274; EZH2 low, n = 60; EZH2 high, n = 60. (**b**) Kaplan-Meier curves comparing overall survival of melanoma specimens (stage I – IV) with respect to EZH2 transcript levels based on TCGA. (**c**) Kaplan-Meier curves comparing distant metastases-free survival of stage I – III melanoma specimens (primary melanoma / lymph node metastases) with respect to EZH2 transcript levels based on TCGA. EZH2 low / high, bottom and top 60 patients with respect to EZH2 transcript levels. TCGA, The Cancer Genome Atlas. P-values calculated with Log-rank (Mantel-Cox) test.

Apart from expression levels, mutations affecting EZH2 activity have been implicated predominantly in malignancies of the hematopoietic system (3.1.4.3. EZH2 function in hematopoietic malignancies), but also in melanoma (3.5.3.3. EZH2 and melanomagenesis). To clarify the significance of these EZH2 mutations for melanomagenesis, I first analyzed the occurrence of *EZH2* somatic mutations in cutaneous melanoma in comparison to 9 different cancer types using TCGA and 4 further datasets (Alexandrov et al., 2013; Hodis et al., 2012; Krauthammer et al., 2012; McCabe et al., 2012a). In this analysis, cutaneous melanoma showed the highest non-synonymous *EZH2* mutation frequency besides primary (non-Hodgkin) lymphomas. In particular, cutaneous melanoma was the only solid cancer with non-synonymous mutations affecting tyrosine 646 (Y646) in the SET domain of EZH2 (Figure 18a, b). Previously, $EZH2^{Y646*}$ mutations were reported to be widely present in primary lymphoma and to lead to increased EZH2 activity resulting in aberrant H3K27me3 (3.1.4.3. EZH2 function in hematopoietic malignancies). Based on *in silico* predictions, the collection of non-synonymous *EZH2* mutations

occurring in melanoma patients are thought of potentially altering EZH2 function (Tiffen et al., 2015). To associate these *EZH2* mutations present in melanoma patients with EZH2 function, I overexpressed selected *EZH2* mutations *in vitro*. However, except $EZH2^{Y646N/F}$, none of the mutations analyzed induced an increase in global H3K27me3. In fact, overexpression of $EZH2^{P132S}$ and $EZH2^{D142V}$ significantly reduced global H3K27me3, indicating a dominant-negative loss-of-function phenotype (Figure 18c, d). Further functional studies will be necessary to uncover properties of these mutations that might allow a functional link to cutaneous melanomagenesis.

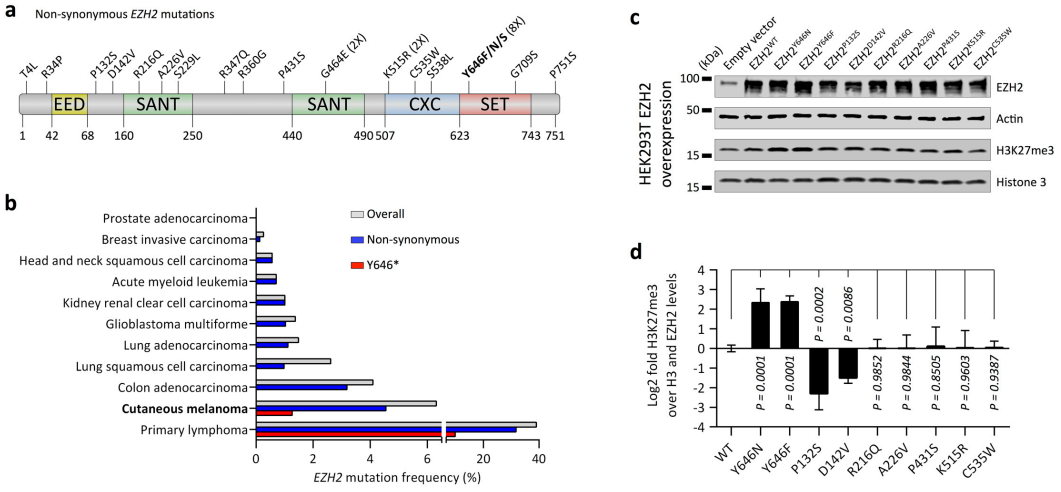

Figure 18 | *EZH2* is frequently mutated in human melanoma. (**a**) *EZH2* non-synonymous mutational landscape including $EZH2^{Y646*}$-activating mutations based on TCGA melanoma dataset and 3 further datasets (Alexandrov et al., 2013; Hodis et al., 2012; Krauthammer et al., 2012). (**b**) *EZH2* mutation frequencies including Y646* in different cancers based on TCGA and 2 further datasets (Hodis et al., 2012; McCabe et al., 2012a). (**c**, **d**) Western blot for EZH2 protein and H3K27me3 on HEK293T cells overexpressing different *EZH2* mutants to quantify changes in H3K27me3. H3, histone 3. Data are mean ± s.e.m. of n = 4. P-values calculated with ANOVA and Fisher's LSD-test.

4.2.3. Ezh2 function is dispensable for homeostasis of melanocytes

Because EZH2 was highly expressed in human and murine melanoma and linked to poor patient survival, I studied its function *in vivo*. To this end, mice carrying floxed alleles of the *Ezh2* locus ($Ezh2^{lox/lox}$) (Hirabayashi et al., 2009) were used to conditionally delete *Ezh2* in the melanocytic lineage (*Tyr* promoter) by tamoxifen (TM)-induced activation of Cre-recombinase ($Tyr::Cre^{ERT2}$) (Bosenberg et al., 2006). Inclusion of a Cre-reporter allele (*R26R::LacZ*) (Soriano, 1999) allowed fate mapping of recombined cells *in vivo*. To address a potential role of Ezh2 in maintaining normal melanocytic

function, *Ezh2* was conditionally depleted in tumor-free *Tyr::Cre^{ERT2} Ezh2$^{lox/lox}$ R26R::LacZ* mice (Figure 19a). TM was applied to 1-month-old animals, and mice were monitored for hair graying (Figure 19b). Hair graying is the phenotype predominantly arising upon interference with homeostasis of melanocyte stem cells in the bulge (Harris et al., 2013; Lang et al., 2005; Nishimura et al., 2010; Rabbani et al., 2011; Shakhova et al., 2015), the permanent niche of epithelial and melanocyte stem cells in hair follicles (Cotsarelis et al., 1990; Nishimura et al., 2002a). However, hair pigmentation remained normal up to 1 year after *Ezh2* depletion (Figure 19c). Importantly, *Ezh2* was efficiently and durably ablated in melanocytes of trunk skin hair follicles, leading to a concomitant loss of H3K27me3 (Figure 19d, e).

4.2.4. *N-Ras^{Q61K}*-expressing nevus cells are Ezh2 independent

This unforeseen independence of the normal melanocyte lineage from Ezh2-mediated gene repression prompted us to investigate a possible function of Ezh2 in maintaining benign nevus-like dermal hyperplasia. Therefore, *Ezh2* was depleted in the genetic *Tyr::N-Ras^{Q61K} Ink4a$^{-/-}$ Tyr::Cre^{ERT2} Ezh2$^{lox/lox}$ R26R::LacZ* melanoma model (Figure 20a - c). As in tumor-free mice, conditional deletion of *Ezh2* in *Tyr::N-Ras^{Q61K} Ink4a$^{-/-}$* animals had no effect on hair pigmentation. Importantly, maintenance of benign dermal hyperplasia was also not affected (Figure 20d), despite efficient *Ezh2* depletion and subsequent loss of H3K27me3 (Figure 20e, f). Even when aged for up to one year after conditional knockout (cKO) of *Ezh2*, *Tyr::N-Ras^{Q61K}* mice with functional *Ink4a^{wt}* loci did not show an overt reduction of recombined melanocytic cells in the dermis (Figure 20e). Accordingly, dermal hyperplasia grew to a similar size with a comparably low proliferation rate in both control and *Ezh2*-depleted mice (Figure 21a, b). Thus, Ezh2-mediated gene repression is dispensable for both physiological homeostasis of normal melanocytes and maintenance of *N-Ras^{Q61K}*-transformed cells in dermal hyperplasia, independent of *Ink4a*-deficiency.

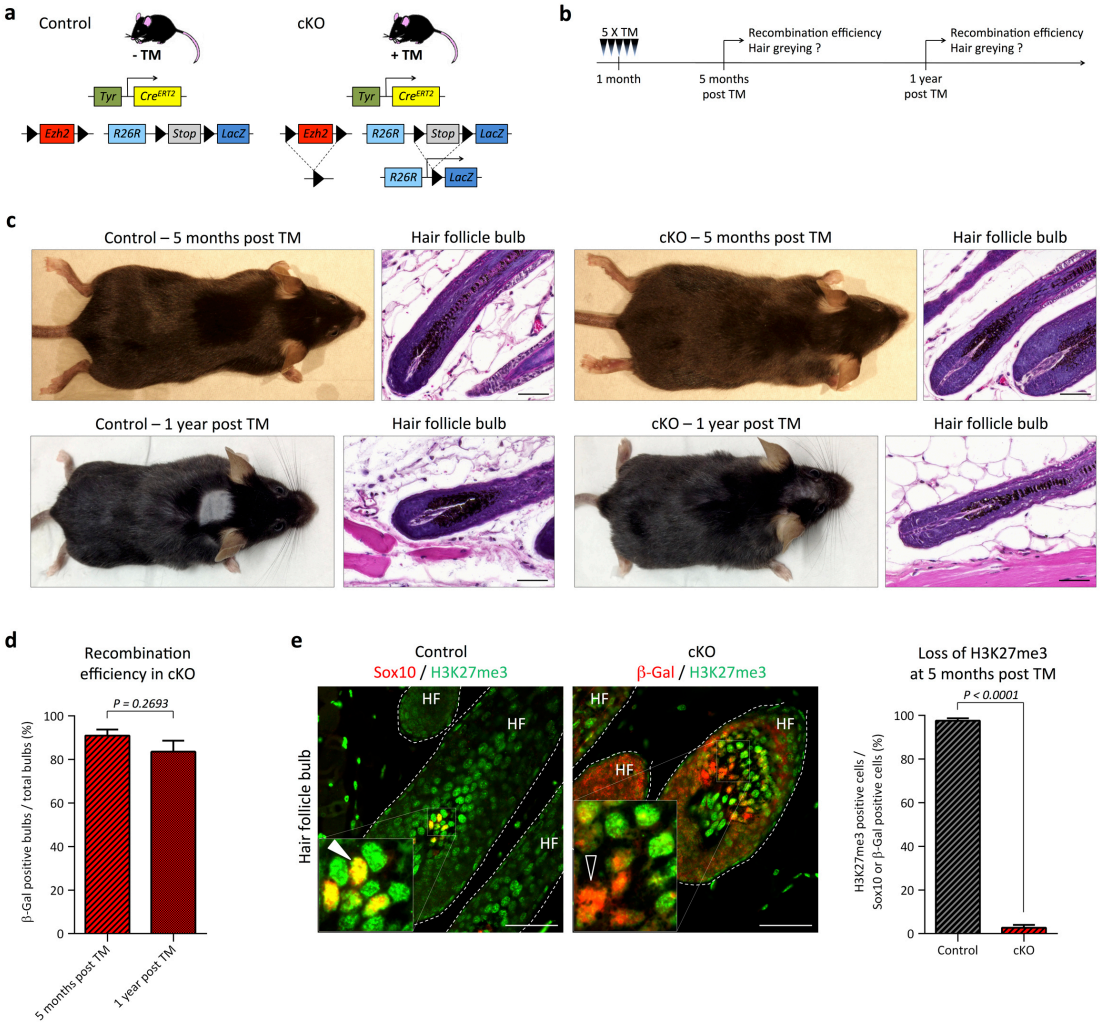

Figure 19 | Ezh2 is not required for normal melanocyte homeostasis. (**a**, **b**) Mouse genotypes and strategy used to analyze the effect of conditional *Ezh2* ablation in the melanocytic lineage of adult *wt* mice. (**c**) Macroscopic pictures and H&E staining on trunk skin sections of control and cKO mice at 5 months and 1 year post conditional *Ezh2* ablation. (**d**) Immunofluorescent staining on trunk skin sections of *wt* mice for β-Gal to quantify recombination efficiencies (representative fields not shown). (**e**) Immunofluorescent staining on trunk skin sections of *wt* mice for Sox10 (control) or β-Gal (cKO) and H3K27me3 to quantify H3K27me3 depletion. White arrowhead, Sox10-positive cell considered H3K27me3-positive; White open arrowhead, β-Gal-positive cell considered H3K27me3-negative. cKO, conditional *Ezh2* knockout; H&E, haematoxylin and eosin; TM, tamoxifen. Data are mean ± s.e.m. of n = 3. P-values calculated with unpaired Student's t-test. Scale bars, 50μm.

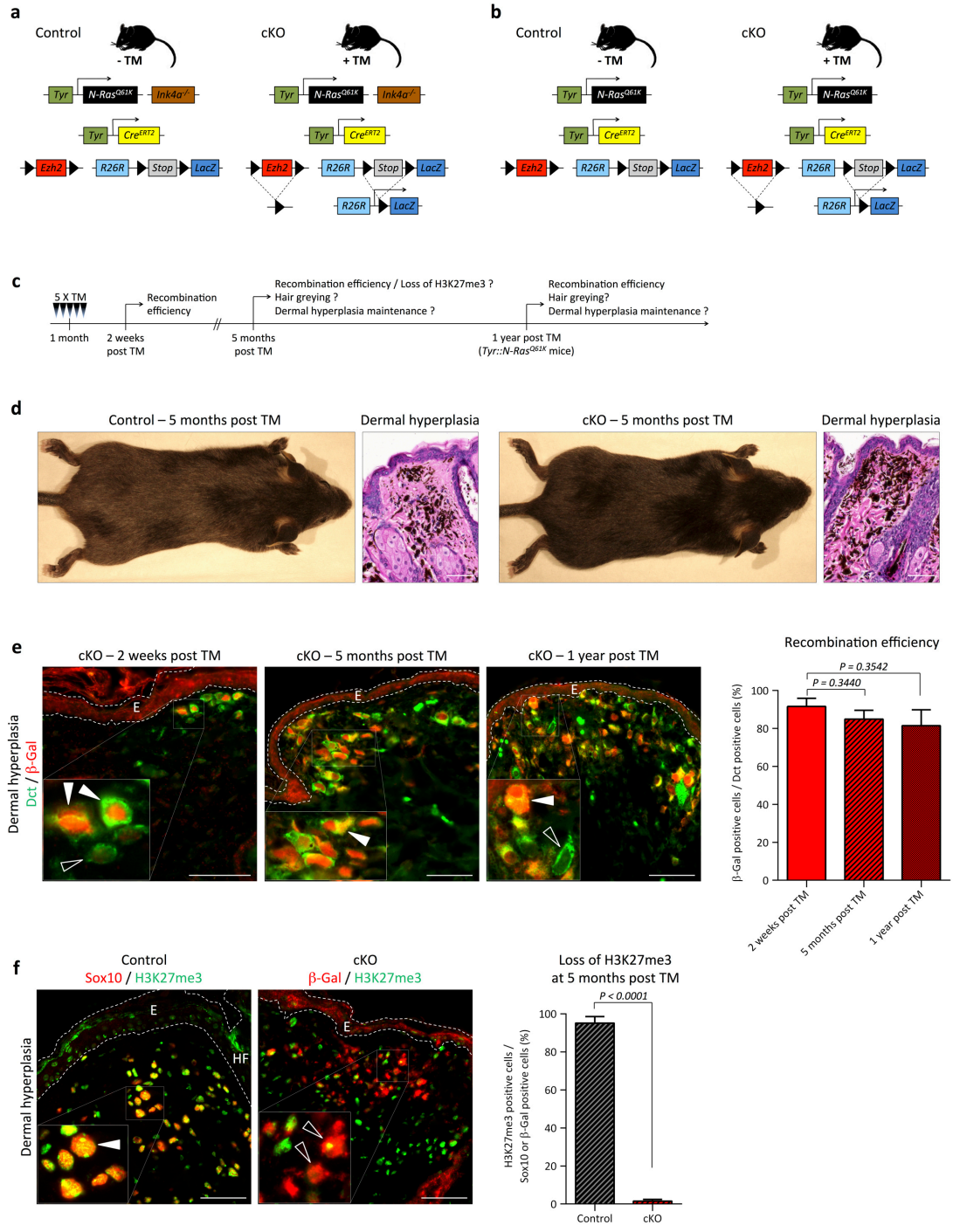

Figure 20 | Ezh2 is not required for maintenance of dermal hyperplasia. (**a - c**) Mouse genotypes and strategy used to analyze the effect of conditional *Ezh2* ablation in the melanocytic lineage of adult *Tyr::N-Ras*^{Q61K} (*Ink4a*$^{-/-}$) mice. (**d**) Macroscopic pictures and H&E staining on trunk skin sections of control and cKO mice at 5 months post conditional *Ezh2* ablation. (**e**) Immunofluorescent staining on trunk skin sections of *Tyr::N-Ras*^{Q61K} (*Ink4a*$^{-/-}$) mice for Dct and β-Gal to quantify recombination efficiencies. White arrowheads, Dct-positive cells considered β-Gal-positive; White open arrowheads, Dct-positive cells considered β-Gal-negative. (**f**) Immunofluorescent staining on trunk skin sections of *Tyr::N-Ras*^{Q61K} *Ink4a*$^{-/-}$ mice for Sox10 (control) or β-Gal (cKO) and H3K27me3 to quantify H3K27me3 depletion. White arrowhead, Sox10-positive cell considered H3K27me3-positive; White open arrowheads, β-Gal-positive cells considered H3K27me3-negative. Data are mean ± s.e.m. of n = 3. P-values calculated with ANOVA and Fisher's LSD-test (**e**), unpaired Student's t-test (**f**). Scale bars, 50µm.

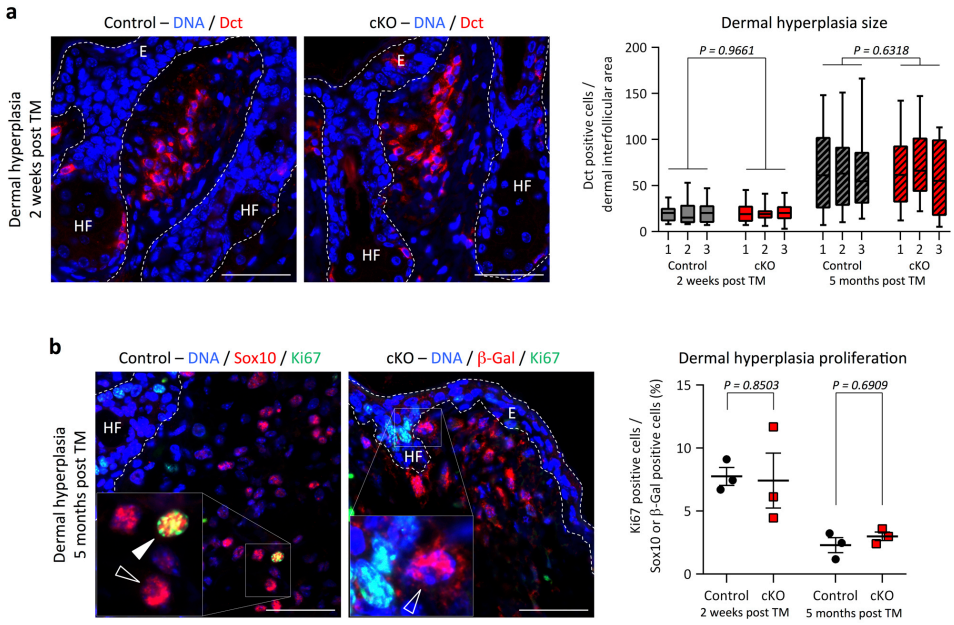

Figure 21 | Ezh2 is not required for dermal hyperplasia growth. (**a**) Immunofluorescent staining for Dct on trunk skin sections 2 weeks after conditional *Ezh2* ablation as in (**Figure 20**) to quantify dermal hyperplasia size. (**b**) Immunofluorescent staining for Sox10 (control) or β-Gal (cKO) and Ki67 on trunk skin sections 5 months after conditional *Ezh2* ablation as in (**Figure 20**) to quantify proliferation rates. White arrowhead, Sox10-positive / Ki67-positive cell; White open arrowheads, Sox10- or β-Gal-positive / Ki67-negative cells. Data are median ± 100% range of n ≥ 20 interfollicular areas, 3 animals per group (**a**), mean ± s.e.m. of n = 3 (**b**). P-values calculated with unpaired Student's t-test. Scale bars, 50µm.

4.2.5. Ezh2 function is essential for melanoma initiation

To assess a possible role of Ezh2 in tumorigenesis, *Ezh2* was conditionally deleted in *Tyr::N-Ras*^{Q61K} *Ink4a*$^{-/-}$ *Tyr::Cre*^{ERT2} *Ezh2*$^{lox/lox}$ *R26R::LacZ* mice before appearance of cutaneous tumors (Figure 22 a, b). While in control mice, many skin melanomas (Ø ≥ 2mm) emerged after approximately 5 months, appearance of tumors was delayed in *Ezh2* cKO animals leading to an increased skin melanoma-free survival (Figure 22c - e). At day of sacrifice, numbers of recombined skin melanomas were drastically reduced in *Ezh2* cKO mice compared to the total tumor load in controls (Figure 22f - h). In accordance with these data, melanoma-specific survival was significantly increased, independently of control type and sex of *Ezh2* cKO mice (Figure 22i, j).

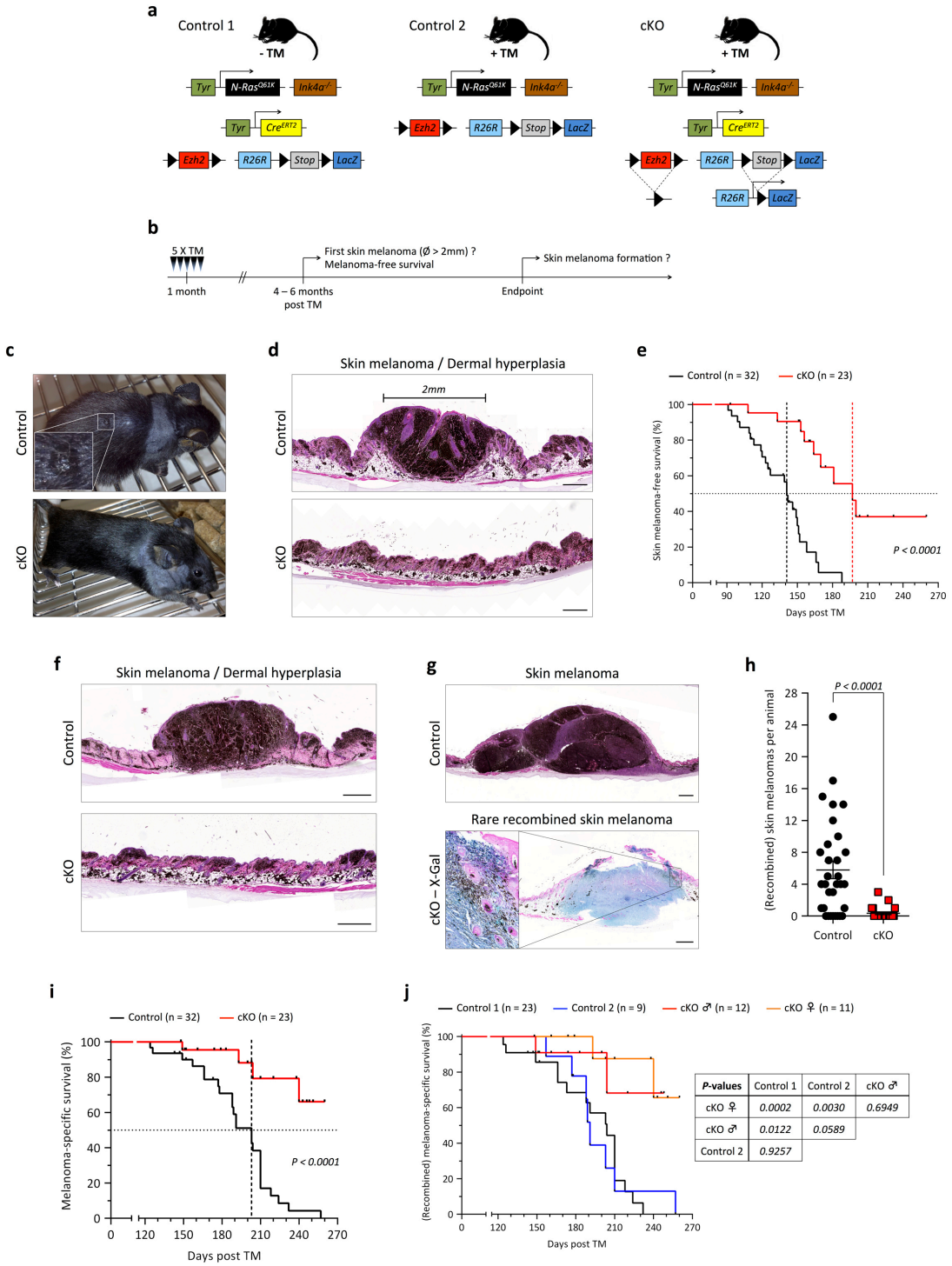

Figure 22 | Ezh2 function is essential for skin melanoma initiation. (**a**, **b**) Mouse genotypes and strategy used to analyze the effect of conditional *Ezh2* ablation in the melanocytic lineage of adult *Tyr::N-Ras*^{Q61K} *Ink4a*$^{-/-}$ mice. (**c**, **d**) Macroscopic pictures and H&E staining on skin sections of a control and a cKO littermate at 5 months post *Ezh2* ablation. (**e**) Kaplan-Meier curves comparing skin melanoma-free survival (skin melanoma = lesion Ø ≥ 2mm) of control and cKO mice taking into count all skin melanomas (recombined and non-recombined). (**f** - **h**) H&E staining on trunk skin sections of control and cKO mice (**f**) and a section of a whole mount X-Gal stained tumor of a cKO animal (**g**) to quantify (recombined) skin melanoma numbers at day of sacrifice (**h**). (**i**, **j**) Kaplan-Meier curves comparing melanoma-specific survival after conditional *Ezh2* ablation. For cKO mice only recombined skin melanomas were taken into count. Data are mean ± s.e.m. of n = 32 (Control), n = 23 (cKO). P-values calculated with Log-rank (Mantel-Cox) test (**e**, **i**, **j**), unpaired Student's t-test (**h**). Scale bars, 500µm.

Next, I addressed whether Ezh2 might also be implicated in melanoma progression after the onset of the disease. To this end, *Tyr::N-Ras*^{Q61K} *Ink4a*$^{-/-}$ *Tyr::Cre*^{ERT2} *Ezh2*$^{lox/lox}$ *R26R::LacZ* mice were individually monitored until appearance of skin melanomas. *Ezh2* deletion was then induced by TM application (Figure 23a, b, g). High recombination efficiency became apparent 1 month post TM application (Figure 23c, d). Concomitantly, this also led to an efficient loss of Ezh2 protein and H3K27me3 in recombined tumor cells (Figure 23e, f). Frequent assessment of the animals showed a marked increase of new melanomas per week in control animals. In striking contrast, the tumor load was stabilized in *Ezh2* cKO mice, in which virtually no new skin melanomas were emerging (Figure 23g). Thus, early genetic interference with Ezh2 activity prevents progression of benign dermal hyperplasia into malignant cutaneous melanoma, while Ezh2 depletion in established melanoma effectively stops emergence of further skin tumors.

4.2.6. Ezh2-targeted therapy interferes with melanoma progression

My findings indicate that interference with EZH2 activity might be a valid strategy for therapy of advanced melanoma. To test this hypothesis, I intended to treat mice with one of the preclinical EZH2 inhibitors (3.1.4.3. EZH2 function in hematopoietic malignancies). I chose to use GSK503 (Figure 5), because it exhibits favorable pharmacokinetics in mice (Béguelin et al., 2013). Independent of the genotype (*wt*, *Ink4a*$^{-/-}$, or *Tyr::N-Ras*^{Q61K} *Ink4a*$^{-/-}$), mice suffered from a tolerable and reversible weight loss of approximately 10% and, in rare cases, from development of ascites after prolonged treatment with GSK503. To investigate the effect of pharmacological Ezh2 inhibition on tumor progression, *Tyr::N-Ras*^{Q61K} *Ink4a*$^{-/-}$ mice were individually monitored until skin melanomas were detectable and subsequently treated daily, either with vehicle or GSK503 for 35 consecutive days (Figure 24a, b, d). This procedure reduced H3K27me3 levels in tumor and stromal cells without affecting Ezh2 levels, confirming inhibition of the catalytic function of Ezh2 (Figure 24c). Comparable to genetic ablation of *Ezh2*, GSK503 treatment drastically reduced the emergence of new skin melanomas over time after treatment start (Figure 24d).

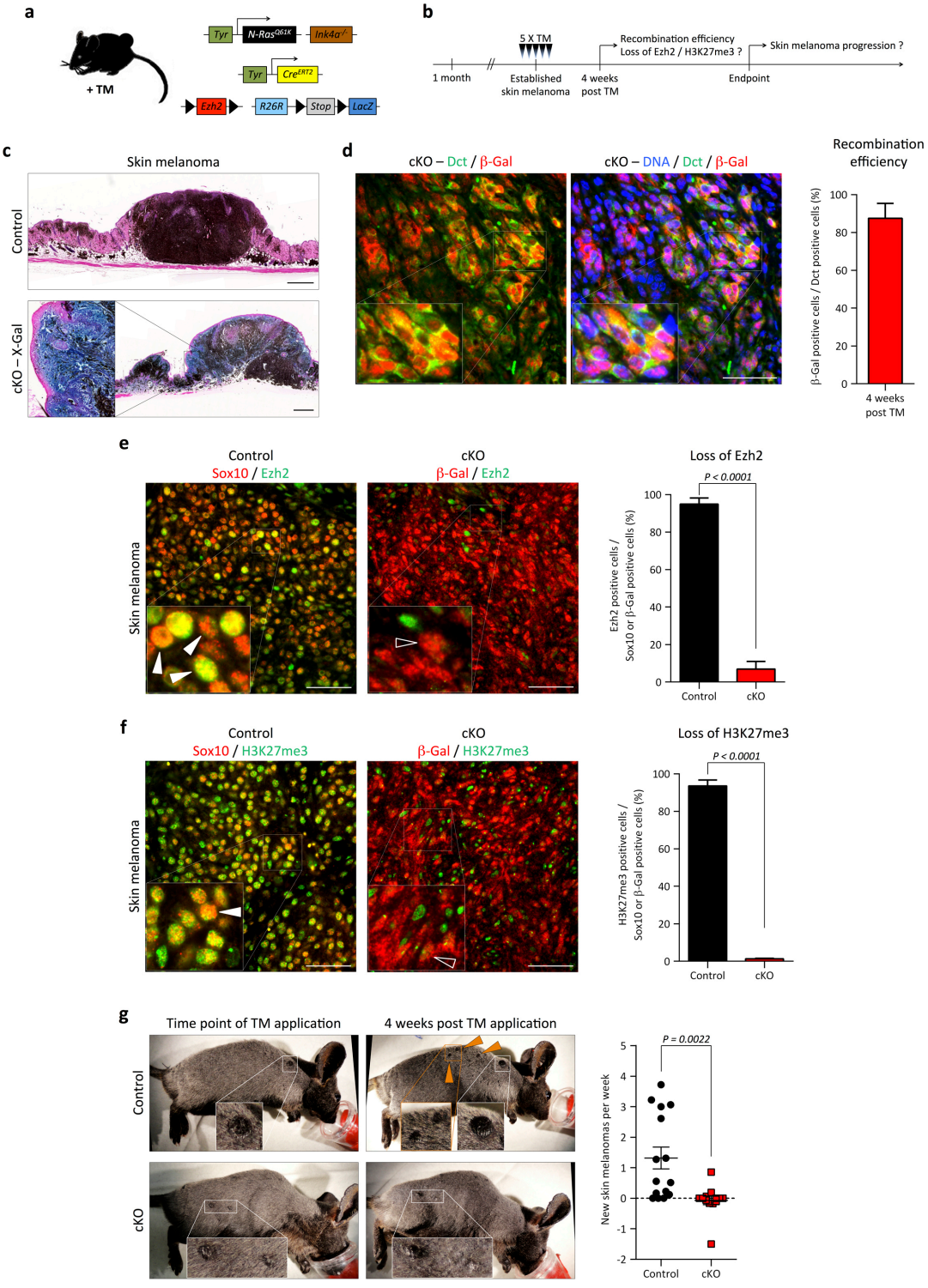

Figure 23 | *Ezh2* ablation in melanoma-bearing mice prevents disease progression. (**a**, **b**) Mouse genotypes and strategy used to analyze the effect of conditional *Ezh2* ablation on melanoma progression in *Tyr::N-Ras*^{Q61K} *Ink4a*$^{-/-}$ mice. (**c**) H&E staining on skin melanoma sections and sections of whole mount X-Gal stained tumors 4 weeks after conditional *Ezh2* ablation. (**d**) Immunofluorescent staining on skin melanoma sections for Dct and β-Gal 4 weeks post conditional *Ezh2* ablation to quantify a recombination efficiency. (**e**, **f**) Immunofluorescent staining on skin melanoma sections for Sox10 (control) or β-Gal (cKO) and Ezh2 (**e**) or H3K27me3 (**f**) 4 weeks post conditional *Ezh2* ablation to quantify Ezh2 and subsequent H3K27me3 depletion in melanoma cells. White arrowheads, Sox10-positive cells considered Ezh2- or H3K27me3-positive; White open arrowheads, β-Gal-positive cells considered Ezh2- or H3K27me3-negative. (**g**) Representative pictures of *Tyr::N-Ras*^{Q61K} *Ink4a*$^{-/-}$ mice at time point of Ezh2 ablation and 4 weeks later to quantify

formation of new skin melanomas per week. Orange arrowheads, new skin melanomas. Data are mean ± s.e.m. of n = 3 (**d** - **f**), mean ± s.e.m. of n = 15 (Control), n = 13 (cKO) (**g**). P-values calculated with unpaired Student's t-test. Scale bars, 500µm (**c**), 50µm (**d** - **f**).

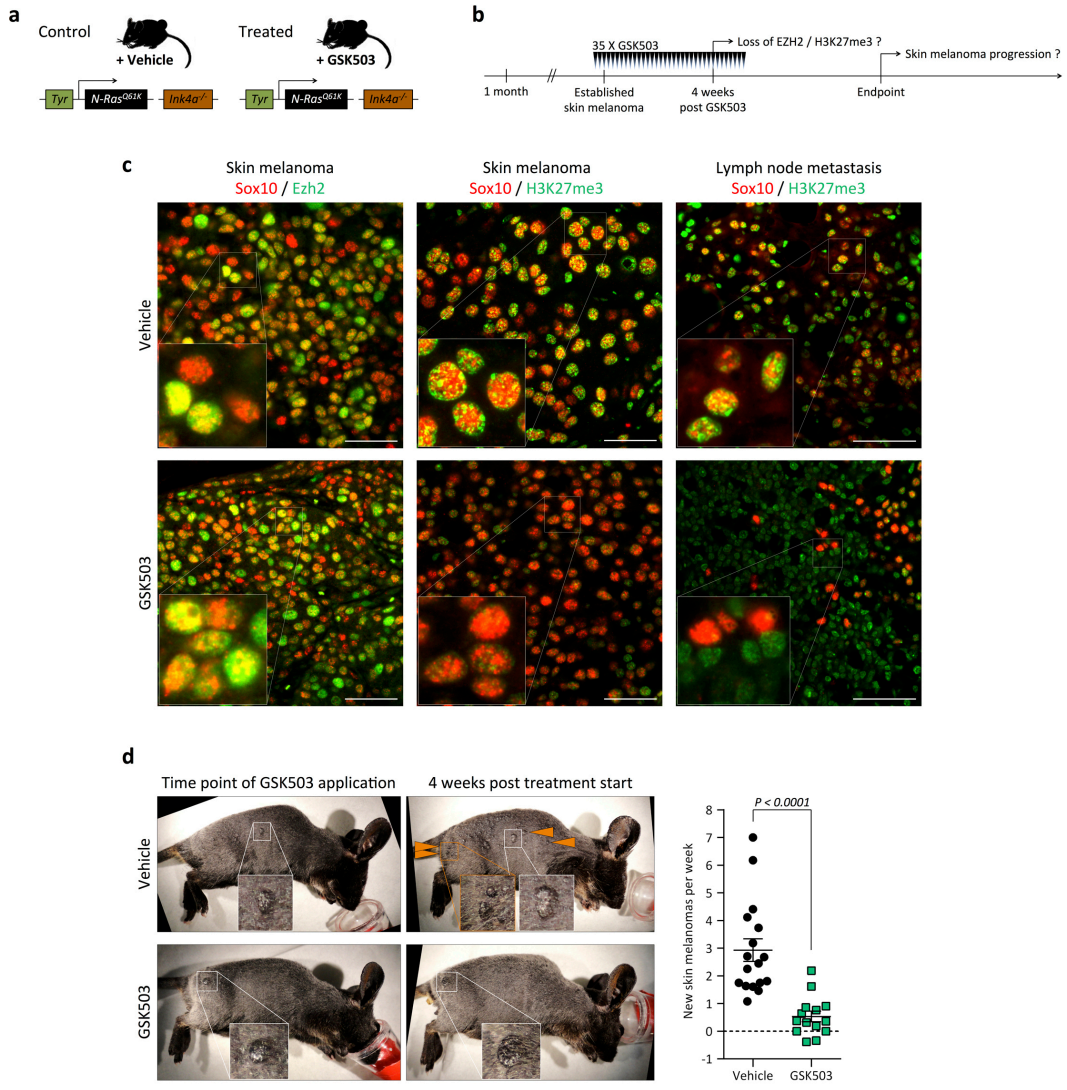

Figure 24 | Temporary GSK503 application in melanoma-bearing mice stabilizes disease. (**a**, **b**) Mouse genotypes and strategy used to analyze the effect of temporary GSK503 treatment on *Tyr::N-Ras*^{Q61K} *Ink4a*$^{-/-}$ mice with established melanoma. (**c**) Immunofluorescent staining on skin melanoma and lymph node sections for Sox10 and Ezh2 or H3K27me3 4 weeks after treatment start with vehicle or GSK503. (**d**) Representative pictures of *Tyr::N-Ras*^{Q61K} *Ink4a*$^{-/-}$ mice treated with vehicle or GSK503 at time point of treatment start and 4 weeks later to quantify formation of new skin melanomas per week. Orange arrowheads, new skin melanomas. Data are mean ± s.e.m. of n = 17 (Vehicle) n = 15 (GSK503). P-values calculated with unpaired Student's t-test. Scale bars, 50µm.

4.2.7. EZH2 is required for growth of human and murine melanoma

My findings demonstrate the requirement of Ezh2 for melanoma initiation. I hypothesized whether this might function through regulation of proliferation, since EZH2 has previously been associated with proliferation of human melanoma cells *in vitro* (Fan et al., 2011; Luo et al., 2012a; 2013). Interestingly, I observed a heterogeneity with respect to EZH2 expression in melanoma cells of both human biopsies as well as on *Tyr::N-Ras*^{Q61K} *Ink4a*$^{-/-}$ skin tumors and metastases, ranging from high EZH2 expression to almost background levels (Figure 16). EZH2 highly expressing cells significantly correlated with KI67-positive cells, implicating EZH2-regulated proliferation of melanoma at primary tumor and metastatic sites (Figure 25). To address the relevance of these findings for melanoma growth, I first blocked EZH2 activity in human melanoma cell cultures (Zipser et al., 2011), either by RNA interference-mediated silencing (RNAi) or by chemical inhibition using GSK503. In agreement with my *in vivo* findings, RNAi effectively reduced EZH2, while GSK503 application did not affect EZH2 levels. Both approaches, however, led to a considerable loss of H3K27me3 (Figure 26a, b). Notably, neither RNAi nor prolonged GSK503 application for 8 days did affect cell survival (Figure 26c, d). However, suppressing EZH2 activity stimulated a G1 cell cycle arrest (Figure 26e, f) and slowed down cell growth in culture (Figure 26g, h).

To functionally study EZH2-regulated proliferation *in vivo*, I quantified proliferative cells in tumors of *Tyr::N-Ras*^{Q61K} *Ink4a*$^{-/-}$ mice, either after *Ezh2* cKO or GSK503 application. Both approaches led to a striking reduction of proliferative tumor cells (Figure 27). I next engrafted murine B16-F10 melanoma cells into *C57Bl/6* mice (Figure 28a). Depletion of Ezh2 function using RNAi or GSK503 significantly reduced global H3K27me3 levels *in vivo* (Figure 28b - e). Importantly, EZH2 inactivation led to an inhibition of tumor growth (Figure 28b, f). Finally, I engrafted *Tyr::N-Ras*^{Q61K} *Ink4a*$^{-/-}$ skin melanoma (RIM)-derived cells into athymic nude *Foxn1*$^{nu/nu}$ mice (Figure 29a, h, k). These RIM allografts were confirmed to express various melanocytic markers, reassuring their melanoma origin (Figure 30). RIMs were first allowed to reach a considerable size for 15 to 25 days after transplantation (Figure 29a, f, j, m). Subsequent TM-induced *Ezh2* cKO in growing RIMs completely abolished Ezh2 protein and H3K27me3, while GSK503 application significantly reduced H3K27me3 (Figure 29b - e). This was associated with an inhibition of further tumor growth in both cKO and GSK503-treated samples (Figure 29b, f, g, i, j, l, m) highlighting Ezh2 inactivation as an efficient strategy for blocking melanoma growth.

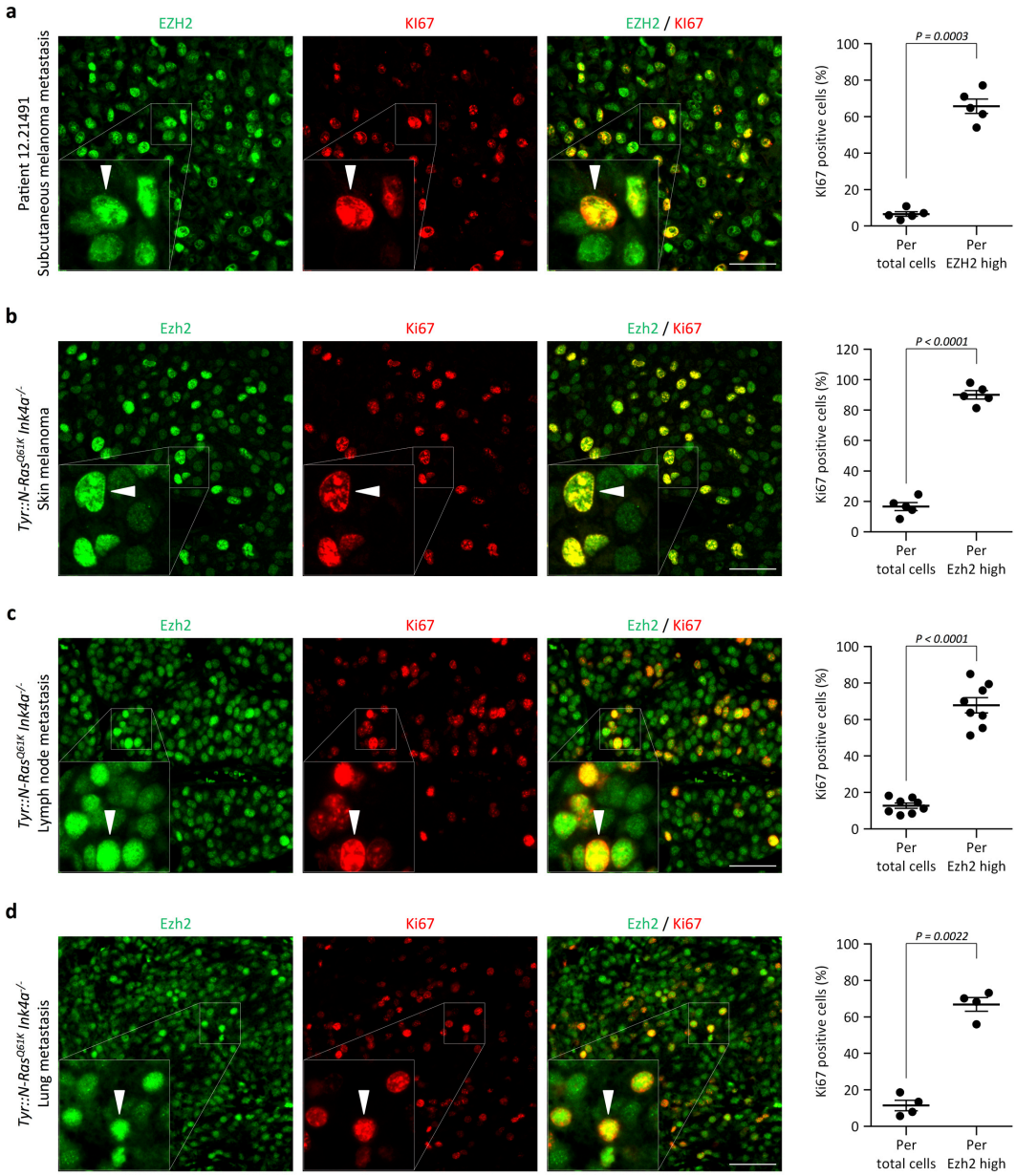

Figure 25 | Heterogeneous high EZH2 expression correlates with KI67 positivity. (**a** - **d**) Immunofluorescent staining on human melanoma metastases sections (**a**) and melanoma sections of *Tyr::N-Ras*^{Q61K} *Ink4a*$^{-/-}$ mice (**b** - **d**) for EZH2 and KI67 to quantify a correlation between high EZH2 expression and KI67 positivity. White arrowheads, EZH2-high cells considered KI67-positive. Data are mean ± s.e.m. of n = 5 (**a**, **b**), mean ± s.e.m. of n = 8 (**c**), mean ± s.e.m. of n = 4 (**d**). P-values calculated with unpaired Student's t-test. Scale bars, 50µm.

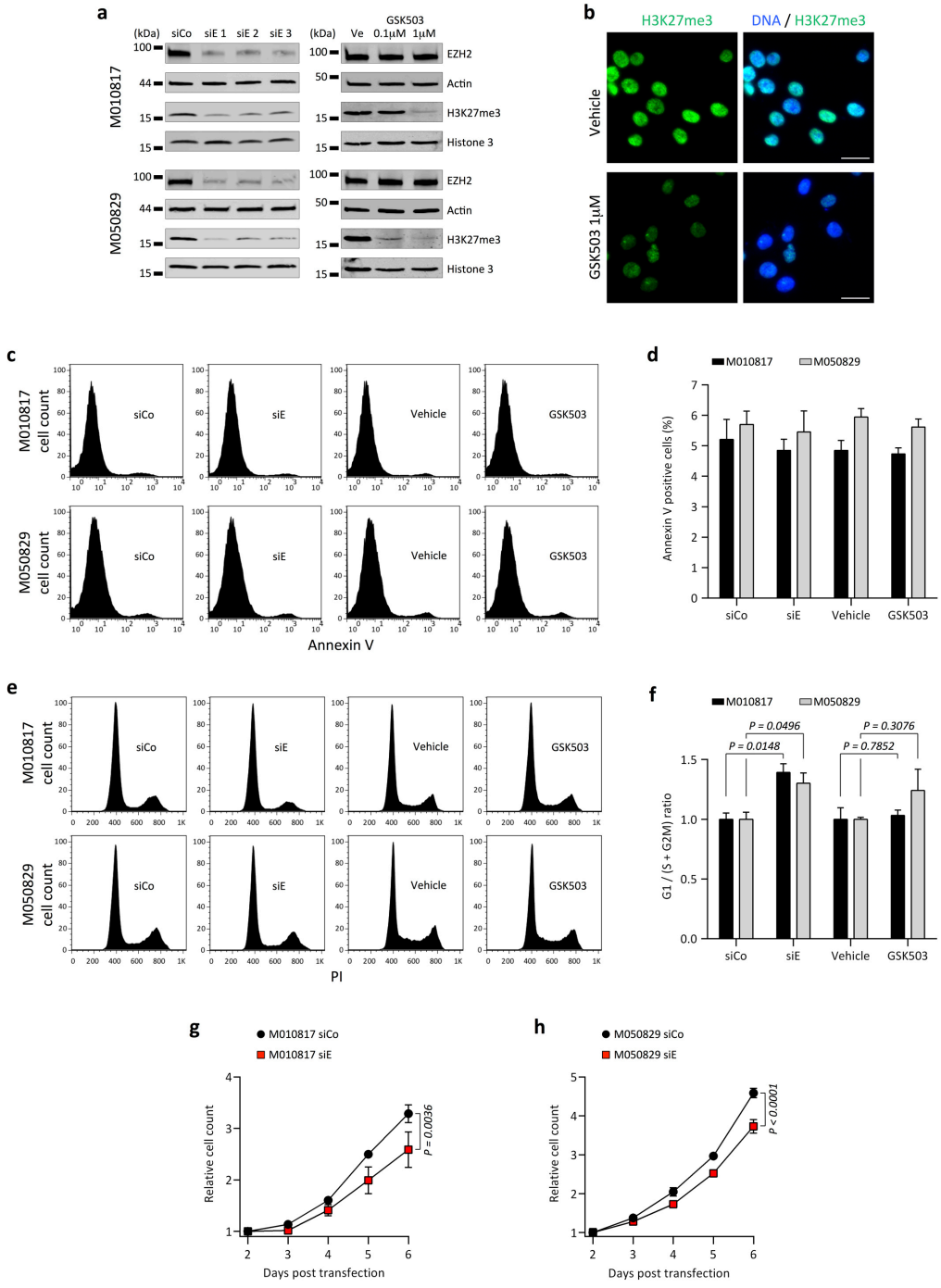

Figure 26 | EZH2 inactivation in human melanoma cells interferes with cell growth. (**a**) Western blot for EZH2 protein and H3K27me3 on whole cell lysates from 2 melanoma cell cultures (M010817, M050829) after *EZH2* depletion with 3 different siEs or EZH2 inhibition using GSK503. (**b**) Immunofluorescent staining on M010817 for H3K27me3 after GSK503 treatment. (**c**, **d**) FACS analysis of M010817 and M050829 for Annexin V positivity after *EZH2* depletion with siE or EZH2 inhibition using GSK503 to quantify induced apoptosis. (**e**, **f**) Cell cycle profiles of M010817 and M050829 using PI after *EZH2* depletion with siE or EZH2 inhibition using GSK503 to quantify a G1 / (S + G2M) ratio. (**g**, **h**) Growth of M010817 and M050829 after EZH2 depletion with siE. PI, propidium iodide; Ve, vehicle. Data are mean ± s.e.m. of n = 3. P-values calculated with unpaired Student's t-test (**f**), ANOVA and Fisher's LSD-test (**g**, **h**). Scale bars, 25µm.

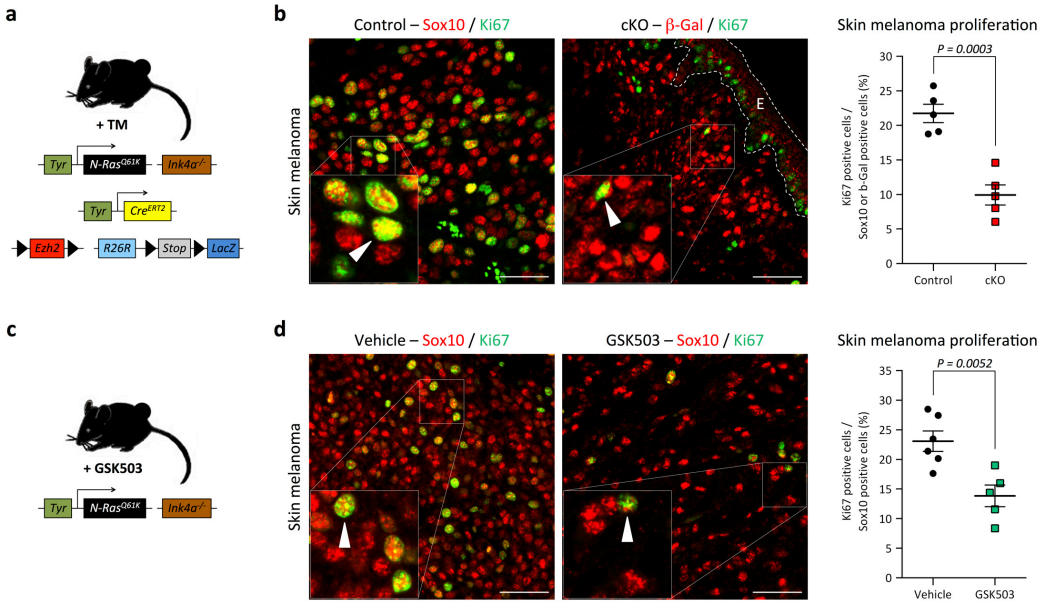

Figure 27 | *Ezh2* ablation and GSK503 treatment attenuates melanoma cell proliferation *in vivo*. (**a**) Mouse genotypes and strategy as in (**Figure 23**) used to analyze the effect of conditional *Ezh2* ablation on melanoma proliferation in *Tyr::N-Ras*^{Q61K} *Ink4a*$^{-/-}$ mice. (**b**) Immunofluorescent staining on skin melanoma sections for Sox10 (control) or β-Gal (cKO) and Ki67 4 weeks after conditional *Ezh2* ablation to quantify a proliferation rate. White arrowheads, Sox10- or β-Gal-positive / Ki67-positive cells. (**c**) Mouse genotypes and strategy as in (**Figure 24**) used to analyze the effect of temporary GSK503 treatment on melanoma proliferation in *Tyr::N-Ras*^{Q61K} *Ink4a*$^{-/-}$ mice. (**d**) Immunofluorescent staining on skin melanoma sections for Sox10 and Ki67 4 weeks after treatment start with vehicle or GSK503 to quantify a proliferation rate. White arrowheads, Sox10-positive / Ki67-positive cells. Data are mean ± s.e.m. of n = 5 (**b**), mean ± s.e.m. of n = 6 (Vehicle), n = 5 (GSK503) (**d**). P-values calculated with unpaired Student's t-test. Scale bars, 50µm.

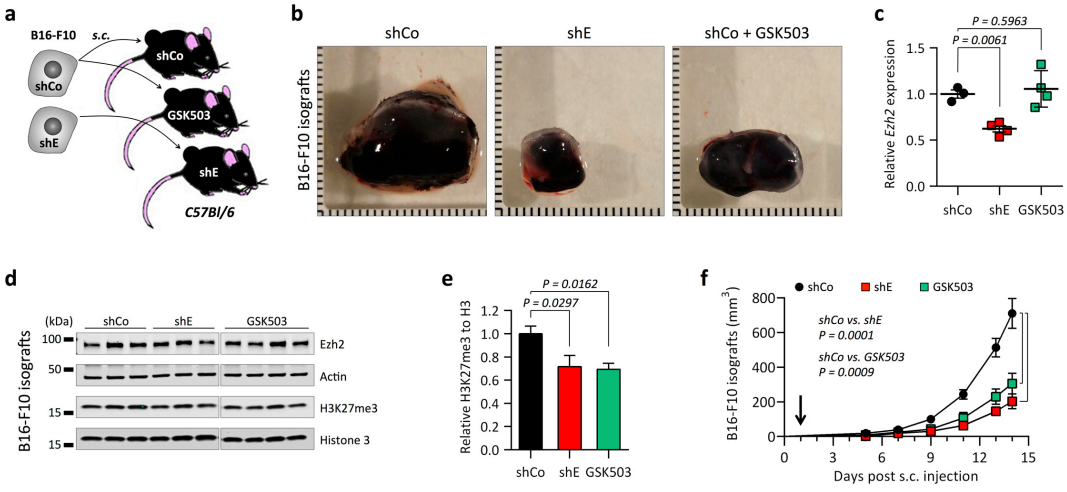

Figure 28 | Ezh2 inactivation interferes with murine B16-F10 melanoma growth. (**a**) Mouse genotypes and strategy used to s.c. engraft B16-F10 cells following *Ezh2* silencing with shE to analyze the effect of *Ezh2* depletion and GSK503 treatment on melanoma growth. (**b**) Representative macroscopic pictures of shCo, shE, and GSK503-treated B16-F10 isografts. (**c**) RT-qPCR for Ezh2 mRNA expression on lysed shCo, shE, and GSK503-treated B16-F10 tumors. (**d**, **e**) Western blot for Ezh2 protein and H3K27me3 on lysed shCo, shE, and GSK503-treated B16-F10 tumors to quantify loss of H3K27me3. (**f**) Growth of shCo, shE, and GSK503-treated B16-F10 isografts. Black arrow, GSK503 treatment start. s.c., subcutaneous. Data are mean ± s.e.m. of n = 3 (shCo), n = 4 (shE, GSK503) (**c**), mean ± s.e.m. of n = 3 (shCo, shE), n = 4 (GSK503) (**d**, **e**), mean ± s.e.m. of n = 5 (**f**). P-values calculated with ANOVA and Fisher's LSD-test. Scale bars, 1mm.

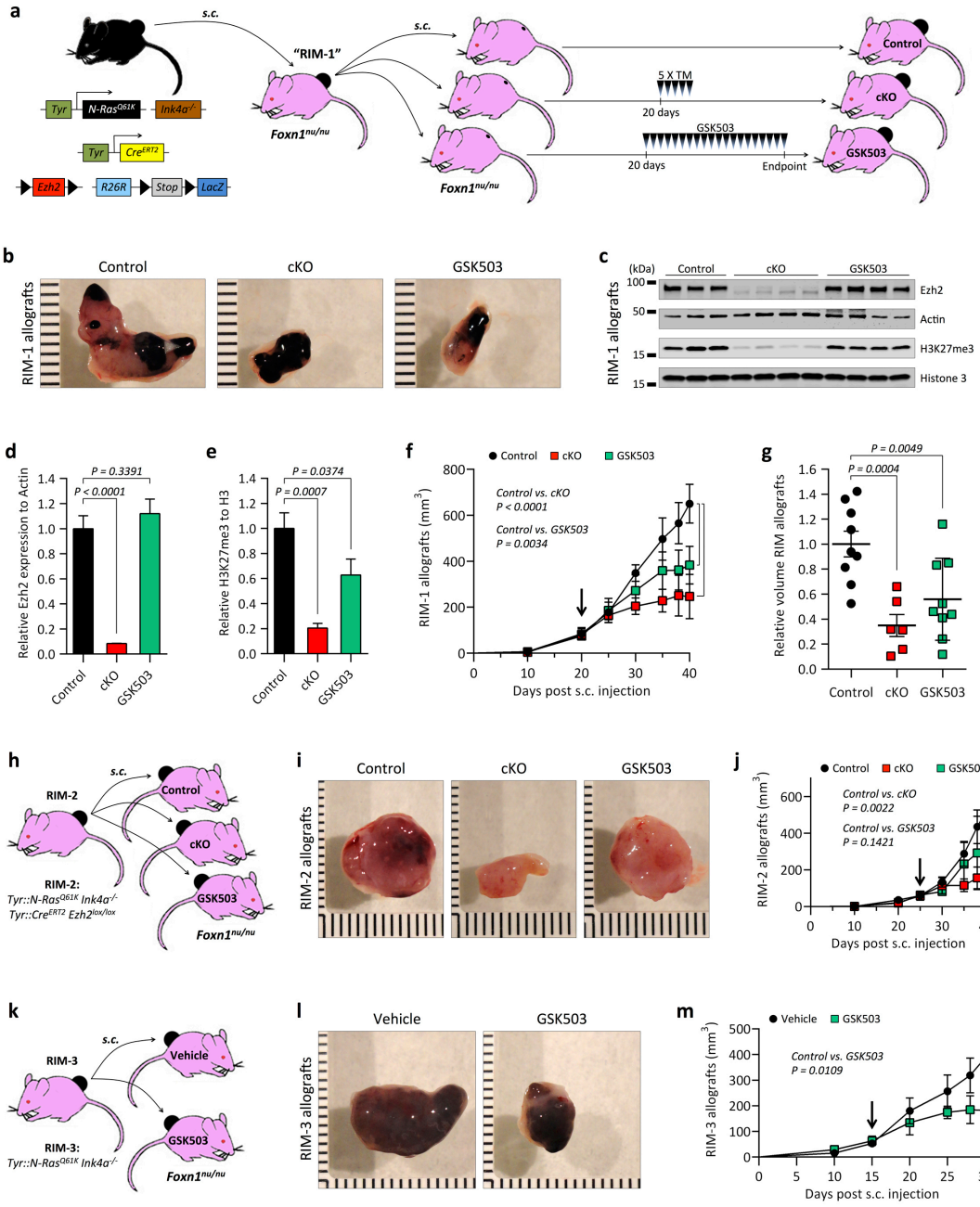

Figure 29 | Ezh2 inactivation prevents growth of allografted *Tyr::N-Ras^{Q61K} Ink4a$^{-/-}$* melanoma. (**a**, **h**, **k**) Mouse genotypes and strategy used to s.c. engraft and expand *Tyr::N-Ras^{Q61K} Ink4a$^{-/-}$* mice-derived melanoma cells in *Foxn1$^{nu/nu}$* animals to analyze the effect of conditional *Ezh2* ablation and GSK503 treatment on melanoma growth. (**b**) Representative macroscopic pictures of control, cKO, and GSK503-treated RIM-1 allografts. (**c** - **e**) Western blot for Ezh2 protein and H3K27me3 on lysed tumors to quantify loss of Ezh2 and H3K27me3. (**f**, **g**) Growth of control, cKO, and GSK503-treated RIM-1 allografts (**f**) and relative tumor volume of RIM-1, RIM-2, and RIM-3 allografts at endpoints (**g**). (**i**, **j**) Representative macroscopic pictures and growth of control, cKO, and GSK503-treated RIM-2 allografts. (**l**, **m**) Representative macroscopic pictures and growth of vehicle- and GSK503-treated RIM-3 allografts. Black arrows, time points of TM application / start of GSK503 treatment. RIM, *Tyr::N-Ras^{Q61K} Ink4a$^{-/-}$* melanoma. Data are mean ± s.e.m. of n = 3 (Control), n = 4 (cKO, GSK503) (**c** - **f**), mean ± s.e.m. of n = 9 (Control, GSK503), n = 6 (cKO) (**g**), mean ± s.e.m. of n = 3 (**j**, **m**). P-values calculated with ANOVA and Fisher's LSD-test. Scale bars, 1mm.

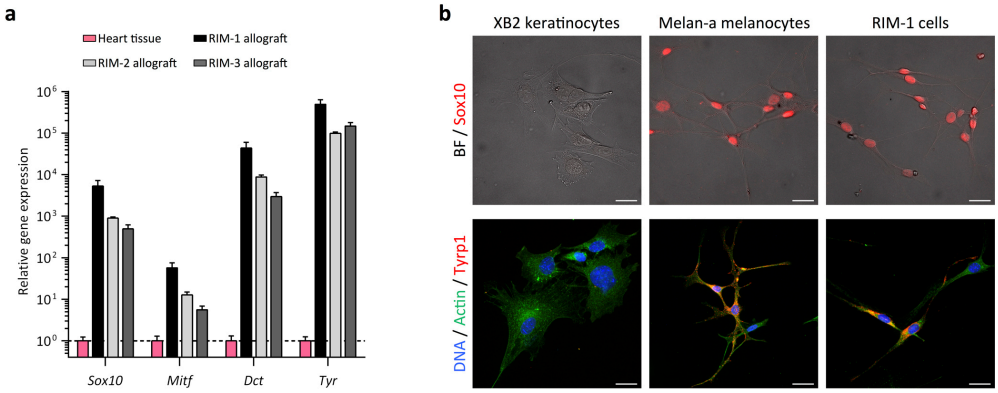

Figure 30 | RIM allografts are of a melanoma origin. (**a**) RT-qPCR for melanocytic lineage genes on lysed heart tissue, RIM-1, RIM-2, and RIM-3 tumors. (**b**) Immunofluorescent staining on XB2, Melan-a, and RIM-1 cells for Sox10 and Tyrp1. BF, bright field. Data are mean ± s.e.m. of n = 3. P-values calculated with ANOVA and Fisher's LSD-test. Scale bars, 25µm.

4.2.8. EZH2 inactivation prevents metastatic spread of melanoma

When depleting Ezh2 in my melanoma model before appearance of skin melanoma (Figure 31a, b), I observed that control mice, apart from skin tumors, frequently developed Sox10-positive melanoma metastases. However, conditional loss of *Ezh2* almost fully prevented the generation of both lymph node and distant lung metastases, drastically increasing metastases-free survival (Figure 31c - e). Distant metastases likely arise from primary skin melanomas. Thus, a lack of metastases was expected, since early *Ezh2* ablation also prevented emergence of skin tumors (Figure 22). In order to functionally analyze metastatic spread from skin tumors, I inactivated Ezh2 function in *Tyr::N-Ras*^{Q61K} *Ink4a*$^{-/-}$ mice already bearing skin tumors (Figure 32a - c). Strikingly, control animals consistently developed metastases, while *Ezh2* cKO mice exhibited a significant reduction in melanoma-positive lymph nodes (Figure 32d) and a virtual absence of distant metastases in the lung (Figure 32e). Consequently, *Ezh2* cKO mice displayed a highly increased melanoma-specific survival compared to controls (Figure 32f). Likewise, GSK503-mediated Ezh2 inhibition counteracted formation of lymph node and lung metastases (Figure 32g, h). Importantly, temporary inhibition of Ezh2 prolonged melanoma-specific survival compared to vehicle-treated animals, resulting in doubling of the median survival time (Figure 32i).

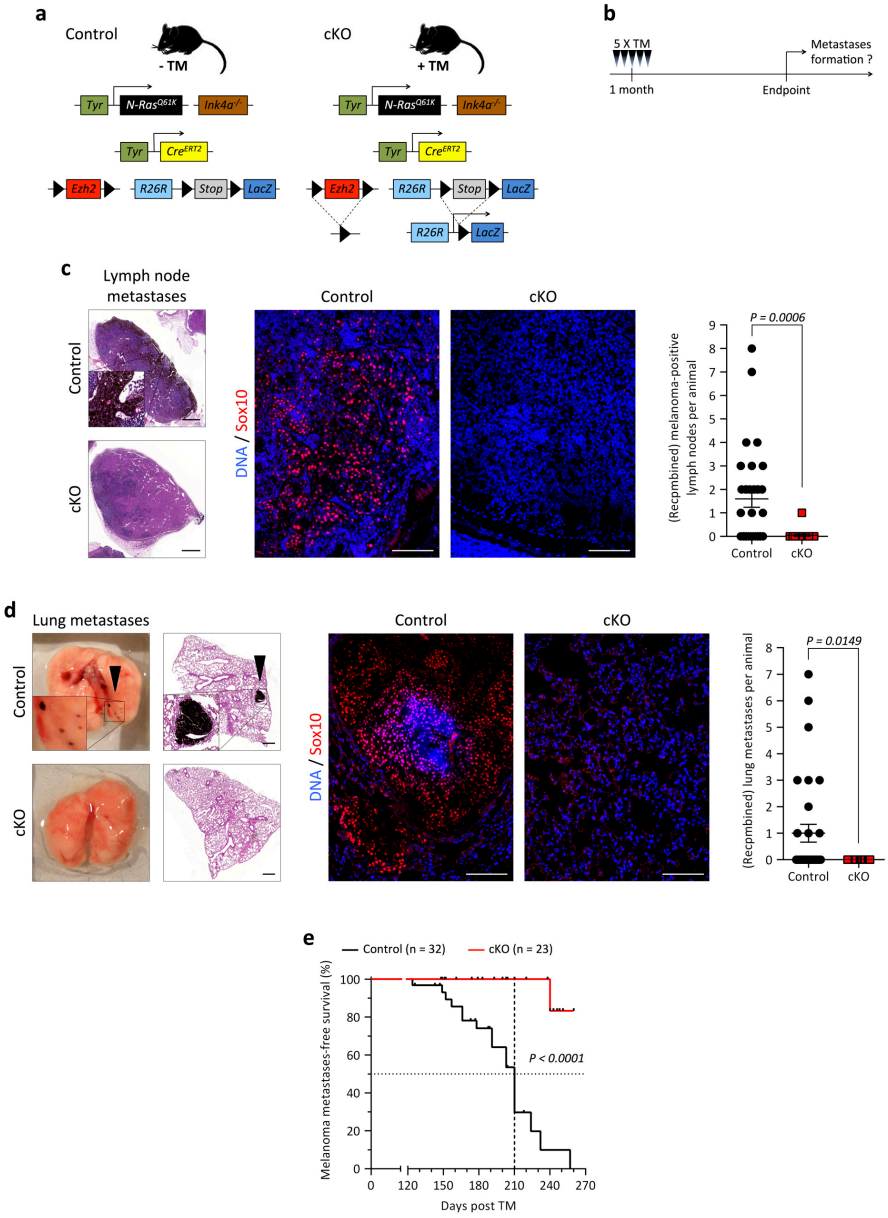

Figure 31 | *Ezh2* ablation before onset of melanomagenesis prevents metastases formation. (**a**, **b**) Mouse genotypes and strategy used to analyze the effect of conditional *Ezh2* ablation on metastases formation in *Tyr::N-Ras*^{Q61K} *Ink4a*$^{-/-}$ mice. (**c**, **d**) Metastases count at day of sacrifice in lymph nodes (**c**) and lung (**d**) of control and cKO animals using macroscopic pictures, H&E staining, and Sox10 staining on sections. Black arrowheads, lung metastases. (**e**) Kaplan-Meier curves comparing melanoma metastases-free survival after conditional *Ezh2* ablation. Data are mean ± s.e.m. of n = 32 (Control), n = 23 (cKO). P-values calculated with unpaired Student's t-test (**c**, **d**), Log-rank (Mantel-Cox) test (**e**). Scale bars, 500µm (H&E in **c**, **d**), 100µm (immunofluorescence in **c**, **d**).

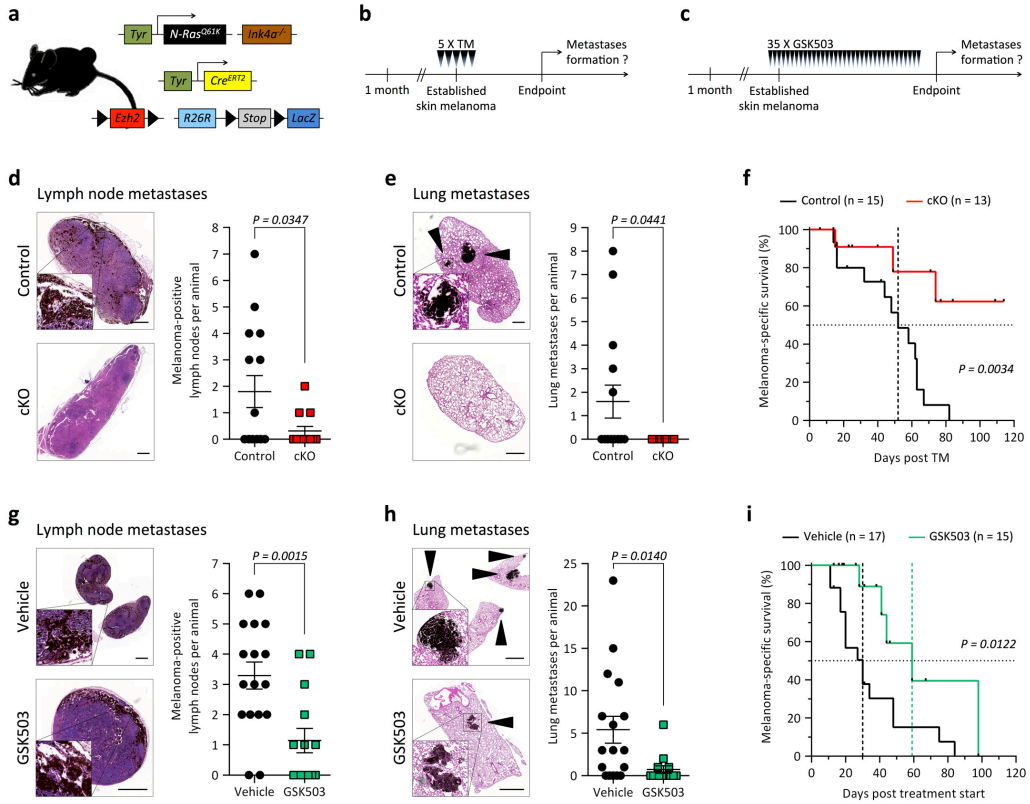

Figure 32 | EZH2 function is required for metastatic progression of *Tyr::N-Ras^{Q61K} Ink4a$^{-/-}$* cutaneous melanoma. (**a** - **c**) Mouse genotypes and strategies used to analyze the effect of conditional *Ezh2* ablation and GSK503 treatment on metastatic spread of *Tyr::N-Ras^{Q61K} Ink4a$^{-/-}$* skin melanoma. (**d**, **e**) Metastases count at day of sacrifice in lymph nodes (**d**) and lung (**e**) of control and cKO animals using macroscopic pictures, H&E staining, and Sox10 staining on sections. Macroscopic pictures and Sox10 staining performed as in (**Figure 31**). Black arrowheads, lung metastases. (**f**) Kaplan-Meier curves comparing melanoma-specific survival after conditional *Ezh2* ablation. (**g**, **h**) Metastases count at day of sacrifice in lymph nodes (**g**) and lung (**h**) of vehicle- and GSK503-treated animals using macroscopic pictures, H&E staining, and Sox10 staining on sections. Macroscopic pictures and Sox10 staining performed as in (**Figure 31**). Black arrowheads, lung metastases. (**i**) Kaplan-Meier curves comparing melanoma-specific survival during and after GSK503 treatment. Data are mean ± s.e.m. of n = 15 (Control) n = 13 (cKO) (**d**, **e**), mean ± s.e.m. of n = 17 (Vehicle) n = 15 (GSK503) (**g**, **h**). P-values calculated with unpaired Student's t-test (**d**, **e**, **g**, **h**), Log-rank (Mantel-Cox) test (**f**, **i**). Scale bars, 500µm (**d**, **e**), 1mm (**g**, **h**).

4.2.9. EZH2 propagates features favorable for melanoma metastasis

Metastatic spread of a human primary melanoma is usually initialized by gain of invasive capacity, which allows a cell to evade from the primary tumor site (Gaggioli and Sahai, 2007; Tam and Weinberg, 2013). Accordingly, both RNAi and drug-mediated inhibition of EZH2 significantly reduced the invasive capacity of human melanoma cell cultures in ECM-mimicking collagen layers referred to as Boyden chambers (Figure 33a). Next I used melanoma cell cultures derived from two distinct patients to perform a comparative global gene expression analysis of control versus EZH2-depleted cells (Figure 34). Cluster analysis of transcriptionally regulated genes indicated that reducing EZH2 levels affected expression of

genes involved, among others, in cytoskeleton remodeling, ECM remodeling, and EMT (Figure 33b). In support of these findings, I observed a gain of melanocyte markers and a loss of NCSC / EMT genes when depleting EZh2 in murine B16-F10 melanoma cells (Figure 33c). Finally, when inoculating B16-F10 cells i.v. into *C57Bl/6* mice, RNAi and importantly also GSK503 treatment drastically reduced lung nodule counts (Figure 33d, e). In summary, EZH2 is crucial throughout several steps of melanoma metastasis, such as EMT and homing to distant sites. Therefore, targeting Ezh2 *in vivo* efficiently prevented metastasis formation in the transgenic melanoma model, and pharmacological EZH2 inhibition might represent a promising treatment strategy in preventing metastasis in patients.

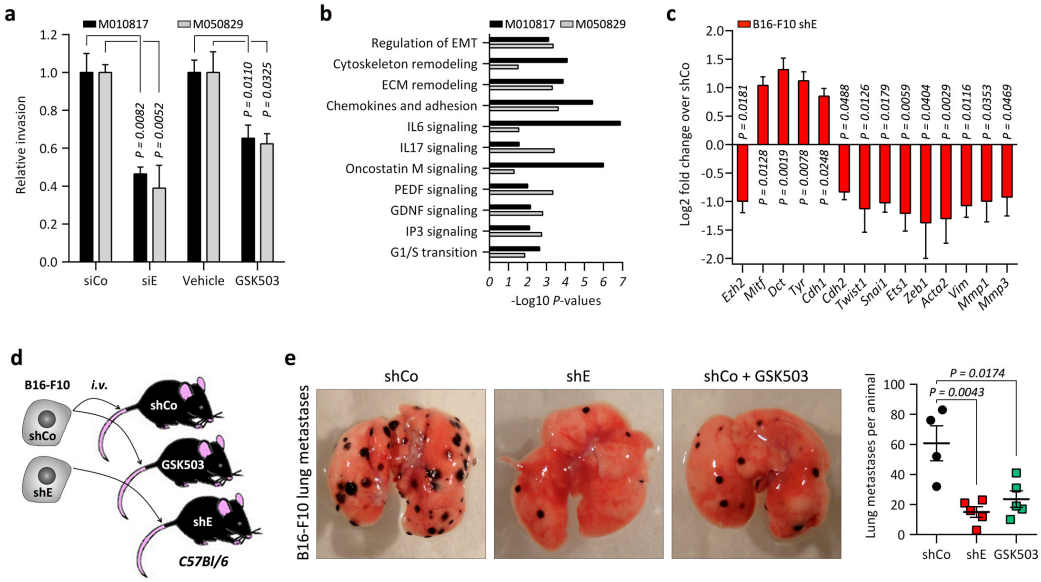

Figure 33 | EZH2 is required for several features of metastatic progression. (**a**) Quantification of relative invasive capacity of M010817 and M050829 following *EZH2* depletion with siE or EZH2 inhibition using GSK503. (**b**) -Log10 P-values based on gene ontology analysis using gene signatures of M010817 and M050829 after *EZH2* depletion with siE (**Figure 34**). (**c**) RT-qPCR for melanocyte differentiation genes and EMT genes on B16-F10 after *Ezh2* depletion with shE. (**d**) Mouse genotypes and strategy used to i.v. engraft B16-F10 cells following *Ezh2* silencing using shE to analyze the effect of *Ezh2* depletion and GSK503 treatment on metastases formation. (**e**) Representative macroscopic pictures of lungs from vehicle and GSK503-treated (from day 1 on until endpoint) animals to quantify lung metastases after i.v. engraftment of shCo and shE B16-F10 cells. ECM, extra cellular matrix; EMT, epithelial to mesenchymal transition; i.v., intravenous. Data are mean ± s.e.m. of n = 4 (**a**), mean ± s.e.m. of n = 3 (**c**), mean ± s.e.m. of n = 4 (shCo), n = 5 (shE, GSK503) (**e**). P-values calculated with unpaired Student's t-test (**a**), ANOVA and Fisher's LSD-test (**c**, **e**).

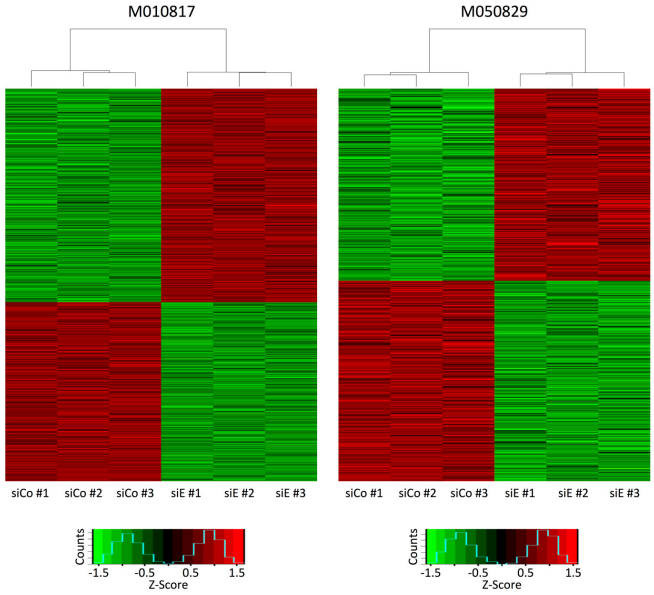

Figure 34 | Gene expression array heat maps. Heat maps of differentially expressed genes in M010817 and M050829 after *EZH2* depletion with siE showing normalized expression values of 3 biological replicates. NCBI Gene Expression Omnibus archive accession code: GSE63165.

4.2.10. EZH2 represses a set of genes connected to patient survival

To further characterize the transcriptional programs controlled by EZH2 activity in melanoma, based on the gene expression arrays (Figure 34), I first defined genes significantly changed in both patient-derived cell cultures after EZH2 depletion (Figure 35a). Next, I performed TCGA-based unbiased analyses to determine the clinical relevance of these EZH2-regulated genes. I correlated expression levels of each of these genes with disease outcome in patients using RNAseq and clinical data from TCGA. Strikingly, for 24% of all genes commonly upregulated upon *EZH2* silencing, high expression levels in patients were associated with improved survival, while only 5.3% correlated with poor survival (Figure 35b; Table 3). Furthermore, for 19.6% of all genes commonly downregulated after *EZH2* silencing, low expression levels in patients correlated with adverse survival (Figure 35c). Thus, EZH2 activity predominantly suppresses a transcriptional program beneficial for human patients and is associated with activation of a considerable fraction of genes linked to poor survival.

The genes upregulated upon *EZH2* silencing and associated with improved patient survival were, first, confirmed to be transcriptionally elevated after *EZH2* depletion in human melanoma cell cultures. Indeed, mRNA of all 18 genes (24% in Figure 35b) was significantly increased after *EZH2* depletion

(Figure 35d; Table 4). Second, ChIP assays for H3K27me3 were performed to determine whether these 18 genes are direct targets of EZH2-mediated histone methylation. Intriguingly, 17 out of these 18 analyzed genes exhibited promoter regions highly enriched for H3K27me3 in comparison to *GAPDH* promoter as negative control, indicating that these genes are targets of EZH2-dependent transcriptional repression (Figure 35e; Table 4).

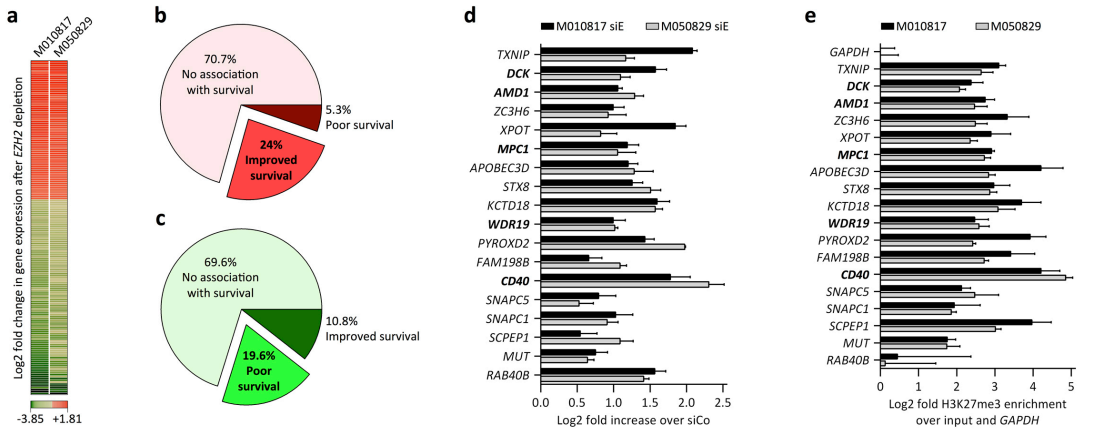

Figure 35 | EZH2 target genes are linked to improved melanoma patient survival. (**a**) Gene expression signature of M010817 and M050829 after *EZH2* depletion using siE. Average Log2 fold change values of 3 siE replicates compared to 3 siCo replicates in (**Figure 34**) and significantly changed in both cell lines are shown. (**b**, **c**) Summary of TCGA-based unbiased analyses of genes upregulated (**b**; **Table 3**) or downregulated (**c**) in (**a**). For upregulated genes in (**a**), specimens with high RNAseq reads for the corresponding genes were compared to specimens with low RNAseq reads. For downregulated genes in (**a**), specimens with low RNAseq reads for the corresponding genes were compared to specimens with high RNAseq reads. (**d**) RT-qPCR for genes associated with improved survival in (**b**) on M010817 and M050829 after *EZH2* depletion using siE (relative to *GAPDH*). (**e**) H3K27me3 ChIP and subsequent qPCR for promoters of genes associated with improved survival in (**b**) on untreated M010817 and M050829. Genes highlighted in bold were functionally analyzed. Data are mean ± s.e.m. of n = 3 (**d**), mean ± s.e.m. of n = 4 (**e**). P-values calculated with ANOVA and Fisher's LSD-test.

Table 3 | TCGA-based association of high gene expression in (Figure 35a) with melanoma patient survival.

Gene	Association with patient survival	Gene	Association with patient survival
TXNIP	improved	*MXRA7*	NS
WDTC1	NS	*DIS3L*	NS
ACO2	poor	*NFIC*	NS
DCK	improved	*APOBEC3D*	improved
TMEM143	NS	*AGPAT2*	poor
WDR34	poor	*KREMEN1*	NS
CAMKK2	NS	*SNAPC5*	improved
ZDHHC1	NS	*GNG7*	NS
ZC3H6	improved	*EIF2C4*	NS
XPOT	improved	*IL17RC*	NS
MPC1	improved	*MSRB2*	NS
CNN2	NS	*FAM198B*	improved
QPRT	NS	*SNAPC1*	improved
TCFL5	NS	*TMEM129*	NS
LAMTOR1	NS	*CDC42EP4*	NS
HIBADH	NS	*HDAC5*	NS
DDR2	NS	*NNT*	NS
HSBP1L1	NS	***CD40***	improved
ECSIT	NS	*DNAJC4*	NS
MCAT	NS	*SAYSD1*	NS
DCAKD	NS	*STX8*	improved
CYP27A1	NS	*SWAP70*	NS
CRYL1	NS	*MUT*	improved
XYLT2	NS	*SCPEP1*	improved
TMEM161A	NS	*RETSAT*	poor
REEP6	NS	*PYROXD2*	improved
RBFOX2	NS	*HDHD2*	NS
R3HDM2	NS	*TGS1*	NS
KCTD18	improved	*WBP1L*	NS
BCAS3	NS	*APOOL*	NS
NFIA	NS	*MCOLN3*	NS
FAM210B	NS	*ANKRD44*	NS
ADAM10	NS	*ST6GALNAC2*	NS
WDR19	improved	*TMEM140*	NS
AMD1	improved	*UBE3B*	NS
STARD5	NS	*GAS2L3*	NS
IER5	NS	*RAB40B*	improved
CTSF	NS		

Genes highlighted in bold were functionally analyzed. improved, improved survival for specimens with high RNAseq reads for a specific gene compared to specimens with low RNAseq reads; poor, poor survival for specimens with high RNAseq reads for a specific gene compared to specimens with low RNAseq reads; NS, no significant difference between the high and the low group.

Table 4 | P-values related to (Figure 35d, e).

Figure 35d	*P*-values		Figure 35e	*P*-values	
Gene	M010817	M050829	Gene	M010817	M050829
TXNIP	*< 0.0001*	*0.0047*	*TXNIP*	*0.0003*	*0.0030*
DCK	*0.0009*	*0.0029*	***DCK***	*0.0051*	*0.0039*
AMD1	*0.0080*	*0.0017*	***AMD1***	*0.0012*	*0.0045*
ZC3H6	*0.0052*	*0.0329*	*ZC3H6*	*0.0189*	*0.0036*
XPOT	*0.0041*	*0.0288*	*XPOT*	*0.0195*	*0.0022*
MPC1	*0.0056*	*0.0177*	***MPC1***	*0.0018*	*0.0016*
APOBEC3D	*0.0075*	*0.0125*	*APOBEC3D*	*0.0114*	*0.0012*
STX8	*0.0065*	*0.0039*	*STX8*	*0.0088*	*0.0011*
KCTD18	*0.0016*	*0.0002*	*KCTD18*	*0.0102*	*0.0080*
WDR19	*0.0065*	*0.0001*	***WDR19***	*0.0078*	*0.0021*
PYROXD2	*0.0012*	*0.0007*	*PYROXD2*	*0.0040*	*0.0064*
FAM198B	*0.0272*	*0.0006*	*FAM198B*	*0.0238*	*0.0028*
CD40	*0.0046*	*0.0007*	***CD40***	*0.0066*	*0.0002*
SNAPC5	*0.0374*	*0.0539*	*SNAPC5*	*0.0025*	*0.0420*
SNAPC1	*0.0162*	*0.0071*	*SNAPC1*	*0.0914*	*0.0068*
SCPEP1	*0.0706*	*0.0058*	*SCPEP1*	*0.0083*	*0.0014*
MUT	*0.0133*	*0.0033*	*MUT*	*0.0039*	*0.0156*
RAB40B	*0.0008*	*0.0013*	*RAB40B*	*0.8299*	*0.9101*

Genes highlighted in bold were functionally analyzed.

4.2.11. EZH2 target genes are functionally distinct suppressors of melanoma

To relate these EZH2 target genes (ETG) functionally to aspects of melanomagenesis, I performed functional screens in human melanoma cell cultures. I focused on a potential rescue of, first, EZH2 depletion-induced G1 cell cycle arrest and, second, *EZH2* depletion-induced loss of invasive capacity. Among the tested ETGs, deoxycytidine kinase (*DCK*), adenosyl-methionine decarboxylase 1 *(AMD1)*, and WD repeat domain 19 (*WDR19*) displayed promising features. I first established efficient RNAi-mediated silencing of these ETGs (Figure 36a). ETG silencing did not affect the efficiency of *EZH2* knockdown achieved by siEZH2 (Figure 36b). However, *EZH2* silencing-dependent upregulation of *DCK*, *AMD1*, or *WDR19* was strongly counteracted with the double RNAi approach (Figure 36c). Interestingly, when simultaneously depleting *EZH2* and *DCK* or *WDR19*, the G1 cell cycle arrest induced by *EZH2* silencing was significantly reverted (Figure 36d - f). Depletion of *AMD1*, however, was not sufficient to induce such a rescue (Figure 36d). In contrary, simultaneous depletion of *EZH2* and *AMD1* efficiently led to a regain of the invasive capacity that was lost upon silencing of *EZH2* alone (Figure 36g - i). *DCK* and *WDR19* silencing, however, had no effect on invasion of human melanoma cells (Figure 36g).

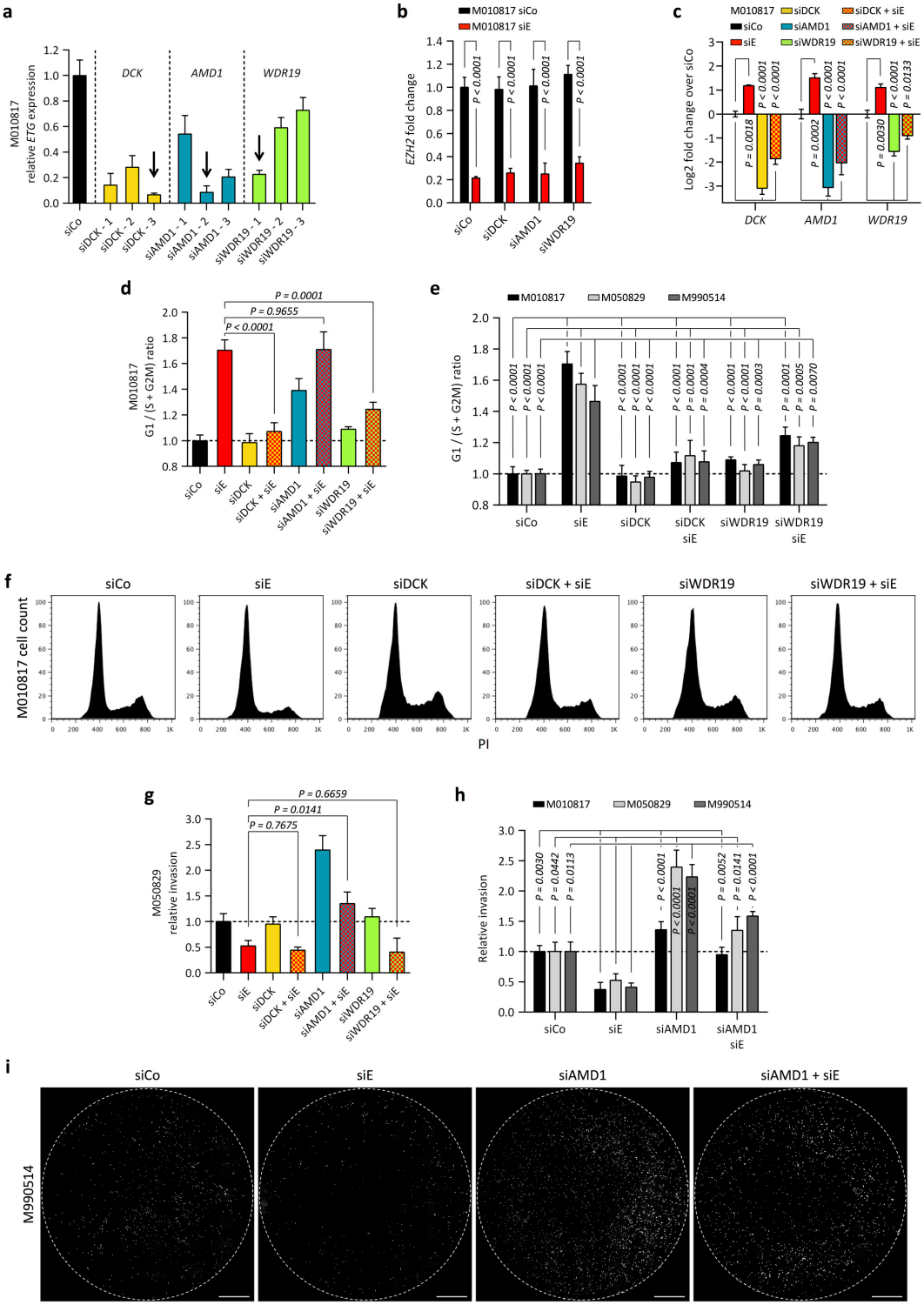

Figure 36 | Depletion of EZH2 target genes rescues EZH2 inactivation phenotypes. (**a**) RT-qPCR for selected ETGs on M010817 after *DCK*, *AMD1*, or *WDR19* depletion with siRNAs targeting these genes. Black arrows, siRNAs chosen for further experiments. (**b**) RT-qPCR for EZH2 on M010817 after *EZH2* and *DCK* / *AMD1* / *WDR19* depletion with siE and siDCK / siAMD1 / siWDR19. (**c**) RT-qPCR for selected ETGs on M010817 after *EZH2* and *DCK* / *AMD1* / *WDR19* depletion. (**d**) Quantification of G1 / (S + G2M) ratio of M010817 after *EZH2* and *DCK* / AMD1 / *WDR19* depletion. (**e**) Quantification of G1 / (S + G2M) ratio of M010817, M050829, and M990514 after depletion of *EZH2* and *DCK* / *WDR19*. (**f**) Cell cycle profiles of M010817 using PI, representative of quantifications in (**e**). (**g**) Quantification of relative invasive capacity of M050829 after *EZH2* and *DCK* / *AMD1* / *WDR19* depletion. (**h**) Quantification of relative invasive capacity of M010817, M050829, and M990514 after depletion of *EZH2* and *AMD1*. (**i**) Immunofluorescence fields of transvaded

M990514 cells after a Boyden chamber assay using Hoechst 33342, representative of quantifications in (**h**). White, DNA. ETG, EZH2 target gene. Data are mean ± s.e.m. of n = 3. P-values calculated with unpaired Student's t-test (**b**), ANOVA and Fisher's LSD-test (**c** - **e**, **g**, **h**). Scale bars, 1mm.

I then reconfirmed these genes as direct ETGs through a ChIP assay on control and *EZH2*-depleted cells. Indeed, upon RNAi targeting *EZH2*, H3K27me3 mark was significantly reduced in promoter regions of *DCK*, *AMD1*, and *WDR19* loci (Figure 37a). Importantly, in both B16-F10 isografts and RIM-1 allografts (Figure 28b; Figure 29b) *Dck*, *Amd1*, and *Wdr19* were consistently upregulated upon Ezh2 inactivation through either cKO (or RNAi) or GSK503 treatment (Figure 37b, c), identifying these ETGs as likely tumor suppressors *in vivo*. Thus, throughout melanomagenesis EZH2 might dynamically repress diverse tumor suppressor genes in order to achieve either favorable growth or invasion kinetics.

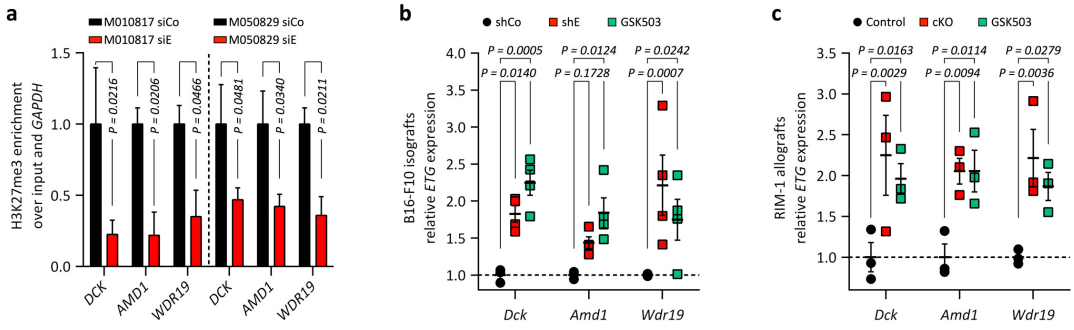

Figure 37 | ETGs are de-repressed *in vivo* upon Ezh2 inactivation. (**a**) H3K27me3 ChIP and subsequent qPCR for gene promoters of selected ETGs on M010817 and M050829 after *EZH2* depletion using siE. (**b**) RT-qPCR for selected ETGs on lysed shCo, shE, and GSK503-treated B16-F10 tumors from (**Figure 28b**). (**c**) RT-qPCR for selected ETGs on lysed control, cKO, and GSK503-treated RIM-1 tumors from (**Figure 29b**). Data are mean ± s.e.m. of n = 3 (**a**, **c**), mean ± s.e.m. of n = 3 (shCo), n = 4 (shE, GSK503) (**b**). P-values calculated with ANOVA and Fisher's LSD-test.

4.2.12. AMD1 suppresses EMT and metastatic spread of melanoma

Interestingly, silencing of *AMD1* in human melanoma cultures induced an increase in invasion on its own (Figure 36g - i). Therefore, I further focused on the relevance of this tumor suppressor in preventing melanoma EMT and metastasis. Based on TCGA, patients with low AMD1 mRNA expression displayed a significantly shorter overall survival as compared to those with high AMD1 expression (Figure 38a). Further, stage I – III patients of the AMD1 low group showed a considerably reduced distant metastases-free survival (Figure 38b). Comparably, low AMD1 expression correlated with more advanced vertical

invasion of primary melanomas (Figure 38c). Finally, depletion of *AMD1* in human melanoma cells induced expression of NCSC- / EMT-relevant genes including *SNAI1*, *TWIST1*, and *ZEB1* (Figure 38d). Similarly, when silencing *Amd1* in B16-F1 (Figure 38e), a murine melanoma cell line with negligible metastatic potential, a comparable EMT gene set was upregulated (Figure 38f). Therefore, in order to functionally link loss of *Amd1* to metastasis, I first i.v. transplanted *Amd1*-silenced B16-F1 cells into *C57Bl/6* mice (Figure 39a).

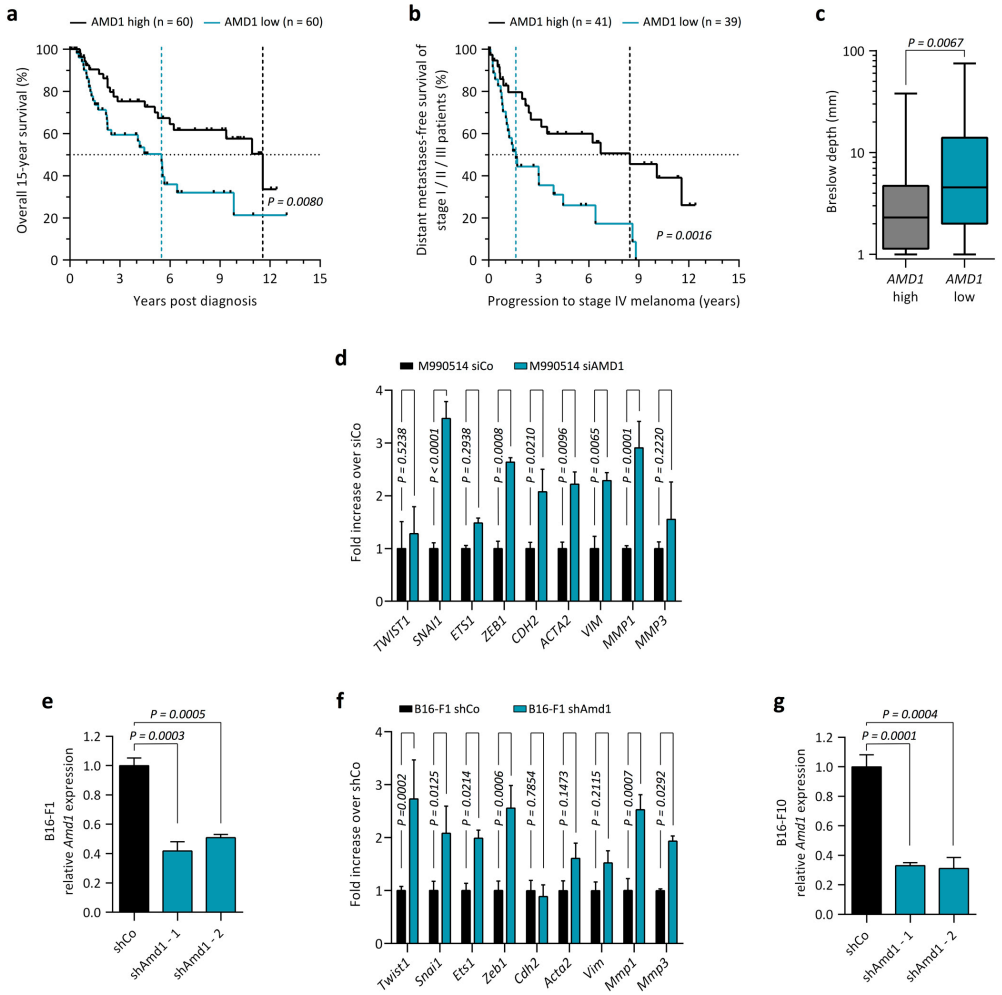

Figure 38 | The ETG *AMD1* is a tumor suppressor that circumvents EMT. (**a**) Kaplan-Meier curves comparing overall survival of melanoma specimens (stage I – IV) with respect to AMD1 transcript levels based on TCGA. (**b**) Kaplan-Meier curves comparing distant metastases-free survival of stage I – III melanoma specimens (primary melanoma / lymph node metastases) with respect to AMD1 transcript levels based on TCGA. (**c**) Breslow depths of melanoma specimens' primary melanomas with respect to AMD1 transcript levels based on TCGA. (**d**) RT-qPCR for EMT genes on M990514 after *AMD1* depletion with siAMD1. (**e**, **f**) RT-qPCR for *Amd1* (**e**) and EMT genes (**f**) on B16-F1 after *Amd1* depletion with shAmd1. (**g**) RT-qPCR for *Amd1* on B16-F10 after *Amd1* depletion with shAmd1. AMD1 low / high, bottom and top 60 patients with respect to AMD1 transcript levels. Data are median ± 100% range of n = 48 (AMD1 high), n = 43 (AMD1 low) (**c**), mean ± s.e.m. of n = 3 (**d** - **g**). P-values calculated with Log-rank (Mantel-Cox) test (**a**, **b**), unpaired Student's t-test (**c**), ANOVA and Fisher's LSD-test (**d** - **g**).

Strikingly, loss of *Amd1* strongly induced nodule formation in the lung (Figure 39b). Next, I depleted *Amd1* in highly metastatic B16-F10 cells (Figure 38g). Comparable to B16-F1, *Amd1* silencing further enhanced the metastatic potential of B16-F10 cells. Most importantly, when inhibiting lung nodule formation through Ezh2 inactivation by GSK503 treatment, depletion of *Amd1* was sufficient to significantly re-induce metastasis (Figure 39a, c). Thus, during melanomagenesis EZH2 epigenetically represses the tumor suppressor *AMD1* allowing metastatic spread, while EZH2-targeted therapy successfully counteracts disease progression.

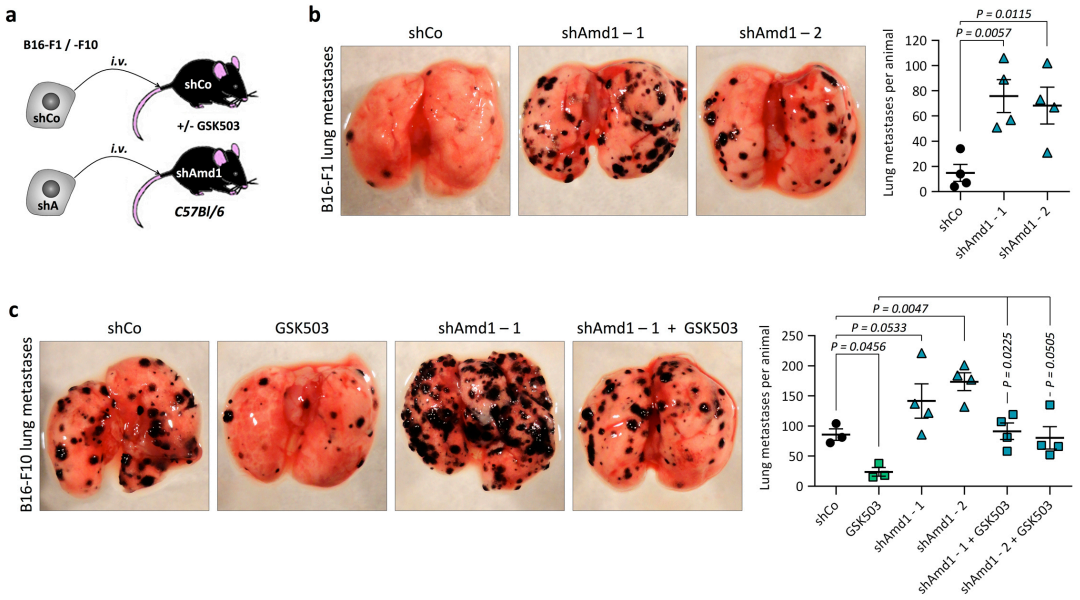

Figure 39 | *Amd1* suppression promotes *in vivo* melanoma metastasis. (**a**) Mouse genotypes and strategies used to i.v. engraft B16-F1 or B16-F10 cells following *Amd1* silencing with shAmd1 to analyze the effect of *Amd1* depletion and GSK503 treatment on metastases formation. (**b**) Representative macroscopic pictures of lungs from *C57Bl/6* animals after i.v. engraftment of shCo and shAmd1 B16-F1 cells to quantify lung metastases. (**c**) Representative macroscopic pictures of lungs from vehicle- and GSK503-treated (from day 1 on until endpoint) animals to quantify lung metastases after i.v. engraftment of shCo and shAmd1 B16-F10 cells. shA, shAmd1. Data are mean ± s.e.m. of n = 4 (**b**, **c**), n = 3 (shCo, GSK503 in **c**). P-values calculated with ANOVA and Fisher's LSD-test.

4.3. Roles of EZH2 in melanoma immunoediting

4.3.1. EZH2 mediates immunomodulation

Besides ETGs interfering with melanoma growth or metastasis, CD40 caught my attention. Notably, in contrast to *DCK*, *AMD1*, and *WDR19*, ablation of *CD40* in *EZH2*-silenced human melanoma cell cultures was neither sufficient to revert the observed growth arrest nor capable of stimulating invasion (data not shown). Nevertheless, *CD40* was the ETG with the highest enrichment for H3K27 promoter methylation and the strongest upregulation upon *EZH2* silencing (Figure 35d, e). CD40 is a positive immune checkpoint regulator that is expressed on tumor cells and stimulates CTLs through binding to CD40 ligand (Pardoll, 2012). Thus, EZH2-dependent *CD40* repression might possibly be involved in attenuating CTL-mediated anti-melanoma responses. To test this hypothesis, I first analyzed Cd40 expression in control and Ezh2-inactivated B16-F10 melanoma samples. Importantly, B16-F10 melanoma was grown in syngeneic, fully immunocompetent *C57Bl/6* mice (Figure 28a, b). Intriguingly, *Cd40* as much as a set of further positive immune checkpoint regulators (*Cd70*, *Cd80*, *Cd86*, *Fas*, *Ox40l*) were upregulated upon *Ezh2* depletion or GSK503-mediated Ezh2 inhibition in comparison to control samples. In contrast, expression of both the immunosuppressant *Tgfb1* and *Pd-L1*, the ligand of the negative immune checkpoint regulator Pd-1 (Pardoll, 2012), was decreased upon Ezh2 inactivation (Figure 40a).

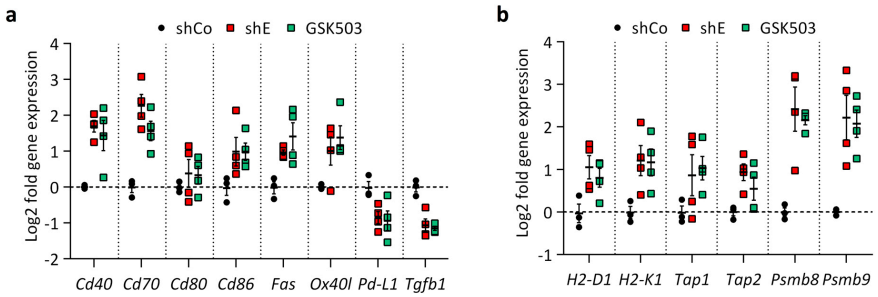

Figure 40 | Ezh2 inactivation promotes upregulation of immune stimulators in B16-F10 melanoma. (**a**, **b**) RT-qPCR for selected immune modulators (**a**) and members of the antigen-processing machinery (**b**) on lysed shCo, shE, and GSK503-treated B16-F10 tumors from (**Figure 28b**). Data are mean ± s.e.m. of n = 3 (shCo), n = 4 (shE, GSK503). P-values calculated with ANOVA and Fisher's LSD-test.

Furthermore, loss of PRC2 activity not only shifted the immune checkpoint balance towards CTL activation, but also promoted induction of the antigen-processing machinery including antigen-presenting MHC-I subunits (*H2-D1*, *H2-K1*), transporters associated with antigen-shuttling into the endoplasmatic reticulum (*Tap1*, *Tap2*), and antigen-generating proteasome subunits (*Psmb8*, *Psmb9*) (Figure 40b). Importantly, based on TCGA, high expression of these immune sensitizers correlated with prolonged melanoma patient survival (Table 5). Thus, EZH2 likely mediates immune evasion and resistance through epigenetic silencing of immunostimulatory genes ultimately resulting in melanoma progression.

Table 5 | TCGA-based association of high expression of immunogenic genes with melanoma patient survival.

Gene	Association with patient survival	Gene	Association with patient survival
HLA-A	improved	*CD40*	improved
HLA-B	improved	*CD70*	improved
HLA-C	improved	*CD80*	improved
TAP1	improved	*CD86*	improved
TAP2	NS	*FAS*	improved
PSMB8	improved	*OX40L*	improved
PSMB9	improved		

HLA-A/B/C, loci encoding human MHC-I subunits; improved, improved survival for specimens with high RNAseq reads for a specific gene compared to specimens with low RNAseq reads; NS, no significant difference between the high and the low group.

4.3.2. EZH2 inactivation promotes immune sensitivity and synergizes with immunotherapy

To strengthen these findings, I *in vivo*-stimulated CTLs in *Tyr::N-Ras*^{Q61K} *Ink4a*$^{-/-}$ mice by continuous treatment with IL2-Cx (Figure 41a, b). Activation of CTLs substantially prolonged skin melanoma-free survival (Figure 41c, d). Comparably, IL2-Cx as well as α-CTLA4 checkpoint blockade treatment interfered with B16-F10 melanoma growth (Figure 41e - i). Analysis of peripheral blood samples confirmed that IL2-Cx treatment promoted T-cell proliferation resulting in a highly increased number of CTLs and especially memory T-cells (Figure 42 a, b). Furthermore, IL2-Cx treatment stimulated tumor infiltration of CTL clones targeting well-established melanoma antigens, such as Dct and Pmel, while these clones were not enriched in tumor-draining lymph nodes (Figure 42c). Thus, CTL activation generated a pool of functional anti-melanoma T-lymphocytes.

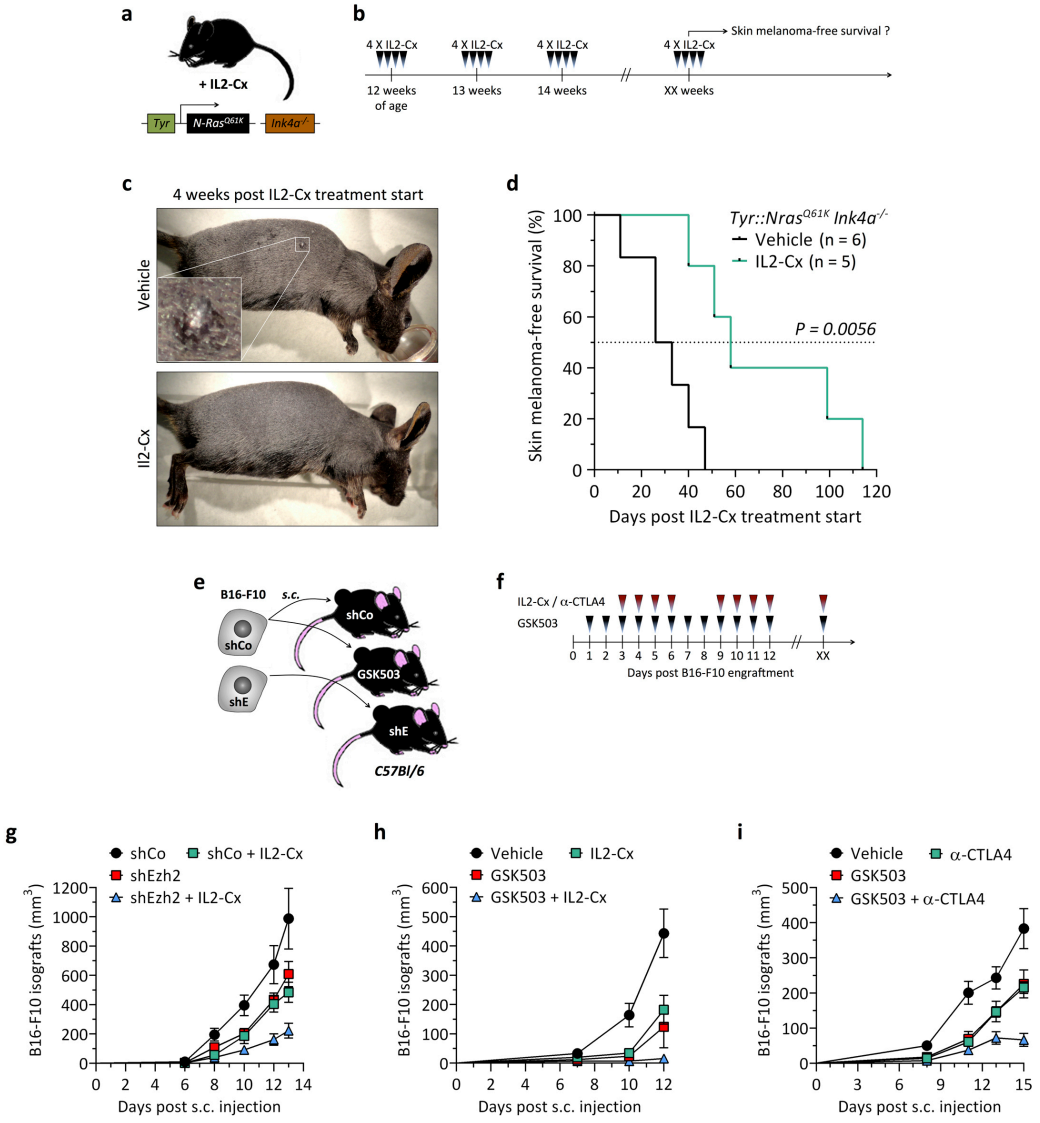

Figure 41 | Ezh2 inactivation and immunotherapy synergistically abolish melanoma growth. (**a**, **b**) Mouse genotypes and strategy used to analyze the effect of prolonged IL2-Cx treatment on melanoma development in *Tyr::N-Ras^{Q61K} Ink4a$^{-/-}$* mice. (**c**) Representative pictures of vehicle- and IL2-Cx-treated *Tyr::N-Ras^{Q61K} Ink4a$^{-/-}$* mice 4 weeks post treatment start. (**d**) Kaplan-Meier curves comparing skin melanoma-free survival (skin melanoma = lesion Ø ≥ 2mm) of vehicle- and IL2-Cx-treated mice. (**e**, **f**) Mouse genotypes and strategy used to s.c. engraft B16-F10 cells following Ezh2 silencing with shE to analyze the effect of Ezh2 depletion and GSK503 treatment in combination with IL2-Cx / α-CTLA4 application on melanoma growth. (**g - i**) Growth of shCo, shE, and GSK503-treated and IL2-Cx / α-CTLA4 co-treated B16-F10 isografts. α-CTLA4, anti-CTL antigen 4 antibody; IL2-Cx, Complexes of IL2 and α-IL2 antibodies. Data are mean ± s.e.m. of n = 5 (**g - i**), n = 6 (Vehicle in **i**), n = 7 (GSK503 in **i**). P-values calculated with Log-rank (Mantel-Cox) test (**d**), ANOVA and Fisher's LSD-test (**g - i**).

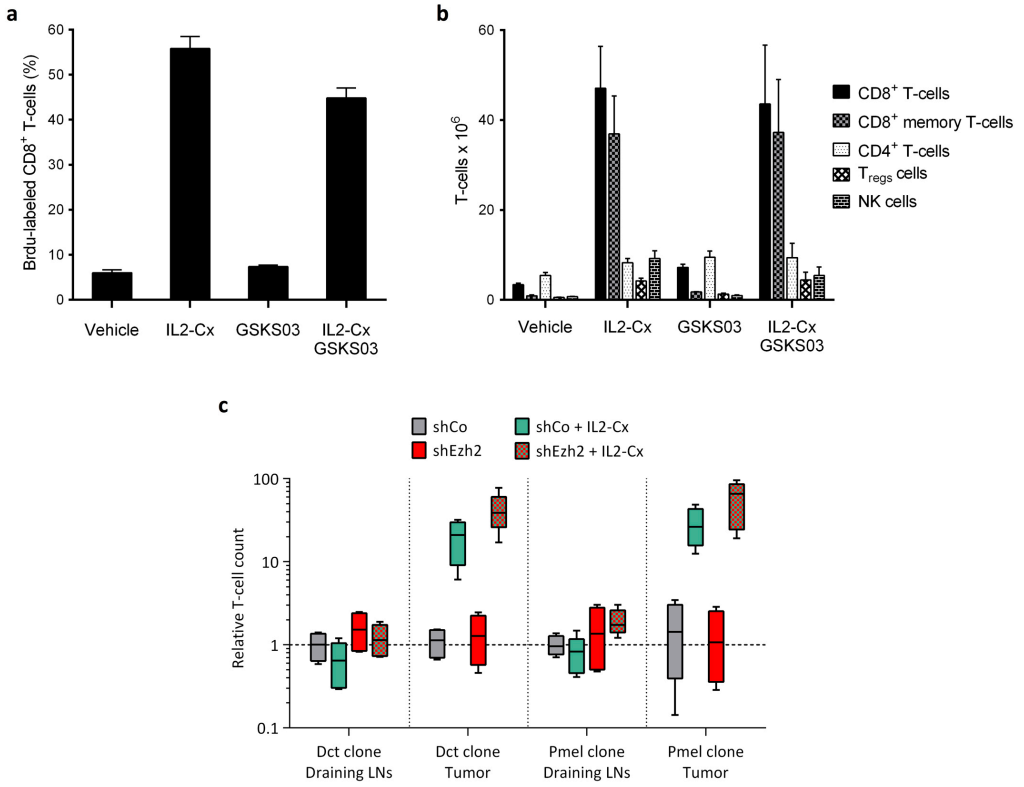

Figure 42 | Ezh2 inactivation and immunotherapy co-promotes CTL tumor infiltration. (**a**, **b**) Quantifications of proliferative T-cells (**a**) and composition of T-cell phenotypes (**b**) using BrdU labeling and FACS analysis on peripheral blood samples from tumor-growing mice in (**Figure 41h**). (**c**) Quantifications of Dct and Pmel antigen-specific T-cells using FACS analysis on tumor samples and tumor-draining lymph nodes from (**Figure 41g**). LN, lymph node. Data are mean ± s.e.m. of n = 4 (**a**, **b**), median ± 100% range of n = 5 (**c**). P-values calculated with ANOVA and Fisher's LSD-test.

Simultaneously, CTL stimulation promoted downregulation of melanoma antigens, members of the antigen-processing machinery, and positive immune checkpoint regulators in the tumor samples (Figure 43). This partly explained the surprisingly inefficient anti-tumor responses in *Tyr::N-Ras*^{Q61K} *Ink4a*$^{-/-}$ and B16-F10-bearing mice (Figure 41). However, adaptive immune evasion and resistance was substantially counteracted by *Ezh2* silencing, which reinforced expression of immunogenic genes (Figure 43). This led to a further increase in tumor-infiltrating, melanoma antigen-specific CTLs (Figure 42c). Accordingly, only CTL activation and concomitant ablation of Ezh2 function through either RNAi or GSK503 completely abolished tumor growth (Figure 41e - i). Taken together, in the melanoma compartment, ablation of PRC2 function de-repressed a set of immunogenic genes, which re-exposed the tumor to CTLs, was favorable for a potent interaction with CTLs, and circumvented immune resistance. Hence, in melanoma patients, EZH2-targeted therapy might functionally synergize with CTL stimulating-immunotherapy potentially resulting in a highly efficient anti-tumor response.

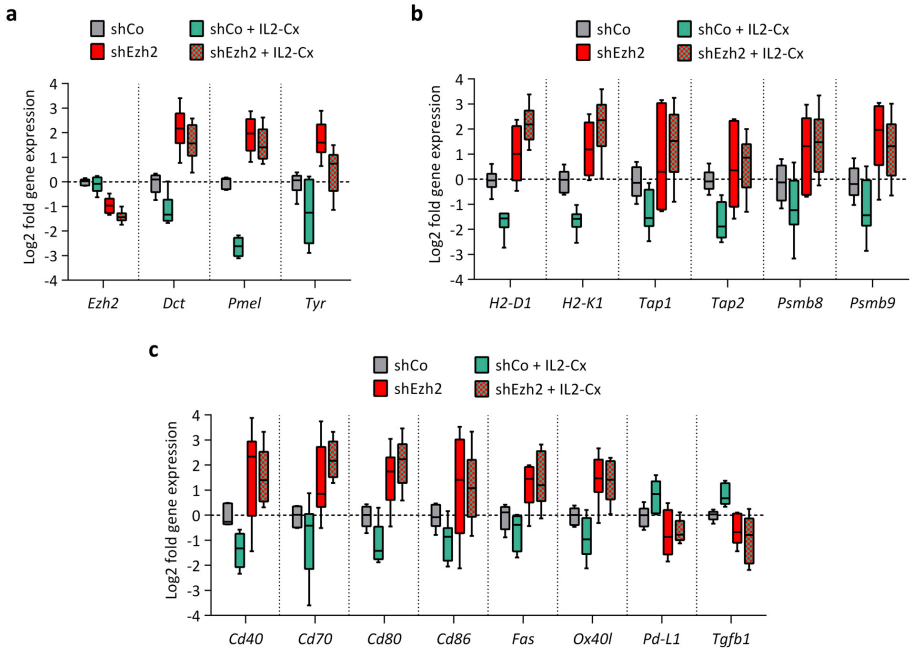

Figure 43 | Ezh2 inactivation counteracts adaptive immune evasion and resistance. (**a - c**) RT-qPCR for melanoma antigens (**a**), members of the antigen-processing machinery (**b**), and selected immune modulators (**c**) on lysed shCo, shE, and IL2-Cx co-treated B16-F10 tumors from (**Figure 41g**). Data are median ± 100% range of n = 6. P-values calculated with ANOVA and Fisher's LSD-test.

5. Discussion

In my PhD thesis, I demonstrate EZH2 to be a key player in promoting malignant melanoma progression in a genetic mouse model of cutaneous melanoma. Importantly, conditional deletion of *Ezh2* did not interfere with normal melanocyte function and benign dermal hyperplasia, underlining the particular roles of Ezh2 in melanoma growth and progression to metastatic disease. Supporting these data, temporary pharmacological inhibition of Ezh2 counteracted growth and metastasis *in vivo*, and blocking EZH2 activity in human melanoma cells affected their growth as well as invasive capacity. In line with these findings, human melanoma patients showed particularly poor survival when EZH2 transcript levels were high or when a newly identified set of ETGs was low-expressed. Furthermore, these ETGs displayed tumor-suppressive functions affecting either melanoma growth or metastatic spread, while a third group of ETGs efficiently mediated immune sensitivity. Hence, EZH2 activity exhibits functionally distinct roles in driving malignant melanoma progression that appear to be highly relevant for human patients (Figure 44).

5.1. EZH2 function in melanoma partly resembles its role in NC development

In many tissues as much as in corresponding malignancies a central function of EZH2 is to sustain stem cell identity and proliferation by transcriptional repression of senescence and differentiation genes (3.1.4. Histone methyltransferases). In contrast, in murine embryonic NCSCs, Ezh2 regulates neither stem cell maintenance nor differentiation of the trunk NC. However, *Ezh2* is required for mesenchymal fate acquisition of the cranial NC (Schwarz et al., 2014). Comparably, *in ovo*, Ezh2 forms a complex with Snai2 to repress *Cdh1*, which promotes EMT and NC delamination (Tien et al., 2015). In melanoma, the role of EZH2 function appears to be analogous, at least in part, to its function during embryonic cranial NC development. In line with previous reports (3.5.3.3. EZH2 and melanomagenesis), EZH2 inactivation in human melanoma cell cultures reduced invasive capacity (Figure 33a). Furthermore, in B16-F10, *Cdh1* and melanocyte differentiation genes including *Mitf* were induced upon *Ezh2* silencing.

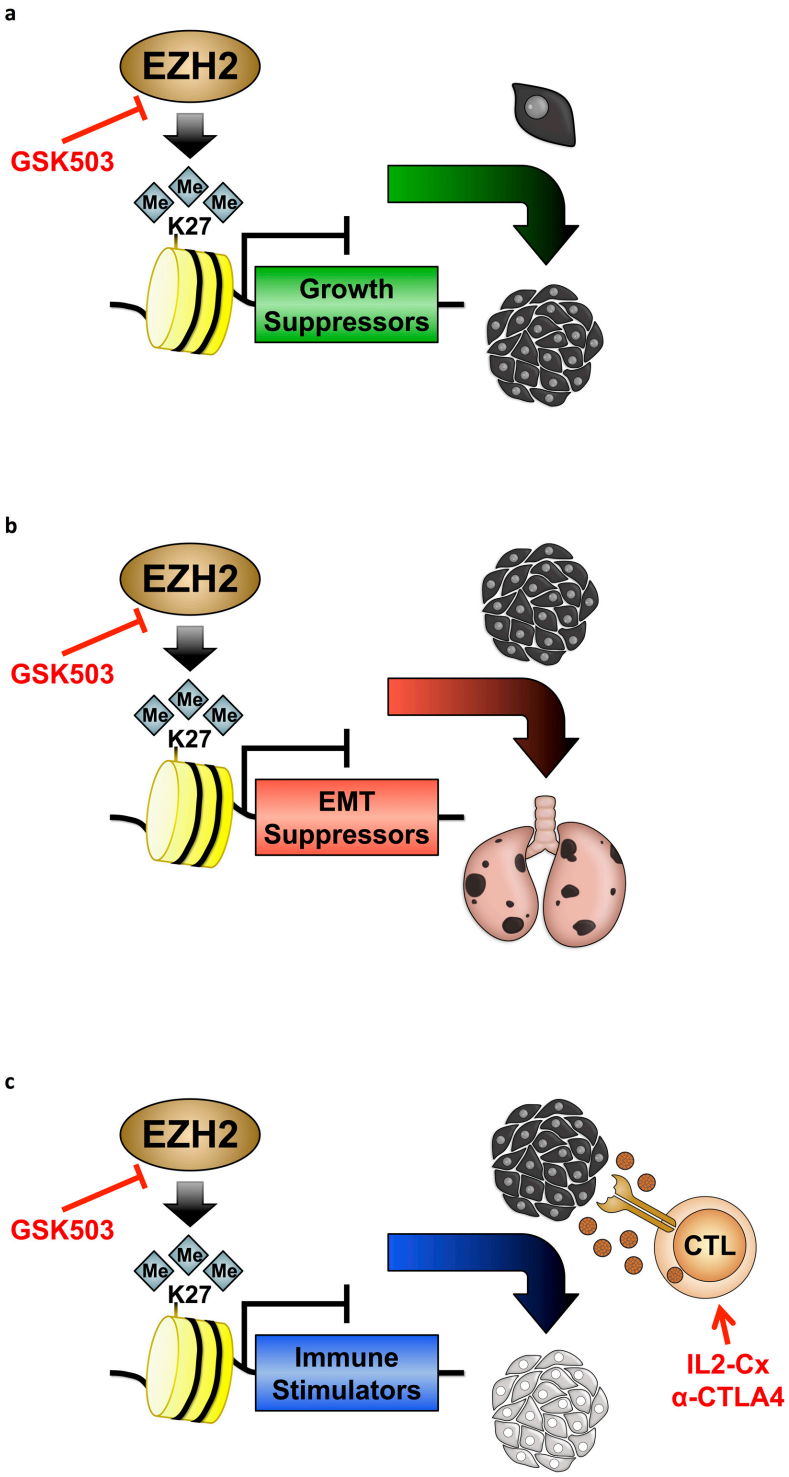

Figure 44 | Graphical summaries of distinct roles of EZH2 during melanomagenesis. During melanoma growth and metastasis, EZH2 mediates repression of functionally distinct tumor suppressors through H3K27me3 in the promoter regions of these genes. The tumor suppressors are either involved in attenuating tumor growth (**a**) or EMT and metastasis (**b**). A third group of tumor suppressors is involved in stimulating CTLs, which in turn release perforin and granzymes triggering tumor cell apoptosis (**c**). Therefore, EZH2 represents a central node that propagates diverse aspects of melanomagenesis. Importantly, these processes can be targeted effectively through GSK503-mediated EZH2 inhibition, potentially in combination with immunotherapy.

Simultaneously, this promoted a reduction in EMT transcription factor expression, among which was Snai1, Twist1, and Zeb1 (Figure 33c). Thus, EZH2 sustains EMT resulting in melanoma cell motility, which is reminiscent of embryonic NC delamination. The process of melanoma metastasis is thought to be triggered by acquisition of mesenchymal features (Gaggioli and Sahai, 2007; Tam and Weinberg, 2013). Indeed, when inactivating Ezh2 in melanoma-bearing *Tyr::N-Ras*^{Q61K} *Ink4a*$^{-/-}$ mice, distant metastases formation was drastically impaired (Figure 32).

However, apart from driving metastatic spread, Ezh2 has further roles during melanomagenesis that do not resemble its function in embryonic NC. When deleting *Ezh2* in benign hyperplasia of *Tyr::N-Ras*^{Q61K} *Ink4a*$^{-/-}$ mice, emergence of cutaneous tumors was almost completely prevented (Figure 22). Likewise, Ezh2 function was required for *Tyr::N-Ras*^{Q61K} *Ink4a*$^{-/-}$ melanoma growth (Figure 29). In carcinomas of breast and prostate, EZH2 similarly propagates tumor initiation and growth, and at later stages, EZH2 activity is necessary for EMT and metastasis (3.1.4.4. EZH2 function in solid cancers). Thus, the abilities of EZH2 to drive functionally distinct aspects of tumorigenesis seem to be a common trait among different cancers entities. Likely, this is achieved through dynamic repression of specific sets of genes with either growth- or EMT-suppressive attributes. Indeed, in human melanoma cells, EZH2 regulated functionally distinct target genes, which will be discussed below (5.5. EZH2 target genes and their melanoma-suppressive functions).

5.2. Significance of Ezh2 activity for melanocytes and malignant melanoma

In *Tyr::N-Ras*^{Q61K} *Ink4a*$^{-/-}$ mice, melanoma is initiated and grows spontaneously in an undisturbed environment without prior *ex vivo* manipulation of tumor cells. Thus, an inducible and conditional knockout strategy in these mice allowed studying functional implications of Ezh2 for different stages of melanomagenesis in an intact environment. A few previous *in vivo* studies have also taken advantage of the cKO technique in genetic mouse models of melanoma, although most reports on gene function in melanoma are based on cell culture and xenotransplantation assays. However, up to date, genes shown to be involved in melanoma formation turned out to be also important for normal melanocytes and benign hyperplasia cells. For instance, *Sox10* haploinsufficiency affects embryonic melanoblast development and similarly counteracts hyperplasia and melanoma formation in *Tyr::N-Ras*^{Q61K} *Ink4a*$^{-/-}$ mice, while

Sox10 cKO completely abrogates the melanocytic lineage (Harris et al., 2013; Shakhova et al., 2012; 2015). Likewise, Wnt and Tgfβ signaling are required for MSC homeostasis, while both *Ctnnb1* and *Smad4* ablation interferes with melanomagenesis in transgenic mouse models (Damsky et al., 2011; Delmas et al., 2007; Gallagher et al., 2013; Nishimura et al., 2010; Rabbani et al., 2011; Zingg and Tuncer, in preparation).

I found Ezh2 function to be relevant for malignant tumor growth at initial stages of melanoma formation, while a striking effect of Ezh2 inactivation was on metastatic spread of melanoma. However, in great contrast to the above-mentioned studies, Ezh2 was required neither for normal melanocyte function nor maintenance of benign hyperplasia (Figure 19; 20; 21). This suggests that in melanoma, Ezh2 plays a unique tumor-specific role, in accordance with the strong upregulation of its expression during malignant melanoma progression (Figure 16; Table 2). Thus, unlike in many other cancers and their respective tissues of origin (3.1.4. Histone methyltransferases), EZH2 function appears to be of no relevance for the cells from which melanoma arises. In HSCs, Ezh2 and its homolog Ezh1 have partially redundant functions. Likewise, in basal skin progenitors, only simultaneous depletion of *Ezh1* and *Ezh2* severely compromises skin homeostasis (3.1.4.2. Ezh2 function in development and tissue homeostasis). Therefore, Ezh1 might functionally compensate loss of *Ezh2* in the melanocytic lineage. However, when inactivating Ezh2 during melanomagenesis, Ezh1 is apparently incapable of compensating the tumorigenic function of Ezh2 in a sufficient manner.

During lymphomagenesis, both $EZH2^{WT}$ and $EZH2^{Y646*}$ act as oncogenes and drive neoplastic transformation of germinal center B-cells (3.1.4.3. EZH2 function in hematopoietic malignancies). Based on TCGA and 2 further datasets (Hodis et al., 2012; McCabe et al., 2012a), cutaneous melanoma was defined as the only solid cancer with recurrent $EZH2^{Y646*}$ gain-of-function mutations (Figure 18b). $EZH2^{Y646N}$ enhances *in vitro* proliferation and motility of a human melanoma cell line (Barsotti et al., 2015). Therefore, it will be of high interest to investigate whether $EZH2^{WT}$ and especially $EZH2^{Y646*}$ operate as *de novo* oncogenic drivers of metastasizing melanoma *in vivo*. To do so, we plan to cross *Tyr::N-*Ras^{Q61K} or *B-*Raf^{V600E}-inducible mice with $Ezh2^{Y646N}$-inducible animals (Béguelin et al., 2013). Mice solely expressing *N-*Ras^{Q61K} or *B-*Raf^{V600E} rarely develop malignant melanoma (3.3.4. Molecular pathogenesis: oncogenic drivers of cutaneous melanoma). Thus, a gain in cutaneous melanoma and metastasis events upon $Ezh2^{Y646N}$ overexpression would confirm $Ezh2^{Y646N}$ to be a melanoma-driving oncogene *in vivo*.

5.3. Possible transcriptional effectors of *EZH2*

During malignant melanoma progression, EZH2 expression is highly increased (Figure 16; Table 2). However, so far no transcriptional effectors of *EZH2* have been described that might accurately explain this upregulation upon melanoma malignancy. In breast carcinoma, *CRAF* amplifications sustain oncogenic MAPK signaling, which induces *EZH2* transcription (Chang et al., 2011; Fujii et al., 2011). Likewise, in cancers of the prostate and the pancreas, $KRAS^{G12D/V}$ mutations are recurrent and promote MAPK signaling, which enhances *EZH2* expression (Cai et al., 2012; Fujii et al., 2012). Furthermore, EZH2 epigenetically represses disabled homolog 2-interacting protein (*DAB2IP*), which is a suppressor of RAS (Min et al., 2010). Thus, EZH2 promotes MAPK signaling, which in turn further enhances *EZH2* transcription. In the vast majority of cutaneous melanomas, MAPK pathway is activated (3.3.4. Molecular pathogenesis: oncogenic drivers of cutaneous melanoma). In analogy to MAPK-driven carcinomas, MAPK signaling might, therefore, also trigger EZH2 upregulation in melanoma. However, human nevi never displayed high levels of EZH2 expression, despite the presence of either $BRAF^{V600E}$ or $NRAS^{Q61K}$ in these tissues. Likewise, $N\text{-}Ras^{Q61K}$ promotes dermal hyperplasia in mice. In spite of activated MAPK signaling, Ezh2 was marginally expressed in hyperplasia and only upregulated upon tumorigenesis (Figure 16; Table 2). Furthermore, MEK inhibition does not reduce EZH2 levels in human melanoma cell cultures (Zingg and Schaefer, unpublished data). Thus, in melanoma, MAPK signaling unlikely acts as a transcriptional enhancer of *EZH2*.

Several transcription factors independent of MAPK pathway have been indicative of increasing *EZH2* expression. For instance, NF-κB induces *EZH2* transcription in lymphocytes and similarly enhances EZH2 in multiple myeloma and leukemia cells (Neo et al., 2014a). In prostate cancer cells, both ETS and MYC transcription factors activate *EZH2* expression (Koh et al., 2011; Kunderfranco et al., 2010), while FOXM1 maintains glioblastoma stem cells through transcriptional upregulation of *EZH2* (Kim et al., 2015). In breast carcinoma, TGFβ signaling induces *SOX4*, which activates *EZH2* transcription and promotes EMT (Tiwari et al., 2013). Comparably, TGFβ signaling sustains *EED* expression in lung cancer cells. This results in aberrant PRC2 activity-mediated EMT (Oktyabri et al., 2014). In *Tyr::N-*Ras^{Q61K} $Ink4a^{-/-}$ mice, enhanced Smad2/3 activity promotes metastatic spread of cutaneous melanoma (Zingg and Tuncer, in preparation), while *Ezh2* ablation prevented metastasis (Figure 31; 32). Therefore,

in resemblance of carcinomas, activated SMAD complexes might drive *EZH2* overexpression in melanoma, thus promoting EMT and metastasis.

Apart from transcriptional activators, loss of transcriptional repressors conceivably induces *EZH2*. Indeed, miR-31, miR-101, miR-124, and miR-137 have been shown to suppress *EZH2* in several melanoma cell lines (Asangani et al., 2012; Chen et al., 2013; Luo et al., 2012a; 2013). It remains to be deciphered, whether a decrease in miRs is causative for EZH2 upregulation during melanoma formation *in vivo*. Besides transcriptional regulation, post-translational modifications alter EZH2 activity during tumorigenesis (Yamaguchi and Hung, 2014). For instance, AKT phosphorylates EZH2 at serine 21 resulting in aberrant EZH2 activity in prostate cancer and glioblastoma (Kim et al. 2013; Xu et al., 2012). A considerable number of melanomas harbor activated PI3K signaling, especially in response to MAPK-targeted therapy (3.3.5.2. *PTEN* as tumor suppressor; 3.4.3.1. PI3K signaling-dependent resistance). In these melanomas, activated AKT might likewise phosphorylate EZH2. Hence, PI3K signaling possibly propagates melanoma progression and adaptive MAPK resistance through phospho-EZH2-mediated epigenetic rewiring.

5.4. Drivers of EZH2 target gene specificity

In melanoma samples, I found high EZH2 expression to correlate with KI67-positive, proliferative cells (Figure 25), while others have described connections between increased EZH2 levels and the invasive front of human melanomas or motile cells in B16-F10 tumors, respectively (Kampilafkos et al., 2015; Manning et al., 2014). Thus, EZH2 might dynamically regulate target genes that suppress either proliferation or motility of melanoma cells. Indeed, I identified ETGs with distinct functions favorable for either growth inhibition or cell immotility (Figure 36). This raises the question of how PRC2 is recruited to such defined loci in the course of melanomagenesis. In *Drosophila*, polycomb response elements (PRE), short *cis*-regulatory DNA sequences in gene promoters, recruit PRC2 to specific loci, thus initiating and mediating gene repression. In contrast, the very existence of PRE-like elements also in mammals remains controversial (Ringrose and Paro, 2007; Simon and Kingston, 2009). In fact, in murine ESCs, absence of the transcriptional machinery recruits PRC2 to maintain transcriptional repression rather than gene silencing would be initiated by PRC2 through recognition of *in cis* DNA

motifs (Riising et al., 2014). Notably, during tumorigenesis, aberrant PRC2 function might still enforce gene repression.

Independent of the mode of PRC2-dependent gene repression, transcription factors have been reported to guide PRC2 *in trans* to specific loci. For instance, a considerable number of loci, which are H3K27me3-repressed during murine ESC differentiation towards neural progenitors, share a Snai1 binding motif in their promoter region. In addition, Snai1 has been shown to mediate, through PRC2 recruitment, the repression of these genes, among which is *Cdh1* (Arnold et al., 2013). Interestingly, in nasopharyngeal carcinoma and pancreatic cancer, PRC2 similarly forms a complex with SNAI1 to repress *CDH1*, thus promoting EMT (Herranz et al., 2008; Tong et al., 2012). Likewise, *in ovo*, Snai2 recruits Ezh2 to the *Cdh1* promoter, and *Cdh1* silencing enables NC delamination (Tien et al., 2015). Comparably, TWIST1 is able to recruit PRC2 to the *CDKN2A* locus in human mesenchymal stem cells, thus propagating self-renewal and mesenchymal identity (Cakouros et al., 2012). Notably, PRC2 silences *CDKN2A* in several cancers (Popov and Gil, 2010), while TWIST1 regulates metastatic progression of basal cell carcinoma and melanoma (Beck et al., 2015; Caramel et al., 2013; Weiss et al., 2012). In murine B16-F10 melanoma cells, ablation of *Ezh2* induced *Cdh1* and melanocyte differentiation genes, accompanied by a reduction in Snai1 and Twist1 expression (Figure 33c). It remains to be deciphered, whether TWIST1 and SNAI1 propagate melanoma EMT and metastasis in cooperation with PRC2-mediated gene repression.

In murine ESCs, the pluripotency factor Sox2 binds to a large number of gene promoters that are enriched in H3K27me3 (Boyer et al., 2006; Lee et al., 2006). Therefore, Sox2 might recruit PRC2 in a comparable fashion as Snai1. Interestingly, *SOX2* is re-expressed in a fraction of melanomas (3.3.7.2. Melanoma stem cell markers beyond CD271), while *SOX2* deletion in melanoma cell cultures induces *CDH1* and melanocyte differentiation genes. Remarkably, *SOX2* ablation also promotes a global H3K27me3 reduction, albeit EZH2 expression remains intact (Zingg and Schaefer, unpublished data). Therefore, SOX2 likely mediates repression of *CDH1* and melanocyte differentiation genes through PRC2 recruitment, which may result in tumor stemness and metastasis.

Besides transcription factor-based PRC2 recruitment, putative histone modification readers might guide PRC2 to specific loci. Previously, H2A-K119ub was thought to be established by PRC1 in a subsequent manner to H3K27me3 (Bracken and Helin, 2009) (Figure 3). However, recent studies in murine ESCs

have challenged this model and propose that H2A-K119ub is placed by PRC1 prior to PRC2 activity. PRC2 is then recruited to H2A-K119ub through a so far unidentified reader subunit to maintain gene repression by H3K27me3 (Blackledge et al., 2014; Cooper et al., 2014; Kalb et al., 2014). In a conceptually similar way, in murine ESCs, Jarid2 can recruit PRC2 to target loci, possibly through binding to yet unknown DNA motifs or nucleosome components (Pasini et al., 2010; Peng et al., 2009; Son et al., 2013). This cascade might include methylation of Jarid2 by Ezh2 as much as long non-coding RNAs (lncRNA) functioning as scaffolds between Jarid2, PRC2, and chromatin (Kaneko et al., 2014; Sanulli et al., 2015). Conceivably, *Jarid2* is relevant for adult tissue stem cell homeostasis (Kinkel et al., 2015; Mejetta et al., 2011), whereas JARID2 incorporates TGFβ signaling resulting in an EMT of several carcinoma cell lines (Tange et al., 2014). These findings emphasize the significance of unraveling the precise recruitment paths encircling PRC2, which might help uncovering how PRC2 perturbations contribute to tumorigenesis.

5.5. EZH2 target genes and their melanoma-suppressive functions

Since EZH2 acts as a transcriptional repressor (3.1.4. Histone methyltransferases), genes upregulated upon *EZH2* silencing are likely candidates for being direct targets of EZH2-mediated H3K27me3. In agreement with this, promoters of genes selected based on my TCGA analyses were indeed confirmed to be enriched in H3K27me3 (Figure 35e), while *EZH2* ablation led to a loss of H3K27me3 at these promoters (Figure 37a). This defined a number of direct ETGs, while functional characterizations of these ETGs allowed assignment of growth-suppressive, metastasis-suppressive, or immunostimulatory features (Figures 36 - 40).

5.5.1. EZH2 target gene *DCK*

For instance, following *EZH2* ablation, silencing of the ETG *DCK* was sufficient to significantly re-induce melanoma cell proliferation (Figure 36). Thus, epigenetic repression of *DCK* might sustain cutaneous melanoma growth. DCK is required for the phosphorylation of several deoxyribonucleosides and their nucleoside analogs (Spasokoukotskaja et al., 1995). In several cancers, DCK expression is

reduced, which confers resistance to DNA-demethylating agents, such as azacitidine and decitabine (Qin et al., 2009; Saiki et al., 2012). Likewise, inactivation of *Dck* enhances resistance to these cytidine analogues in a rat model of AML (Stegmann et al., 1995). Importantly, the melanoma cell cultures used to define ETGs were never exposed to cytidine analogues. Therefore, loss of DCK function appears to have biological relevance for melanoma cell proliferation independent from any cytidine analog resistance mechanism. Interestingly, efficiency of nucleoside transporters is attenuated in pancreatic adenocarcinoma, while overexpression of these transporters counteracts tumor growth (Pérez-Torras et al., 2013). In line with these data, enhanced degradation of pyrimidine deoxynucleosides promotes EMT and metastasis in breast cancer (Shaul et al., 2014). Thus, dynamic influx, turnover, and phosphorylation of nucleosides seem to influence tumorigenesis. However, the underlying mechanisms of this appearance remain to be deciphered.

5.5.2. EZH2 target gene *WDR19*

Comparably to *DCK*, depletion of the ETG *WDR19* counteracted an EZH2 inactivation-provoked growth arrest of melanoma cells (Figure 36). WDR19 is a critical component required for the structural and functional integrity of the intraflagellar transport machinery of primary, immotile cilia (Efimenko et al., 2006; Wei et al., 2012). *Wdr19*-defficient mouse embryos have patterning defects affecting the limbs, the skeleton, and the nervous system (Ashe et al., 2012; Wainwright et al., 2014). These anomalies appear reminiscent of a broad spectrum of human ciliopathies. Indeed, patients affected by these disorders frequently harbor *WDR19* mutations (Bredrup et al., 2011; Coussa et al., 2013; Fehrenbach et al., 2014; Schmidts et al., 2013). A primary cilium is a non-motile, microtubule-based organelle that is maintained by the intraflagellar transport machinery and projects from the surface of vertebrate cells. Primary cilia function as sensory antennae that coordinate a large number of signaling pathways coupled to cell division and differentiation. Hence, they play critical roles in embryonic patterning, organogenesis, and tissue homeostasis (Goetz and Anderson, 2010). Interestingly, upon differentiation-induced quiescence, melanocytes form primary cilia *in vitro* (Le Coz et al., 2014), in accordance with the observation that human epidermal melanocytes harbor these organelles (Wandel et al., 1984). Primary cilia are similarly detectable in melanocytic cells of nevi. However, these structures are completely absent in samples of malignant melanoma (Kim et al., 2011b; Snedecor et al., 2015). Comparably, primary cilia are lost in

advanced prostate carcinoma (Hassounah et al., 2013), while low WDR19 expression is connected to poor prostate cancer patient survival (Lin et al., 2008). Therefore, EZH2 might dynamically repress members of the intraflagellar transport machinery including *WDR19* resulting in disassembly of the primary cilium, which sustains melanomagenesis through yet unidentified mechanisms.

5.5.3. EZH2 target gene *AMD1*

In contrast to *DCK* and *WDR19*, the ETG *AMD1* was not relevant for melanoma growth, but *AMD1* loss promoted melanoma EMT and metastasis (Figure 36; 38; 39). AMD1 is an enzyme that catalyzes the conversion of S-adenosyl-methionine (SAM) to decarboxylated SAM (dcSAM), which serves as a substrate for the biosynthesis network of the polyamines spermine and spermidine. Spermidine itself is required for the conversion of lysine 50 in eukaryotic translation initiation factor 5A (EIF5A) into the non-canonical amino acid hypusine, which is critical for EIF5A function. EIF5A initiates and elongates translation of proteins through recruitment of initiator methionyl-tRNA as well as prolyl-tRNAs to ribosomes (Gutierrez et al., 2013; Park et al., 2010; Scuoppo et al., 2012) (Figure 45a). Besides EIF5A activation, spermine and spermidine directly influence a variety of biological processes including transcription, translation, diverse signaling cascades, and cytoskeleton remodeling (Pegg, 2009). Likewise, SAM, apart from being decarboxylated by AMD1, interacts with lncRNAs and influences transcription and translation. But most importantly, SAM is also the methyl group donor for DNMTs and histone methyltransferases including EZH2. Catalysis of SAM results in methylated DNA and histones and produces S-adenosyl-homocysteine (SAH) as by-product (Loenen, 2006) (Figure 45b).

The relevance of AMD1 and polyamine metabolism becomes apparent in early lethality of *Amd1*-deficient embryos, while *Amd1* deletion abolishes self-renewal of ESC cultures, which is restored by spermidine application (Nishimura et al., 2002b; Zhang et al., 2012a; Zhao et al., 2012). This proliferation defect is thought of resulting from impaired protein synthesis due to a lack in functional EIF5A. Indeed, *EIF5A* depletion affects growth of xenotransplanted pancreatic cancer and melanoma cells (Fujimura et al., 2014, Jasiulionis et al., 2007). Notably, *AMD1* ablation similarly induced a G1 cell cycle arrest in melanoma cell cultures (Figure 36d). In contrast, *Amd1* and *Eif5a* function as tumor suppressor genes in a murine lymphoma model (Scuoppo et al., 2012), while I saw an *Amd1* depletion-dependent increase in melanoma EMT and metastasis (Figure 39).

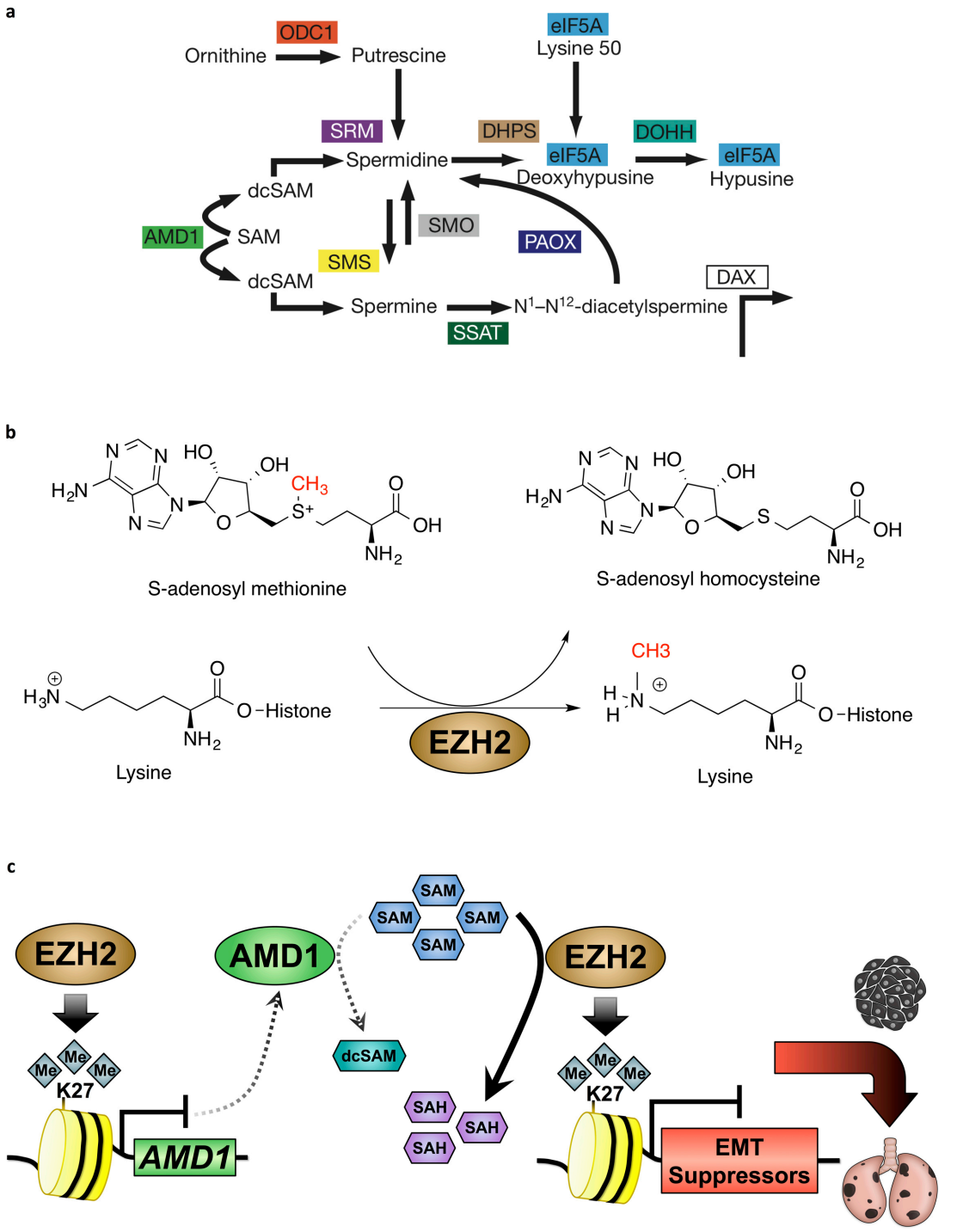

Figure 45 | Polyamine synthesis and connection to EZH2 activity. (**a**) Schematic representation of the polyamine-hypusine metabolic network. SAM is the substrate for AMD1, which produces dcSAM. This intermediate metabolite serves as substrate to generate the polyamines spermine and spermidine. Spermidine is essential to convert lysine 50 in EIF5A into hypusine. This non-canonical amino acid is critical for EIF5A function. (**b**) SAM is also the methyl group-donating substrate for methyltransferases, such as EZH2, which results in methylated DNA or proteins and SAH as by-product. (**c**) Hypothetical working model of *AMD1* repression influencing increased EZH2 activity: EZH2 mediates *AMD1* repression, which reduces AMD1 protein. This increases SAM availability for EZH2, which sustains EZH2 efficacy in silencing target genes, such as EMT / metastasis suppressors. Hence, melanoma cells secure availability of EZH2 substrate through epigenetic repression of substrate-competing metabolic networks. AMD1, adenosyl-methionine decarboxylase 1; EIF5A, eukaryotic translation initiation factor 5A; SAH, S-adenosyl-homocysteine; SAM, S-adenosyl-methionine; dcSAM, decarboxylated SAM (adapted from: Scuoppo et al., 2012).

Thus, polyamine metabolism is required for proliferative cells due to its relevance in sustaining protein synthesis through EIF5A. However, diminutions in protein synthesis seem to be critical for EMT and metastatic tumor progression. Indeed, in prostate cancer, mTOR promotes metastasis by steering a pro-metastatic translational landscape (Hsieh et al., 2012). Likewise, reduction in the translation initiation factor family member EIF3E in breast cancer cells causes a global loss of protein synthesis but unexpectedly enhances SNAI1 and ZEB2 translation, thus promoting EMT (Gillis and Lewis, 2013).

AMD1 depletion likely increases the abundance of SAM. Therefore, in an alternative scenario, AMD1 reductions might influence EMT through accumulation of SAM, rather than by attenuating protein synthesis. An increase in SAM would facilitate aberrant EZH2 function, as EZH2-mediated H3K27me3 is dependent on SAM as methyl group-donating substrate (Loenen, 2006). Hence, in this proposed model, EZH2 represses *AMD1*, which elevates SAM abundance, thus ultimately enhancing EZH2 efficacy in silencing further EMT- / metastasis-suppressive genes (Figure 45c). Interestingly, in rheumatoid arthritis, increased SAM-dependent polyamine synthesis leads to DNA hypomethylation (Karouzakis et al., 2012). Thus, AMD1 and methyltransferases indeed directly compete for SAM usage.

Previously, changes in metabolites have been connected to epigenetic rewiring. For instance, elevated levels of the tricarboxylic (TCA) cycle metabolite alpha ketoglutarate (αKG) maintain ESC pluripotency. Histone demethylases including JMJD3 and UTX utilize αKG as substrate. Therefore, an increase in αKG promotes demethylation of H3K9me3 and H3K27me3, which sustains pluripotency (Carey et al., 2015). Interestingly, the locus encoding the TCA cycle enzyme isocitrate dehydrogenase 1 (*IDH1*) harbors recurrent mutations in diverse cancers (Lu and Thompson, 2012). Under physiologic conditions, IDH1 catabolizes isocitrate to αKG. However, mutant *IDH1* displays neomorphic activity of converting αKG to 2-hydroxyglutarate (2HG) (Dang et al., 2009; Ward et al., 2010). αKG serves as histone demethylase substrate, whereas 2HG sterically hinders these enzymes (Chowdhury et al., 2011; Xu et al., 2011). Therefore, mutant *IDH1* causes a vast increase in H3K9me3 and H3K27me3, which contributes to aberrant epigenetic gene silencing. Likewise, loss-of-function mutations affecting the TCA cycle enzyme succinate dehydrogenase (*SDH*) lead to an accumulation of succinate. Succinate inhibits histone demethylases similarly as 2HG, thus inducing global hypermethylation, which promotes tumor growth and especially EMT in several malignancies (Aspuria et al., 2014; Cervera et al., 2009; Letouzé et al., 2013). Thus, in a conceptually similar mode, an *AMD1* repression-provoked raise in SAM levels

might indeed give rise to EZH2-mediated metastatic melanoma progression (Figure 45c). It will be of high interest to further decipher the interplay between abundance of metabolites and epigenetic gene regulation and its significance for aspects of tumorigenesis.

5.5.4. EZH2 target gene *MPC1*

Another ETG that caught my attention is mitochondrial pyruvate carrier 1 (*MPC1*). Comparably to *AMD1*, depletion of *MPC1* enhances melanoma cell invasion. *Mpc1* loss also promotes s.c. tumor growth of B16-F1 melanoma and, importantly, induces distant metastasis arising from these transplants (Zingg, Leu, and Antunes, unpublished data). MPC1 is a transporter that shuffles pyruvate, the end product of glycolysis, into mitochondria, thus providing the organelle with oxidative fuel (Bender et al., 2015; Bricker et al., 2012; Herzig et al., 2012). Cancer cells, however, divert pyruvate to fuel other anabolic processes or convert it to lactate for excretion from the cell, a phenomenon referred to as Warburg effect (Warburg, 1956; Warburg et al., 1927). In accordance with Warburg effect, depletion of *MPC1* reroutes metabolism to, first, increased glycolysis at the expense of pyruvate oxidation and, second, an increase in glutaminolysis and fatty acid oxidation to maintain TCA cycle (Schell et al., 2014; Vacanti et al., 2014; Yang et al., 2014a). Indeed, in several cancers, MPC1 is low-expressed, thus conferring Warburg effect-associated growth advantages (Schell et al., 2014). Conceivably, *Mpc1* silencing promotes B16-F1 melanoma growth. However, it is less apparent, how such a Warburg-like metabolic rerouting would trigger melanoma cell invasion resulting in distant metastasis (Zingg, Leu, and Antunes, unpublished data).

In support of these observations, expression of the TCA cycle malic enzyme 2 (ME2) is increased in invasive melanoma, while *ME2* depletion interferes with cell motility. ME2 maintains constant anaplerosis by replenishing pyruvate from glutamine (Chang et al., 2015). Comparably, pyruvate dehydrogenase (PDH) is the enzyme that converts pyruvate into acetyl co-enzyme A (acetyl-CoA), which is fueled into TCA cycle. Pyruvate dehydrogenase kinases (PDK) inhibit PDH. Interestingly, in melanoma-bearing mice, *Pdk1* cKO enhances acetyl-CoA production, which drives oxidative phosphorylation, thus reversing the Warburg effect. Importantly, loss of *Pdk1* abolishes metastasis formation (Kaplon et al., 2013; Scortegagna et al., 2014). Similarly, SNAI1 represses *PDH* in canine kidney cells, while in lung cancer cells, TGFβ signaling represses lipogenesis in a SNAI1-dependent

manner. Suppression of both PDH activity and lipogenesis promotes EMT (Haraguchi et al., 2013; Jiang et al., 2014). Thus, metabolic rewiring, for instance by EZH2-dependent repression of *MPC1*, is sufficient to promote EMT and metastasis, while EMT transcription factors reshape the metabolic landscape in favor of cell motility and metastasis. Intriguingly, dynamic epigenetic regulation might be at the source of guiding this complex interplay between metabolism and phenotypic plasticity of cancer.

5.6. Epigenetic regulation of immunoediting

I found ETGs to suppress either melanoma growth or metastasis. However, in B16-F10 melanoma samples, Ezh2 inactivation also promoted upregulation of an immunostimulatory gene signature. In contrast, immunotherapy in B16-F10 melanoma-bearing mice led to a downregulation of these immunogenic genes, which was significantly counteracted by *Ezh2* depletion (Figure 40 - 43). Previously, immunogenicity has been connected to chemical blockade of epigenetic modifiers. For instance, DNMT and HDAC inhibition induces *FAS* de-repression in melanoma cells, osteosarcoma cells, and *H-Ras*-transformed fibroblasts. FAS is a death receptor recognized by FAS ligand on CTLs, which in turn triggers apoptosis of the target cells (Maecker et al., 2002; Mologhoni et al., 2011; Rao-Bindal et al., 2012). Likewise, *Dnmt3a* silencing promotes upregulation of MHC-I subunits in B16-F10 melanoma cells (Deng et al., 2009), while both DNMT and HDAC inhibition is sufficient to similarly induce the antigen-processing machinery in human and murine cell lines of melanoma and further cancers (Chou et al., 2012; Coral et al., 2012; Gregorie et al., 2009; Khan et al., 2008; Krishnadas et al., 2014; Kumari et al., 2013; Magner et al., 2000; Manning et al., 2008; Setiadi et al., 2008; Woods et al., 2013; Wrangle et al., 2013; Xiao et al., 2013). Furthermore, epigenetic inhibitors also promote de-repression of immune checkpoint effectors, such as CD40, CD80, CD86, and OX40L, but also PD-L1 (Kumari et al., 2013; Magner et al., 2000; Woods et al., 2013; Wrangle et al., 2013; Yang et al., 2014b). Importantly, PD-L1 is an immune checkpoint inhibitor, thus PD-L1 upregulation might rather attenuate CTL efficacy (3.4.4.3. Immune checkpoint blockade as therapeutic approaches). In contrast, Ezh2 inactivation only induced expression of positive immune checkpoint regulators, while expression of Pd-L1, as well as of the immunosuppressant Tgfβ, was reduced (Figure 40a). Therefore, EZH2-targeted therapy might represent a more efficient strategy to reinforce immunogenicity than DNMT or HDAC inhibition.

In mice bearing B16-F10 melanoma or renal cell carcinoma tumors, combinatorial treatment with HDAC inhibitors and IL2 synergistically attenuates tumor growth through concomitant stimulation of lymphocytes by IL2 and reinforced immune sensitivity in the tumor compartment (Kato et al., 2007; 2014). Comparably, we observed a synergistic growth reduction of B16-F10 melanoma upon Ezh2 inactivation and simultaneous administration of immunotherapeutics (Figure 41). However, in contrast to previous studies, we provide direct evidence that the synergistic growth mitigation was based on, first, selective CTL stimulation through IL2-Cx or α-CTLA4, second, melanoma antigen-specific CTL infiltration into the tumor, and third, Ezh2 inactivation-dependent upregulation of immunogenic surface receptors in the tumor cells. Furthermore, we demonstrate that PRC2 mediated *de novo* repression of immune modulators in the course of immunotherapeutic pressure resulting in adaptive immune evasion and resistance (Figure 42; 43). This provides a rationale for combining immunotherapy and EZH2-targeting agents likely resulting in an effective anti-melanoma response.

Noteworthy, in activated Tregs, Ezh2 stabilizes the transcriptional program including *Foxp3* expression, while *Ezh2* deletion in Tregs impairs immunotolerance resulting in autoimmunity (Arvey et al., 2014; DuPage et al., 2015; He et al., 2014). Furthermore, an *Ezh2* knockout in the T-cell compartment promotes spontaneous leukemogenicity in aged mice (Simon et al., 2012), while T-ALL patients frequently harbor *EZH2* and *SUZ12* loss-of-function mutations (Ntziachristos et al., 2012; Zhang et al., 2012b). Therefore, melanoma patients, which would undergo a prolonged systemic therapy with EZH2 inhibitors, had to be carefully monitored for possible autoimmunity side effects, especially in the case of simultaneous immunotherapy. Furthermore, dependent on genetic predispositions, systemic EZH2 blockade might promote T-cell proliferations possibly advancing to leukemia.

5.7. Possible roles of EZH2 in MAPK-targeted therapy resistance

Efficacy of current melanoma treatments, such as MAPK-targeted therapy, is limited because of acquired resistances resulting in tumor relapse (3.4. Melanoma therapies) (Figure 13). In xenotransplantation models of human melanoma, continuous vemurafenib administration rapidly causes drug resistance. However, these resistant tumors become drug dependent, such as cessation of drug administration leads to a temporary tumor regression, while a discontinuous dosing strategy exploits this vemurafenib

dependency and forestalls the onset of progressive disease (Thakur et al., 2013). This plastic behavior of melanoma upon intermittent vemurafenib exposure supposedly underlies dynamic epigenetic rearrangements. Likewise, the acquirement of resistances to MAPK-targeting therapy is prevalently based on transcriptional dynamics (3.4. Melanoma therapies) (Figure 13), thus might depend on aberrant PRC2 activity.

Indeed, in a set of solid tumor entities, inactivation of PRC2 function synergizes with chemotherapy in attenuating tumorigenesis, while PRC2 activity is required to establish chemoresistance (Hu et al., 2010; Iliopoulos et al., 2010; Ougolkov et al., 2008). Comparably, increased EZH2 activity protects glioblastoma stem cells from radiation therapy, while EZH2 inhibition extenuates radioresistance (Kim et al., 2015). Therefore, to more efficiently medicate malignant melanoma, apart from combining EZH2 inhibitors with immunotherapy, a possibly highly effective treatment strategy might incorporate MAPK-targeting therapeutics and EZH2 inhibition.

A considerable number of melanomas harbor damaging alterations in the *NF1* locus (De Raedt et al., 2014; Hodis et al., 2012; Krauthammer et al., 2012), while *NF1* is frequently lost upon MAPK inhibition, thus re-establishing MAPK signaling (Maertens et al., 2013; Van Allen et al., 2014; Whittaker et al., 2013). Importantly, in several cancers including MPNSTs and cutaneous melanoma, *NF1* aberrances co-occur with *EED* or *SUZ12* loss, which expedites tumorigenesis (3.5.2. Epigenetic regulation of neurocristopathies). Comparably, I observed a subset of the *EZH2* mutations occurring in melanoma specimens to be damaging for PRC2 function (Figure 18). Interestingly, in *NF1*-deficient melanoma cells, *SUZ12* depletion enhances growth, while *SUZ12* ablation counteracts growth of $NF1^{WT}$ cells. Therefore, in melanoma patients bearing loss of PRC2 function, EZH2 inhibition might exacerbate tumorigenesis rather than counteracting it. However, loss of *EED* or *SUZ12* sensitizes tumors to BET bromodomain inhibitors (De Raedt et al., 2014). Hence, careful genomic screening would be absolutely prudent prior to subjecting melanoma patients to an EZH2-inhibiting therapy to minimize adverse clinical responses, while BRD4 inhibition might represent an alternative treatment strategy for the PRC2-inactivated subset of melanoma patients.

5.8. EZH2 inhibition as possible future melanoma therapy

In a murine model of glioblastoma, *Ezh2* depletion first abolishes tumor growth, but prolonged *Ezh2* ablation epigenetically redirects remaining tumor cells to an undifferentiated, stem cell-like state, which eventually results in tumor progression. In this model, stemness of glioblastoma cells upon *Ezh2* loss is promoted by de-repression of pluripotency genes, which confers tumor aggressiveness. However, release from *Ezh2* depletion abolishes the acquired stemness features and attenuates the growth advantages (de Vries et al., 2015). A small group of *Tyr::N-Ras*^{Q61K} *Ink4a*$^{-/-}$ mice similarly developed *Ezh2*-deficient melanomas despite knockout of *Ezh2* in benign hyperplasia long prior to tumor initiation (Figure 23g, h). Therefore, also in melanoma, cells rarely escape Ezh2 dependence and form progressing tumors. These observations highlight the importance of carefully establishing regimens for possible future EZH2 inhibition-based therapies, potentially including intermittent EZH2 blockade.

Dependent on the mutational landscape, levels of oxidative and metabolic stress, the stromal context including the immune system, and the history of exposure to melanoma therapeutics, the set of aberrantly silenced tumor suppressor genes might be assembled differently in a given melanoma and at a given time point (Figure 6). However, I have demonstrated that EZH2 itself represents a central node in the control of melanoma progression through epigenetic regulation of such genes (Figure 44). In support of this, pharmacological inhibition of Ezh2 using the preclinical drug GSK503 in melanoma-bearing mice efficiently counteracted metastatic melanoma progression, resulting in a doubled survival time (Figure 32). Therefore, my PhD thesis reveals that EZH2 inhibition, likely in combination with immunotherapeutics or MAPK-targeting therapeutics, might be a promising strategy for future therapies of human melanoma patients.

6. Materials and Methods

6.1. *In vivo* experiments

6.1.1. Human biopsies

Human biopsies were isolated and genotyped as described (Zipser et al., 2011). Usage of nevus and melanoma biopsies as well as melanoma-derived cell cultures was approved by the official ethical authorities of Canton of Zurich, Switzerland. Written informed consent was obtained from all subjects and approved by the local institutional review boards (EK647, EK800).

6.1.2. Mice

Tyr::N-Ras^{Q61K} animals and *Ink4a*-defficient mice have previously been described (Ackermann et al., 2005; Serrano et al., 1996; Shakhova et al., 2012; 2015). The *Tyr::Cre*^{ERT2} line (Bosenberg et al., 2006; Harris and Pavan, 2013; Harris et al., 2013; Shakhova et al., 2012; 2015), *Ezh2*^{lox} animals (Hirabayashi et al., 2009; Schwarz et al., 2014), and *R26R::LacZ* mice (Soriano, 1999) have been analyzed elsewhere. Mouse genotyping was performed according to a standard DNA isolation protocol (Laird et al., 1991), followed by PCR using a Taq PCR Core Kit (201225, Qiagen) and primers indicated in (Table 6). Genetic background of (*Tyr::N-Ras*^{Q61K} *Ink4a*$^{-/-}$) *Tyr::Cre*^{ERT2} *Ezh2*$^{lox/lox}$ *R26R::LacZ* mice was mixed, while background of *Tyr::N-Ras*^{Q61K} *Ink4a*$^{-/-}$ animals was Black 6. Mice were born with the expected ratio of Mendelian inheritance, and no changes in gender ratios were observed. Transgenic mice used were of both genders and were subjected to experiments either at the age of 1 month, or upon tumor development (5 to 7 months). Melanoma-developing mice were frequently monitored and sacrificed at an endpoint defined by adverse clinical symptoms, such as multiple skin tumors (Ø > 5mm), weight loss (Δm > 15%), or hunched back. 3-month-old female *C57Bl/6J* and athymic nude *Foxn1*$^{nu/nu}$ mice were purchased (Charles River Laboratories). Mice engrafted s.c. with melanoma cells were sacrificed at an endpoint defined by tumor volume (V > 1'000mm^3). Tumor volume was calculated as follows: $V = 2/3 \times \pi \times ((a + b) / 4))^3$, a (mm) was the length and b (mm) was the width of the tumor. Mice engrafted i.v. with melanoma cells were sacrificed 12 days post engraftment. All animal experiments have been approved by the veterinary authorities of Canton of Zurich, Switzerland, and were performed in accordance with Swiss law and the GlaxoSmithKline policy on the Care, Welfare, and Treatment of Animals.

Table 6 | Mouse genotyping primers.

Allele	Forward sequence	Reverse sequence
Cre	CTATCCAGCAACATTTGGGCCAGC	CCAGGTTACGGATATAGTTCATGAC
Ezh2^{wt}	AAGGCTGTGTACAGGAAACAATC	AGTACTCCAGAGGTACTGAAGTTTG
Ezh2^{lox}	AAGGCTGTGTACAGGAAACAATC	TCACCTTAATATGCGAAGTGGAC
Ink4a^{wt}	ATGATGATGGGCAACGTTC	CAAATATCGCACGATGTC
Ink4a-knockout	CTATCAGGACATAGCGTTGG	AGTGAGAGTTTGGGGACAGAG
LacZ	GGTCGGCTTACGGCGGTGATTT	AGCGGCGTCAGCAGTTGTTTTT
N-Ras^{Q61K}	GATCCCACCATAGAGGATT	CTGGCGTATTTCTCTTACC

6.1.3. *In vivo* Tamoxifen, GSK503, IL2-Cx, and α-CTLA4 application

In order to conditionally ablate *Ezh2*, (*Tyr::N-Ras*^{Q61K} *Ink4a*$^{-/-}$) *Tyr::Cre*^{ERT2} *Ezh2*$^{lox/lox}$ *R26R::LacZ* mice were subjected to treatment with tamoxifen (TM, T5648, Sigma-Aldrich), which was diluted (10mg/ml) in ethanol and sunflower oil (1:9 ratio). Conditional ablation of *Ezh2* was achieved by daily intraperitoneal injections of 2mg TM for 5 consecutive days. Mice were either 4 weeks old or at an age of 5 to 7 months, when first skin melanomas had become macroscopically detectable (Ø ≥ 2mm). In order to pharmacologically inhibit Ezh2 activity, *Tyr::N-Ras*^{Q61K} *Ink4a*$^{-/-}$, *Ink4a*$^{-/-}$, and *C57Bl/6* mice were subjected to treatment with GSK503 (Béguelin et al., 2013), which was diluted (15mg/ml) in 20% Captisol solution (Cydex). Efficient Ezh2 inhibition was achieved by daily intraperitoneal injections of 150mg/kg GSK503 over 35 consecutive days. *Ink4a*$^{-/-}$ and *C57Bl/6* mice were 5 months old. *Tyr::N-Ras*^{Q61K} *Ink4a*$^{-/-}$ animals were at an age of 5 to 7 months, when first skin melanomas had become macroscopically detectable (Ø ≥ 2mm). Mice were monitored during and after treatment to measure GSK503-induced reversible weight loss. Moreover, a few GSK503 treated animals developed ascites, independently of the genotype, and had to be excluded from the studies. *C57Bl/6* and *Foxn1*$^{nu/nu}$ mice engrafted with melanoma cells were subjected to TM and GSK503 treatment as described above. *C57Bl/6* mice engrafted with melanoma cells were subjected to IL2-Cx and α-CTLA4 treatment as previously specified (Krieg et al., 2010; Létourneau et al., 2010).

6.1.4. Quantification of skin melanomas and metastases

When *Ezh2* ablation was done at 1 month, developing trunk skin lesions were considered as melanomas above a diameter of 2mm (Ø ≥ 2mm). At day of sacrifice, a final skin melanoma count was established. In conditional *Ezh2* knockout mice (cKO) whole mount X-Gal staining was used to quantify recombined tumors, and X-Gal negative tumors were excluded from cKO melanoma count. To quantify metastases, accessory axillary, proper axillary, sciatic, and subiliac lymph nodes (total of 8) (Van den Broeck et al., 2006) as well as the lung were subjected to further analyses. Lymph nodes were considered melanoma-positive, when Sox10-positive cells were found on histological sections. Black dots on lung surface were counted and confirmed as melanoma metastases using Sox10 staining on histological sections. Melanoma-specific survival curves were based on presence of (recombined) skin melanomas and/or metastases. When *Ezh2* ablation or GSK503 treatment was done in established melanoma, newly forming skin melanomas (Ø ≥ 2mm) were counted weekly. At day of sacrifice, skin melanoma and metastases counts were established as described for early *Ezh2* ablation, except skin melanoma numbers were not based on recombination but solely on tumor numbers. Melanoma-specific survival curves were based on presence of newly formed skin melanomas and/or metastases.

6.1.5. Isografting and allografting of murine melanoma cells

Skin melanomas from *Tyr::N-Ras*^{Q61K} *Ink4a*$^{-/-}$ (*Tyr::Cre*^{ERT2} *Ezh2*$^{lox/lox}$ *R26R::LacZ*) animals were dissociated into small pieces using forceps and scissors. Tissue was digested using 0.25mg/ml Liberase DH Research Grade (05401054001, Roche) in RPMI 1640 (42401, Life Technologies) for 45min at 37°C followed by a treatment with 0.55mg/ml Dispase II (17105, Life Technologies) and 0.2mg/ml DNase I (10104159001, Roche) for 15min at 37°C. Single cells were separated from remaining tissue using a 70μm cell strainer and engrafted s.c. into *Foxn1*$^{nu/nu}$ mice in PBS or cultured *in vitro* using growth medium as described below. *Foxn1*$^{nu/nu}$ mice were s.c. engrafted with either 500'000 *Tyr::N-Ras*^{Q61K} *Ink4a*$^{-/-}$ Melanoma (RIM)-1 cells, 500'000 RIM-2 cells, or 1 Mio RIM-3 cells. *C57Bl/6* mice were either s.c. engrafted with 1 Mio B16-F10 cells or tail vein-injected with 400'000 B16-F1 cells / 100'000 B16-F10 cells.

6.1.6. Histological analysis and immunofluorescence

Human and mouse tissue samples were fixed in 4% buffered formaldehyde and embedded in paraffin, except for whole mount X-Gal staining. Therefore, mouse tissue samples were fixed in formaldehyde for 20min and subjected to X-Gal staining as described (Shakhova et al., 2012). Human samples were processed into sections of 3mm thickness, while mouse samples were processed into 5mm sections. Slides were stained with haematoxylin and eosin (H&E) according to standard protocols. Sections were subjected either to immunohistochemical analyses or to immunofluorescent analyses. Briefly, immunohistochemical stainings were performed using primary antibodies (Table 7) in combination with the iVIEW DAB Detection Kit (760-091, Ventana) or the ChemMate Detection Kit (K5006, Dako) according to manufacturers' protocols. For immunofluorescence, protocols described elsewhere were applied (Shakhova et al., 2012). Briefly, sections were deparaffinized and subjected to an antigen retrieval step using citrate buffer (S2369, Dako). Primary antibodies (Table 7) were applied in blocking buffer (1% BSA in PBS and 0.05% Triton X-100) overnight at 4°C and visualized using secondary antibodies (Table 8) in blocking buffer for 1h at room temperature. For visualization of β-Gal, a biotin α-chicken (1:300, AP194B, Merck Millipore) secondary antibody was combined with further signal amplification using HRP-streptavidin (1:300, 016-030-084, Jackson ImmunoResearch) and the TSA Plus Cy3 Kit (1:50, NEL744001KT, PerkinElmer) according to manufacturer's protocol. Subsequently, nuclei were stained with Hoechst 33342 (14533, Sigma-Aldrich) and slides were mounted with Fluorescent Mounting Medium (S3023, Dako). Immunohistochemical / -fluorescent sections were analyzed using either a Mirax Midi Slide Scanner (Zeiss) or a DMI 6000B microscope (Leica).

Table 7 | Primary antibodies.

Anitgen	Specificity	Company	Serial number	Applications / Dilutions
b-Actin	human / mouse	Sigma-Aldrich	A5316	WB, 1:10'000 / IF, 1:1'000
DCT	human / mouse	Santa Cruz Biotechnology	sc-10451	IF, 1:200
EZH2	human / mouse	Cell Signaling Technology	3147	WB, 1:1'000 / IF, 1:200
b-Gal	mouse	Abcam	ab9361	IF, 1:1'000
Histone 3	human / mouse	Cell Signaling Technology	3638	WB, 1:1'000
H3K27me3	human / mouse	Cell Signaling Technology	9733	WB, 1:1'000 / IF, 1:500
HMB45	human	Dako	IS052	IHC, 1:50
KI67	human	Abcam	ab156956	IF, 1:50
Ki67	mouse	BioLegend	652402	IF, 1:100
MART1	human	Novocastra	PA0233	IHC, 1:50
MART1-HMB45	human	Abcam	ab732	IF, 1:200
SOX10	human / mouse	Santa Cruz Biotechnology	sc-17342	IF, 1:100
Tyrp1	mouse	V. Hearing Lab, NIH (Kobayashi and Hearing, 2007)	aPEP1	IF, 1:500

Table 8 | Secondary antibodies.

Fluorophore	Specificity	Company	Serial number	Applications / Dilutions
Alexa488	goat	Jackson ImmunoResearch	705-545-147	IF, 1:500
Alexa488	rabbit	Jackson ImmunoResearch	711-545-152	IF, 1:500
Alexa488	rat	Jackson ImmunoResearch	712-545-153	IF, 1:500
Alexa546	mouse	Life Technologies	A-11030	IF, 1:500
Cy3	goat	Jackson ImmunoResearch	705-165-147	IF, 1:500
Cy3	rat	Jackson ImmunoResearch	712-165-153	IF, 1:500
IRDye-800CW	mouse	LI-COR Biosciences	926-32212	WB, 1:10'000
IRDye-680LT	rabbit	LI-COR Biosciences	926-68023	WB, 1:10'000

6.1.7. Peripheral blood sample and tumor-infiltrating CTL analysis

Blood samples, tumors, and tumor-draining lymph nodes were collected and processed as previously described (Krieg et al., 2010; Létourneau et al., 2010). BrdU, immunophenotype, and CTL antigen-specific clone labeling for flow cytometry was performed according to previous reports (Krieg et al., 2010; Létourneau et al., 2010) and cell populations were quantified using a BD FACSCanto II flow cytometer (BD Biosciences) and FlowJo software (Tree Star).

6.2. *In vitro* experiments

6.2.1. *EZH2* mutagenesis and mutation analysis

EZH2 mutations were chosen based on specimens in the Somatic Mutations dataset for Skin Cutaneous Melanoma (SKCM) as described below. Specimens showing non-synonymous mutations in the coding sequence of *EZH2* and for which clinical data was available were selected. A previously validated pRetro-X construct containing human $EZH2^{WT}$, $EZH2^{Y646N}$, or $EZH2^{Y646F}$ cDNA was used (Béguelin et al., 2013). Further mutations were introduced into $EZH2^{WT}$ cDNA using a QuikChange II Site-Directed Mutagenesis Kit (200523, Agilent Technologies) according to manufacturer's protocol. For each mutation, 10ng of template $EZH2^{WT}$ cDNA was used with the appropriate primers containing the corresponding sequence modification (Table 9), and constructs were sequenced using 3 pairs of primers covering the *EZH2* sequence (Table 10).

Table 9 | Human *EZH2* mutagenesis primers.

EZH2 mutation		Sequence
$EZH2^{P132S}$	forward	CTAAAACTTCATCTCCCATATAAGAAATGTTATGTAAAACAGTTTCATCTTC
$EZH2^{P132S}$	reverse	GAAGATGAAACTGTTTTACATAACATTTCTTATATGGGAGATGAAGTTTTAG
$EZH2^{D142V}$	forward	TAGTTCTTCAATGAAAGTACCAACCTGATCTAAAACTTCATCTCC
$EZH2^{D142V}$	reverse	GGAGATGAAGTTTTAGATCAGGTTGGTACTTTCATTGAAGAACTA
$EZH2^{R216Q}$	forward	TCAAAAATTTTATCAGAAGGAAATTTTTGAGGTGGGCGGCTTTCTTTATCATC
$EZH2^{R216Q}$	reverse	GATGATAAAGAAAGCCGCCCACCTCAAAAATTTCCTTCTGATAAAATTTTTGA
$EZH2^{A226V}$	forward	CTTATCTGGAAACATTGAGGAAATGACTTCAAAAATTTTATCAGAAGGAAAT
$EZH2^{A226V}$	reverse	ATTTCCTTCTGATAAAATTTTTGAAGTCATTTCCTCAATGTTTCCAGATAAG
$EZH2^{P431S}$	forward	CCACATTCTCAGGAGATTCAATATTTGGCTTCATCTTTATTGGT
$EZH2^{P431S}$	reverse	ACCAATAAAGATGAAGCCAAATATTGAATCTCCTGAGAATGTGG
$EZH2^{K515R}$	forward	GAGGAGCCGTCCCTTTTCAGCTGTATCTTTCTGCAG
$EZH2^{K515R}$	reverse	CTGCAGAAAGATACAGCTGAAAAGGGACGGCTCCTC
$EZH2^{C535W}$	forward	GGCACGAACTGTCCCAAGGCTGCCGTG
$EZH2^{C535W}$	reverse	CACGGCAGCCTTGGGACAGTTCGTGCC

Table 10 | Human *EZH2* sequencing primers.

Gene location	Forward sequence	Reverse sequence
EZH2 N-term	TGTTCGGTGACCAGTGACTT	TTTGGTCCATCTATGTTGGGG
EZH2 middle	ATACAGACAGTGATAGGGAAGCA	CATCCCGGAAAGCGGTTTTG
EZH2 C-term	CAAGAACTGCAGTATTCAGCG	CCGACATACTTCAGGGCATC

6.2.2. Cell cultures

Human melanoma cell cultures were characterized before (Zipser et al., 2011), XB2 and Melan-a cell lines were previously described (Bennett et al., 1987), and HEK293T, B16-F1, and B16-F10 cell lines were purchased (ATCC). All cells (including primary RIM cells) were cultured in growth medium, which was RPMI 1640 (42401, Life Technologies) supplemented with 10% FCS (16140, Life Technologies), 4mM L-Glutamine (25030, Life Technologies), Penicillin-Streptomycin (15070, Life Technologies), and Fungizone Antimycotic (15290, Life Technologies) as previously specified (Shakhova et al., 2012; Zipser et al., 2011).

6.2.3. Cell transfections and *in vitro* GSK503 treatment

In order to overexpress $EZH2^{WT}$ and mutated *EZH2*, HEK293T cells were grown in growth medium devoid of antibiotics and transfected with 10μg *EZH2*-expressing plasmids using 2.5M $CaCl_2$ in HEPES buffer according to standard protocols, and cells were subjected to functional analyses after 36h. In order to temporarily deplete EZH2, DCK, AMD1, and WDR19, human melanoma cells were transfected with small interfering RNAs (siRNA) indicated in (Table 11). 25nM siRNA was applied in combination with jetPRIME siRNA Transfection Reagent (114-15, Polyplus Transfection) according to manufacturer's guidelines. Growth medium was exchanged after 24h and cells were subjected to further assays after 72h, unless specified. For all functional assays the most efficient siRNAs underlined in (Supplementary Table 9) were used. In order to stably deplete Ezh2 and Amd1, murine melanoma cells were transfected with small hairpin RNA (shRNA)-expressing plasmids indicated in (Table 11). 10μg plasmid was applied in combination with jetPEI DNA Transfection Reagent (101-10N, Polyplus Transfection) according to manufacturer's guidelines. Transfected cells were selected using 1μg/ml puromycin (A11138-02, Life Technologies) for 1 week before subjection to further assays. Efficiency of shEzh2 was previously validated (Tiwari et al., 2013). In order to pharmacologically inhibit EZH2, melanoma cells were treated either with vehicle (DMSO) or 1μM GSK503. Cells were treated for 8 days before subjection to further assays. Drug was only replenished when cells were passaged during the 8-day period.

Table 11 | RNAi constructs.

Target gene	si/shRNA name	Specificity	Company	Serial numbers
none	siCo	human	Life Technologies	12935-112
EZH2	siE	human	Life Technologies	HSS176653, HSS176652, HSS103462
DCK	siDCK	human	Life Technologies	HSS141795, HSS175996, HSS175997
AMD1	siAMD1	human	Life Technologies	HSS100444, HSS178141, HSS178142
WDR19	siWDR19	human	Life Technologies	HSS126737, HSS126738, HSS184043
none	shCo	mouse	Sigma-Aldrich	SHC002
Ezh2	shE	mouse	Sigma-Aldrich	TRCN0000039040
none	shCo	mouse	GE Healthcare	RHS4346
Amd1	shAmd1	mouse	GE Healthcare	V2LMM_71494, V2LMM_72222

6.2.4. Cell growth and apoptosis assays

To establish growth curves, cell counts were measured daily starting 48h after transfection. For cell cycle analysis, cells were 50% ethanol-fixed, and labeled with propidium iodide including RNase A (F10797, Life Technologies). To measure apoptosis, an Annexin V Apoptosis Detection Kit (559763, BD Biosciences) was used. Cell cycle and apoptotic cells were quantified using a BD FACSCanto II flow cytometer (BD Biosciences) and FlowJo software (Tree Star).

6.2.5. Boyden chamber invasion assay

After 24h of transfection or 8d of GSK503 treatment, cells were starved for 48h in starvation medium containing all supplements except 1% FCS. Subsequent Boyden chamber invasion assays were done according to manufacturer's protocol. Briefly, 150'000 cells were subjected to Matrigel-coated well inserts (354480, BD Biosciences) in empty medium (0% FCS, 0% L-Glutamine). Growth medium was used as chemoattractant for 24h. Transvaded cells were 4% buffered formaldehyde-fixed and visualized using Hoechst 33342 (14533, Sigma-Aldrich). Membranes were mounted to glass slides, and cell numbers were quantified using a DMI 6000B microscope (Leica) and CellProfiler software (Carpenter et al., 2006).

6.2.6. Immunofluorescence on cells

Cells were grown on cover slips, 50% ethanol-fixed, and subjected to immunofluorescent labeling using primary antibodies (Table 7) in blocking buffer (1% BSA in PBS) overnight at 4°C and secondary antibodies (Table 8) for 1h at room temperature. Nuclei were stained with Hoechst 33342 (14533, Sigma-Aldrich), and cells were recorded with a DMI 6000B microscope (Leica).

6.2.7. Protein isolation and western blotting

Protein isolation and western blotting was done as previously described (Shakhova et al., 2012), unless specified. Briefly, cells were lysed in RIPA buffer (89900, Thermo Scientific) containing Halt Phosphatase and Protease Inhibitor Cocktail (78420, 87786, Thermo Scientific), while tumor biopsies were homogenized in such buffer using a tissue homogenizer (Polytron). SDS-PAGE was carried out on 4-20% Mini-PROTEAN TGX Gels (456-1094, Bio Rad). Primary antibodies (Table 7) were applied in Odyssey blocking buffer (927-40000, LI-COR Biosciences) overnight at 4°C and visualized using secondary antibodies (Table 8) in Odyssey blocking buffer (927-40000, LI-COR Biosciences) for 45min at room temperature. Blots were scanned and quantified with an Odyssey imaging system (LI-COR Biosciences). Quantified band intensities were normalized using either β-Actin or Histone 3 as housekeeping protein. Full scans are shown in (Figure 46).

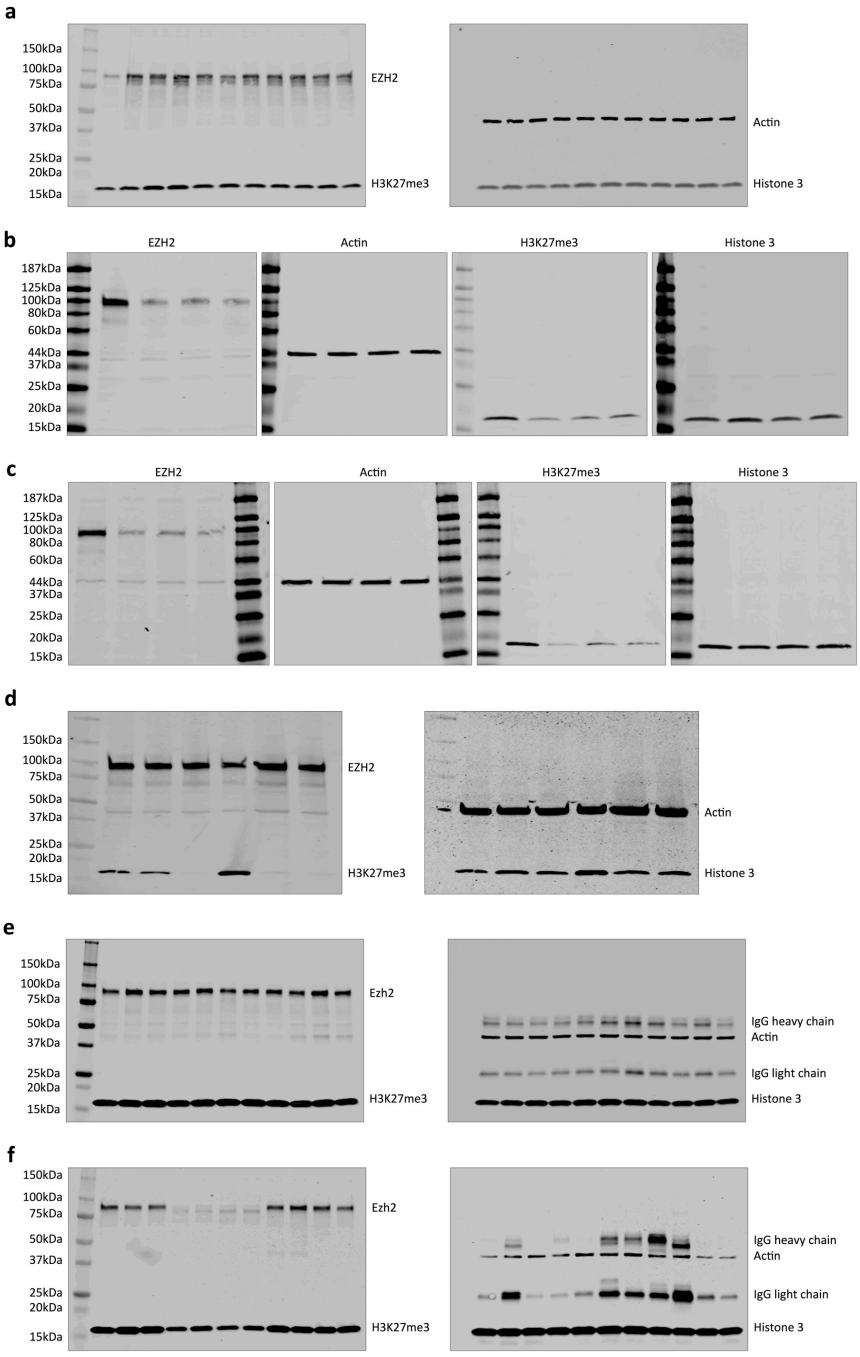

Figure 46 | Full scans of western blots. (**a**) Full scans corresponding to (**Figure 18c**). (**b - d**) Full scans of M010817 (**b**, **d**) and M050829 (**c**, **d**) after siE (**b**, **c**) or GSK503 (**d**) corresponding to (**Figure 26a**). (**e**) Full scans corresponding to (**Figure 28d**). (**f**) Full scans corresponding to (**Figure 29c**).

6.2.8. RNA isolation and RT-qPCR

RNA extraction and DNase treatment of samples was performed using the RNeasy Mini Kit (74104, Qiagen) and the RNase-Free DNase Set (79254, Qiagen) according to manufacturer's guidelines. Purified RNA was quantified using nanodrop and subjected to reverse transcriptase reaction using Maxima First Strand cDNA Synthesis Kit (K1641, Thermo Scientific) followed by an RNase H (EN0202, Thermo Scientific) digestion step according to manufacturer's recommendations. Quantitative real-time PCR was performed on a LightCycler 480 System (Roche) using LightCycler 480 SYBR Green I Master (4707516001, Roche). Primers used are indicated in (Table 12; 13). Each sample was analyzed in technical triplicates, and relative quantified RNA was normalized using *USF1* or *GAPDH*, when specified, as housekeeping transcript.

Table 12 | Mouse RT-qPCR primers.

Gene	Forward sequence	Reverse sequence
Acta2	TGACAGAGGCACCACTGAAC	AGAGGCATAGAGGGACAGCA
Amd1	TGTGGAAGTCTTCAAGCCAGG	CGAAGAAAGCACTGTGCGAC
Cd40	TCCTCATCACCATTTTCGGGG	TCCATCTCCTGGGGATCTTG
Cd70	CGCACACAGCTGAGTTACAG	CTCTGGTCCGTGTGTGAAGG
Cd80	CGACTCGCAACCACACCAT	GCTATCAGGAGGGTCTTCTGG
Cd86	AGCTTCAGTTACTGTGGCCC	TGTCAGCGTTACTATCCCGC
Cdh1	CTGCTGCCACCAGATGATGA	CTGTGCAGCTGGCTCAAATC
Cdh2	GCGCCATCATCGCTATCCTT	TCCCGCCGTTTCATCCATAC
Dck	AAGCTGGCTCCTTCATCGGA	TAACATCCAGTGTGAGGACGG
Dct	CCTGAATGGGACCAATGCCT	AGGCATCTGTGGAAGGGTTG
Ets1	GCCAACCCTACCTACCCAGA	GAGGGAGGAACACACTGAGC
Ezh2	GTGACCACAGGATAGGCATCT	CAAGGGATTTCCATTTCTCG
Fas (Cd95)	TCCCAGAAATCGCCTATGGT	CCTGTCTCCTTTTCCAGCACT
H2-D1	GGAGCTATGGCCATCATTGGA	TCTCGGAGAGACATTTCAGAGC
H2-K1	CTGGAGCTGTGGTGGCTTT	GACAGATCAGAGGTCTGGGAG
Mitf	CCCCAAGTCAAATGATCCAG	GCAACTTCCGGATGTAGTCC
Mmp1	GAACACGGGGAAGACCCTCT	TTCCTCTTCTATGAGGCGGGG
Mmp3	GACTCAAGGGTGGATGCTGT	CCAACTGCGAAGATCCACTG
Ox40l (Tnfsf4)	GGACCCTCCAATCCAAAGACT	CCGAATTGTTCTGCACCTCC
Pd-L1 (Cd274)	GGACTACAAGCGAATCACGC	TTCTGGATAACCCTCGGCCT
Pmel	GGGGATGCATTTGAGCTGAC	CTGGCACCCTGGTGATGAAA
Psmb8	AGCATCCAAGCTGCTTTCCAA	CCGAGTCCCATTGTCATCTACG
Psmb9	GGTTCCGGAAGCTCCTACAT	AGAGCCATCTCGGTTCATGG
Snai1	GTGGAAAGGCCTTCTCTAGGC	GGTTGGAGCGGTCAGCAAAA
Sox10	GAAGAAGGCTCCCCCATGTC	GCTCTGTCTTTGGGGTGGTT
Tap1	TCCCTCAGGGCTATGACACA	ATAAGCAGGAGTGGCTTCCG
Tap2	ACTGTGAGGACGCTCAAGTG	TAACTGGCCCCCTTTTTCCC
Tgfb1	ATGCCAACTTCTGTCTGGGAC	CGGGTTGTGTTGGTTGTAGAG
Twist1	CGGCCAGGTACATCGACTTC	TGCAGCTTGCCATCTTGGAG
Tyr	GTACTTGGGAGGTCGTCACC	GTCCCTCAGGTGTTCCATCG
Usf1	CAGGGCTCAGAGGCACTACT	GCTCCCTCCCTGCAATACTT
Vim	GCGAGGAGAGCAGGATTTCT	TGAGTGGGTGTCAACCAGAG
Wdr19	ACCACCCCATGTCCATTCTG	CGTCTTTCAACATGTGTCGGC
Zeb1	GATCCAGCCAAACGGAAACC	TGGCGTGGAGTCAGAGTCAT

Table 13 | Human RT-qPCR primers.

Gene	Forward sequence	Reverse sequence
ACTA2	GGCAAGTGATCACCATCGGA	GTGGTTTCATGGATGCCAGC
AMD1	CCAGGAAAATTTGTGACCACCT	ACTCTGGCAATCAAGACGCT
APOBEC3D	AAGCACCACTCAGCTGTCTTC	CCAGGTGACCTCGTAGTTTGT
CD40	AGTCAGTGCTGTTCTTTGTGC	TTCGCTTTCACCGCAAGGA
CDH2	ACAGTGGCCACCTACAAAGG	CCGAGATGGGGTTGATAATG
DCK	AAAGCTGGCTCCTGCATAGG	TCCAGTGTTAAGATAGGCACCTC
ETS1	GATAGTTGTGATCGCCTCACC	GTCCTCTGAGTCGAAGCTGTC
EZH2	CCCTGACCTCTGTCTTACTTGTGGA	ACGTCAGATGGTGCCAGCAATA
FAM198B	AGCGAAAGCATGACCCAAGG	CCGTAAGTGCTGGCTCTTCAA
GAPDH	ACCCAGAAGACTGTGGATGG	TCTAGACGGCAGGTCAGGTC
KCTD18	TGCGTCACATGGCTCCAAT	CTGAGGCCGAGTTCTTGACTT
MMP1	TTGTGGCCAGAAAACAGAAA	TTCGGGGAGAAGTGATGTTC
MMP3	CAATTTCATGAGCAGCAACG	AGGGATTAATGGAGATGCCC
MPC1	ATCAGTGGGCGGATGACATT	GGCATGCAAACAGAAGCCAG
MUT	ACTTAACTCCCTTGGACGGC	CGAGTCCCAGGACCAAATACA
PYROXD2	AGCAGGAGAGAGACGCTTATG	TGAGGATGTCTCTGCCAACC
RAB40B	ATGGGATGGACCGGCTCT	TTAAGGCAATGGGGAGCGG
SCPEP1	AGCATTGTGGACGAGTTGCT	ACTTCAGTTTCCGCACCCAG
SNAI1	CCTCCCTGTCAGATGAGGAC	CCAGGCTGAGGTATTCCTTG
SNAPC1	TGAAAGGGCAGAATCATTAGCG	TTGACTTGCCCTTGACCAGA
SNAPC5	GAAGAGGGGATGAGATGCTGTC	CAGCTCCAGGGTTGTTTGGT
STX8	TCGCCAAAAACAAATGGGGC	TGTTTACCCGCCTGGTTTCA
TWIST1	GTCCGCAGTCTTACGAGGAG	CCAGCTTGAGGGTCTGAATC
TXNIP	TATCCTGGGCTGCAACATCC	TCTGCTGCCAATTACCAGGG
USF1	TACTACCCAGGGCTCAGAGG	TCCCTGCAGTACTTCTTGTGG
VIM	GAGAACTTTGCCGTTGAAGC	GCTTCCTGTAGGTGGCAATC
WDR19	TGATGAGGCCTGAATACCGC	AATGGACATGGAGTCGTGGC
XPOT	GACCTGGCAGATGCACAAAC	GCAAGGAGGGCAGGTATTCT
ZC3H6	ATGAGTCCCTGCAAAACCCAG	TGGGCAAATTCACCATGCCA
ZEB1	GCACAACCAAGTGCAGAAGA	CATTTGCAGATTGAGGCTGA

6.2.9. Chromatin isolation and ChIP

Chromatin isolation and ChIP was done as previously described (Santoro, 2014). Briefly, an antibody against H3K27me3 (1:250, 9733, Cell Signaling Technology) and Dynabeads Protein A (10002D, Life Technologies) were used. Quantitative real-time PCR was performed on a Rotor Gene RG-3000A (Qiagen) using the SensiFAST Probe Hi-ROX Kit (BIO-82005, Bioline). Primers were designed to amplify genomic DNA from a region flanking the transcriptional starting site -500bp to +100bp devoid of local CpG islands using CpG island prediction (Li and Dahiya, 2002). Primers used are indicated in (Table 14). Relative promoter enrichment was normalized to chromatin inputs and to *GAPDH* promoter as negative control.

Table 14 | Human ChIP primers.

Promoter	Forward sequence	Reverse sequence
AMD1	ACAGCTGGAACAATCCGCAG	CGTGAGACTAGCGAACAACCA
APOBEC3D	TTTGCAATTGCCTTGGGTCC	GCCCTGGGACGCTTTATCTT
CD40	GAGTTGTTTTTGCCCCGACC	CTGCCCCCACAAAAATCAGC
DCK	CAGCCTGGCTCTCTAAGTGG	CATCTGGGGAGAAGGCACTG
FAM198B	CCCTGTCCCCTTTCTGTCTTC	TGTCCTAGCACAAAGGCAGG
GAPDH	TACTAGCGGTTTTACGGGCG	TCGAACAGGAGGAGCAGAGAGCG
KCTD18	AGTGACCTTGGACAATCGCA	CACACGGTAGAGAAGGCCAG
MPC1	GAGAGGGTGCGCTTGTCAG	CACTGTCACCGGCTCTCTAC
MUT	CGCGCCCAAACATTCGTAAA	AGGGTTAGATGCCCGTTTCC
PYROXD2	GCATGGAGTTGGAGCAGAGT	CAGAGTGGAGCTCGAAAGGG
RAB40B	AACTGGACCGACCCCGA	GAACTCGCTCCCACGGTC
SCPEP1	TGGTCTGAGTGCTTCCGTTC	CGGGGAAACCTCATTGACCA
SNAPC1	AGACCTAAAACCGCTCGTGA	TTGCTTTCACCCAGAGTGCT
SNAPC5	AGGTATTGACCAGCAGCCTC	CTGGCTTTGTCATGCCTGTG
STX8	TACAGAGAGGTCTTGCAGCG	CTGCGGACAGTACACTGGAG
TXNIP	AAGGAGTGCTTGTGGAGATCG	TACGCCGCTGGTTACACTAAG
WDR19	CTCCTCCCTTCTACCCCAGA	GGAGGCAGGATGGGCTAAAT
XPOT	CTGCTGTACTCGGGACACTT	GGATTCACGAATCAGGATGACG
ZC3H6	AAACTGCATGGCAAGCTATTTTCC	AAGGCGGCTGTAGAGTCCTTA

6.3. *In silico* analyses

6.3.1. Microarray analysis

Total RNA was isolated as described for RT-qPCR. Total RNA was amplified and biotin-labeled using the MessageAmp II-Biotin Enhanced aRNA Amplification Kit (AM1791, Life Technologies). Biotin-labeled RNA was hybridized to Human Gene 2.1 ST Array (902136, Affymetrix) following the manufacturer's protocol. After hybridization, microarrays were washed and stained using a GeneChip Fluidics Station 450 (Affymetrix), and scanned with a GeneChip Scanner 7G (Affymetrix). Differential gene expression was determined by R package limma (Smyth, 2005). Microarray data have been deposited in the NCBI Gene Expression Omnibus (GEO) archive under the accession code GSE63165. Gene ontology network analysis was performed with MetaCore (Thomson Reuters).

6.3.2. TCGA analysis

The RNAseq, Somatic Mutations, and Clinical datasets for Skin Cutaneous Melanoma (SKCM), and the Somatic Mutations datasets for Colon Adenocarcinoma (COAD), Lung Squamous Cell Carcinoma (LUSC), Lung Adenocarcinoma (LUAD), Glioblastoma Multiforme (GBM), Kidney Renal Clear Cell Carcinoma (KIRC), Acute Myeloid Leukemia (LAML), Head And Neck Squamous Cell Carcinoma (HNSC), Breast Invasive Carcinoma (BRCA), and Prostate Adenocarcinoma (PRAD) were downloaded on September 29, 2013 from The Cancer Genome Atlas (TCGA, http://cancergenome.nih.gov/). Somatic mutation data was annotated using ANNOVAR (Wang et al., 2010b). Non-synonymous *EZH2* mutations were mapped to functional EZH2 domains based on previous reports (Ciferri et al., 2012; Tiffen et al., 2015). Raw RNAseq reads were normalized with edgeR (Robinson et al., 2010) and differential RNA expression was analyzed with voom from R package limma (Smyth, 2005). Specimens with top and bottom transcript levels for a gene of interest were used for analysis. Patient numbers were gradually increased from a minimum of top and bottom 7% (19 out of 274) to a maximum of top and bottom 25% (69 out of 274), in order to optimize potential segregation of Kaplan-Meier curves. This procedure was performed for *EZH2* and all commonly differentially expressed genes form the microarray datasets (Figure 35a) in an unbiased way.

6.3.3. Statistical analyses

Quantifications of immunofluorescent stainings were done on sections of at least 3 different mice. Therefore, at least 150 hair follicles or at least 300 label-positive cells were counted. Cell culture-based experiments were done at least in biological triplicates. *P*-values for comparison of 2 groups were calculated with unpaired Student's t-test, except for paired data (follow-up measurements on the same mouse). Therefore, paired Student's t-test was applied. *P*-values for comparison of multiple groups were calculated with ANOVA and Fisher's LSD-test. *P*-values for comparison of Kaplan-Meier curves were calculated with Log-rank (Mantel-Cox) test. $P < 0.05$ was considered significant.

7. References

Abdel-Wahab, O., Pardanani, A., Patel, J., Wadleigh, M., Lasho, T., Heguy, A., Beran, M., Gilliland, D.G., Levine, R.L., and Tefferi, A. (2011). Concomitant analysis of EZH2 and ASXL1 mutations in myelofibrosis, chronic myelomonocytic leukemia and blast-phase myeloproliferative neoplasms. Leukemia *25*, 1200–1202.

Abel, E.V., and Aplin, A.E. (2010). FOXD3 is a mutant B-RAF-regulated inhibitor of G(1)-S progression in melanoma cells. Cancer Res. *70*, 2891–2900.

Abel, E.V., Basile, K.J., Kugel, C.H., Witkiewicz, A.K., Le, K., Amaravadi, R.K., Karakousis, G.C., Xu, X., Xu, W., Schuchter, L.M., et al. (2013). Melanoma adapts to RAF/MEK inhibitors through FOXD3-mediated upregulation of ERBB3. J. Clin. Invest. *123*, 2155–2168.

Ackermann, J., Frutschi, M., Kaloulis, K., McKee, T., Trumpp, A., and Beermann, F. (2005). Metastasizing melanoma formation caused by expression of activated N-RasQ61K on an INK4a-deficient background. Cancer Res. *65*, 4005–4011.

Adameyko, I., Lallemend, F., Aquino, J.B., Pereira, J.A., Topilko, P., Müller, T., Fritz, N., Beljajeva, A., Mochii, M., Liste, I., et al. (2009). Schwann cell precursors from nerve innervation are a cellular origin of melanocytes in skin. Cell *139*, 366–379.

Adameyko, I., Lallemend, F., Furlan, A., Zinin, N., Aranda, S., Kitambi, S.S., Blanchart, A., Favaro, R., Nicolis, S., Lübke, M., et al. (2012). Sox2 and Mitf cross-regulatory interactions consolidate progenitor and melanocyte lineages in the cranial neural crest. Development *139*, 397–410.

Agnarsdóttir, M., Ponten, F., Garmo, H., Wagenius, G., Mucci, L., Magnusson, K., Holmberg, L., and Eaker-Fält, S. (2012). MITF Expression in Cutaneous Malignant Melanoma. J. Mol. Biomark. Diagn. *03*, 1–7.

Agnarsdóttir, M., Sooman, L., Bolander, A., Strömberg, S., Rexhepaj, E., Bergqvist, M., Ponten, F., Gallagher, W., Lennartsson, J., Ekman, S., et al. (2010). SOX10 expression in superficial spreading and nodular malignant melanomas. Melanoma Res. *20*, 468–478.

Akiyama, H., Chaboissier, M.-C., Behringer, R.R., Rowitch, D.H., Schedl, A., Epstein, J.A., and de Crombrugghe, B. (2004). Essential role of Sox9 in the pathway that controls formation of cardiac valves and septa. Proc. Natl. Acad. Sci. USA *101*, 6502–6507.

Akiyama, H., Chaboissier, M.-C., Martin, J.F., Schedl, A., and de Crombrugghe, B. (2002). The transcription factor Sox9 has essential roles in successive steps of the chondrocyte differentiation pathway and is required for expression of Sox5 and Sox6. Genes Dev. *16*, 2813–2828.

Albino, A.P., Le Strange, R., Oliff, A.I., Furth, M.E., and Old, L.J. (1984). Transforming ras genes from human melanoma: a manifestation of tumour heterogeneity? Nature *308*, 69–72.

Alcazar, O., Achberger, S., Aldrich, W., Hu, Z., Negrotto, S., Saunthararajah, Y., and Triozzi, P. (2012). Epigenetic regulation by decitabine of melanoma differentiation in vitro and in vivo. Int. J. Cancer. *131*, 18–29.

Alexaki, V.-I., Javelaud, D., Van Kempen, L.C.L., Mohammad, K.S., Dennler, S., Luciani, F., Hoek, K.S., Juárez, P., Goydos, J.S., Fournier, P.J., et al. (2010). GLI2-mediated melanoma invasion and metastasis. J. Natl. Cancer Inst. *102*, 1148–1159.

Alexandrov, L.B., Nik-Zainal, S., Wedge, D.C., Aparicio, S.A.J.R., Behjati, S., Biankin, A.V., Bignell, G.R., Bolli, N., Borg, A., Børresen-Dale, A.-L., et al. (2013). Signatures of mutational processes in human cancer. Nature *500*, 415–421.

Allie, S.R., Zhang, W., Fuse, S., and Usherwood, E.J. (2011). Programmed death 1 regulates development of central memory CD8 T cells after acute viral infection. J. Immunol. *186*, 6280–6286.

Amatangelo, M.D., Garipov, A., Li, H., Conejo-Garcia, J.R., Speicher, D.W., and Zhang, R. (2013). Three-dimensional culture sensitizes epithelial ovarian cancer cells to EZH2 methyltransferase inhibition. Cell Cycle *12*, 2113–2119.

Anaka, M., Hudson, C., Lo, P.-H., Do, H., Caballero, O.L., Davis, I.D., Dobrovic, A., Cebon, J., and Behren, A. (2013). Intratumoral genetic heterogeneity in metastatic melanoma is accompanied by variation in malignant behaviors. BMC Med. Genomics *6*, 40.

Anderson, D.J., and Axel, R. (1986). A bipotential neuroendocrine precursor whose choice of cell fate is determined by NGF and glucocorticoids. Cell *47*, 1079–1090.

Anderson, D.J., Carnahan, J.F., Michelsohn, A., and Patterson, P.H. (1991). Antibody markers identify a common progenitor to sympathetic neurons and chromaffin cells in vivo and reveal the timing of commitment to neuronal differentiation in the sympathoadrenal lineage. J. Neurosci. *11*, 3507–3519.

Aoki, Y., Saint-Germain, N., Gyda, M., Magner-Fink, E., Lee, Y.-H., Credidio, C., and Saint-Jeannet, J.-P. (2003). Sox10 regulates the development of neural crest-derived melanocytes in Xenopus. Dev. Biol. *259*, 19–33.

Arima, Y., Hayashi, H., Kamata, K., Goto, T.M., Sasaki, M., Kuramochi, A., and Saya, H. (2010). Decreased expression of neurofibromin contributes to epithelial-mesenchymal transition in neurofibromatosis type 1. Exp. Dermatol. *19*, e136–e141.

Arnold, P., Schöler, A., Pachkov, M., Balwierz, P.J., Jorgensen, H., Stadler, M.B., van Nimwegen, E., and Schübeler, D. (2013). Modeling of epigenome dynamics identifies transcription factors that mediate Polycomb targeting. Genome Res. *23*, 60–73.

Arozarena, I., Bischof, H., Gilby, D., Belloni, B., Dummer, R., and Wellbrock, C. (2011). In melanoma, beta-catenin is a suppressor of invasion. Oncogene *30*, 4531–4543.

Arvey, A., van der Veeken, J., Samstein, R.M., Feng, Y., Stamatoyannopoulos, J.A., and Rudensky, A.Y. (2014). Inflammation-induced repression of chromatin bound by the transcription factor Foxp3 in regulatory T cells. Nat. Immunol. *15*, 580–587.

Asangani, I.A., Dommeti, V.L., Wang, X., Malik, R., Cieslik, M., Yang, R., Escara-Wilke, J., Wilder-Romans, K., Dhanireddy, S., Engelke, C., et al. (2014). Therapeutic targeting of BET bromodomain proteins in castration-resistant prostate cancer. Nature *510*, 278–282.

Asangani, I.A., Harms, P.W., Dodson, L., Pandhi, M., Kunju, L.P., Maher, C.A., Fullen, D.R., Johnson, T.M., Giordano, T.J., Palanisamy, N., et al. (2012). Genetic and epigenetic loss of microRNA-31 leads to feed-forward expression of EZH2 in melanoma. Oncotarget *3*, 1011–1025.

Ascierto, P.A., Schadendorf, D., Berking, C., Agarwala, S.S., van Herpen, C.M., Queirolo, P., Blank, C.U., Hauschild, A., Beck, J.T., St-Pierre, A., et al. (2013). MEK162 for patients with advanced melanoma harbouring NRAS or Val600 BRAF mutations: a non-randomised, open-label phase 2 study. Lancet Oncol. *14*, 249–256.

Ashe, A., Butterfield, N.C., Town, L., Courtney, A.D., Cooper, A.N., Ferguson, C., Barry, R., Olsson, F., Liem, K.F., Parton, R.G., et al. (2012). Mutations in mouse Ift144 model the craniofacial, limb and rib defects in skeletal ciliopathies. Hum. Mol. Genet. *21*, 1808–1823.

Aspuria, P.-J.P., Lunt, S.Y., Väremo, L., Vergnes, L., Gozo, M., Beach, J.A., Salumbides, B., Reue, K., Wiedemeyer, W.R., Nielsen, J., et al. (2014). Succinate dehydrogenase inhibition leads to epithelial-mesenchymal transition and reprogrammed carbon metabolism. Cancer Metab. *2*, 21.

Atkins, M.B., Lotze, M.T., Dutcher, J.P., Fisher, R.I., Weiss, G., Margolin, K., Abrams, J., Sznol, M., Parkinson, D., Hawkins, M., et al. (1999). High-dose recombinant interleukin 2 therapy for patients with metastatic melanoma: analysis of 270 patients treated between 1985 and 1993. J. Clin. Oncol. *17*, 2105–2116.

Avilion, A.A., Nicolis, S.K., Pevny, L.H., Perez, L., Vivian, N., and Lovell-Badge, R. (2003). Multipotent cell lineages in early mouse development depend on SOX2 function. Genes Dev. *17*, 126–140.

Azad, N., Zahnow, C.A., Rudin, C.M., and Baylin, S.B. (2013). The future of epigenetic therapy in solid tumours--lessons from the past. Nat. Rev. Clin. Oncol. *10*, 256–266.

Azimi, F., Scolyer, R.A., Rumcheva, P., Moncrieff, M., Murali, R., McCarthy, S.W., Saw, R.P., and Thompson, J.F. (2012). Tumor-infiltrating lymphocyte grade is an independent predictor of sentinel lymph node status and survival in patients with cutaneous melanoma. J. Clin. Oncol. *30*, 2678–2683.

Azuara, V., Perry, P., Sauer, S., Spivakov, M., Jørgensen, H.F., John, R.M., Gouti, M., Casanova, M., Warnes, G., Merkenschlager, M., et al. (2006). Chromatin signatures of pluripotent cell lines. Nat. Cell Biol. *8*, 532–538.

Bachmann, I.M., Halvorsen, O.J., Collett, K., Stefansson, I.M., Straume, O., Haukaas, S.A., Salvesen, H.B., Otte, A.P., and Akslen, L.A. (2006). EZH2 expression is associated with high proliferation rate and aggressive tumor subgroups in cutaneous melanoma and cancers of the endometrium, prostate, and breast. J. Clin. Oncol. *24*, 268–273.

Bachmann, I.M., Straume, O., Puntervoll, H.E., Kalvenes, M.B., and Akslen, L.A. (2005). Importance of P-cadherin, beta-catenin, and Wnt5a/frizzled for progression of melanocytic tumors and prognosis in cutaneous melanoma. Clin. Cancer Res. *11*, 8606–8614.

Baggiolini, A., Varum, S., Mateos, J.M., Bettosini, D., John, N., Bonalli, M., Ziegler, U., Dimou, L., Clevers, H., Furrer, R., et al. (2015). Premigratory and Migratory Neural Crest Cells Are Multipotent In Vivo. Cell Stem Cell *16*, 314–322.

Baitsch, L., Baumgaertner, P., Devêvre, E., Raghav, S.K., Legat, A., Barba, L., Wieckowski, S., Bouzourene, H., Deplancke, B., Romero, P., et al. (2011). Exhaustion of tumor-specific $CD8^+$ T cells in metastases from melanoma patients. J. Clin. Invest. *121*, 2350–2360.

Bakos, R.M., Maier, T., Besch, R., Mestel, D.S., Ruzicka, T., Sturm, R.A., and Berking, C. (2010). Nestin and SOX9 and SOX10 transcription factors are coexpressed in melanoma. Exp. Dermatol. *19*, e89–e94.

Balch, C.M., Soong, S.J., Gershenwald, J.E., Thompson, J.F., Reintgen, D.S., Cascinelli, N., Urist, M., McMasters, K.M., Ross, M.I., Kirkwood, J.M., et al. (2001). Prognostic factors analysis of 17,600 melanoma patients: validation of the American Joint Committee on Cancer melanoma staging system. J. Clin. Oncol. *19*, 3622–3634.

Bald, T., Quast, T., Landsberg, J., Rogava, M., Glodde, N., Lopez-Ramos, D., Kohlmeyer, J., Riesenberg, S., van den Boorn-Konijnenberg, D., Hömig-Hölzel, C., et al. (2014). Ultraviolet-radiation-induced inflammation promotes angiotropism and metastasis in melanoma. Nature *507*, 109–113.

Bandopadhayay, P., Bergthold, G., Nguyen, B., Schubert, S., Gholamin, S., Tang, Y., Bolin, S., Schumacher, S.E., Zeid, R., Masoud, S., et al. (2014). BET Bromodomain Inhibition of MYC-Amplified Medulloblastoma. Clin. Cancer Res. *20*, 912–925.

Banerjee, S.S., and Eyden, B. (2008). Divergent differentiation in malignant melanomas: a review. Histopathology *52*, 119–129.

Bannister, A.J., Zegerman, P., Partridge, J.F., Miska, E.A., Thomas, J.O., Allshire, R.C., and Kouzarides, T. (2001). Selective recognition of methylated lysine 9 on histone H3 by the HP1 chromo domain. Nature *410*, 120–124.

Bardeesy, N., Bastian, B.C., Hezel, A., Pinkel, D., DePinho, R.A., and Chin, L. (2001). Dual inactivation of RB and p53 pathways in RAS-induced melanomas. Mol. Cell Biol. *21*, 2144–2153.

Bardot, E.S., Valdes, V.J., Zhang, J., Perdigoto, C.N., Nicolis, S., Hearn, S.A., Silva, J.M., and Ezhkova, E. (2013). Polycomb subunits Ezh1 and Ezh2 regulate the Merkel cell differentiation program in skin stem cells. Embo J. *32*, 1990–2000.

Baroffio, A., Dupin, E., and Le Douarin, N.M. (1991). Common precursors for neural and mesectodermal derivatives in the cephalic neural crest. Development *112*, 301–305.

Barsotti, A.M., Ryskin, M., Zhong, W., Zhang, W.-G., Giannakou, A., Loreth, C., Diesl, V., Follettie, M., Golas, J., Lee, M., et al. (2015). Epigenetic reprogramming by tumor-derived EZH2 gain-of-function mutations promotes aggressive 3D cell morphologies and enhances melanoma tumor growth. Oncotarget *6*, 2928-2938.

Basile, K.J., Abel, E.V., and Aplin, A.E. (2012). Adaptive upregulation of FOXD3 and resistance to PLX4032/4720-induced cell death in mutant B-RAF melanoma cells. Oncogene *31*, 2471–2479.

Bastian, B.C., LeBoit, P.E., and Pinkel, D. (2000). Mutations and copy number increase of HRAS in Spitz nevi with distinctive histopathological features. Am. J. Pathol. *157*, 967–972.

Basu, T.N., Gutmann, D.H., Fletcher, J.A., Glover, T.W., Collins, F.S., and Downward, J. (1992). Aberrant regulation of ras proteins in malignant tumour cells from type 1 neurofibromatosis patients. Nature *356*, 713–715.

Bauer, J., Curtin, J.A., Pinkel, D., and Bastian, B.C. (2007). Congenital melanocytic nevi frequently harbor NRAS mutations but no BRAF mutations. J. Invest. Dermatol. *127*, 179–182.

Bauer, N., Fonseca, A.-V., Florek, M., Freund, D., Jászai, J., Bornhäuser, M., Fargeas, C.A., and Corbeil, D. (2008). New insights into the cell biology of hematopoietic progenitors by studying prominin-1 (CD133). Cells Tissues Organs *188*, 127–138.

Baynash, A.G., Hosoda, K., Giaid, A., Richardson, J.A., Emoto, N., Hammer, R.E., and Yanagisawa, M. (1994). Interaction of endothelin-3 with endothelin-B receptor is essential for development of epidermal melanocytes and enteric neurons. Cell *79*, 1277–1285.

Beck, B., and Blanpain, C. (2013). Unravelling cancer stem cell potential. Nat. Rev. Cancer *13*, 727–738.

Beck, B., Lapouge, G., Rorive, S., Drogat, B., Desaedelaere, K., Delafaille, S., Dubois, C., Salmon, I., Willekens, K., Marine, J.-C., et al. (2015). Different levels of twist1 regulate skin tumor initiation, stemness, and progression. Cell Stem Cell *16*, 67–79.

Bender, T., Pena, G., and Martinou, J.-C. (2015). Regulation of mitochondrial pyruvate uptake by alternative pyruvate carrier complexes. Embo J., doi:10.15252/embj.201490197.

Benevolenskaya, E.V. (2007). Histone H3K4 demethylases are essential in development and differentiation. Biochem. Cell Biol. *85*, 435–443.

Bennett, D.C., Cooper, P.J., and Hart, I.R. (1987). A line of non-tumorigenic mouse melanocytes, syngeneic with the B16 melanoma and requiring a tumour promoter for growth. Int. J. Cancer *39*, 414–418.

Benoist, L.B.L., and van Looij, M.A.J. (2013). Images in clinical medicine. Melanoma of the oral cavity. N. Engl. J. Med. *368*, e14.

Berg, T., Thoene, S., Yap, D., Wee, T., Schoeler, N., Rosten, P., Lim, E., Bilenky, M., Mungall, A.J., Oellerich, T., et al. (2014). A transgenic mouse model demonstrating the oncogenic role of mutations in the polycomb-group gene EZH2 in lymphomagenesis. Blood *123*, 3914–3924.

Bernstein, B.E., Mikkelsen, T.S., Xie, X., Kamal, M., Huebert, D.J., Cuff, J., Fry, B., Meissner, A., Wernig, M., Plath, K., et al. (2006). A bivalent chromatin structure marks key developmental genes in embryonic stem cells. Cell *125*, 315–326.

Bertolotto, C., Lesueur, F., Giuliano, S., Strub, T., de Lichy, M., Bille, K., Dessen, P., d'Hayer, B., Mohamdi, H., Remenieras, A., et al. (2011). A SUMOylation-defective MITF germline mutation predisposes to melanoma and renal carcinoma. Nature *480*, 94–98.

Besaratinia, A., and Pfeifer, G.P. (2006). Investigating human cancer etiology by DNA lesion footprinting and mutagenicity analysis. Carcinogenesis *27*, 1526–1537.

Besser, M.J., Shapira-Frommer, R., Treves, A.J., Zippel, D., Itzhaki, O., Hershkovitz, L., Levy, D., Kubi, A., Hovav, E., Chermoshniuk, N., et al. (2010). Clinical responses in a phase II study using adoptive transfer of short-term cultured tumor infiltration lymphocytes in metastatic melanoma patients. Clin. Cancer Res. *16*, 2646–2655.

Bestor, T.H. (2005). Transposons reanimated in mice. Cell *122*, 322–325.

Betancur, P., Bronner-Fraser, M., and Sauka-Spengler, T. (2010). Assembling neural crest regulatory circuits into a gene regulatory network. Annu. Rev. Cell Dev. Biol. *26*, 581–603.

Bevona, C., Goggins, W., Quinn, T., Fullerton, J., and Tsao, H. (2003). Cutaneous melanomas associated with nevi. Arch. Dermatol. *139*, 1620–1624.

Béguelin, W., Popovic, R., Teater, M., Jiang, Y., Bunting, K.L., Rosen, M., Shen, H., Yang, S.N., Wang, L., Ezponda, T., et al. (2013). EZH2 Is Required for Germinal Center Formation and Somatic EZH2 Mutations Promote Lymphoid Transformation. Cancer Cell *23*, 677–692.

Biernaskie, J., Sparling, J.S., Liu, J., Shannon, C.P., Plemel, J.R., Xie, Y., Miller, F.D., and Tetzlaff, W. (2007). Skin-derived precursors generate myelinating Schwann cells that promote remyelination and functional recovery after contusion spinal cord injury. J. Neurosci. *27*, 9545–9559.

Bilodeau, S., Kagey, M.H., Frampton, G.M., Rahl, P.B., and Young, R.A. (2009). SetDB1 contributes to repression of genes encoding developmental regulators and maintenance of ES cell state. Genes Dev. *23*, 2484–2489.

Bird, A. (2002). DNA methylation patterns and epigenetic memory. Genes Dev. *16*, 6–21.

Bixby, S., Kruger, G.M., Mosher, J.T., Joseph, N.M., and Morrison, S.J. (2002). Cell-intrinsic differences between stem cells from different regions of the peripheral nervous system regulate the generation of neural diversity. Neuron *35*, 643–656.

Blackledge, N.P., Farcas, A.M., Kondo, T., King, H.W., McGouran, J.F., Hanssen, L.L.P., Ito, S., Cooper, S., Kondo, K., Koseki, Y., et al. (2014). Variant PRC1 complex-dependent H2A ubiquitylation drives PRC2 recruitment and polycomb domain formation. Cell *157*, 1445–1459.

Blair, L.P., Cao, J., Zou, M.R., Sayegh, J., and Yan, Q. (2011). Epigenetic Regulation by Lysine Demethylase 5 (KDM5) Enzymes in Cancer. Cancers *3*, 1383–1404.

Blank, C., Brown, I., Peterson, A.C., Spiotto, M., Iwai, Y., Honjo, T., and Gajewski, T.F. (2004). PD-L1/B7H-1 inhibits the effector phase of tumor rejection by T cell receptor (TCR) transgenic CD8+ T cells. Cancer Res. *64*, 1140–1145.

Bloom, M.B., Perry-Lalley, D., Robbins, P.F., Li, Y., el-Gamil, M., Rosenberg, S.A., and Yang, J.C. (1997). Identification of tyrosinase-related protein 2 as a tumor rejection antigen for the B16 melanoma. J. Exp. Med. *185*, 453–459.

Boiko, A.D., Razorenova, O.V., van de Rijn, M., Swetter, S.M., Johnson, D.L., Ly, D.P., Butler, P.D., Yang, G.P., Joshua, B., Kaplan, M.J., et al. (2010). Human melanoma-initiating cells express neural crest nerve growth factor receptor CD271. Nature *466*, 133–137.

Bollag, G., Hirth, P., Tsai, J., Zhang, J., Ibrahim, P.N., Cho, H., Spevak, W., Zhang, C., Zhang, Y., Habets, G., et al. (2010). Clinical efficacy of a RAF inhibitor needs broad target blockade in BRAF-mutant melanoma. Nature *467*, 596–599.

Bonazzi, V.F., Nancarrow, D.J., Stark, M.S., Moser, R.J., Boyle, G.M., Aoude, L.G., Schmidt, C., and Hayward, N.K. (2011). Cross-platform array screening identifies COL1A2, THBS1, TNFRSF10D and UCHL1 as genes frequently silenced by methylation in melanoma. PLoS ONE *6*, e26121.

Bondurand, N., Kobetz, A., Pingault, V., Lemort, N., Encha-Razavi, F., Couly, G., Goerich, D.E., Wegner, M., Abitbol, M., and Goossens, M. (1998). Expression of the SOX10 gene during human development. FEBS Lett. *432*, 168–172.

Bondurand, N., Pingault, V., Goerich, D.E., Lemort, N., Sock, E., Le Caignec, C., Wegner, M., and Goossens, M. (2000). Interaction among SOX10, PAX3 and MITF, three genes altered in Waardenburg syndrome. Hum Mol Genet *9*, 1907–1917.

Boonyaratanakornkit, J.B., Yue, L., Strachan, L.R., Scalapino, K.J., LeBoit, P.E., Lu, Y., Leong, S.P., Smith, J.E., and Ghadially, R. (2010). Selection of tumorigenic melanoma cells using ALDH. J. Invest. Dermatol. *130*, 2799–2808.

Bosenberg, M., Muthusamy, V., Curley, D.P., Wang, Z., Hobbs, C., Nelson, B., Nogueira, C., Horner, J.W., Depinho, R., and Chin, L. (2006). Characterization of melanocyte-specific inducible Cre recombinase transgenic mice. Genesis *44*, 262–267.

Botton, T., Yeh, I., Nelson, T., Vemula, S.S., Sparatta, A., Garrido, M.C., Allegra, M., Rocchi, S., Bahadoran, P., McCalmont, T.H., et al. (2013). Recurrent BRAF kinase fusions in melanocytic tumors offer an opportunity for targeted therapy. Pigment Cell & Melanoma Research *26*, 845–851.

Box, N.F., and Terzian, T. (2008). The role of p53 in pigmentation, tanning and melanoma. Pigment Cell & Melanoma Research *21*, 525–533.

Boyer, L.A., Plath, K., Zeitlinger, J., Brambrink, T., Medeiros, L.A., Lee, T.I., Levine, S.S., Wernig, M., Tajonar, A., Ray, M.K., et al. (2006). Polycomb complexes repress developmental regulators in murine embryonic stem cells. Nature *441*, 349–353.

Boyman, O., and Sprent, J. (2012). The role of interleukin-2 during homeostasis and activation of the immune system. Nat. Rev. Immunol. *12*, 180–190.

Boyman, O., Kovar, M., Rubinstein, M.P., Surh, C.D., and Sprent, J. (2006). Selective stimulation of T cell subsets with antibody-cytokine immune complexes. Science *311*, 1924–1927.

Bödör, C., O'Riain, C., Wrench, D., Matthews, J., Iyengar, S., Tayyib, H., Calaminici, M., Clear, A., Iqbal, S., Quentmeier, H., et al. (2011). EZH2 Y641 mutations in follicular lymphoma. Leukemia *25*, 726–729.

Bödör, C., Grossmann, V., Popov, N., Okosun, J., O'Riain, C., Tan, K., Marzec, J., Araf, S., Wang, J., Lee, A.M., et al. (2013). EZH2 mutations are frequent and represent an early event in follicular lymphoma. Blood *122*, 3165–3168.

Bracken, A.P., and Helin, K. (2009). Polycomb group proteins: navigators of lineage pathways led astray in cancer. Nat. Rev. Cancer *9*, 773–784.

Bracken, A.P., Pasini, D., Capra, M., Prosperini, E., Colli, E., and Helin, K. (2003). EZH2 is downstream of the pRB-E2F pathway, essential for proliferation and amplified in cancer. Embo J. *22*, 5323–5335.

Brahmer, J.R., Tykodi, S.S., Chow, L.Q.M., Hwu, W.-J., Topalian, S.L., Hwu, P., Drake, C.G., Camacho, L.H., Kauh, J., Odunsi, K., et al. (2012). Safety and activity of anti-PD-L1 antibody in patients with advanced cancer. N. Engl. J. Med. *366*, 2455–2465.

Brault, V., Moore, R., Kutsch, S., Ishibashi, M., Rowitch, D.H., McMahon, A.P., Sommer, L., Boussadia, O., and Kemler, R. (2001). Inactivation of the beta-catenin gene by Wnt1-Cre-mediated deletion results in dramatic brain malformation and failure of craniofacial development. Development *128*, 1253–1264.

Bredrup, C., Saunier, S., Oud, M.M., Fiskerstrand, T., Hoischen, A., Brackman, D., Leh, S.M., Midtbø, M., Filhol, E., Bole-Feysot, C., et al. (2011). Ciliopathies with skeletal anomalies and renal insufficiency due to mutations in the IFT-A gene WDR19. Am. J. Hum. Genet. *89*, 634–643.

Breslow, A. (1970). Thickness, cross-sectional areas and depth of invasion in the prognosis of cutaneous melanoma. Ann. Surg. *172*, 902–908.

Bricker, D.K., Taylor, E.B., Schell, J.C., Orsak, T., Boutron, A., Chen, Y.-C., Cox, J.E., Cardon, C.M., Van Vranken, J.G., Dephoure, N., et al. (2012). A mitochondrial pyruvate carrier required for pyruvate uptake in yeast, Drosophila, and humans. Science *337*, 96–100.

Britsch, S., Goerich, D.E., Riethmacher, D., Peirano, R.I., Rossner, M., Nave, K.A., Birchmeier, C., and Wegner, M. (2001). The transcription factor Sox10 is a key regulator of peripheral glial development. Genes Dev. *15*, 66–78.

Bronner, M.E., and Ledouarin, N.M. (2012). Development and evolution of the neural crest: an overview. Dev. Biol. *366*, 2–9.

Bronner-Fraser, M., and Fraser, S. (1989). Developmental potential of avian trunk neural crest cells in situ. Neuron *3*, 755–766.

Brownbridge, G.G., Gold, J., Edward, M., and MacKie, R.M. (2001). Evaluation of the use of tyrosinase-specific and melanA/MART-1-specific reverse transcriptase-coupled--polymerase chain reaction to detect melanoma cells in peripheral blood samples from 299 patients with malignant melanoma. Br. J. Dermatol. *144*, 279–287.

Buhrman, G., Wink, G., and Mattos, C. (2007). Transformation Efficiency of RasQ61 Mutants Linked to Structural Features of the Switch Regions in the Presence of Raf. Structure *15*, 1618–1629.

Busam, K.J., Chen, Y.T., Old, L.J., Stockert, E., Iversen, K., Coplan, K.A., Rosai, J., Barnhill, R.L., and Jungbluth, A.A. (1998). Expression of melan-A (MART1) in benign melanocytic nevi and primary cutaneous malignant melanoma. Am. J. Surg. Pathol. *22*, 976–982.

Cacheux, V., Dastot-Le Moal, F., Kääriäinen, H., Bondurand, N., Rintala, R., Boissier, B., Wilson, M., Mowat, D., and Goossens, M. (2001). Loss-of-function mutations in SIP1 Smad interacting protein 1 result in a syndromic Hirschsprung disease. Hum. Mol. Genet. *10*, 1503–1510.

Cadet, J., Sage, E., and Douki, T. (2005). Ultraviolet radiation-mediated damage to cellular DNA. Mutat. Res. *571*, 3–17.

Cadigan, K.M., and Liu, Y.I. (2006). Wnt signaling: complexity at the surface. J. Cell Sci. *119*, 395–402.

Cadili, A., and Dabbs, K. (2010). Predictors of sentinel lymph node metastasis in melanoma. Can. J. Surg. *53*, 32–36.

Caganova, M., Carrisi, C., Varano, G., Mainoldi, F., Zanardi, F., Germain, P.-L., George, L., Alberghini, F., Ferrarini, L., Talukder, A.K., et al. (2013). Germinal center dysregulation by histone methyltransferase EZH2 promotes lymphomagenesis. J. Clin. Invest. *123*, 5009–5022.

Cai, H., Memarzadeh, S., Stoyanova, T., Beharry, Z., Kraft, A.S., and Witte, O.N. (2012). Collaboration of Kras and androgen receptor signaling stimulates EZH2 expression and tumor-propagating cells in prostate cancer. Cancer Res. *72*, 4672–4681.

Cakouros, D., Isenmann, S., Cooper, L., Zannettino, A., Anderson, P., Glackin, C., and Gronthos, S. (2012). Twist-1 induces Ezh2 recruitment regulating histone methylation along the Ink4A/Arf locus in mesenchymal stem cells. Mol. Cell. Biol. *32*, 1433–1441.

Cao, Q., Yu, J., Dhanasekaran, S.M., Kim, J.H., Mani, R.-S., Tomlins, S.A., Mehra, R., Laxman, B., Cao, X., Yu, J., et al. (2008). Repression of E-cadherin by the polycomb group protein EZH2 in cancer. Oncogene *27*, 7274–7284.

Cao, R., and Zhang, Y. (2004). SUZ12 is required for both the histone methyltransferase activity and the silencing function of the EED-EZH2 complex. Mol. Cell *15*, 57–67.

Cao, R., Wang, L., Wang, H., Xia, L., Erdjument-Bromage, H., Tempst, P., Jones, R.S., and Zhang, Y. (2002). Role of histone H3 lysine 27 methylation in Polycomb-group silencing. Science *298*, 1039–1043.

Capello, D., Gloghini, A., Martini, M., Spina, M., Tirelli, U., Bertoni, F., Rinaldi, A., Morra, E., Rambaldi, A., Sinigaglia, F., et al. (2011). Mutations of CD79A, CD79B and EZH2 genes in immunodeficiency-related non-Hodgkin lymphomas. Br. J. Haematol. *152*, 777–780.

Caramel, J., Papadogeorgakis, E., Hill, L., Browne, G.J., Richard, G., Wierinckx, A., Saldanha, G., Osborne, J., Hutchinson, P., Tse, G., et al. (2013). A Switch in the Expression of Embryonic EMT-Inducers Drives the Development of Malignant Melanoma. Cancer Cell *24*, 466–480.

Carbonnelle-Puscian, A., Vidal, V., Laurendeau, I., Valeyrie-Allanore, L., Vidaud, D., Bièche, I., Leroy, K., Lantieri, L., Wolkenstein, P., Schedl, A., et al. (2011). SOX9 expression increases with malignant potential in tumors from patients with neurofibromatosis 1 and is not correlated to desert hedgehog. Human Pathology *42*, 434–443.

Carey, B.W., Finley, L.W.S., Cross, J.R., Allis, C.D., and Thompson, C.B. (2015). Intracellular α-ketoglutarate maintains the pluripotency of embryonic stem cells. Nature *518*, 413–416.

Carpenter, A.E., Jones, T.R., Lamprecht, M.R., Clarke, C., Kang, I.H., Friman, O., Guertin, D.A., Chang, J.H., Lindquist, R.A., Moffat, J., et al. (2006). CellProfiler: image analysis software for identifying and quantifying cell phenotypes. Genome Biol. *7*, R100.

Carreira, S., Goodall, J., Denat, L., Rodriguez, M., Nuciforo, P., Hoek, K.S., Testori, A., Larue, L., and Goding, C.R. (2006). Mitf regulation of Dia1 controls melanoma proliferation and invasiveness. Genes Dev. *20*, 3426–3439.

Carroll, S.L. (2012). Molecular mechanisms promoting the pathogenesis of Schwann cell neoplasms. Acta Neuropathol. *123*, 321–348.

Catchpole, S., Spencer-Dene, B., Hall, D., Santangelo, S., Rosewell, I., Guenatri, M., Beatson, R., Scibetta, A.G., Burchell, J.M., and Taylor-Papadimitriou, J. (2011). PLU-1/JARID1B/KDM5B is required for embryonic survival and contributes to cell proliferation in the mammary gland and in ER+ breast cancer cells. Int. J. Oncol. *38*, 1267–1277.

Ceol, C.J., Houvras, Y., Jane-Valbuena, J., Bilodeau, S., Orlando, D.A., Battisti, V., Fritsch, L., Lin, W.M., Hollmann, T.J., Ferré, F., et al. (2011). The histone methyltransferase SETDB1 is recurrently amplified in melanoma and accelerates its onset. Nature *471*, 513–517.

Cervera, A.M., Bayley, J.-P., Devilee, P., and McCreath, K.J. (2009). Inhibition of succinate dehydrogenase dysregulates histone modification in mammalian cells. Mol. Cancer *8*, 89.

Chamberlain, S.J., Yee, D., and Magnuson, T. (2008). Polycomb repressive complex 2 is dispensable for maintenance of embryonic stem cell pluripotency. Stem Cells *26*, 1496–1505.

Chang, A.E., Karnell, L.H., and Menck, H.R. (1998). The National Cancer Data Base report on cutaneous and noncutaneous melanoma: a summary of 84,836 cases from the past decade. The American College of Surgeons Commission on Cancer and the American Cancer Society. Cancer *83*, 1664–1678.

Chang, C.-J., Yang, J.-Y., Xia, W., Chen, C.-T., Xie, X., Chao, C.-H., Woodward, W.A., Hsu, J.-M., Hortobagyi, G.N., and Hung, M.-C. (2011). EZH2 promotes expansion of breast tumor initiating cells through activation of RAF1-β-catenin signaling. Cancer Cell *19*, 86–100.

Chang, Y.-L., Gao, H.-W., Chiang, C.-P., Wang, W.-M., Huang, S.-M., Ku, C.-F., Liu, G.-Y., and Hung, H.-C. (2015). Human Mitochondrial NAD(P)(+)-Dependent Malic Enzyme Participates in Cutaneous Melanoma Progression and Invasion. J. Invest. Dermatol. *135*, 807–815.

Chapman, P.B., Hauschild, A., Robert, C., Haanen, J.B., Ascierto, P., Larkin, J., Dummer, R., Garbe, C., Testori, A., Maio, M., et al. (2011). Improved survival with vemurafenib in melanoma with BRAF V600E mutation. N. Engl. J. Med. *364*, 2507–2516.

Chapuy, B., McKeown, M.R., Lin, C.Y., Monti, S., Roemer, M.G.M., Qi, J., Rahl, P.B., Sun, H.H., Yeda, K.T., Doench, J.G., et al. (2013). Discovery and Characterizationof Super-Enhancer-Associated Dependencies in Diffuse Large B Cell Lymphoma. Cancer Cell *24*, 777–790.

Charbel, C., Fontaine, R.H., Malouf, G.G., Picard, A., Kadlub, N., El-Murr, N., How-Kit, A., Su, X., Coulomb-L'Hermine, A., Tost, J., et al. (2014). NRAS mutation is the sole recurrent somatic mutation in large congenital melanocytic nevi. J. Invest. Dermatol. *134*, 1067–1074.

Chartrain, M., Riond, J., Stennevin, A., Vandenberghe, I., Gomes, B., Lamant, L., Meyer, N., Gairin, J.E., Guilbaud, N., and Annereau, J.P. (2012). Melanoma chemotherapy leads to the selection of ABCB5-expressing cells. PLoS ONE *7*, e36762.

Cheli, Y., Giuliano, S., Fenouille, N., Allegra, M., Hofman, V., Hofman, P., Bahadoran, P., Lacour, J.-P., Tartare-Deckert, S., Bertolotto, C., et al. (2012). Hypoxia and MITF control metastatic behaviour in mouse and human melanoma cells. Oncogene *31*, 2461–2470.

Chen, X., He, D., Dong, X.D., Dong, F., Wang, J., Wang, L., Tang, J., Hu, D.-N., Yan, D., and Tu, L. (2013). MicroRNA-124a is epigenetically regulated and acts as a tumor suppressor by controlling multiple targets in uveal melanoma. Invest. Ophthalmol. Vis. Sci. *54*, 2248–2256.

Chen, Y., Wang, H., Yoon, S.O., Xu, X., Hottiger, M.O., Svaren, J., Nave, K.A., Kim, H.A., Olson, E.N., and Lu, Q.R. (2011). HDAC-mediated deacetylation of NF-κB is critical for Schwann cell myelination. Nat. Neurosci. *14*, 437–441.

Cheng, P.F., Shahkova, O., Widmer, D.S., Eichhoff, O.M., Zingg, D., Frommel, S.C., Belloni, B., Raaijmakers, M.M., Goldinger, S.M., Santoro, R., et al. (2015). Methylation-dependent SOX9 expression mediates invasion in human melanoma cells and is a negative prognostic factor in advanced melanoma. Genome Biol. *16*, 3016.

Cheng, Z., Gong, Y., Ma, Y., Lu, K., Lu, X., Pierce, L.A., Thompson, R.C., Muller, S., Knapp, S., and Wang, J. (2013). Inhibition of BET Bromodomain Targets Genetically Diverse Glioblastoma. Clin. Cancer Res. *19*, 1748–1759.

Chesa, P.G., Rettig, W.J., Thomson, T.M., Old, L.J., and Melamed, M.R. (1988). Immunohistochemical analysis of nerve growth factor receptor expression in normal and malignant human tissues. J. Histochem. Cytochem. *36*, 383–389.

Cheung, N.-K.V., and Dyer, M.A. (2013). Neuroblastoma: developmental biology, cancer genomics and immunotherapy. Nat. Rev. Cancer *13*, 397–411.

Chien, A.J., Moore, E.C., Lonsdorf, A.S., Kulikauskas, R.M., Rothberg, B.G., Berger, A.J., Major, M.B., Hwang, S.T., Rimm, D.L., and Moon, R.T. (2009). Activated Wnt/beta-catenin signaling in melanoma is associated with decreased proliferation in patient tumors and a murine melanoma model. Proc. Natl. Acad. Sci. USA *106*, 1193–1198.

Chin, L., Pomerantz, J., Polsky, D., Jacobson, M., Cohen, C., Cordon-Cardo, C., Horner, J.W., and DePinho, R.A. (1997). Cooperative effects of INK4a and ras in melanoma susceptibility in vivo. Genes Dev. *11*, 2822–2834.

Chin, L., Tam, A., Pomerantz, J., Wong, M., Holash, J., Bardeesy, N., Shen, Q., O'Hagan, R., Pantginis, J., Zhou, H., et al. (1999). Essential role for oncogenic Ras in tumour maintenance. Nature *400*, 468–472.

Chou, J., Voong, L.N., Mortales, C.L., Towlerton, A.M.H., Pollack, S.M., Chen, X., Yee, C., Robbins, P.F., and Warren, E.H. (2012). Epigenetic modulation to enable antigen-specific T-cell therapy of colorectal cancer. J. Immunother. *35*, 131–141.

Chou, W.C., Takeo, M., Rabbani, P., Hu, H., Lee, W., Chung, Y.R., Carucci, J., Overbeek, P., and Ito, M. (2013). Direct migration of follicular melanocyte stem cells to the epidermis after wounding or UVB irradiation is dependent on Mc1r signaling. Nat. Med. *19*, 924–929.

Chowdhury, R., Yeoh, K.K., Tian, Y.-M., Hillringhaus, L., Bagg, E.A., Rose, N.R., Leung, I.K.H., Li, X.S., Woon, E.C.Y., Yang, M., et al. (2011). The oncometabolite 2-hydroxyglutarate inhibits histone lysine demethylases. EMBO Rep. *12*, 463–469.

Christensen, J., Agger, K., Cloos, P.A.C., Pasini, D., Rose, S., Sennels, L., Rappsilber, J., Hansen, K.H., Salcini, A.E., and Helin, K. (2007). RBP2 belongs to a family of demethylases, specific for tri-and dimethylated lysine 4 on histone 3. Cell *128*, 1063–1076.

Chung, Y.R., Schatoff, E., and Abdel-Wahab, O. (2012). Epigenetic alterations in hematopoietic malignancies. Int. J. Hematol. *96*, 413–427.

Cichowski, K., Shih, T.S., Schmitt, E., Santiago, S., Reilly, K., McLaughlin, M.E., Bronson, R.T., and Jacks, T. (1999). Mouse models of tumor development in neurofibromatosis type 1. Science *286*, 2172–2176.

Ciferri, C., Lander, G.C., Maiolica, A., Herzog, F., Aebersold, R., and Nogales, E. (2012). Molecular architecture of human polycomb repressive complex 2. Elife *1*, e00005.

Cimadamore, F., Shah, M., Amador-Arjona, A., Navarro-Peran, E., Chen, C., Huang, C.-T., and Terskikh, A.V. (2012). SOX2 modulates levels of MITF in normal human melanocytes, and melanoma lines in vitro. Pigment Cell & Melanoma Research *25*, 533–536.

Civenni, G., Walter, A., Kobert, N., Mihic-Probst, D., Zipser, M., Belloni, B., Seifert, B., Moch, H., Dummer, R., van den Broek, M., et al. (2011). Human CD271-positive melanoma stem cells associated with metastasis establish tumor heterogeneity and long-term growth. Cancer Res. *71*, 3098–3109.

Clark, W.H., Elder, D.E., Guerry, D., Epstein, M.N., Greene, M.H., and Van Horn, M. (1984). A study of tumor progression: the precursor lesions of superficial spreading and nodular melanoma. Human Pathology *15*, 1147–1165.

Coles, E.G., Taneyhill, L.A., and Bronner-Fraser, M. (2007). A critical role for Cadherin6B in regulating avian neural crest emigration. Dev. Biol. *312*, 533–544.

Conway, K., Edmiston, S.N., Khondker, Z.S., Groben, P.A., Zhou, X., Chu, H., Kuan, P.-F., Hao, H., Carson, C., Berwick, M., et al. (2011). DNA-methylation profiling distinguishes malignant melanomas from benign nevi. Pigment Cell & Melanoma Research *24*, 352–360.

Cook, A.L., Donatien, P.D., Smith, A.G., Murphy, M., Jones, M.K., Herlyn, M., Bennett, D.C., Leonard, J.H., and Sturm, R.A. (2003). Human melanoblasts in culture: expression of BRN2 and synergistic regulation by fibroblast growth factor-2, stem cell factor, and endothelin-3. J. Invest. Dermatol. *121*, 1150–1159.

Cooper, S., Dienstbier, M., Hassan, R., Schermelleh, L., Sharif, J., Blackledge, N.P., De Marco, V., Elderkin, S., Koseki, H., Klose, R., et al. (2014). Targeting polycomb to pericentric heterochromatin in embryonic stem cells reveals a role for H2AK119u1 in PRC2 recruitment. Cell Rep. *7*, 1456–1470.

Coral, S., Covre, A., Nicolay, H.J., Parisi, G., Rizzo, A., Colizzi, F., Santa, S.D., Fonsatti, E., Fratta, E., Sigalotti, L., et al. (2012). Epigenetic remodelling of gene expression profiles of neoplastic and normal tissues: immunotherapeutic implications. Br. J. Cancer *107*, 1116–1124.

Costello, J.F., Frühwald, M.C., Smiraglia, D.J., Rush, L.J., Robertson, G.P., Gao, X., Wright, F.A., Feramisco, J.D., Peltomäki, P., Lang, J.C., et al. (2000). Aberrant CpG-island methylation has non-random and tumour-type-specific patterns. Nat. Genet. *24*, 132–138.

Cotsarelis, G., Sun, T.T., and Lavker, R.M. (1990). Label-retaining cells reside in the bulge area of pilosebaceous unit: implications for follicular stem cells, hair cycle, and skin carcinogenesis. Cell *61*, 1329–1337.

Coussa, R.G., Otto, E.A., Gee, H.-Y., Arthurs, P., Ren, H., Lopez, I., Keser, V., Fu, Q., Faingold, R., Khan, A., et al. (2013). WDR19: an ancient, retrograde, intraflagellar ciliary protein is mutated in autosomal recessive retinitis pigmentosa and in Senior-Loken syndrome. Clin. Genet. *84*, 150–159.

Cronin, J.C., Watkins-Chow, D.E., Incao, A., Hasskamp, J.H., Schönewolf, N., Aoude, L.G., Hayward, N.K., Bastian, B.C., Dummer, R., Loftus, S.K., et al. (2013). SOX10 ablation arrests cell cycle, induces senescence, and suppresses melanomagenesis. Cancer Res. *73*, 5709–5718.

Cronin, J.C., Wunderlich, J., Loftus, S.K., Prickett, T.D., Wei, X., Ridd, K., Vemula, S., Burrell, A.S., Agrawal, N.S., Lin, J.C., et al. (2009). Frequent mutations in the MITF pathway in melanoma. Pigment Cell & Melanoma Research *22*, 435–444.

Cruz, J., Reis-Filho, J.S., and Lopes, J.M. (2003). Primary cutaneous malignant melanoma with lipoblast-like cells. Arch. Pathol. Lab. Med. *127*, 370–371.

Cui, J., Shen, L.Y., and Wang, G.C. (1991). Role of hair follicles in the repigmentation of vitiligo. J. Invest. Dermatol. *97*, 410–416.

Curado, M.P., Edwards, B., Shin, H.R., Ferlay, J., and Storm, H. (2007). Cancer incidence in five continents, Volume IX (Lyon: World Health Organization).

Curtin, J.A., Fridlyand, J., Kageshita, T., Patel, H.N., Busam, K.J., Kutzner, H., Cho, K.-H., Aiba, S., Bröcker, E.-B., LeBoit, P.E., et al. (2005). Distinct sets of genetic alterations in melanoma. N. Engl. J. Med. *353*, 2135–2147.

Czermin, B., Melfi, R., McCabe, D., Seitz, V., Imhof, A., and Pirrotta, V. (2002). Drosophila enhancer of Zeste/ESC complexes have a histone H3 methyltransferase activity that marks chromosomal Polycomb sites. Cell *111*, 185–196.

Damsky, W.E., Curley, D.P., Santhanakrishnan, M., Rosenbaum, L.E., Platt, J.T., Gould Rothberg, B.E., Taketo, M.M., Dankort, D., Rimm, D.L., McMahon, M., et al. (2011). β-catenin signaling controls metastasis in Braf-activated Pten-deficient melanomas. Cancer Cell *20*, 741–754.

Dang, L., White, D.W., Gross, S., Bennett, B.D., Bittinger, M.A., Driggers, E.M., Fantin, V.R., Jang, H.G., Jin, S., Keenan, M.C., et al. (2009). Cancer-associated IDH1 mutations produce 2-hydroxyglutarate. Nature *462*, 739–744.

Dankort, D., Curley, D.P., Cartlidge, R.A., Nelson, B., Karnezis, A.N., Damsky, W.E., You, M.J., DePinho, R.A., McMahon, M., and Bosenberg, M. (2009). Braf(V600E) cooperates with Pten loss to induce metastatic melanoma. Nat. Genet. *41*, 544–552.

Davies, H., Bignell, G.R., Cox, C., Stephens, P., Edkins, S., Clegg, S., Teague, J., Woffendin, H., Garnett, M.J., Bottomley, W., et al. (2002). Mutations of the BRAF gene in human cancer. Nature *417*, 949–954.

Davies, M.A., Stemke-Hale, K., Tellez, C., Calderone, T.L., Deng, W., Prieto, V.G., Lazar, A.J.F., Gershenwald, J.E., and Mills, G.B. (2008). A novel AKT3 mutation in melanoma tumours and cell lines. Br. J. Cancer *99*, 1265–1268.

Dawson, M.A., Prinjha, R.K., Dittmann, A., Giotopoulos, G., Bantscheff, M., Chan, W.-I., Robson, S.C., Chung, C.-W., Hopf, C., Savitski, M.M., et al. (2011). Inhibition of BET recruitment to chromatin as an effective treatment for MLL-fusion leukaemia. Nature *478*, 529–533.

De Raedt, T., Beert, E., Pasmant, E., Luscan, A., Brems, H., Ortonne, N., Helin, K., Hornick, J.L., Mautner, V., Kehrer-Sawatzki, H., et al. (2014). PRC2 loss amplifies Ras-driven transcription and confers sensitivity to BRD4-based therapies. Nature *514*, 247–251.

de Vries, N.A., Hulsman, D., Akhtar, W., de Jong, J., Miles, D.C., Blom, M., van Tellingen, O., Jonkers, J., and van Lohuizen, M. (2015). Prolonged Ezh2 Depletion in Glioblastoma Causes a Robust Switch in Cell Fate Resulting in Tumor Progression. Cell Rep. *10*, 383–397.

Delmas, V., Beermann, F., Martinozzi, S., Carreira, S., Ackermann, J., Kumasaka, M., Denat, L., Goodall, J., Luciani, F., Viros, A., et al. (2007). Beta-catenin induces immortalization of melanocytes by suppressing p16INK4a expression and cooperates with N-Ras in melanoma development. Genes Dev. *21*, 2923–2935.

Delmore, J.E., Issa, G.C., Lemieux, M.E., Rahl, P.B., Shi, J., Jacobs, H.M., Kastritis, E., Gilpatrick, T., Paranal, R.M., Qi, J., et al. (2011). BET bromodomain inhibition as a therapeutic strategy to target c-Myc. Cell *146*, 904–917.

Denecker, G., Vandamme, N., Akay, O., Koludrovic, D., Taminau, J., Lemeire, K., Gheldof, A., De Craene, B., Van Gele, M., Brochez, L., et al. (2014). Identification of a ZEB2-MITF-ZEB1 transcriptional network that controls melanogenesis and melanoma progression. Cell Death Differ. *21*, 1250–1261.

Deng, T., Kuang, Y., Wang, L., Li, J., Wang, Z., and Fei, J. (2009). An essential role for DNA methyltransferase 3a in melanoma tumorigenesis. Biochem. Biophys. Res. Commun. *387*, 611–616.

Deng, W., Gopal, Y.N.V., Scott, A., Chen, G., Woodman, S.E., and Davies, M.A. (2012). Role and therapeutic potential of PI3K-mTOR signaling in de novo resistance to BRAF inhibition. Pigment Cell & Melanoma Research *25*, 248–258.

Der, C.J., Finkel, T., and Cooper, G.M. (1986). Biological and biochemical properties of human rasH genes mutated at codon 61. Cell *44*, 167–176.

Dey, A., Nishiyama, A., Karpova, T., McNally, J., and Ozato, K. (2009). Brd4 marks select genes on mitotic chromatin and directs postmitotic transcription. Mol. Biol. Cell *20*, 4899–4909.

Dhomen, N., Reis-Filho, J.S., da Rocha Dias, S., Hayward, R., Savage, K., Delmas, V., Larue, L., Pritchard, C., and Marais, R. (2009). Oncogenic Braf induces melanocyte senescence and melanoma in mice. Cancer Cell *15*, 294–303.

Di Cristofano, A., Pesce, B., Cordon-Cardo, C., and Pandolfi, P.P. (1998). Pten is essential for embryonic development and tumour suppression. Nat. Genet. *19*, 348–355.

Di Micco, R., Fontanals-Cirera, B., Low, V., Ntziachristos, P., Yuen, S.K., Lovell, C.D., Dolgalev, I., Yonekubo, Y., Zhang, G., Rusinova, E., et al. (2014). Control of Embryonic Stem Cell Identity by BRD4- Dependent Transcriptional Elongation of Super- Enhancer-Associated Pluripotency Genes. Cell Rep. *9*, 234–247.

Divito, K.A., Trabosh, V.A., Chen, Y.-S., Chen, Y., Albanese, C., Javelaud, D., Mauviel, A., Simbulan-Rosenthal, C.M., and Rosenthal, D.S. (2010). Smad7 restricts melanoma invasion by restoring N-cadherin expression and establishing heterotypic cell-cell interactions in vivo. Pigment Cell & Melanoma Research *23*, 795–808.

Dong, H., Strome, S.E., Salomao, D.R., Tamura, H., Hirano, F., Flies, D.B., Roche, P.C., Lu, J., Zhu, G., Tamada, K., et al. (2002). Tumor-associated B7-H1 promotes T-cell apoptosis: a potential mechanism of immune evasion. Nat. Med. *8*, 793–800.

Dorsky, R.I., Moon, R.T., and Raible, D.W. (1998). Control of neural crest cell fate by the Wnt signalling pathway. Nature *396*, 370–373.

Dovey, O.M., Foster, C.T., and Cowley, S.M. (2010). Histone deacetylase 1 (HDAC1), but not HDAC2, controls embryonic stem cell differentiation. Proc. Natl. Acad. Sci. USA *107*, 8242–8247.

Driscoll, D.A., Spinner, N.B., Budarf, M.L., McDonald-McGinn, D.M., Zackai, E.H., Goldberg, R.B., Shprintzen, R.J., Saal, H.M., Zonana, J., and Jones, M.C. (1992). Deletions and microdeletions of 22q11.2 in velo-cardio-facial syndrome. Am. J. Med. Genet. *44*, 261–268.

Du, J., Widlund, H.R., Horstmann, M.A., Ramaswamy, S., Ross, K., Huber, W.E., Nishimura, E.K., Golub, T.R., and Fisher, D.E. (2004). Critical role of CDK2 for melanoma growth linked to its melanocyte-specific transcriptional regulation by MITF. Cancer Cell *6*, 565–576.

Ducatman, B.S., and Scheithauer, B.W. (1984). Malignant peripheral nerve sheath tumors with divergent differentiation. Cancer *54*, 1049–1057.

Dudley, M.E., Wunderlich, J.R., Robbins, P.F., Yang, J.C., Hwu, P., Schwartzentruber, D.J., Topalian, S.L., Sherry, R., Restifo, N.P., Hubicki, A.M., et al. (2002). Cancer regression and autoimmunity in patients after clonal repopulation with antitumor lymphocytes. Science *298*, 850–854.

Dundr, P., and Ehrmann, J. (2012). Neural Crest Cell-Derived Tumors: An Overview. In Stem Cells and Cancer Stem Cells, (Clifton, NJ: Springer), pp. 29–40.

DuPage, M., Chopra, G., Quiros, J., Rosenthal, W.L., Morar, M.M., Holohan, D., Zhang, R., Turka, L., Marson, A., and Bluestone, J.A. (2015). The chromatin-modifying enzyme Ezh2 is critical for the maintenance of regulatory T cell identity after activation. Immunity *42*, 227–238.

Dupin, E., and Sommer, L. (2012). Neural crest progenitors and stem cells: from early development to adulthood. Dev. Biol. *366*, 83–95.

Dutton-Regester, K., Kakavand, H., Aoude, L.G., Stark, M.S., Gartside, M.G., Johansson, P., O'Connor, L., Lanagan, C., Tembe, V., Pupo, G.M., et al. (2013). Melanomas of unknown primary have a mutation profile consistent with cutaneous sun-exposed melanoma. Pigment Cell & Melanoma Research *26*, 852–860.

Duvic, M., Talpur, R., Ni, X., Zhang, C., Hazarika, P., Kelly, C., Chiao, J.H., Reilly, J.F., Ricker, J.L., Richon, V.M., et al. (2007). Phase 2 trial of oral vorinostat (suberoylanilide hydroxamic acid, SAHA) for refractory cutaneous T-cell lymphoma (CTCL). Blood *109*, 31–39.

Eccles, M.R., He, S., Ahn, A., Slobbe, L.J., Jeffs, A.R., Yoon, H.-S., and Baguley, B.C. (2013). MITF and PAX3 Play Distinct Roles in Melanoma Cell Migration; Outline of a "Genetic Switch" Theory Involving MITF and PAX3 in Proliferative and Invasive Phenotypes of Melanoma. Front. Oncol. *3*, 229.

Eden, A., Gaudet, F., Waghmare, A., and Jaenisch, R. (2003). Chromosomal instability and tumors promoted by DNA hypomethylation. Science *300*, 455.

Efimenko, E., Blacque, O.E., Ou, G., Haycraft, C.J., Yoder, B.K., Scholey, J.M., Leroux, M.R., and Swoboda, P. (2006). Caenorhabditis elegans DYF-2, an orthologue of human WDR19, is a component of the intraflagellar transport machinery in sensory cilia. Mol. Biol. Cell *17*, 4801–4811.

Eggermont, A.M.M., and Kirkwood, J.M. (2004). Re-evaluating the role of dacarbazine in metastatic melanoma: what have we learned in 30 years? Eur. J. Cancer *40*, 1825–1836.

Eggermont, A.M.M., Spatz, A., and Robert, C. (2014). Cutaneous melanoma. Lancet *383*, 816–827.

Elgin, S.C.R., and Workman, J.L. (2000). Chromatin Structure and Gene Expression (Oxford: Oxford University Press).

Emery, C.M., Vijayendran, K.G., Zipser, M.C., Sawyer, A.M., Niu, L., Kim, J.J., Hatton, C., Chopra, R., Oberholzer, P.A., Karpova, M.B., et al. (2009). MEK1 mutations confer resistance to MEK and B-RAF inhibition. Proc. Natl. Acad. Sci. USA *106*, 20411–20416.

Ennen, M., Keime, C., Kobi, D., Mengus, G., Lipsker, D., Thibault-Carpentier, C., and Davidson, I. (2014). Single-cell gene expression signatures reveal melanoma cell heterogeneity. Oncogene, doi:10.1038/onc.2014.262.

Epsztejn-Litman, S., Feldman, N., Abu-Remaileh, M., Shufaro, Y., Gerson, A., Ueda, J., Deplus, R., Fuks, F., Shinkai, Y., Cedar, H., et al. (2008). De novo DNA methylation promoted by G9a prevents reprogramming of embryonically silenced genes. Nat. Struct. Mol. Biol. *15*, 1176–1183.

Erdag, G., Schaefer, J.T., Smolkin, M.E., Deacon, D.H., Shea, S.M., Dengel, L.T., Patterson, J.W., and Slingluff, C.L. (2012). Immunotype and immunohistologic characteristics of tumor-infiltrating immune cells are associated with clinical outcome in metastatic melanoma. Cancer Res. *72*, 1070–1080.

Ernst, T., Chase, A.J., Score, J., Hidalgo-Curtis, C.E., Bryant, C., Jones, A.V., Waghorn, K., Zoi, K., Ross, F.M., Reiter, A., et al. (2010). Inactivating mutations of the histone methyltransferase gene EZH2 in myeloid disorders. Nat. Genet. *42*, 722–726.

Eskandarpour, M., Hashemi, J., Kanter, L., Ringborg, U., Platz, A., and Hansson, J. (2003). Frequency of UV-inducible NRAS mutations in melanomas of patients with germline CDKN2A mutations. J. Natl. Cancer Inst. *95*, 790–798.

Esteller, M., Corn, P.G., Baylin, S.B., and Herman, J.G. (2001a). A gene hypermethylation profile of human cancer. Cancer Res. *61*, 3225–3229.

Esteller, M., Fraga, M.F., Guo, M., Garcia-Foncillas, J., Hedenfalk, I., Godwin, A.K., Trojan, J., Vaurs-Barrière, C., Bignon, Y.J., Ramus, S., et al. (2001b). DNA methylation patterns in hereditary human cancers mimic sporadic tumorigenesis. Hum. Mol. Genet. *10*, 3001–3007.

Esteller, M. (2007). Cancer epigenomics: DNA methylomes and histone-modification maps. Nat. Rev. Genet. *8*, 286–298.

Etchevers, H.C., Amiel, J., and Lyonnet, S. (2006). Molecular bases of human neurocristopathies. Adv. Exp. Med. Biol. *589*, 213–234.

Ezhkova, E., Lien, W.-H., Stokes, N., Pasolli, H.A., Silva, J.M., and Fuchs, E. (2011). EZH1 and EZH2 cogovern histone H3K27 trimethylation and are essential for hair follicle homeostasis and wound repair. Genes Dev. *25*, 485–498.

Ezhkova, E., Pasolli, H.A., Parker, J.S., Stokes, N., Su, I.-H., Hannon, G., Tarakhovsky, A., and Fuchs, E. (2009). Ezh2 orchestrates gene expression for the stepwise differentiation of tissue-specific stem cells. Cell *136*, 1122–1135.

Falabella, R. (2009). Vitiligo and the melanocyte reservoir. Indian J. Dermatol. *54*, 313–318.

Fan, T., Jiang, S., Chung, N., Alikhan, A., Ni, C., Lee, C.-C.R., and Hornyak, T.J. (2011). EZH2-dependent suppression of a cellular senescence phenotype in melanoma cells by inhibition of p21/CDKN1A expression. Mol. Cancer Res. *9*, 418–429.

Fang, D., Nguyen, T.K., Leishear, K., Finko, R., Kulp, A.N., Hotz, S., Van Belle, P.A., Xu, X., Elder, D.E., and Herlyn, M. (2005). A tumorigenic subpopulation with stem cell properties in melanomas. Cancer Res. *65*, 9328–9337.

Fang, R., Zhang, G., Guo, Q., Ning, F., Wang, H., Cai, S., and Du, J. (2013). Nodal promotes aggressive phenotype via Snail-mediated epithelial-mesenchymal transition in murine melanoma. Cancer Lett. *333*, 66–75.

Fang, S., Wu, L., Li, M., Yi, H., Gao, G., Sheng, Z., Gong, P., Ma, Y., and Cai, L. (2014). ZEB1 knockdown mediated using polypeptide cationic micelles inhibits metastasis and effects sensitization to a chemotherapeutic drug for cancer therapy. Nanoscale *6*, 10084–10094.

Faust, C., Lawson, K.A., Schork, N.J., Thiel, B., and Magnuson, T. (1998). The Polycomb-group gene eed is required for normal morphogenetic movements during gastrulation in the mouse embryo. Development *125*, 4495–4506.

Faust, C., Schumacher, A., Holdener, B., and Magnuson, T. (1995). The eed mutation disrupts anterior mesoderm production in mice. Development *121*, 273–285.

Fehrenbach, H., Decker, C., Eisenberger, T., Frank, V., Hampel, T., Walden, U., Amann, K.U., Krüger-Stollfuß, I., Bolz, H.J., Häffner, K., et al. (2014). Mutations in WDR19 encoding the intraflagellar transport component IFT144 cause a broad spectrum of ciliopathies. Pediatr. Nephrol. *29*, 1451–1456.

Feldman, N., Gerson, A., Fang, J., Li, E., Zhang, Y., Shinkai, Y., Cedar, H., and Bergman, Y. (2006). G9a-mediated irreversible epigenetic inactivation of Oct-3/4 during early embryogenesis. Nat. Cell Biol. *8*, 188–194.

Fenaux, P., Mufti, G.J., Hellstrom-Lindberg, E., Santini, V., Finelli, C., Giagounidis, A., Schoch, R., Gattermann, N., Sanz, G., List, A., et al. (2009). Efficacy of azacitidine compared with that of conventional care regimens in the treatment of higher-risk myelodysplastic syndromes: a randomised, open-label, phase III study. Lancet Oncol. *10*, 223–232.

Ferraro, A., Boni, T., and Pintzas, A. (2014). EZH2 Regulates Cofilin Activity and Colon Cancer Cell Migration by Targeting ITGA2 Gene. PLoS ONE *9*, e115276.

Fife, K.M., Colman, M.H., Stevens, G.N., Firth, I.C., Moon, D., Shannon, K.F., Harman, R., Petersen-Schaefer, K., Zacest, A.C., Besser, M., et al. (2004). Determinants of outcome in melanoma patients with cerebral metastases. J. Clin. Oncol. *22*, 1293–1300.

Filippakopoulos, P., Picaud, S., Mangos, M., Keates, T., Lambert, J.-P., Barsyte-Lovejoy, D., Felletar, I., Volkmer, R., Müller, S., Pawson, T., et al. (2012). Histone recognition and large-scale structural analysis of the human bromodomain family. Cell *149*, 214–231.

Filippakopoulos, P., Qi, J., Picaud, S., Shen, Y., Smith, W.B., Fedorov, O., Morse, E.M., Keates, T., Hickman, T.T., Felletar, I., et al. (2010). Selective inhibition of BET bromodomains. Nature *468*, 1067–1073.

Flaherty, K.T., Infante, J.R., Daud, A., Gonzalez, R., Kefford, R.F., Sosman, J., Hamid, O., Schuchter, L., Cebon, J., Ibrahim, N., et al. (2012a). Combined BRAF and MEK inhibition in melanoma with BRAF V600 mutations. N. Engl. J. Med. *367*, 1694–1703.

Flaherty, K.T., Puzanov, I., Kim, K.B., Ribas, A., McArthur, G.A., Sosman, J.A., O'Dwyer, P.J., Lee, R.J., Grippo, J.F., Nolop, K., et al. (2010). Inhibition of mutated, activated BRAF in metastatic melanoma. N. Engl. J. Med. *363*, 809–819.

Flaherty, K.T., Robert, C., Hersey, P., Nathan, P., Garbe, C., Milhem, M., Demidov, L.V., Hassel, J.C., Rutkowski, P., Mohr, P., et al. (2012b). Improved survival with MEK inhibition in BRAF-mutated melanoma. N. Engl. J. Med. *367*, 107–114.

Flammiger, A., Besch, R., Cook, A.L., Maier, T., Sturm, R.A., and Berking, C. (2009). SOX9 and SOX10 but not BRN2 are required for nestin expression in human melanoma cells. J. Invest. Dermatol. *129*, 945–953.

Fraga, M.F., Herranz, M., Espada, J., Ballestar, E., Paz, M.F., Ropero, S., Erkek, E., Bozdogan, O., Peinado, H., Niveleau, A., et al. (2004). A mouse skin multistage carcinogenesis model reflects the aberrant DNA methylation patterns of human tumors. Cancer Res. *64*, 5527–5534.

Frank, E., and Sanes, J.R. (1991). Lineage of neurons and glia in chick dorsal root ganglia: analysis in vivo with a recombinant retrovirus. Development *111*, 895–908.

Frank, N.Y., Margaryan, A., Huang, Y., Schatton, T., Waaga-Gasser, A.M., Gasser, M., Sayegh, M.H., Sadee, W., and Frank, M.H. (2005). ABCB5-mediated doxorubicin transport and chemoresistance in human malignant melanoma. Cancer Res. *65*, 4320–4333.

French, C.A., Miyoshi, I., Aster, J.C., Kubonishi, I., Kroll, T.G., Dal Cin, P., Vargas, S.O., Perez-Atayde, A.R., and Fletcher, J.A. (2001). BRD4 bromodomain gene rearrangement in aggressive carcinoma with translocation t(15;19). Am. J. Pathol. *159*, 1987–1992.

French, C.A., Ramirez, C.L., Kolmakova, J., Hickman, T.T., Cameron, M.J., Thyne, M.E., Kutok, J.L., Toretsky, J.A., Tadavarthy, A.K., Kees, U.R., et al. (2008). BRD-NUT oncoproteins: a family of closely related nuclear proteins that block epithelial differentiation and maintain the growth of carcinoma cells. Oncogene *27*, 2237–2242.

French, C.A., Miyoshi, I., Kubonishi, I., Grier, H.E., Perez-Atayde, A.R., and Fletcher, J.A. (2003). BRD4-NUT fusion oncogene: a novel mechanism in aggressive carcinoma. Cancer Res. *63*, 304–307.

Fujii, S., Tokita, K., Wada, N., Ito, K., Yamauchi, C., Ito, Y., and Ochiai, A. (2011). MEK-ERK pathway regulates EZH2 overexpression in association with aggressive breast cancer subtypes. Oncogene *30*, 4118–4128.

Fujii, S., Fukamachi, K., Tsuda, H., Ito, K., Ito, Y., and Ochiai, A. (2012). RAS oncogenic signal upregulates EZH2 in pancreatic cancer. Biochem. Biophys. Res. Commun. *417*, 1074–1079.

Fujimura, K., Wright, T., Strnadel, J., Kaushal, S., Metildi, C., Lowy, A.M., Bouvet, M., Kelber, J.A., and Klemke, R.L. (2014). A hypusine-eIF5A-PEAK1 switch regulates the pathogenesis of pancreatic cancer. Cancer Res. *74*, 6671–6681.

Furney, S.J., Turajlic, S., Fenwick, K., Lambros, M.B., MacKay, A., Ricken, G., Mitsopoulos, C., Kozarewa, I., Hakas, J., Zvelebil, M., et al. (2012). Genomic characterisation of acral melanoma cell lines. Pigment Cell & Melanoma Research *25*, 488–492.

Furney, S.J., Turajlic, S., Stamp, G., Nohadani, M., Carlisle, A., Thomas, J.M., Hayes, A., Strauss, D., Gore, M., van den Oord, J., et al. (2013). Genome sequencing of mucosal melanomas reveals that they are driven by distinct mechanisms from cutaneous melanoma. J. Pathol. *230*, 261–269.

Furney, S.J., Turajlic, S., Stamp, G., Thomas, J.M., Hayes, A., Strauss, D., Gavrielides, M., Xing, W., Gore, M., Larkin, J., et al. (2014). The mutational burden of acral melanoma revealed by whole-genome sequencing and comparative analysis. Pigment Cell & Melanoma Research *27*, 835–838.

Füchtbauer, E.M. (1995). Expression of M-twist during postimplantation development of the mouse. Dev. Dyn. *204*, 316–322.

Gaggioli, C., and Sahai, E. (2007). Melanoma invasion - current knowledge and future directions. Pigment Cell Res. *20*, 161–172.

Gallagher, S.J., Rambow, F., Kumasaka, M., Champeval, D., Bellacosa, A., Delmas, V., and Larue, L. (2013). Beta-catenin inhibits melanocyte migration but induces melanoma metastasis. Oncogene *32*, 2230–2238.

Gallagher, S.J., Mijatov, B., Gunatilake, D., Gowrishankar, K., Tiffen, J., James, W., Jin, L., Pupo, G., Cullinane, C., McArthur, G.A., et al. (2014a). Control of NF-kB activity in human melanoma by bromodomain and extra-terminal protein inhibitor I-BET151. Pigment Cell & Melanoma Research *27*, 1126–1137.

Gallagher, S.J., Mijatov, B., Gunatilake, D., Tiffen, J.C., Gowrishankar, K., Jin, L., Pupo, G.M., Cullinane, C., Prinjha, R.K., Smithers, N., et al. (2014b). The epigenetic regulator I-BET151 induces BIM-dependent apoptosis and cell cycle arrest of human melanoma cells. J. Invest. Dermatol. *134*, 2795–2805.

Gandini, S., Sera, F., Cattaruzza, M.S., Pasquini, P., Abeni, D., Boyle, P., and Melchi, C.F. (2005a). Meta-analysis of risk factors for cutaneous melanoma: I. Common and atypical naevi. Eur. J. Cancer *41*, 28–44.

Gandini, S., Sera, F., Cattaruzza, M.S., Pasquini, P., Picconi, O., Boyle, P., and Melchi, C.F. (2005b). Meta-analysis of risk factors for cutaneous melanoma: II. Sun exposure. Eur. J. Cancer *41*, 45–60.

Gandini, S., Sera, F., Cattaruzza, M.S., Pasquini, P., Zanetti, R., Masini, C., Boyle, P., and Melchi, C.F. (2005c). Meta-analysis of risk factors for cutaneous melanoma: III. Family history, actinic damage and phenotypic factors. Eur. J. Cancer *41*, 2040–2059.

Garapaty-Rao, S., Nasveschuk, C., Gagnon, A., Chan, E.Y., Sandy, P., Busby, J., Balasubramanian, S., Campbell, R., Zhao, F., Bergeron, L., et al. (2013). Identification of EZH2 and EZH1 small molecule inhibitors with selective impact on diffuse large B cell lymphoma cell growth. Chem. Biol. *20*, 1329–1339.

Garibyan, L., and Fisher, D.E. (2010). How sunlight causes melanoma. Curr. Oncol. Rep. *12*, 319–326.

Garraway, L.A., Widlund, H.R., Rubin, M.A., Getz, G., Berger, A.J., Ramaswamy, S., Beroukhim, R., Milner, D.A., Granter, S.R., Du, J., et al. (2005). Integrative genomic analyses identify MITF as a lineage survival oncogene amplified in malignant melanoma. Nature *436*, 117–122.

Garrido, F., Cabrera, T., and Aptsiauri, N. (2010). "Hard" and “soft” lesions underlying the HLA class I alterations in cancer cells: implications for immunotherapy. Int. J. Cancer *127*, 249–256.

Garrido, M.C., and Bastian, B.C. (2010). KIT as a therapeutic target in melanoma. J. Invest. Dermatol. *130*, 20–27.

Gaudet, F., Hodgson, J.G., Eden, A., Jackson-Grusby, L., Dausman, J., Gray, J.W., Leonhardt, H., and Jaenisch, R. (2003). Induction of tumors in mice by genomic hypomethylation. Science *300*, 489–492.

Gembarska, A., Luciani, F., Fedele, C., Russell, E.A., Dewaele, M., Villar, S.E.P., Zwolinska, A., Haupt, S., de Lange, J., Yip, D., et al. (2012). MDM4 is a key therapeutic target in cutaneous melanoma. Nat. Med. *18*, 1239–1247.

Gershon, T.R., Oppenheimer, O., Chin, S.S., and Gerald, W.L. (2005). Temporally regulated neural crest transcription factors distinguish neuroectodermal tumors of varying malignancy and differentiation. Neoplasia *7*, 575–584.

Gibson, W.T., Hood, R.L., Zhan, S.H., Bulman, D.E., Fejes, A.P., Moore, R., Mungall, A.J., Eydoux, P., Babul-Hirji, R., An, J., et al. (2012). Mutations in EZH2 cause Weaver syndrome. Am. J. Hum. Genet. *90*, 110–118.

Gillis, L.D., and Lewis, S.M. (2013). Decreased eIF3e/Int6 expression causes epithelial-to-mesenchymal transition in breast epithelial cells. Oncogene *32*, 3598–3605.

Gilmartin, A.G., Bleam, M.R., Groy, A., Moss, K.G., Minthorn, E.A., Kulkarni, S.G., Rominger, C.M., Erskine, S., Fisher, K.E., Yang, J., et al. (2011). GSK1120212 (JTP-74057) is an inhibitor of MEK activity and activation with favorable pharmacokinetic properties for sustained in vivo pathway inhibition. Clin. Cancer Res. *17*, 989–1000.

Girotti, M.R., Pedersen, M., Sanchez-Laorden, B., Viros, A., Turajlic, S., Niculescu-Duvaz, D., Zambon, A., Sinclair, J., Hayes, A., Gore, M., et al. (2013). Inhibiting EGF Receptor or SRC Family Kinase Signaling Overcomes BRAF Inhibitor Resistance in Melanoma. Cancer Discovery *3*, 158–167.

Girouard, S.D., Laga, A.C., Mihm, M.C., Scolyer, R.A., Thompson, J.F., Zhan, Q., Widlund, H.R., Lee, C.-W., and Murphy, G.F. (2012). SOX2 contributes to melanoma cell invasion. Lab. Invest. *92*, 362–370.

Goel, V.K., Ibrahim, N., Jiang, G., Singhal, M., Fee, S., Flotte, T., Westmoreland, S., Haluska, F.S., Hinds, P.W., and Haluska, F.G. (2009). Melanocytic nevus-like hyperplasia and melanoma in transgenic BRAFV600E mice. Oncogene *28*, 2289–2298.

Goel, V.K., Lazar, A.J.F., Warneke, C.L., Redston, M.S., and Haluska, F.G. (2006). Examination of mutations in BRAF, NRAS, and PTEN in primary cutaneous melanoma. J. Invest. Dermatol. *126*, 154–160.

Goetz, E.M., Ghandi, M., Treacy, D.J., Wagle, N., and Garraway, L.A. (2014). ERK Mutations Confer Resistance to Mitogen-Activated Protein Kinase Pathway Inhibitors. Cancer Res. *74*, 7079–7089.

Goetz, S.C., and Anderson, K.V. (2010). The primary cilium: a signalling centre during vertebrate development. Nat. Rev. Genet. *11*, 331–344.

Goldstein, A.M., and Tucker, M.A. (2001). Genetic epidemiology of cutaneous melanoma: a global perspective. Arch. Dermatol. *137*, 1493–1496.

Gonzalez, M.E., Li, X., Toy, K., DuPrie, M., Ventura, A.C., Banerjee, M., Ljungman, M., Merajver, S.D., and Kleer, C.G. (2009). Downregulation of EZH2 decreases growth of estrogen receptor-negative invasive breast carcinoma and requires BRCA1. Oncogene *28*, 843–853.

Gonzalez, M.E., Moore, H.M., Li, X., Toy, K.A., Huang, W., Sabel, M.S., Kidwell, K.M., and Kleer, C.G. (2014). EZH2 expands breast stem cells through activation of NOTCH1 signaling. Proc. Natl. Acad. Sci. USA *111*, 3098–3103.

Goodall, J., Carreira, S., Denat, L., Kobi, D., Davidson, I., Nuciforo, P., Sturm, R.A., Larue, L., and Goding, C.R. (2008). Brn-2 represses microphthalmia-associated transcription factor expression and marks a distinct subpopulation of microphthalmia-associated transcription factor-negative melanoma cells. Cancer Res. *68*, 7788–7794.

Gopal, Y.N.V., Deng, W., Woodman, S.E., Komurov, K., Ram, P., Smith, P.D., and Davies, M.A. (2010). Basal and treatment-induced activation of AKT mediates resistance to cell death by AZD6244 (ARRY-142886) in Braf-mutant human cutaneous melanoma cells. Cancer Res. *70*, 8736–8747.

Gopal, Y.N.V., Rizos, H., Chen, G., Deng, W., Frederick, D.T., Cooper, Z.A., Scolyer, R.A., Pupo, G., Komurov, K., Sehgal, V., et al. (2014). Inhibition of mTORC1/2 overcomes resistance to MAPK pathway inhibitors mediated by PGC1α and oxidative phosphorylation in melanoma. Cancer Res. *74*, 7037–7047.

Gorelik, L., and Flavell, R.A. (2001). Immune-mediated eradication of tumors through the blockade of transforming growth factor-beta signaling in T cells. Nat. Med. *7*, 1118–1122.

Gould Rothberg, B.E., Berger, A.J., Molinaro, A.M., Subtil, A., Krauthammer, M.O., Camp, R.L., Bradley, W.R., Ariyan, S., Kluger, H.M., and Rimm, D.L. (2009). Melanoma prognostic model using tissue microarrays and genetic algorithms. J. Clin. Oncol. *27*, 5772–5780.

Gown, A.M., Vogel, A.M., Hoak, D., Gough, F., and McNutt, M.A. (1986). Monoclonal antibodies specific for melanocytic tumors distinguish subpopulations of melanocytes. Am. J. Pathol. *123*, 195–203.

Graf, S.A., Busch, C., Bosserhoff, A.K., Besch, R., and Berking, C. (2014). SOX10 promotes melanoma cell invasion by regulating melanoma inhibitory activity. J. Invest. Dermatol. *134*, 2212–2220.

Gray-Schopfer, V., Wellbrock, C., and Marais, R. (2007). Melanoma biology and new targeted therapy. Nature *445*, 851–857.

Greger, V., Passarge, E., Höpping, W., Messmer, E., and Horsthemke, B. (1989). Epigenetic changes may contribute to the formation and spontaneous regression of retinoblastoma. Hum. Genet. *83*, 155–158.

Gregorie, C.J., Wiesen, J.L., Magner, W.J., Lin, A.W., and Tomasi, T.B. (2009). Restoration of immune response gene induction in trophoblast tumor cells associated with cellular senescence. J. Reprod. Immunol. *81*, 25–33.

Grossmann, V., Kohlmann, A., Eder, C., Haferlach, C., Kern, W., Cross, N.C.P., Haferlach, T., and Schnittger, S. (2011). Molecular profiling of chronic myelomonocytic leukemia reveals diverse mutations in >80% of patients with TET2 and EZH2 being of high prognostic relevance. Leukemia *25*, 877–879.

Guglielmelli, P., Biamonte, F., Score, J., Hidalgo-Curtis, C., Cervantes, F., Maffioli, M., Fanelli, T., Ernst, T., Winkelman, N., Jones, A.V., et al. (2011). EZH2 mutational status predicts poor survival in myelofibrosis. Blood *118*, 5227–5234.

Gui, Y., Guo, G., Huang, Y., Hu, X., Tang, A., Gao, S., Wu, R., Chen, C., Li, X., Zhou, L., et al. (2011). Frequent mutations of chromatin remodeling genes in transitional cell carcinoma of the bladder. Nat. Genet. *43*, 875–878.

Guldberg, P., thor Straten, P., Birck, A., Ahrenkiel, V., Kirkin, A.F., and Zeuthen, J. (1997). Disruption of the MMAC1/PTEN gene by deletion or mutation is a frequent event in malignant melanoma. Cancer Res. *57*, 3660–3663.

Guris, D.L., Fantes, J., Tara, D., Druker, B.J., and Imamoto, A. (2001). Mice lacking the homologue of the human 22q11.2 gene CRKL phenocopy neurocristopathies of DiGeorge syndrome. Nat. Genet. *27*, 293–298.

Gutierrez, E., Shin, B.-S., Woolstenhulme, C.J., Kim, J.-R., Saini, P., Buskirk, A.R., and Dever, T.E. (2013). eIF5A promotes translation of polyproline motifs. Mol. Cell *51*, 35–45.

Haberland, M., Mokalled, M.H., Montgomery, R.L., and Olson, E.N. (2009). Epigenetic control of skull morphogenesis by histone deacetylase 8. Genes Dev. *23*, 1625–1630.

Hagedorn, L., Floris, J., Suter, U., and Sommer, L. (2000). Autonomic neurogenesis and apoptosis are alternative fates of progenitor cell communities induced by TGFbeta. Dev. Biol. *228*, 57–72.

Hagedorn, L., Suter, U., and Sommer, L. (1999). P0 and PMP22 mark a multipotent neural crest-derived cell type that displays community effects in response to TGF-beta family factors. Development *126*, 3781–3794.

Hanahan, D., and Weinberg, R.A. (2011). Hallmarks of cancer: the next generation. Cell *144*, 646–674.

Hansen, R.S., Wijmenga, C., Luo, P., Stanek, A.M., Canfield, T.K., Weemaes, C.M., and Gartler, S.M. (1999). The DNMT3B DNA methyltransferase gene is mutated in the ICF immunodeficiency syndrome. Proc. Natl. Acad. Sci. USA *96*, 14412–14417.

Haqq, C., Nosrati, M., Sudilovsky, D., Crothers, J., Khodabakhsh, D., Pulliam, B.L., Federman, S., Miller, J.R., Allen, R.E., Singer, M.I., et al. (2005). The gene expression signatures of melanoma progression. Proc. Natl. Acad. Sci. USA *102*, 6092–6097.

Haraguchi, M., Indo, H.P., Iwasaki, Y., Iwashita, Y., Fukushige, T., Majima, H.J., Izumo, K., Horiuchi, M., Kanekura, T., Furukawa, T., et al. (2013). Snail modulates cell metabolism in MDCK cells. Biochem. Biophys. Res. Commun. *432*, 618–625.

Hari, L., Brault, V., Kléber, M., Lee, H.-Y., Ille, F., Leimeroth, R., Paratore, C., Suter, U., Kemler, R., and Sommer, L. (2002). Lineage-specific requirements of beta-catenin in neural crest development. J. Cell. Biol. *159*, 867–880.

Hari, L., Miescher, I., Shakhova, O., Suter, U., Chin, L., Taketo, M., Richardson, W.D., Kessaris, N., and Sommer, L. (2012). Temporal control of neural crest lineage generation by Wnt/β-catenin signaling. Development *139*, 2107–2117.

Harms, P.W., Hristov, A.C., Kim, D.S., Anens, T., Quist, M.J., Siddiqui, J., Carskadon, S., Mehra, R., Fullen, D.R., Johnson, T.M., et al. (2014). Activating mutations of the oncogene EZH2 in cutaneous melanoma revealed by next generation sequencing. Human Pathology: Case Reports *1*, 21–28.

Harris, M.L., and Pavan, W.J. (2013). Postnatal lineage mapping of follicular melanocytes with the Tyr::CreER(T) (2) transgene. Pigment Cell & Melanoma Research *26*, 269–274.

Harris, M.L., Buac, K., Shakhova, O., Hakami, R.M., Wegner, M., Sommer, L., and Pavan, W.J. (2013). A Dual Role for SOX10 in the Maintenance of the Postnatal Melanocyte Lineage and the Differentiation of Melanocyte Stem Cell Progenitors. PLoS Genet. *9*, e1003644.

Hassounah, N.B., Nagle, R., Saboda, K., Roe, D.J., Dalkin, B.L., and McDermott, K.M. (2013). Primary cilia are lost in preinvasive and invasive prostate cancer. PLoS ONE *8*, e68521.

Hatzivassiliou, G., Song, K., Yen, I., Brandhuber, B.J., Anderson, D.J., Alvarado, R., Ludlam, M.J.C., Stokoe, D., Gloor, S.L., Vigers, G., et al. (2010). RAF inhibitors prime wild-type RAF to activate the MAPK pathway and enhance growth. Nature *464*, 431–435.

Hauschild, A., Grob, J.-J., Demidov, L.V., Jouary, T., Gutzmer, R., Millward, M., Rutkowski, P., Blank, C.U., Miller, W.H., Kaempgen, E., et al. (2012). Dabrafenib in BRAF-mutated metastatic melanoma: a multicentre, open-label, phase 3 randomised controlled trial. Lancet *380*, 358–365.

He, H., Ni, B., Tian, Y., Tian, Z., Chen, Y., Liu, Z., Yang, X., Lv, Y., and Zhang, Y. (2014). Histone methylation mediates plasticity of human FOXP3(+) regulatory T cells by modulating signature gene expressions. Immunology *141*, 362–376.

He, S., Li, C.G., Slobbe, L., Glover, A., Marshall, E., Baguley, B.C., and Eccles, M.R. (2011). PAX3 knockdown in metastatic melanoma cell lines does not reduce MITF expression. Melanoma Res. *21*, 24–34.

He, S., Yoon, H.-S., Suh, B.-J., and Eccles, M.R. (2010). PAX3 Is extensively expressed in benign and malignant tissues of the melanocytic lineage in humans. J. Invest. Dermatol. *130*, 1465–1468.

Heck, J.E., Ritz, B., Hung, R.J., Hashibe, M., and Boffetta, P. (2009). The epidemiology of neuroblastoma: a review. Paediatr. Perinat. Epidemiol. *23*, 125–143.

Heidorn, S.J., Milagre, C., Whittaker, S., Nourry, A., Niculescu-Duvas, I., Dhomen, N., Hussain, J., Reis-Filho, J.S., Springer, C.J., Pritchard, C., et al. (2010). Kinase-dead BRAF and oncogenic RAS cooperate to drive tumor progression through CRAF. Cell *140*, 209–221.

Heinen, A., Tzekova, N., Graffmann, N., Torres, K.J., Uhrberg, M., Hartung, H.-P., and Küry, P. (2012). Histone methyltransferase enhancer of zeste homolog 2 regulates Schwann cell differentiation. Glia *60*, 1696–1708.

Henssen, A., Thor, T., Odersky, A., Heukamp, L., El-Hindy, N., Beckers, A., Speleman, F., Althoff, K., Schäfers, S., Schramm, A., et al. (2013). BET bromodomain protein inhibition is a therapeutic option for medulloblastoma. Oncotarget *4*, 2080–2095.

Herbst, R.S., Soria, J.-C., Kowanetz, M., Fine, G.D., Hamid, O., Gordon, M.S., Sosman, J.A., McDermott, D.F., Powderly, J.D., Gettinger, S.N., et al. (2014). Predictive correlates of response to the anti-PD-L1 antibody MPDL3280A in cancer patients. Nature *515*, 563–567.

Herman, J.G., and Baylin, S.B. (2003). Gene silencing in cancer in association with promoter hypermethylation. N. Engl. J. Med. *349*, 2042–2054.

Herranz, N., Pasini, D., Díaz, V.M., Francí, C., Gutierrez, A., Dave, N., Escrivà, M., Hernandez-Muñoz, I., Di Croce, L., Helin, K., et al. (2008). Polycomb complex 2 is required for E-cadherin repression by the Snail1 transcription factor. Mol. Cell Biol. *28*, 4772–4781.

Herrera-Merchan, A., Arranz, L., Ligos, J.M., de Molina, A., Dominguez, O., and Gonzalez, S. (2012). Ectopic expression of the histone methyltransferase Ezh2 in haematopoietic stem cells causes myeloproliferative disease. Nat. Commun. *3*, 623.

Herzig, S., Raemy, E., Montessuit, S., Veuthey, J.-L., Zamboni, N., Westermann, B., Kunji, E.R.S., and Martinou, J.-C. (2012). Identification and functional expression of the mitochondrial pyruvate carrier. Science *337*, 93–96.

Hidalgo, I., Herrera-Merchan, A., Ligos, J.M., Carramolino, L., Nuñez, J., Martinez, F., Dominguez, O., Torres, M., and Gonzalez, S. (2012). Ezh1 is required for hematopoietic stem cell maintenance and prevents senescence-like cell cycle arrest. Cell Stem Cell *11*, 649–662.

Hirabayashi, Y., Suzki, N., Tsuboi, M., Endo, T.A., Toyoda, T., Shinga, J., Koseki, H., Vidal, M., and Gotoh, Y. (2009). Polycomb Limits the Neurogenic Competence of Neural Precursor Cells to Promote Astrogenic Fate Transition. Neuron *63*, 600–613.

Hirobe, T. (1984). Histochemical survey of the distribution of the epidermal melanoblasts and melanocytes in the mouse during fetal and postnatal periods. Anat. Rec. *208*, 589–594.

His, W. (1868). Untersuchungen über die erste Anlage des Wirbeltierleibes. Die erste Entwickelung des Hühnchens im Ei. (Leipzig: FCW Vogel).

Hocker, T., and Tsao, H. (2007). Ultraviolet radiation and melanoma: a systematic review and analysis of reported sequence variants. Hum. Mutat. *28*, 578–588.

Hodi, F.S., O'Day, S.J., McDermott, D.F., Weber, R.W., Sosman, J.A., Haanen, J.B., Gonzalez, R., Robert, C., Schadendorf, D., Hassel, J.C., et al. (2010). Improved survival with ipilimumab in patients with metastatic melanoma. N. Engl. J. Med. *363*, 711–723.

Hodis, E., Watson, I.R., Kryukov, G.V., Arold, S.T., Imielinski, M., Theurillat, J.-P., Nickerson, E., Auclair, D., Li, L., Place, C., et al. (2012). A landscape of driver mutations in melanoma. Cell *150*, 251–263.

Hoek, K.S., Eichhoff, O.M., Schlegel, N.C., Döbbeling, U., Kobert, N., Schaerer, L., Hemmi, S., and Dummer, R. (2008). In vivo switching of human melanoma cells between proliferative and invasive states. Cancer Res. *68*, 650–656.

Hoek, K.S., Schlegel, N.C., Brafford, P., Sucker, A., Ugurel, S., Kumar, R., Weber, B.L., Nathanson, K.L., Phillips, D.J., Herlyn, M., et al. (2006). Metastatic potential of melanomas defined by specific gene expression profiles with no BRAF signature. Pigment Cell Res. *19*, 290–302.

Holliday, R. (1987). The inheritance of epigenetic defects. Science *238*, 163–170.

Holtkamp, N., Atallah, I., Okuducu, A.-F., Mucha, J., Hartmann, C., Mautner, V.-F., Friedrich, R.E., Mawrin, C., and Deimling, von, A. (2007). MMP-13 and p53 in the progression of malignant peripheral nerve sheath tumors. Neoplasia *9*, 671–677.

Horne, G.A., Stewart, H.J.S., Dickson, J., Knapp, S., Ramsahoye, B., and Chevassut, T. (2014). Nanog Requires BRD4 to Maintain Murine Embryonic Stem Cell Pluripotency and Is Suppressed by Bromodomain Inhibitor JQ1 Together with Lefty1. Stem Cells Dev., doi:10.1089/scd.2014.0302.

Hosoda, K., Hammer, R.E., Richardson, J.A., Baynash, A.G., Cheung, J.C., Giaid, A., and Yanagisawa, M. (1994). Targeted and natural (piebald-lethal) mutations of endothelin-B receptor gene produce megacolon associated with spotted coat color in mice. Cell *79*, 1267–1276.

Houzelstein, D., Bullock, S.L., Lynch, D.E., Grigorieva, E.F., Wilson, V.A., and Beddington, R.S.P. (2002). Growth and early postimplantation defects in mice deficient for the bromodomain-containing protein Brd4. Mol. Cell Biol. *22*, 3794–3802.

Hsieh, A.C., Liu, Y., Edlind, M.P., Ingolia, N.T., Janes, M.R., Sher, A., Shi, E.Y., Stumpf, C.R., Christensen, C., Bonham, M.J., et al. (2012). The translational landscape of mTOR signalling steers cancer initiation and metastasis. Nature *485*, 55–61.

Hsieh, C.L. (1999). In vivo activity of murine de novo methyltransferases, Dnmt3a and Dnmt3b. Mol. Cell Biol. *19*, 8211–8218.

Hsu, Y.-C., and Fuchs, E. (2012). A family business: stem cell progeny join the niche to regulate homeostasis. Nat. Rev. Mol. Cell. Biol. *13*, 103–114.

Hu, D.N. (2000). Regulation of growth and melanogenesis of uveal melanocytes. Pigment Cell Res. *13*, 81–86.

Hu, N., Strobl-Mazzulla, P.H., Simoes-Costa, M., Sánchez-Vásquez, E., and Bronner, M.E. (2014). DNA methyltransferase 3B regulates duration of neural crest production via repression of Sox10. Proc. Natl. Acad. Sci. USA *111*, 17911–17916.

Hu, N., Strobl-Mazzulla, P., Sauka-Spengler, T., and Bronner, M.E. (2012). DNA methyltransferase3A as a molecular switch mediating the neural tube-to-neural crest fate transition. Genes Dev. *26*, 2380–2385.

Hu, S., Yu, L., Li, Z., Shen, Y., Wang, J., Cai, J., Xiao, L., and Wang, Z. (2010). Overexpression of EZH2 contributes to acquired cisplatin resistance in ovarian cancer cells in vitro and in vivo. Cancer Biol. Ther. *10*, 788–795.

Huang, H., Sabari, B.R., Garcia, B.A., Allis, C.D., and Zhao, Y. (2014). SnapShot: Histone Modifications. Cell *159*, 458–458.e1.

Huijbers, I.J., Krimpenfort, P., Chomez, P., van der Valk, M.A., Song, J.-Y., Inderberg-Suso, E.-M., Schmitt-Verhulst, A.-M., Berns, A., and Van den Eynde, B.J. (2006). An inducible mouse model of melanoma expressing a defined tumor antigen. Cancer Res. *66*, 3278–3286.

Ignatius, M.S., Moose, H.E., El-Hodiri, H.M., and Henion, P.D. (2008). colgate/hdac1 Repression of foxd3 expression is required to permit mitfa-dependent melanogenesis. Dev. Biol. *313*, 568–583.

Ignatius, M.S., Unal Eroglu, A., Malireddy, S., Gallagher, G., Nambiar, R.M., and Henion, P.D. (2013). Distinct functional and temporal requirements for zebrafish Hdac1 during neural crest-derived craniofacial and peripheral neuron development. PLoS ONE *8*, e63218.

Ikeya, M., Lee, S.M., Johnson, J.E., McMahon, A.P., and Takada, S. (1997). Wnt signalling required for expansion of neural crest and CNS progenitors. Nature *389*, 966–970.

Iliopoulos, D., Lindahl-Allen, M., Polytarchou, C., Hirsch, H.A., Tsichlis, P.N., and Struhl, K. (2010). Loss of miR-200 inhibition of Suz12 leads to polycomb-mediated repression required for the formation and maintenance of cancer stem cells. Mol. Cell *39*, 761–772.

Innominato, P.F., Libbrecht, L., and van den Oord, J.J. (2001). Expression of neurotrophins and their receptors in pigment cell lesions of the skin. J. Pathol. *194*, 95–100.

Ito, Y., Yeo, J.Y., Chytil, A., Han, J., Bringas, P., Nakajima, A., Shuler, C.F., Moses, H.L., and Chai, Y. (2003). Conditional inactivation of Tgfbr2 in cranial neural crest causes cleft palate and calvaria defects. Development *130*, 5269–5280.

Itzhaki, O., Hovav, E., Ziporen, Y., Levy, D., Kubi, A., Zikich, D., Hershkovitz, L., Treves, A.J., Shalmon, B., Zippel, D., et al. (2011). Establishment and large-scale expansion of minimally cultured "young" tumor infiltrating lymphocytes for adoptive transfer therapy. J. Immunother. *34*, 212–220.

Ivanova, N., Dobrin, R., Lu, R., Kotenko, I., Levorse, J., DeCoste, C., Schafer, X., Lun, Y., and Lemischka, I.R. (2006). Dissecting self-renewal in stem cells with RNA interference. Nature *442*, 533–538.

Iwamoto, S., Burrows, R.C., Agoff, S.N., Piepkorn, M., Bothwell, M., and Schmidt, R. (2001). The p75 neurotrophin receptor, relative to other Schwann cell and melanoma markers, is abundantly Expressed in spindled melanomas. The American Journal of Dermatopathology *23*, 288–294.

Jacob, C., Christen, C.N., Pereira, J.A., Somandin, C., Baggiolini, A., Lötscher, P., Ozçelik, M., Tricaud, N., Meijer, D., Yamaguchi, T., et al. (2011). HDAC1 and HDAC2 control the transcriptional program of myelination and the survival of Schwann cells. Nat. Neurosci. *14*, 429–436.

Jacob, C., Lötscher, P., Engler, S., Baggiolini, A., Varum Tavares, S., Brügger, V., John, N., Büchmann-Møller, S., Snider, P.L., Conway, S.J., et al. (2014). HDAC1 and HDAC2 Control the Specification of Neural Crest Cells into Peripheral Glia. J. Neurosci. *34*, 6112–6122.

Janebodin, K., Horst, O.V., Ieronimakis, N., Balasundaram, G., Reesukumal, K., Pratumvinit, B., and Reyes, M. (2011). Isolation and characterization of neural crest-derived stem cells from dental pulp of neonatal mice. PLoS ONE *6*, e27526.

Jasiulionis, M.G., Luchessi, A.D., Moreira, A.G., Souza, P.P.C., Suenaga, A.P.M., Correa, M., Costa, C.A.S., Curi, R., and Costa-Neto, C.M. (2007). Inhibition of eukaryotic translation initiation factor 5A (eIF5A) hypusination impairs melanoma growth. Cell Biochem. Funct. *25*, 109–114.

Javelaud, D., Alexaki, V.-I., Pierrat, M.-J., Hoek, K.S., Dennler, S., van Kempen, L., Bertolotto, C., Ballotti, R., Saule, S., Delmas, V., et al. (2011). GLI2 and M-MITF transcription factors control exclusive gene expression programs and inversely regulate invasion in human melanoma cells. Pigment Cell & Melanoma Research *24*, 932–943.

Javelaud, D., Delmas, V., Möller, M., Sextius, P., André, J., Menashi, S., Larue, L., and Mauviel, A. (2005). Stable overexpression of Smad7 in human melanoma cells inhibits their tumorigenicity in vitro and in vivo. Oncogene *24*, 7624–7629.

Javelaud, D., Mohammad, K.S., McKenna, C.R., Fournier, P., Luciani, F., Niewolna, M., André, J., Delmas, V., Larue, L., Guise, T.A., et al. (2007). Stable overexpression of Smad7 in human melanoma cells impairs bone metastasis. Cancer Res. *67*, 2317–2324.

Jäger, E., Ringhoffer, M., Altmannsberger, M., Arand, M., Karbach, J., Jäger, D., Oesch, F., and Knuth, A. (1997). Immunoselection in vivo: independent loss of MHC class I and melanocyte differentiation antigen expression in metastatic melanoma. Int. J. Cancer *71*, 142–147.

Jenuwein, T., and Allis, C.D. (2001). Translating the histone code. Science *293*, 1074–1080.

Jiang, L., Xiao, L., Sugiura, H., Huang, X., Ali, A., Kuro-O, M., DeBerardinis, R.J., and Boothman, D.A. (2014). Metabolic reprogramming during TGFβ1-induced epithelial-to-mesenchymal transition. Oncogene, doi:10.1038/onc.2014.321.

Jiang, X., Rowitch, D.H., Soriano, P., McMahon, A.P., and Sucov, H.M. (2000). Fate of the mammalian cardiac neural crest. Development *127*, 1607–1616.

Jin, E.J., Erickson, C.A., Takada, S., and Burrus, L.W. (2001). Wnt and BMP signaling govern lineage segregation of melanocytes in the avian embryo. Dev. Biol. *233*, 22–37.

Johannessen, C.M., Boehm, J.S., Kim, S.Y., Thomas, S.R., Wardwell, L., Johnson, L.A., Emery, C.M., Stransky, N., Cogdill, A.P., Barretina, J., et al. (2010). COT drives resistance to RAF inhibition through MAP kinase pathway reactivation. Nature *468*, 968–972.

Johannessen, C.M., Johnson, L.A., Piccioni, F., Townes, A., Frederick, D.T., Donahue, M.K., Narayan, R., Flaherty, K.T., Wargo, J.A., Root, D.E., et al. (2013). A melanocyte lineage program confers resistance to MAP kinase pathway inhibition. Nature *504*, 138–142.

John, N., Cinelli, P., Wegner, M., and Sommer, L. (2011). Transforming growth factor β-mediated Sox10 suppression controls mesenchymal progenitor generation in neural crest stem cells. Stem Cells *29*, 689–699.

Johnston, A.P.W., Naska, S., Jones, K., Jinno, H., Kaplan, D.R., and Miller, F.D. (2013). Sox2-Mediated Regulation of Adult Neural Crest Precursors and Skin Repair. Stem Cell Reports *1*, 38–45.

Jones, D.T.W., Jäger, N., Kool, M., Zichner, T., Hutter, B., Sultan, M., Cho, Y.-J., Pugh, T.J., Hovestadt, V., Stütz, A.M., et al. (2012). Dissecting the genomic complexity underlying medulloblastoma. Nature *488*, 100–105.

Jones, P.A., and Taylor, S.M. (1980). Cellular differentiation, cytidine analogs and DNA methylation. Cell *20*, 85–93.

Jonsson, A., Tuominen, R., Grafström, E., Hansson, J., and Egyhazi, S. (2010). High Frequency of p16(INK4A) Promoter Methylation in NRAS-Mutated Cutaneous Melanoma. J. Invest. Dermatol. *130*, 2809–2817.

Joseph, N.M., Mosher, J.T., Buchstaller, J., Snider, P., McKeever, P.E., Lim, M., Conway, S.J., Parada, L.F., Zhu, Y., and Morrison, S.J. (2008). The loss of Nf1 transiently promotes self-renewal but not tumorigenesis by neural crest stem cells. Cancer Cell *13*, 129–140.

Kageshita, T., Hamby, C.V., Ishihara, T., Matsumoto, K., Saida, T., and Ono, T. (2001). Loss of beta-catenin expression associated with disease progression in malignant melanoma. Br. J. Dermatol. *145*, 210–216.

Kalb, R., Latwiel, S., Baymaz, H.I., Jansen, P.W.T.C., Müller, C.W., Vermeulen, M., and Müller, J. (2014). Histone H2A monoubiquitination promotes histone H3 methylation in Polycomb repression. Nat. Struct. Mol. Biol. *21*, 569–571.

Kamb, A., Gruis, N.A., Weaver-Feldhaus, J., Liu, Q., Harshman, K., Tavtigian, S.V., Stockert, E., Day, R.S., Johnson, B.E., and Skolnick, M.H. (1994). A cell cycle regulator potentially involved in genesis of many tumor types. Science *264*, 436–440.

Kamminga, L.M., Bystrykh, L.V., de Boer, A., Houwer, S., Douma, J., Weersing, E., Dontje, B., and de Haan, G. (2006). The Polycomb group gene Ezh2 prevents hematopoietic stem cell exhaustion. Blood *107*, 2170–2179.

Kampilafkos, P., Melachrinou, M., Kefalopoulou, Z., Lakoumentas, J., and Sotiropoulou-Bonikou, G. (2015). Epigenetic Modifications in Cutaneous Malignant Melanoma: EZH2, H3K4me2, and H3K27me3 Immunohistochemical Expression is Enhanced at the Invasion Front of the Tumor. The American Journal of Dermatopathology *37*, 138–144.

Kamposioras, K., Pentheroudakis, G., Pectasides, D., and Pavlidis, N. (2011). Malignant melanoma of unknown primary site. To make the long story short. A systematic review of the literature. Crit. Rev. Oncol. Hematol. *78*, 112–126.

Kaneko, S., Bonasio, R., Saldaña-Meyer, R., Yoshida, T., Son, J., Nishino, K., Umezawa, A., and Reinberg, D. (2014). Interactions between JARID2 and Noncoding RNAs Regulate PRC2 Recruitment to Chromatin. Mol. Cell *53*, 290–300.

Kaplon, J., Zheng, L., Meissl, K., Chaneton, B., Selivanov, V.A., Mackay, G., van der Burg, S.H., Verdegaal, E.M.E., Cascante, M., Shlomi, T., et al. (2013). A key role for mitochondrial gatekeeper pyruvate dehydrogenase in oncogene-induced senescence. Nature *498*, 109–112.

Kapur, R.P. (1999). Early death of neural crest cells is responsible for total enteric aganglionosis in Sox10(Dom)/Sox10(Dom) mouse embryos. Pediatr. Dev. Pathol. *2*, 559–569.

Karouzakis, E., Gay, R.E., Gay, S., and Neidhart, M. (2012). Increased recycling of polyamines is associated with global DNA hypomethylation in rheumatoid arthritis synovial fibroblasts. Arthritis Rheum. *64*, 1809–1817.

Karpf, A.R., and Matsui, S.-I. (2005). Genetic disruption of cytosine DNA methyltransferase enzymes induces chromosomal instability in human cancer cells. Cancer Res. *65*, 8635–8639.

Kato, Y., Yoshimura, K., Shin, T., Verheul, H., Hammers, H., Sanni, T.B., Salumbides, B.C., Van Erp, K., Schulick, R., and Pili, R. (2007). Synergistic in vivo antitumor effect of the histone deacetylase inhibitor MS-275 in combination with interleukin 2 in a murine model of renal cell carcinoma. Clin. Cancer Res. *13*, 4538–4546.

Kato, Y., Yoshino, I., Egusa, C., Maeda, T., Pili, R., and Tsuboi, R. (2014). Combination of HDAC inhibitor MS-275 and IL-2 increased anti-tumor effect in a melanoma model via activated cytotoxic T cells. J. Dermatol. Sci. *75*, 140–147.

Kelderman, S., Schumacher, T.N.M., and Haanen, J.B.A.G. (2014). Acquired and intrinsic resistance in cancer immunotherapy. Mol. Oncol. *8*, 1132–1139.

Kelly, R.D.W., and Cowley, S.M. (2013). The physiological roles of histone deacetylase (HDAC) 1 and 2: complex co-stars with multiple leading parts. Biochem. Soc. Trans. *41*, 741–749.

Keshet, G.I., Goldstein, I., Itzhaki, O., Cesarkas, K., Shenhav, L., Yakirevitch, A., Treves, A.J., Schachter, J., Amariglio, N., and Rechavi, G. (2008). MDR1 expression identifies human melanoma stem cells. Biochem. Biophys. Res. Commun. *368*, 930–936.

Khan, A.N.H., Gregorie, C.J., and Tomasi, T.B. (2008). Histone deacetylase inhibitors induce TAP, LMP, Tapasin genes and MHC class I antigen presentation by melanoma cells. Cancer Immunol. Immunother. *57*, 647–654.

Khong, H.T., Wang, Q.J., and Rosenberg, S.A. (2004). Identification of multiple antigens recognized by tumor-infiltrating lymphocytes from a single patient: tumor escape by antigen loss and loss of MHC expression. J. Immunother. *27*, 184–190.

Kim, E., Kim, M., Woo, D.-H., Shin, Y., Shin, J., Chang, N., Oh, Y.T., Kim, H., Rheey, J., Nakano, I., et al. (2013). Phosphorylation of EZH2 Activates STAT3 Signaling via STAT3 Methylation and Promotes Tumorigenicity of Glioblastoma Stem-like Cells. Cancer Cell *23*, 839–852.

Kim, H., Kang, K., Ekram, M.B., Roh, T.-Y., and Kim, J. (2011a). Aebp2 as an epigenetic regulator for neural crest cells. PLoS ONE *6*, e25174.

Kim, J., Dabiri, S., and Seeley, E.S. (2011b). Primary cilium depletion typifies cutaneous melanoma in situ and malignant melanoma. PLoS ONE *6*, e27410.

Kim, J., Lo, L., Dormand, E., and Anderson, D.J. (2003). SOX10 maintains multipotency and inhibits neuronal differentiation of neural crest stem cells. Neuron *38*, 17–31.

Kim, S.-H., Joshi, K., Ezhilarasan, R., Myers, T.R., Siu, J., Gu, C., Nakano-Okuno, M., Taylor, D., Minata, M., Sulman, E.P., et al. (2015). EZH2 protects glioma stem cells from radiation-induced cell death in a MELK/FOXM1-dependent manner. Stem Cell Reports *4*, 226–238.

King, R., Weilbaecher, K.N., McGill, G., Cooley, E., Mihm, M., and Fisher, D.E. (1999). Microphthalmia transcription factor. A sensitive and specific melanocyte marker for MelanomaDiagnosis. Am. J. Pathol. *155*, 731–738.

Kinkel, S.A., Galeev, R., Flensburg, C., Keniry, A., Breslin, K., Gilan, O., Lee, S., Liu, J., Chen, K., Gearing, L.J., et al. (2015). Jarid2 regulates hematopoietic stem cell function by acting with polycomb repressive complex 2. Blood, doi:10. 1182/blood-2014-10-603969.

Kinsler, V.A., Thomas, A.C., Ishida, M., Bulstrode, N.W., Loughlin, S., Hing, S., Chalker, J., McKenzie, K., Abu-Amero, S., Slater, O., et al. (2013). Multiple congenital melanocytic nevi and neurocutaneous melanosis are caused by postzygotic mutations in codon 61 of NRAS. J. Invest. Dermatol. *133*, 2229–2236.

Kleer, C.G., Cao, Q., Varambally, S., Shen, R., Ota, I., Tomlins, S.A., Ghosh, D., Sewalt, R.G.A.B., Otte, A.P., Hayes, D.F., et al. (2003). EZH2 is a marker of aggressive breast cancer and promotes neoplastic transformation of breast epithelial cells. Proc. Natl. Acad. Sci. USA *100*, 11606–11611.

Kléber, M., Lee, H.-Y., Wurdak, H., Buchstaller, J., Riccomagno, M.M., Ittner, L.M., Suter, U., Epstein, D.J., and Sommer, L. (2005). Neural crest stem cell maintenance by combinatorial Wnt and BMP signaling. J. Cell Biol. *169*, 309–320.

Knoechel, B., Roderick, J.E., Williamson, K.E., Zhu, J., Lohr, J.G., Cotton, M.J., Gillespie, S.M., Fernandez, D., Ku, M., Wang, H., et al. (2014). An epigenetic mechanism of resistance to targeted therapy in T cell acute lymphoblastic leukemia. Nat. Genet. *46*, 364–370.

Knutson, S.K., Warholic, N.M., Wigle, T.J., Klaus, C.R., Allain, C.J., Raimondi, A., Porter Scott, M., Chesworth, R., Moyer, M.P., Copeland, R.A., et al. (2013). Durable tumor regression in genetically altered malignant rhabdoid tumors by inhibition of methyltransferase EZH2. Proc. Natl. Acad. Sci. USA *110*, 7922–7927.

Knutson, S.K., Wigle, T.J., Warholic, N.M., Sneeringer, C.J., Allain, C.J., Klaus, C.R., Sacks, J.D., Raimondi, A., Majer, C.R., Song, J., et al. (2012). A selective inhibitor of EZH2 blocks H3K27 methylation and kills mutant lymphoma cells. Nat. Chem. Biol. *8*, 890–896.

Kobayashi, T., and Hearing, V.J. (2007). Direct interaction of tyrosinase with Tyrp1 to form hetero-dimeric complexes in vivo. J. Cell. Sci. 120, 4261–4268.

Koh, C.M., Iwata, T., Zheng, Q., Bethel, C., Yegnasubramanian, S., and De Marzo, A.M. (2011). Myc enforces overexpression of EZH2 in early prostatic neoplasia via transcriptional and post-transcriptional mechanisms. Oncotarget *2*, 669–683.

Koh, H.K. (1991). Cutaneous melanoma. N. Engl. J. Med. *325*, 171–182.

Konieczkowski, D.J., Johannessen, C.M., Abudayyeh, O., Kim, J.W., Cooper, Z.A., Piris, A., Frederick, D.T., Barzily-Rokni, M., Straussman, R., Haq, R., et al. (2014). A melanoma cell state distinction influences sensitivity to MAPK pathway inhibitors. Cancer Discovery *4*, 816–827.

Konze, K.D., Ma, A., Li, F., Barsyte-Lovejoy, D., Parton, T., Macnevin, C.J., Liu, F., Gao, C., Huang, X.-P., Kuznetsova, E., et al. (2013). An orally bioavailable chemical probe of the Lysine Methyltransferases EZH2 and EZH1. ACS Chem. Biol. *8*, 1324–1334.

Kos, R., Reedy, M.V., Johnson, R.L., and Erickson, C.A. (2001). The winged-helix transcription factor FoxD3 is important for establishing the neural crest lineage and repressing melanogenesis in avian embryos. Development *128*, 1467–1479.

Kostaki, M., Manona, A.D., Stavraka, I., Korkolopoulou, P., Levidou, G., Trigka, E.-A., Christofidou, E., Champsas, G., Stratigos, A.J., Katsambas, A., et al. (2014). High-frequency p16(INK) (4A) promoter methylation is associated with histone methyltransferase SETDB1 expression in sporadic cutaneous melanoma. Exp. Dermatol. *23*, 332–338.

Kourea, H.P., Orlow, I., Scheithauer, B.W., Cordón-Cardo, C., and Woodruff, J.M. (1999). Deletions of the INK4A Gene Occur in Malignant Peripheral Nerve Sheath Tumors but not in Neurofibromas. Am. J. Pathol. *155*, 1855–1860.

Kouzarides, T. (2007). Chromatin modifications and their function. Cell *128*, 693–705.

Krasagakis, K., Krüger-Krasagakes, S., Fimmel, S., Eberle, J., Thölke, D., Ohe, von der, M., Mansmann, U., and Orfanos, C.E. (1999). Desensitization of melanoma cells to autocrine TGF-beta isoforms. J. Cell. Physiol. *178*, 179–187.

Krauthammer, M., Kong, Y., Ha, B.H., Evans, P., Bacchiocchi, A., McCusker, J.P., Cheng, E., Davis, M.J., Goh, G., Choi, M., et al. (2012). Exome sequencing identifies recurrent somatic RAC1 mutations in melanoma. Nat. Genet. *44*, 1006–1014.

Krejcí, J., Uhlírová, R., Galiová, G., Kozubek, S., Smigová, J., and Bártová, E. (2009). Genome-wide reduction in H3K9 acetylation during human embryonic stem cell differentiation. J. Cell. Physiol. *219*, 677–687.

Krengel, U., Schlichting, I., Scherer, A., Schumann, R., Frech, M., John, J., Kabsch, W., Pai, E.F., and Wittinghofer, A. (1990). Three-dimensional structures of H-ras p21 mutants: molecular basis for their inability to function as signal switch molecules. Cell *62*, 539–548.

Kreso, A., and Dick, J.E. (2014). Evolution of the cancer stem cell model. Cell Stem Cell *14*, 275–291.

Krieg, C., Létourneau, S., Pantaleo, G., and Boyman, O. (2010). Improved IL-2 immunotherapy by selective stimulation of IL-2 receptors on lymphocytes and endothelial cells. Proc. Natl. Acad. Sci. USA *107*, 11906–11911.

Krishnadas, D.K., Bao, L., Bai, F., Chencheri, S.C., and Lucas, K. (2014). Decitabine facilitates immune recognition of sarcoma cells by upregulating CT antigens, MHC molecules, and ICAM-1. Tumour Biol. *35*, 5753–5762.

Kruger, G.M., Mosher, J.T., Bixby, S., Joseph, N., Iwashita, T., and Morrison, S.J. (2002). Neural crest stem cells persist in the adult gut but undergo changes in self-renewal, neuronal subtype potential, and factor responsiveness. Neuron *35*, 657–669.

Kubic, J.D., Young, K.P., Plummer, R.S., Ludvik, A.E., and Lang, D. (2008). Pigmentation PAX-ways: the role of Pax3 in melanogenesis, melanocyte stem cell maintenance, and disease. Pigment Cell & Melanoma Research *21*, 627–645.

Kumari, A., Cacan, E., Greer, S.F., and Garnett-Benson, C. (2013). Turning T cells on: epigenetically enhanced expression of effector T-cell costimulatory molecules on irradiated human tumor cells. J Immunother Cancer *1*, 17.

Kunderfranco, P., Mello-Grand, M., Cangemi, R., Pellini, S., Mensah, A., Albertini, V., Malek, A., Chiorino, G., Catapano, C.V., and Carbone, G.M. (2010). ETS transcription factors control transcription of EZH2 and epigenetic silencing of the tumor suppressor gene Nkx3.1 in prostate cancer. PLoS ONE *5*, e10547.

Kuzmichev, A., Nishioka, K., Erdjument-Bromage, H., Tempst, P., and Reinberg, D. (2002). Histone methyltransferase activity associated with a human multiprotein complex containing the Enhancer of Zeste protein. Genes Dev. *16*, 2893–2905.

Kuźbicki, L., Lange, D., Strączyńska-Niemiec, A., and Chwirot, B.W. (2013). JARID1B expression in human melanoma and benign melanocytic skin lesions. Melanoma Res. *23*, 8–12.

Kwong, L.N., Costello, J.C., Liu, H., Jiang, S., Helms, T.L., Langsdorf, A.E., Jakubosky, D., Genovese, G., Muller, F.L., Jeong, J.H., et al. (2012). Oncogenic NRAS signaling differentially regulates survival and proliferation in melanoma. Nat. Med. *18*, 1503–1510.

Laga, A.C., and Murphy, G.F. (2010). Cellular heterogeneity in vertical growth phase melanoma. Arch. Pathol. Lab. Med. *134*, 1750–1757.

Laga, A.C., Lai, C.-Y., Zhan, Q., Huang, S.J., Velazquez, E.F., Yang, Q., Hsu, M.-Y., and Murphy, G.F. (2010). Expression of the embryonic stem cell transcription factor SOX2 in human skin: relevance to melanocyte and merkel cell biology. Am. J. Pathol. *176*, 903–913.

Laga, A.C., Zhan, Q., Weishaupt, C., Ma, J., Frank, M.H., and Murphy, G.F. (2011). SOX2 and nestin expression in human melanoma: an immunohistochemical and experimental study. Exp. Dermatol. *20*, 339–345.

Lagger, G., O'Carroll, D., Rembold, M., Khier, H., Tischler, J., Weitzer, G., Schuettengruber, B., Hauser, C., Brunmeir, R., Jenuwein, T., et al. (2002). Essential function of histone deacetylase 1 in proliferation control and CDK inhibitor repression. Embo J. *21*, 2672–2681.

Laird, P.W., Zijderveld, A., Linders, K., Rudnicki, M.A., Jaenisch, R., and Berns, A. (1991). Simplified mammalian DNA isolation procedure. Nucleic Acids Res. *19*, 4293.

Landsberg, J., Gaffal, E., Cron, M., Kohlmeyer, J., Renn, M., and Tüting, T. (2010). Autochthonous primary and metastatic melanomas in Hgf-Cdk4 R24C mice evade T-cell-mediated immune surveillance. Pigment Cell & Melanoma Research *23*, 649–660.

Landsberg, J., Kohlmeyer, J., Renn, M., Bald, T., Rogava, M., Cron, M., Fatho, M., Lennerz, V., Wölfel, T., Hölzel, M., et al. (2012). Melanomas resist T-cell therapy through inflammation-induced reversible dedifferentiation. Nature *490*, 412–416.

Lane, A.A., and Chabner, B.A. (2009). Histone deacetylase inhibitors in cancer therapy. J. Clin. Oncol. *27*, 5459–5468.

Lang, D., Lu, M.M., Huang, L., Engleka, K.A., Zhang, M., Chu, E.Y., Lipner, S., Skoultchi, A., Millar, S.E., and Epstein, J.A. (2005). Pax3 functions at a nodal point in melanocyte stem cell differentiation. Nature *433*, 884–887.

Larkin, J., Ascierto, P.A., Dreno, B., Atkinson, V., Liszkay, G., Maio, M., Mandalà, M., Demidov, L., Stroyakovskiy, D., Thomas, L., et al. (2014). Combined vemurafenib and cobimetinib in BRAF-mutated melanoma. N. Engl. J. Med. *371*, 1867–1876.

Lasithiotakis, K.G., Sinnberg, T.W., Schittek, B., Flaherty, K.T., Kulms, D., Maczey, E., Garbe, C., and Meier, F.E. (2008). Combined inhibition of MAPK and mTOR signaling inhibits growth, induces cell death, and abrogates invasive growth of melanoma cells. J. Invest. Dermatol. *128*, 2013–2023.

Lassen, A., Atefi, M., Robert, L., Wong, D.J., Cerniglia, M., Comin-Anduix, B., and Ribas, A. (2014). Effects of AKT inhibitor therapy in response and resistance to BRAF inhibition in melanoma. Mol. Cancer *13*, 83.

Lauden, L., Siewiera, J., Boukouaci, W., Ramgolam, K., Mourah, S., Lebbe, C., Charron, D., Aoudjit, F., Jabrane-Ferrat, N., and Al-Daccak, R. (2014). TGF-β-induced (TGFBI) protein in melanoma: a signature of high metastatic potential. J. Invest. Dermatol. *134*, 1675–1685.

Laugesen, A., and Helin, K. (2014). Chromatin repressive complexes in stem cells, development, and cancer. Cell Stem Cell *14*, 735–751.

Lavoie, J.-F., Biernaskie, J.A., Chen, Y., Bagli, D., Alman, B., Kaplan, D.R., and Miller, F.D. (2009). Skin-derived precursors differentiate into skeletogenic cell types and contribute to bone repair. Stem Cells Dev. *18*, 893–906.

Le Coz, M., Benmerah, A., and Larue, L. (2014). Quiescent melanocytes form primary cilia. Exp. Dermatol. *23*, 426–427.

Leach, D.R., Krummel, M.F., and Allison, J.P. (1996). Enhancement of antitumor immunity by CTLA-4 blockade. Science *271*, 1734–1736.

Lee, H.-Y., Kléber, M., Hari, L., Brault, V., Suter, U., Taketo, M.M., Kemler, R., and Sommer, L. (2004). Instructive role of Wnt/beta-catenin in sensory fate specification in neural crest stem cells. Science *303*, 1020–1023.

Lee, S.T., Li, Z., Wu, Z., Aau, M., Guan, P., Karuturi, R.K.M., Liou, Y.C., and Yu, Q. (2011). Context-specific regulation of NF-κB target gene expression by EZH2 in breast cancers. Mol. Cell *43*, 798–810.

Lee, T.I., Jenner, R.G., Boyer, L.A., Guenther, M.G., Levine, S.S., Kumar, R.M., Chevalier, B., Johnstone, S.E., Cole, M.F., Isono, K.-I., et al. (2006). Control of developmental regulators by Polycomb in human embryonic stem cells. Cell *125*, 301–313.

Lee, W., Teckie, S., Wiesner, T., Ran, L., Prieto Granada, C.N., Lin, M., Zhu, S., Cao, Z., Liang, Y., Sboner, A., et al. (2014). PRC2 is recurrently inactivated through EED or SUZ12 loss in malignant peripheral nerve sheath tumors. Nat. Genet. *46*, 1227–1232.

Legius, E., Marchuk, D.A., Collins, F.S., and Glover, T.W. (1993). Somatic deletion of the neurofibromatosis type 1 gene in a neurofibrosarcoma supports a tumour suppressor gene hypothesis. Nat. Genet. *3*, 122–126.

Lehnertz, B., Ueda, Y., Derijck, A.A.H.A., Braunschweig, U., Perez-Burgos, L., Kubicek, S., Chen, T., Li, E., Jenuwein, T., and Peters, A.H.F.M. (2003). Suv39h-mediated histone H3 lysine 9 methylation directs DNA methylation to major satellite repeats at pericentric heterochromatin. Curr. Biol. *13*, 1192–1200.

Letouzé, E., Martinelli, C., Loriot, C., Burnichon, N., Abermil, N., Ottolenghi, C., Janin, M., Menara, M., Nguyen, A.T., Benit, P., et al. (2013). SDH Mutations Establish a Hypermethylator Phenotype in Paraganglioma. Cancer Cell *23*, 739–752.

Levin, A.M., Bates, D.L., Ring, A.M., Krieg, C., Lin, J.T., Su, L., Moraga, I., Raeber, M.E., Bowman, G.R., Novick, P., et al. (2012). Exploiting a natural conformational switch to engineer an interleukin-2 'superkine'. Nature *484*, 529–533.

Létourneau, S., van Leeuwen, E.M.M., Krieg, C., Martin, C., Pantaleo, G., Sprent, J., Surh, C.D., and Boyman, O. (2010). IL-2/anti-IL-2 antibody complexes show strong biological activity by avoiding interaction with IL-2 receptor alpha subunit CD25. Proc. Natl. Acad. Sci. USA *107*, 2171–2176.

Lévy, P., Vidaud, D., Leroy, K., Laurendeau, I., Wechsler, J., Bolasco, G., Parfait, B., Wolkenstein, P., Vidaud, M., and Bièche, I. (2004). Molecular profiling of malignant peripheral nerve sheath tumors associated with neurofibromatosis type 1, based on large-scale real-time RT-PCR. Mol. Cancer *3*, 1–13.

Li, E., Bestor, T.H., and Jaenisch, R. (1992). Targeted mutation of the DNA methyltransferase gene results in embryonic lethality. Cell *69*, 915–926.

Li, L.-C., and Dahiya, R. (2002). MethPrimer: designing primers for methylation PCRs. Bioinformatics *18*, 1427–1431.

Li, X., Gonzalez, M.E., Toy, K., Filzen, T., Merajver, S.D., and Kleer, C.G. (2009). Targeted overexpression of EZH2 in the mammary gland disrupts ductal morphogenesis and causes epithelial hyperplasia. Am. J. Pathol. *175*, 1246–1254.

Liao, Y., Wei, Y., Zhou, X., Yang, J.-Y., Dai, C., Chen, Y.-J., Agarwal, N.K., Sarbassov, D., Shi, D., Yu, D., et al. (2009). Peptidyl-prolyl cis/trans isomerase Pin1 is critical for the regulation of PKB/Akt stability and activation phosphorylation. Oncogene *28*, 2436–2445.

Lin, B., Utleg, A.G., Gravdal, K., White, J.T., Halvorsen, O.J., Lu, W., True, L.D., Vessella, R., Lange, P.H., Nelson, P.S., et al. (2008). WDR19 Expression is Increased in Prostate Cancer Compared with Normal Cells, but Low-Intensity Expression in Cancers is Associated with Shorter Time to Biochemical Failures and Local Recurrence. Clin. Cancer Res. *14*, 1397–1406.

Lin, J.Y., and Fisher, D.E. (2007). Melanocyte biology and skin pigmentation. Nature *445*, 843–850.

Lin, W., Cao, J., Liu, J., Beshiri, M.L., Fujiwara, Y., Francis, J., Cherniack, A.D., Geisen, C., Blair, L.P., Zou, M.R., et al. (2011). Loss of the retinoblastoma binding protein 2 (RBP2) histone demethylase suppresses tumorigenesis in mice lacking Rb1 or Men1. Proc. Natl. Acad. Sci. USA *108*, 13379–13386.

Lin, W.M., Luo, S., Muzikansky, A., Lobo, A.Z.C., Tanabe, K.K., Sober, A.J., Cosimi, A.B., Tsao, H., and Duncan, L.M. (2015). Outcome of patients with de novo versus nevus-associated melanoma. J. Am. Acad. Dermatol. *72*, 54–58.

Lindroth, A.M., Park, Y.J., McLean, C.M., Dokshin, G.A., Persson, J.M., Herman, H., Pasini, D., Miró, X., Donohoe, M.E., Lee, J.T., et al. (2008). Antagonism between DNA and H3K27 methylation at the imprinted Rasgrf1 locus. PLoS Genet *4*, e1000145.

Lipson, E.J., and Drake, C.G. (2011). Ipilimumab: an anti-CTLA-4 antibody for metastatic melanoma. Clin. Cancer Res. *17*, 6958–6962.

Lito, P., Pratilas, C.A., Joseph, E.W., Tadi, M., Halilovic, E., Zubrowski, M., Huang, A., Wong, W.L., Callahan, M.K., Merghoub, T., et al. (2012). Relief of profound feedback inhibition of mitogenic signaling by RAF inhibitors attenuates their activity in BRAFV600E melanomas. Cancer Cell *22*, 668–682.

Liu, G., Bollig-Fischer, A., Kreike, B., van de Vijver, M.J., Abrams, J., Ethier, S.P., and Yang, Z.-Q. (2009). Genomic amplification and oncogenic properties of the GASC1 histone demethylase gene in breast cancer. Oncogene *28*, 4491–4500.

Liu, T.-P., Lo, H.-L., Wei, L.-S., Hao-Yun Hsiao, H., and Yang, P.-M. (2015). S-Adenosyl-L-methionine-competitive inhibitors of the histone methyltransferase EZH2 induce autophagy and enhance drug sensitivity in cancer cells. Anticancer Drugs *26*, 139–147.

Liu, W., Stein, P., Cheng, X., Yang, W., Shao, N.-Y., Morrisey, E.E., Schultz, R.M., and You, J. (2014). BRD4 regulates Nanog expression in mouse embryonic stem cells and preimplantation embryos. Cell Death Differ. *21*, 1950–1960.

Lo, J.A., and Fisher, D.E. (2014). The melanoma revolution: from UV carcinogenesis to a new era in therapeutics. Science *346*, 945–949.

Loenen, W.A.M. (2006). S-adenosylmethionine: jack of all trades and master of everything? Biochem. Soc. Trans. *34*, 330–333.

Lohr, J.G., Stojanov, P., Lawrence, M.S., Auclair, D., Chapuy, B., Sougnez, C., Cruz-Gordillo, P., Knoechel, B., Asmann, Y.W., Slager, S.L., et al. (2012). Discovery and prioritization of somatic mutations in diffuse large B-cell lymphoma (DLBCL) by whole-exome sequencing. Proc Natl Acad Sci USA *109*, 3879–3884.

Lomuto, M., Calabrese, P., and Giuliani, A. (2004). Prognostic signs in melanoma: state of the art. J. Eur. Acad. Dermatol. Venereol. *18*, 291–300.

Long, G.V., Stroyakovskiy, D., Gogas, H., Levchenko, E., de Braud, F., Larkin, J., Garbe, C., Jouary, T., Hauschild, A., Grob, J.-J., et al. (2014). Combined BRAF and MEK inhibition versus BRAF inhibition alone in melanoma. N. Engl. J. Med. *371*, 1877–1888.

Lovén, J., Hoke, H.A., Lin, C.Y., Lau, A., Orlando, D.A., Vakoc, C.R., Bradner, J.E., Lee, T.I., and Young, R.A. (2013). Selective Inhibition of Tumor Oncogenes by Disruption of Super-Enhancers. Cell *153*, 320–334.

Luger, K., Mäder, A.W., Richmond, R.K., Sargent, D.F., and Richmond, T.J. (1997). Crystal structure of the nucleosome core particle at 2.8 A resolution. Nature *389*, 251–260.

Luo, C., Merz, P.R., Chen, Y., Dickes, E., Pscherer, A., Schadendorf, D., and Eichmüller, S.B. (2013). MiR-101 inhibits melanoma cell invasion and proliferation by targeting MITF and EZH2. Cancer Lett. *341*, 240–247.

Luo, C., Tetteh, P.W., Merz, P.R., Dickes, E., Abukiwan, A., Hotz-Wagenblatt, A., Holland-Cunz, S., Sinnberg, T., Schittek, B., Schadendorf, D., et al. (2012a). miR-137 Inhibits the Invasion of Melanoma Cells through Downregulation of Multiple Oncogenic Target Genes. J. Invest. Dermatol. *133*, 768–775.

Luo, Y., Dallaglio, K., Chen, Y., Robinson, W.A., Robinson, S.E., McCarter, M.D., Wang, J., Gonzalez, R., Thompson, D.C., Norris, D.A., et al. (2012b). ALDH1A isozymes are markers of human melanoma stem cells and potential therapeutic targets. Stem Cells *30*, 2100–2113.

Lyon, V.B. (2010). Congenital melanocytic nevi. Pediatr. Clin. North Am. *57*, 1155–1176.

Lu, C., and Thompson, C.B. (2012). Metabolic regulation of epigenetics. Cell Metab. *16*, 9–17.

Madhunapantula, S.V., and Robertson, G.P. (2009). The PTEN-AKT3 signaling cascade as a therapeutic target in melanoma. Pigment Cell & Melanoma Research *22*, 400–419.

Madore, J., Vilain, R.E., Menzies, A.M., Kakavand, H., Wilmott, J.S., Hyman, J., Yearley, J.H., Kefford, R.F., Thompson, J.F., Long, G.V., et al. (2014). PD-L1 expression in melanoma shows marked heterogeneity within and between patients: implications for anti-PD-1/PD-L1 clinical trials. Pigment Cell & Melanoma Research, doi:10.1111/pcmr.12340.

Maecker, H.L., Yun, Z., Maecker, H.T., and Giaccia, A.J. (2002). Epigenetic changes in tumor Fas levels determine immune escape and response to therapy. Cancer Cell *2*, 139–148.

Maelandsmo, G.M., Holm, R., Nesland, J.M., Fodstad, O., and Florenes, V.A. (2003). Reduced beta-catenin expression in the cytoplasm of advanced-stage superficial spreading malignant melanoma. Clin. Cancer Res. *9*, 3383–3388.

Maertens, O., Johnson, B., Hollstein, P., Frederick, D.T., Cooper, Z.A., Messiaen, L., Bronson, R.T., McMahon, M., Granter, S., Flaherty, K., et al. (2013). Elucidating distinct roles for NF1 in melanomagenesis. Cancer Discovery *3*, 338–349.

Magner, W.J., Kazim, A.L., Stewart, C., Romano, M.A., Catalano, G., Grande, C., Keiser, N., Santaniello, F., and Tomasi, T.B. (2000). Activation of MHC class I, II, and CD40 gene expression by histone deacetylase inhibitors. J. Immunol. *165*, 7017–7024.

Maison, C., Bailly, D., Peters, A.H.F.M., Quivy, J.-P., Roche, D., Taddei, A., Lachner, M., Jenuwein, T., and Almouzni, G. (2002). Higher-order structure in pericentric heterochromatin involves a distinct pattern of histone modification and an RNA component. Nat. Genet. *30*, 329–334.

Majer, C.R., Jin, L., Scott, M.P., Knutson, S.K., Kuntz, K.W., Keilhack, H., Smith, J.J., Moyer, M.P., Richon, V.M., Copeland, R.A., et al. (2012). A687V EZH2 is a gain-of-function mutation found in lymphoma patients. FEBS Lett. *586*, 3448–3451.

Makishima, H., Jankowska, A.M., Tiu, R.V., Szpurka, H., Sugimoto, Y., Hu, Z., Sauntharajah, Y., Guinta, K., Keddache, M.A., Putnam, P., et al. (2010). Novel homo- and hemizygous mutations in EZH2 in myeloid malignancies. Leukemia *24*, 1799–1804.

Manning, C.S., Hooper, S., and Sahai, E.A. (2014). Intravital imaging of SRF and Notch signalling identifies a key role for EZH2 in invasive melanoma cells. Oncogene, doi:10.1038/onc.2014.362.

Manning, J., Indrova, M., Lubyova, B., Pribylova, H., Bieblova, J., Hejnar, J., Simova, J., Jandlova, T., Bubenik, J., and Reinis, M. (2008). Induction of MHC class I molecule cell surface expression and epigenetic activation of antigen-processing machinery components in a murine model for human papilloma virus 16-associated tumours. Immunology *123*, 218–227.

Margolin, K.A., Rayner, A.A., Hawkins, M.J., Atkins, M.B., Dutcher, J.P., Fisher, R.I., Weiss, G.R., Doroshow, J.H., Jaffe, H.S., and Roper, M. (1989). Interleukin-2 and lymphokine-activated killer cell therapy of solid tumors: analysis of toxicity and management guidelines. J. Clin. Oncol. *7*, 486–498.

Margueron, R., Justin, N., Ohno, K., Sharpe, M.L., Son, J., Drury, W.J., Voigt, P., Martin, S.R., Taylor, W.R., De Marco, V., et al. (2009). Role of the polycomb protein EED in the propagation of repressive histone marks. Nature *461*, 762–767.

Marine, J.-C., and Jochemsen, A.G. (2005). Mdmx as an essential regulator of p53 activity. Biochem. Biophys. Res. Commun. *331*, 750–760.

Martins-Taylor, K., Schroeder, D.I., LaSalle, J.M., Lalande, M., and Xu, R.-H. (2012). Role of DNMT3B in the regulation of early neural and neural crest specifiers. Epigenetics *7*, 71–82.

Mayer, T.C. (1973). The migratory pathway of neural crest cells into the skin of mouse embryos. Dev. Biol. *34*, 39–46.

Mayes, D.A., Rizvi, T.A., Cancelas, J.A., Kolasinski, N.T., Ciraolo, G.M., Stemmer-Rachamimov, A.O., and Ratner, N. (2011). Perinatal or Adult Nf1 Inactivation Using Tamoxifen-Inducible PlpCre Each Cause Neurofibroma Formation. Cancer Res. *71*, 4675–4685.

McCabe, M.T., Graves, A.P., Ganji, G., Diaz, E., Halsey, W.S., Jiang, Y., Smitheman, K.N., Ott, H.M., Pappalardi, M.B., Allen, K.E., et al. (2012a). Mutation of A677 in histone methyltransferase EZH2 in human B-cell lymphoma promotes hypertrimethylation of histone H3 on lysine 27 (H3K27). Proc. Natl. Acad. Sci. USA *109*, 2989–2994.

McCabe, M.T., Ott, H.M., Ganji, G., Korenchuk, S., Thompson, C., Van Aller, G.S., Liu, Y., Graves, A.P., Pietra, Della, A., Diaz, E., et al. (2012b). EZH2 inhibition as a therapeutic strategy for lymphoma with EZH2-activating mutations. Nature *492*, 108–112.

McHugh, J.B., Fullen, D.R., Ma, L., Kleer, C.G., and Su, L.D. (2007). Expression of polycomb group protein EZH2 in nevi and melanoma. J. Cutan. Pathol. *34*, 597–600.

McKenzie, I.A., Biernaskie, J., Toma, J.G., Midha, R., and Miller, F.D. (2006). Skin-derived precursors generate myelinating Schwann cells for the injured and dysmyelinated nervous system. J. Neurosci. *26*, 6651–6660.

McKeown, S.J., Stamp, L., Hao, M.M., and Young, H.M. (2013). Hirschsprung disease: a developmental disorder of the enteric nervous system. Wiley Interdiscip. Rev. Dev. Biol. *2*, 113–129.

McLaughlin, C.C., Wu, X.-C., Jemal, A., Martin, H.J., Roche, L.M., and Chen, V.W. (2005). Incidence of noncutaneous melanomas in the U.S. Cancer *103*, 1000–1007.

Mejetta, S., Morey, L., Pascual, G., Kuebler, B., Mysliwiec, M.R., Lee, Y., Shiekhattar, R., Di Croce, L., and Benitah, S.A. (2011). Jarid2 regulates mouse epidermal stem cell activation and differentiation. Embo J. *30*, 3635–3646.

Menon, D.R., Das, S., Krepler, C., Vultur, A., Rinner, B., Schauer, S., Kashofer, K., Wagner, K., Zhang, G., Bonyadi Rad, E., et al. (2014). A stress-induced early innate response causes multidrug tolerance in melanoma. Oncogene, doi:10.1038/onc.2014.372.

Menon, D.R., Wels, C., Bonyadi Rad, E., Joshi, S., Knausz, H., Lade-Keller, J., Brandner, J.M., and Schaider, H. (2013). TGF-β1 and TNF-α differentially regulate Twist1 mediated resistance towards BRAF/MEK inhibition in melanoma. Pigment Cell & Melanoma Research *26*, 912–916.

Meshorer, E., Yellajoshula, D., George, E., Scambler, P.J., Brown, D.T., and Misteli, T. (2006). Hyperdynamic plasticity of chromatin proteins in pluripotent embryonic stem cells. Dev. Cell *10*, 105–116.

Messiaen, L.M., Callens, T., Mortier, G., Beysen, D., Vandenbroucke, I., Van Roy, N., Speleman, F., and Paepe, A.D. (2000). Exhaustive mutation analysis of the NF1 gene allows identification of 95% of mutations and reveals a high frequency of unusual splicing defects. Hum. Mutat. *15*, 541–555.

Mete, O., Bilgic, B., and Buyukbabani, N. (2010). A tumor with many faces: metastatic malignant melanoma with extensive cartilaginous differentiation. Int. J. Surg. Pathol. *18*, 217–218.

Meyer, C., Sevko, A., Ramacher, M., Bazhin, A.V., Falk, C.S., Osen, W., Borrello, I., Kato, M., Schadendorf, D., Baniyash, M., et al. (2011). Chronic inflammation promotes myeloid-derived suppressor cell activation blocking antitumor immunity in transgenic mouse melanoma model. Proc. Natl. Acad. Sci. USA *108*, 17111–17116.

Mica, Y., Lee, G., Chambers, S.M., Tomishima, M.J., and Studer, L. (2013). Modeling neural crest induction, melanocyte specification, and disease-related pigmentation defects in hESCs and patient-specific iPSCs. Cell Rep. *3*, 1140–1152.

Michaloglou, C., Vredeveld, L.C.W., Soengas, M.S., Denoyelle, C., Kuilman, T., van der Horst, C.M.A.M., Majoor, D.M., Shay, J.W., Mooi, W.J., and Peeper, D.S. (2005). BRAFE600-associated senescence-like cell cycle arrest of human naevi. Nature *436*, 720–724.

Mihajlovic, M., Vlajkovic, S., Jovanovic, P., and Stefanovic, V. (2012). Primary mucosal melanomas: a comprehensive review. Int. J. Clin. Exp. Pathol. *5*, 739–753.

Mikkelsen, T.S., Ku, M., Jaffe, D.B., Issac, B., Lieberman, E., Giannoukos, G., Alvarez, P., Brockman, W., Kim, T.-K., Koche, R.P., et al. (2007). Genome-wide maps of chromatin state in pluripotent and lineage-committed cells. Nature *448*, 553–560.

Milagre, C., Dhomen, N., Geyer, F.C., Hayward, R., Lambros, M., Reis-Filho, J.S., and Marais, R. (2010). A mouse model of melanoma driven by oncogenic KRAS. Cancer Res. *70*, 5549–5557.

Miller, S.J., Jessen, W.J., Mehta, T., Hardiman, A., Sites, E., Kaiser, S., Jegga, A.G., Li, H., Upadhyaya, M., Giovannini, M., et al. (2009). Integrative genomic analyses of neurofibromatosis tumours identify SOX9 as a biomarker and survival gene. EMBO Mol. Med. *1*, 236–248.

Miller, S.J., Rangwala, F., Williams, J., Ackerman, P., Kong, S., Jegga, A.G., Kaiser, S., Aronow, B.J., Frahm, S., Kluwe, L., et al. (2006). Large-scale molecular comparison of human schwann cells to malignant peripheral nerve sheath tumor cell lines and tissues. Cancer Res. *66*, 2584–2591.

Min, J., Zaslavsky, A., Fedele, G., McLaughlin, S.K., Reczek, E.E., De Raedt, T., Guney, I., Strochlic, D.E., Macconaill, L.E., Beroukhim, R., et al. (2010). An oncogene-tumor suppressor cascade drives metastatic prostate cancer by coordinately activating Ras and nuclear factor-kappaB. Nat. Med. *16*, 286–294.

Miura, S., Maesawa, C., Shibazaki, M., Yasuhira, S., Kasai, S., Tsunoda, K., Maeda, F., Takahashi, K., Akasaka, T., and Masuda, T. (2014). Immunohistochemistry for histone h3 lysine 9 methyltransferase and demethylase proteins in human melanomas. The American Journal of Dermatopathology *36*, 211–216.

Mochizuki-Kashio, M., Mishima, Y., Miyagi, S., Negishi, M., Saraya, A., Konuma, T., Shinga, J., Koseki, H., and Iwama, A. (2011). Dependency on the polycomb gene Ezh2 distinguishes fetal from adult hematopoietic stem cells. Blood *118*, 6553–6561.

Mohamed, A., Gonzalez, R.S., Lawson, D., Wang, J., and Cohen, C. (2013). SOX10 expression in malignant melanoma, carcinoma, and normal tissues. Appl. Immunohistochem. Mol. Morphol. *21*, 506–510.

Mohammad, K.S., Javelaud, D., Fournier, P.G.J., Niewolna, M., McKenna, C.R., Peng, X.H., Duong, V., Dunn, L.K., Mauviel, A., and Guise, T.A. (2011). TGF- -RI Kinase Inhibitor SD-208 Reduces the Development and Progression of Melanoma Bone Metastases. Cancer Res. *71*, 175–184.

Mohan, M., Herz, H.-M., and Shilatifard, A. (2012). SnapShot: Histone Lysine Methylase Complexes. Cell *149*, 498–498.e1.

Molognoni, F., Cruz, A.T., Meliso, F.M., Morais, A.S., Souza, C.F., Xander, P., Bischof, J.M., Costa, F.F., Soares, M.B., Liang, G., et al. (2011). Epigenetic reprogramming as a key contributor to melanocyte malignant transformation. Epigenetics *6*, 450–464.

Montagut, C., Sharma, S.V., Shioda, T., McDermott, U., Ulman, M., Ulkus, L.E., Dias-Santagata, D., Stubbs, H., Lee, D.Y., Singh, A., et al. (2008). Elevated CRAF as a potential mechanism of acquired resistance to BRAF inhibition in melanoma. Cancer Res. *68*, 4853–4861.

Montgomery, R.L., Davis, C.A., Potthoff, M.J., Haberland, M., Fielitz, J., Qi, X., Hill, J.A., Richardson, J.A., and Olson, E.N. (2007). Histone deacetylases 1 and 2 redundantly regulate cardiac morphogenesis, growth, and contractility. Genes Dev. *21*, 1790–1802.

Monzani, E., Facchetti, F., Galmozzi, E., Corsini, E., Benetti, A., Cavazzin, C., Gritti, A., Piccinini, A., Porro, D., Santinami, M., et al. (2007). Melanoma contains CD133 and ABCG2 positive cells with enhanced tumourigenic potential. Eur. J. Cancer *43*, 935–946.

Morgan, R.A., Dudley, M.E., Wunderlich, J.R., Hughes, M.S., Yang, J.C., Sherry, R.M., Royal, R.E., Topalian, S.L., Kammula, U.S., Restifo, N.P., et al. (2006). Cancer regression in patients after transfer of genetically engineered lymphocytes. Science *314*, 126–129.

Mori-Akiyama, Y., Akiyama, H., Rowitch, D.H., and de Crombrugghe, B. (2003). Sox9 is required for determination of the chondrogenic cell lineage in the cranial neural crest. Proc. Natl. Acad. Sci. USA *100*, 9360–9365.

Morin, R.D., Johnson, N.A., Severson, T.M., Mungall, A.J., An, J., Goya, R., Paul, J.E., Boyle, M., Woolcock, B.W., Kuchenbauer, F., et al. (2010). Somatic mutations altering EZH2 (Tyr641) in follicular and diffuse large B-cell lymphomas of germinal-center origin. Nat. Genet. *42*, 181–185.

Morin, R.D., Mendez-Lago, M., Mungall, A.J., Goya, R., Mungall, K.L., Corbett, R.D., Johnson, N.A., Severson, T.M., Chiu, R., Field, M., et al. (2011). Frequent mutation of histone-modifying genes in non-Hodgkin lymphoma. Nature *476*, 298–303.

Morris, E.J., Jha, S., Restaino, C.R., Dayananth, P., Zhu, H., Cooper, A., Carr, D., Deng, Y., Jin, W., Black, S., et al. (2013). Discovery of a novel ERK inhibitor with activity in models of acquired resistance to BRAF and MEK inhibitors. Cancer Discovery *3*, 742–750.

Morrison, S.J., White, P.M., Zock, C., and Anderson, D.J. (1999). Prospective identification, isolation by flow cytometry, and in vivo self-renewal of multipotent mammalian neural crest stem cells. Cell *96*, 737–749.

Moustakas, A., and Heldin, C.-H. (2009). The regulation of TGFbeta signal transduction. Development *136*, 3699–3714.

Mrugala, M.M., Batchelor, T.T., and Plotkin, S.R. (2005). Peripheral and cranial nerve sheath tumors. Curr. Opin. Neurol. *18*, 604–610.

Musselman, C.A., Lalonde, M.-E., Cote, J., and Kutateladze, T.G. (2012). Perceiving the epigenetic landscape through histone readers. Nat. Struct. Mol. Biol. *19*, 1218–1227.

Muthusamy, V., Hobbs, C., Nogueira, C., Cordón-Cardo, C., McKee, P.H., Chin, L., and Bosenberg, M.W. (2006). Amplification of CDK4 and MDM2 in malignant melanoma. Genes Chromosomes Cancer *45*, 447–454.

Müller, J., Krijgsman, O., Tsoi, J., Robert, L., Hugo, W., Song, C., Kong, X., Possik, P.A., Cornelissen-Steijger, P.D.M., Foppen, M.H.G., et al. (2014). Low MITF/AXL ratio predicts early resistance to multiple targeted drugs in melanoma. Nat. Commun. *5*, 5712.

Müller, J., Hart, C.M., Francis, N.J., Vargas, M.L., Sengupta, A., Wild, B., Miller, E.L., O'Connor, M.B., Kingston, R.E., and Simon, J.A. (2002). Histone methyltransferase activity of a Drosophila Polycomb group repressor complex. Cell *111*, 197–208.

Nagashimada, M., Ohta, H., Li, C., Nakao, K., Uesaka, T., Brunet, J.-F., Amiel, J., Trochet, D., Wakayama, T., and Enomoto, H. (2012). Autonomic neurocristopathy-associated mutations in PHOX2B dysregulate Sox10 expression. J. Clin. Invest. *122*, 3145–3158.

Nagoshi, N., Shibata, S., Kubota, Y., Nakamura, M., Nagai, Y., Satoh, E., Morikawa, S., Okada, Y., Mabuchi, Y., Katoh, H., et al. (2008). Ontogeny and multipotency of neural crest-derived stem cells in mouse bone marrow, dorsal root ganglia, and whisker pad. Cell Stem Cell *2*, 392–403.

Nazarian, R., Shi, H., Wang, Q., Kong, X., Koya, R.C., Lee, H., Chen, Z., Lee, M.-K., Attar, N., Sazegar, H., et al. (2010a). Melanomas acquire resistance to B-RAF(V600E) inhibition by RTK or N-RAS upregulation. Nature *468*, 973–977.

Nazarian, R.M., Prieto, V.G., Elder, D.E., and Duncan, L.M. (2010b). Melanoma biomarker expression in melanocytic tumor progression: a tissue microarray study. J. Cutan. Pathol. *37 Suppl. 1*, 41–47.

Nelms, B.L., and Labosky, P.A. (2010). Transcriptional Control of Neural Crest Development (San Rafael (CA): Morgan & Claypool Life Sciences).

Neo, W.H., Lim, J.F., Grumont, R., Gerondakis, S., and Su, I.-H. (2014a). c-Rel regulates Ezh2 expression in activated lymphocytes and malignant lymphoid cells. J. Biol. Chem. *289*, 31693–31707.

Neo, W.H., Yap, K., Lee, S.H., Looi, L.S., Khandelia, P., Neo, S.X., Makeyev, E.V., and Su, I.-H. (2014b). MicroRNA miR-124 Controls the Choice between Neuronal and Astrocyte Differentiation by Fine-tuning Ezh2 Expression. J. Biol. Chem. *289*, 20788–20801.

Nguyen, T., Kuo, C., Nicholl, M.B., Sim, M.-S., Turner, R.R., Morton, D.L., and Hoon, D.S.B. (2011). Downregulation of microRNA-29c is associated with hypermethylation of tumor-related genes and disease outcome in cutaneous melanoma. Epigenetics *6*, 388–394.

Nicodeme, E., Jeffrey, K.L., Schaefer, U., Beinke, S., Dewell, S., Chung, C.-W., Chandwani, R., Marazzi, I., Wilson, P., Coste, H., et al. (2010). Suppression of inflammation by a synthetic histone mimic. Nature *468*, 1119–1123.

Nielsen, G.P., Stemmer-Rachamimov, A.O., Ino, Y., Moller, M.B., Rosenberg, A.E., and Louis, D.N. (1999). Malignant transformation of neurofibromas in neurofibromatosis 1 is associated with CDKN2A/p16 inactivation. Am. J. Pathol. *155*, 1879–1884.

Nikoloski, G., Langemeijer, S.M.C., Kuiper, R.P., Knops, R., Massop, M., Tönnissen, E.R.L.T.M., van der Heijden, A., Scheele, T.N., Vandenberghe, P., de Witte, T., et al. (2010). Somatic mutations of the histone methyltransferase gene EZH2 in myelodysplastic syndromes. Nat. Genet. *42*, 665–667.

Nishikawa, S., Kusakabe, M., Yoshinaga, K., Ogawa, M., Hayashi, S., Kunisada, T., Era, T., Sakakura, T., and Nishikawa, S. (1991). In utero manipulation of coat color formation by a monoclonal anti-c-kit antibody: two distinct waves of c-kit-dependency during melanocyte development. Embo J. *10*, 2111–2118.

Nishimura, E.K., Jordan, S.A., Oshima, H., Yoshida, H., Osawa, M., Moriyama, M., Jackson, I.J., Barrandon, Y., Miyachi, Y., and Nishikawa, S.-I. (2002a). Dominant role of the niche in melanocyte stem-cell fate determination. Nature *416*, 854–860.

Nishimura, E.K., Suzuki, M., Igras, V., Du, J., Lonning, S., Miyachi, Y., Roes, J., Beermann, F., and Fisher, D.E. (2010). Key Roles for Transforming Growth Factor β in Melanocyte Stem Cell Maintenance. Cell Stem Cell *6*, 130–140.

Nishimura, H., Nose, M., Hiai, H., Minato, N., and Honjo, T. (1999). Development of lupus-like autoimmune diseases by disruption of the PD-1 gene encoding an ITIM motif-carrying immunoreceptor. Immunity *11*, 141–151.

Nishimura, K., Nakatsu, F., Kashiwagi, K., Ohno, H., Saito, T., and Igarashi, K. (2002b). Essential role of S-adenosylmethionine decarboxylase in mouse embryonic development. Genes Cells *7*, 41–47.

Nitzan, E., Krispin, S., Pfaltzgraff, E.R., Klar, A., Labosky, P.A., and Kalcheim, C. (2013). A dynamic code of dorsal neural tube genes regulates the segregation between neurogenic and melanogenic neural crest cells. Development *140*, 2269–2279.

Nobori, T., Miura, K., Wu, D.J., Lois, A., Takabayashi, K., and Carson, D.A. (1994). Deletions of the cyclin-dependent kinase-4 inhibitor gene in multiple human cancers. Nature *368*, 753–756.

Nonaka, D., Chiriboga, L., and Rubin, B.P. (2008). Sox10: a pan-schwannian and melanocytic marker. Am. J. Surg. Pathol. *32*, 1291–1298.

Ntziachristos, P., Tsirigos, A., Vlierberghe, P.V., Nedjic, J., Trimarchi, T., Flaherty, M.S., Ferres-Marco, D., da Ros, V., Tang, Z., Siegle, J., et al. (2012). Genetic inactivation of the polycomb repressive complex 2 in T cell acute lymphoblastic leukemia. Nat. Med. *18*, 298–303.

O'Carroll, D., Erhardt, S., Pagani, M., Barton, S.C., Surani, M.A., and Jenuwein, T. (2001). The polycomb-group gene Ezh2 is required for early mouse development. Mol. Cell Biol. *21*, 4330–4336.

O'Reilly, F.M., Brat, D.J., McAlpine, B.E., Grossniklaus, H.E., Folpe, A.L., and Arbiser, J.L. (2001). Microphthalmia transcription factor immunohistochemistry: a useful diagnostic marker in the diagnosis and detection of cutaneous melanoma, sentinel lymph node metastases, and extracutaneous melanocytic neoplasms. Journal of American Dermatology *45*, 414–419.

Offermanns, S., Zhao, L.P., Gohla, A., Sarosi, I., Simon, M.I., and Wilkie, T.M. (1998). Embryonic cardiomyocyte hypoplasia and craniofacial defects in G alpha q/G alpha 11-mutant mice. Embo J. *17*, 4304–4312.

Okano, M., Bell, D.W., Haber, D.A., and Li, E. (1999). DNA methyltransferases Dnmt3a and Dnmt3b are essential for de novo methylation and mammalian development. Cell *99*, 247–257.

Okano, M., Xie, S., and Li, E. (1998). Cloning and characterization of a family of novel mammalian DNA (cytosine-5) methyltransferases. Nat. Genet. *19*, 219–220.

Okosun, J., Bödör, C., Wang, J., Araf, S., Yang, C.-Y., Pan, C., Boller, S., Cittaro, D., Bozek, M., Iqbal, S., et al. (2014). Integrated genomic analysis identifies recurrent mutations and evolution patterns driving the initiation and progression of follicular lymphoma. Nat. Genet. *46*, 176–181.

Okroj, M., Österborg, A., and Blom, A.M. (2013). Effector mechanisms of anti-CD20 monoclonal antibodies in B cell malignancies. Cancer Treat. Rev. *39*, 632–639.

Oktyabri, D., Tange, S., Terashima, M., Ishimura, A., and Suzuki, T. (2014). EED regulates epithelial-mesenchymal transition of cancer cells induced by TGF-β. Biochem. Biophys. Res. Commun. *453*, 124–130.

O'Meara, M.M., and Simon, J.A. (2012). Inner workings and regulatory inputs that control Polycomb repressive complex 2. Chromosoma *121*, 221–234.

Omholt, K., Platz, A., Ringborg, U., and Hansson, J. (2001). Cytoplasmic and nuclear accumulation of beta-catenin is rarely caused by CTNNB1 exon 3 mutations in cutaneous malignant melanoma. Int. J. Cancer *92*, 839–842.

Omholt, K., Karsberg, S., Platz, A., Kanter, L., Ringborg, U., and Hansson, J. (2002). Screening of N-ras codon 61 mutations in paired primary and metastatic cutaneous melanomas: mutations occur early and persist throughout tumor progression. Clin. Cancer Res. *8*, 3468–3474.

Omholt, K., Platz, A., Kanter, L., Ringborg, U., and Hansson, J. (2003). NRAS and BRAF mutations arise early during melanoma pathogenesis and are preserved throughout tumor progression. Clin. Cancer Res. *9*, 6483–6488.

Opdecamp, K., Nakayama, A., Nguyen, M.T., Hodgkinson, C.A., Pavan, W.J., and Arnheiter, H. (1997). Melanocyte development in vivo and in neural crest cell cultures: crucial dependence on the Mitf basic-helix-loop-helix-zipper transcription factor. Development *124*, 2377–2386.

Ortonne, J.P., Schmitt, D., and Thivolet, J. (1980). PUVA-induced repigmentation of vitiligo: scanning electron microscopy of hair follicles. J. Invest. Dermatol. *74*, 40–42.

Orzan, F., Pellegatta, S., Poliani, P.L., Pisati, F., Caldera, V., Menghi, F., Kapetis, D., Marras, C., Schiffer, D., and Finocchiaro, G. (2011). Enhancer of Zeste 2 (EZH2) is up-regulated in malignant gliomas and in glioma stem-like cells. Neuropathol. Appl. Neurobiol. *37*, 381–394.

Osawa, M., Egawa, G., Mak, S.-S., Moriyama, M., Freter, R., Yonetani, S., Beermann, F., and Nishikawa, S.-I. (2005). Molecular characterization of melanocyte stem cells in their niche. Development *132*, 5589–5599.

Oshimori, N., Oristian, D., and Fuchs, E. (2015). TGF-b Promotes Heterogeneity and Drug Resistance in Squamous Cell Carcinoma. Cell *160*, 963–976.

Ott, C.J., Kopp, N., Bird, L., Paranal, R.M., Qi, J., Bowman, T., Rodig, S.J., Kung, A.L., Bradner, J.E., and Weinstock, D.M. (2012). BET bromodomain inhibition targets both c-Myc and IL7R in high-risk acute lymphoblastic leukemia. Blood *120*, 2843–2852.

Ott, H.M., Graves, A.P., Pappalardi, M.B., Huddleston, M., Halsey, W.S., Hughes, A.M., Groy, A., Dul, E., Jiang, Y., Bai, Y., et al. (2014). A687V EZH2 Is a Driver of Histone H3 Lysine 27 (H3K27) Hypertrimethylation. Mol. Cancer Ther. *13*, 3062–3073.

Ougolkov, A.V., Bilim, V.N., and Billadeau, D.D. (2008). Regulation of pancreatic tumor cell proliferation and chemoresistance by the histone methyltransferase enhancer of zeste homologue 2. Clin. Cancer Res. *14*, 6790–6796.

Overwijk, W.W., Tsung, A., Irvine, K.R., Parkhurst, M.R., Goletz, T.J., Tsung, K., Carroll, M.W., Liu, C., Moss, B., Rosenberg, S.A., et al. (1998). gp100/pmel 17 is a murine tumor rejection antigen: induction of "self-"reactive, tumoricidal T cells using high-affinity, altered peptide ligand. J. Exp. Med. *188*, 277–286.

Pan, G., Tian, S., Nie, J., Yang, C., Ruotti, V., Wei, H., Jonsdottir, G.A., Stewart, R., and Thomson, J.A. (2007). Whole-genome analysis of histone H3 lysine 4 and lysine 27 methylation in human embryonic stem cells. Cell Stem Cell *1*, 299–312.

Paraiso, K.H.T., Xiang, Y., Rebecca, V.W., Abel, E.V., Chen, Y.A., Munko, A.C., Wood, E., Fedorenko, I.V., Sondak, V.K., Anderson, A.R.A., et al. (2011). PTEN loss confers BRAF inhibitor resistance to melanoma cells through the suppression of BIM expression. Cancer Res. *71*, 2750–2760.

Paratore, C., Goerich, D.E., Suter, U., Wegner, M., and Sommer, L. (2001). Survival and glial fate acquisition of neural crest cells are regulated by an interplay between the transcription factor Sox10 and extrinsic combinatorial signaling. Development *128*, 3949–3961.

Paratore, C., Eichenberger, C., Suter, U., and Sommer, L. (2002). Sox10 haploinsufficiency affects maintenance of progenitor cells in a mouse model of Hirschsprung disease. Hum. Mol. Genet. *11*, 3075–3085.

Pardoll, D.M. (2012). The blockade of immune checkpoints in cancer immunotherapy. Nat. Rev. Cancer *12*, 252–264.

Parente J.D., Labareda, J.M.P.D.S., Bártolo, E.A.F.L.F., Santos, M.F.S.P.F., and Vale, E.M.S.D. (2013). Cartilaginous melanoma: case report and review of the literature. An. Bras. Dermatol. *88*, 403–407.

Park, M.H., Nishimura, K., Zanelli, C.F., and Valentini, S.R. (2010). Functional significance of eIF5A and its hypusine modification in eukaryotes. Amino Acids *38*, 491–500.

Pasini, D., Bracken, A.P., Hansen, J.B., Capillo, M., and Helin, K. (2007). The polycomb group protein Suz12 is required for embryonic stem cell differentiation. Mol. Cell Biol. *27*, 3769–3779.

Pasini, D., Bracken, A.P., Jensen, M.R., Lazzerini Denchi, E., and Helin, K. (2004). Suz12 is essential for mouse development and for EZH2 histone methyltransferase activity. Embo J. *23*, 4061–4071.

Pasini, D., Cloos, P.A.C., Walfridsson, J., Olsson, L., Bukowski, J.-P., Johansen, J.V., Bak, M., Tommerup, N., Rappsilber, J., and Helin, K. (2010). JARID2 regulates binding of the Polycomb repressive complex 2 to target genes in ES cells. Nature *464*, 306–310.

Pastori, C., Daniel, M., Penas, C., Volmar, C.-H., Johnstone, A.L., Brothers, S.P., Graham, R.M., Allen, B., Sarkaria, J.N., Komotar, R.J., et al. (2014). BET bromodomain proteins are required for glioblastoma cell proliferation. Epigenetics *9*, 611–620.

Patel, A.J., Liao, C.-P., Chen, Z., Liu, C., Wang, Y., and Le, L.Q. (2014). BET Bromodomain Inhibition Triggers Apoptosis of NF1-Associated Malignant Peripheral Nerve Sheath Tumors through Bim Induction. Cell Rep. *6*, 81–92.

Pavan, W.J., and Raible, D.W. (2012). Specification of neural crest into sensory neuron and melanocyte lineages. Dev. Biol. *366*, 55–63.

Pedersen, M., Küsters-Vandevelde, H.V.N., Viros, A., Groenen, P.J.T.A., Sanchez-Laorden, B., Gilhuis, J.H., van Engen-van Grunsven, I.A., Renier, W., Schieving, J., Niculescu-Duvaz, I., et al. (2013). Primary melanoma of the CNS in children is driven by congenital expression of oncogenic NRAS in melanocytes. Cancer Discovery *3*, 458–469.

Pedersen, M., Viros, A., Cook, M., and Marais, R. (2014). (G12D) NRAS and kinase-dead BRAF cooperate to drive naevogenesis and melanomagenesis. Pigment Cell & Melanoma Research *27*, 1162–1166.

Pegg, A.E. (2009). Mammalian polyamine metabolism and function. IUBMB Life *61*, 880–894.

Peng, J.C., Valouev, A., Swigut, T., Zhang, J., Zhao, Y., Sidow, A., and Wysocka, J. (2009). Jarid2/Jumonji coordinates control of PRC2 enzymatic activity and target gene occupancy in pluripotent cells. Cell *139*, 1290–1302.

Pereira, J.D., Sansom, S.N., Smith, J., Dobenecker, M.-W., Tarakhovsky, A., and Livesey, F.J. (2010). Ezh2, the histone methyltransferase of PRC2, regulates the balance between self-renewal and differentiation in the cerebral cortex. Proc. Natl. Acad. Sci. USA *107*, 15957–15962.

Pérez-Torras, S., Vidal-Pla, A., Cano-Soldado, P., Huber-Ruano, I., Mazo, A., and Pastor-Anglada, M. (2013). Concentrative nucleoside transporter 1 (hCNT1) promotes phenotypic changes relevant to tumor biology in a translocation-independent manner. Cell Death Dis. *4*, e648.

Peters, A.H., O'Carroll, D., Scherthan, H., Mechtler, K., Sauer, S., Schöfer, C., Weipoltshammer, K., Pagani, M., Lachner, M., Kohlmaier, A., et al. (2001). Loss of the Suv39h histone methyltransferases impairs mammalian heterochromatin and genome stability. Cell *107*, 323–337.

Peters, A.H.F.M., Kubicek, S., Mechtler, K., O'Sullivan, R.J., Derijck, A.A.H.A., Perez-Burgos, L., Kohlmaier, A., Opravil, S., Tachibana, M., Shinkai, Y., et al. (2003). Partitioning and plasticity of repressive histone methylation states in mammalian chromatin. Mol. Cell *12*, 1577–1589.

Pierrat, M.-J., Marsaud, V., Mauviel, A., and Javelaud, D. (2012). Expression of microphthalmia-associated transcription factor (MITF), which is critical for melanoma progression, is inhibited by both transcription factor GLI2 and transforming growth factor-β. J Biol Chem *287*, 17996–18004.

Piliang, M.P. (2011). Acral lentiginous melanoma. Clin. Lab. Med. *31*, 281–288.

Pingault, V., Bondurand, N., Kuhlbrodt, K., Goerich, D.E., Préhu, M.O., Puliti, A., Herbarth, B., Hermans-Borgmeyer, I., Legius, E., Matthijs, G., et al. (1998). SOX10 mutations in patients with Waardenburg-Hirschsprung disease. Nat. Genet. *18*, 171–173.

Pingault, V., Ente, D., Dastot-Le Moal, F., Goossens, M., Marlin, S., and Bondurand, N. (2010). Review and update of mutations causing Waardenburg syndrome. Hum. Mutat. *31*, 391–406.

Podsypanina, K., Ellenson, L.H., Nemes, A., Gu, J., Tamura, M., Yamada, K.M., Cordon-Cardo, C., Catoretti, G., Fisher, P.E., and Parsons, R. (1999). Mutation of Pten/Mmac1 in mice causes neoplasia in multiple organ systems. Proc. Natl. Acad. Sci. USA *96*, 1563–1568.

Pollock, P.M., Harper, U.L., Hansen, K.S., Yudt, L.M., Stark, M., Robbins, C.M., Moses, T.Y., Hostetter, G., Wagner, U., Kakareka, J., et al. (2003). High frequency of BRAF mutations in nevi. Nat. Genet. *33*, 19–20.

Polsky, D., Bastian, B.C., Hazan, C., Melzer, K., Pack, J., Houghton, A., Busam, K., Cordon-Cardo, C., and Osman, I. (2001). HDM2 protein overexpression, but not gene amplification, is related to tumorigenesis of cutaneous melanoma. Cancer Res. *61*, 7642–7646.

Popov, N., and Gil, J. (2010). Epigenetic regulation of the INK4b-ARF-INK4a locus: in sickness and in health. Epigenetics *5*, 685–690.

Postovit, L.-M., Margaryan, N.V., Seftor, E.A., and Hendrix, M.J.C. (2008). Role of nodal signaling and the microenvironment underlying melanoma plasticity. Pigment Cell & Melanoma Research *21*, 348–357.

Potterf, S.B., Furumura, M., Dunn, K.J., Arnheiter, H., and Pavan, W.J. (2000). Transcription factor hierarchy in Waardenburg syndrome: regulation of MITF expression by SOX10 and PAX3. Hum. Genet. *107*, 1–6.

Potterf, S.B., Mollaaghababa, R., Hou, L., Southard-Smith, E.M., Hornyak, T.J., Arnheiter, H., and Pavan, W.J. (2001). Analysis of SOX10 function in neural crest-derived melanocyte development: SOX10-dependent transcriptional control of dopachrome tautomerase. Dev. Biol. *237*, 245–257.

Poulikakos, P.I., Persaud, Y., Janakiraman, M., Kong, X., Ng, C., Moriceau, G., Shi, H., Atefi, M., Titz, B., Gabay, M.T., et al. (2011). RAF inhibitor resistance is mediated by dimerization of aberrantly spliced BRAF(V600E). Nature *480*, 387–390.

Poulikakos, P.I., Zhang, C., Bollag, G., Shokat, K.M., and Rosen, N. (2010). RAF inhibitors transactivate RAF dimers and ERK signalling in cells with wild-type BRAF. Nature *464*, 427–430.

Pradhan, S., Bacolla, A., Wells, R.D., and Roberts, R.J. (1999). Recombinant human DNA (cytosine-5) methyltransferase. I. Expression, purification, and comparison of de novo and maintenance methylation. J. Biol. Chem. *274*, 33002–33010.

Prieto, P.A., Yang, J.C., Sherry, R.M., Hughes, M.S., Kammula, U.S., White, D.E., Levy, C.L., Rosenberg, S.A., and Phan, G.Q. (2012). CTLA-4 blockade with ipilimumab: long-term follow-up of 177 patients with metastatic melanoma. Clin. Cancer Res. *18*, 2039–2047.

Pugh, T.J., Weeraratne, S.D., Archer, T.C., Pomeranz Krummel, D.A., Auclair, D., Bochicchio, J., Carneiro, M.O., Carter, S.L., Cibulskis, K., Erlich, R.L., et al. (2012). Medulloblastoma exome sequencing uncovers subtype-specific somatic mutations. Nature *488*, 106–110.

Puissant, A., Frumm, S.M., Alexe, G., Bassil, C.F., Qi, J., Chanthery, Y.H., Nekritz, E.A., Zeid, R., Gustafson, W.C., Greninger, P., et al. (2013). Targeting MYCN in Neuroblastoma by BET Bromodomain Inhibition. Cancer Discovery *3*, 308–323.

Qi, W., Chan, H., Teng, L., Li, L., Chuai, S., Zhang, R., Zeng, J., Li, M., Fan, H., Lin, Y., et al. (2012). Selective inhibition of Ezh2 by a small molecule inhibitor blocks tumor cells proliferation. Proc. Natl. Acad. Sci. USA *109*, 21360–21365.

Qin, T., Jelinek, J., Si, J., Shu, J., and Issa, J.-P.J. (2009). Mechanisms of resistance to 5-aza-2'-deoxycytidine in human cancer cell lines. Blood *113*, 659–667.

Qu, X., Shen, L., Zheng, Y., Cui, Y., Feng, Z., Liu, F., and Liu, J. (2014). A signal transduction pathway from TGF-β1 to SKP2 via Akt1 and c-Myc and its correlation with progression in human melanoma. J. Invest. Dermatol. *134*, 159–167.

Quail, D.F., and Joyce, J.A. (2013). Microenvironmental regulation of tumor progression and metastasis. Nat. Med. *19*, 1423–1437.

Raabe, E.H., Laudenslager, M., Winter, C., Wasserman, N., Cole, K., LaQuaglia, M., Maris, D.J., Mosse, Y.P., and Maris, J.M. (2008). Prevalence and functional consequence of PHOX2B mutations in neuroblastoma. Oncogene *27*, 469–476.

Rabbani, P., Takeo, M., Chou, W., Myung, P., Bosenberg, M., Chin, L., Taketo, M.M., and Ito, M. (2011). Coordinated activation of Wnt in epithelial and melanocyte stem cells initiates pigmented hair regeneration. Cell *145*, 941–955.

Rajakulendran, T., Sahmi, M., Lefrançois, M., Sicheri, F., and Therrien, M. (2009). A dimerization-dependent mechanism drives RAF catalytic activation. Nature *461*, 542–545.

Rao-Bindal, K., Zhou, Z., and Kleinerman, E.S. (2012). MS-275 sensitizes osteosarcoma cells to Fas ligand-induced cell death by increasing the localization of Fas in membrane lipid rafts. Cell Death Dis. *3*, e369.

Rawles, M.E. (1947). Origin of pigment cells from the neural crest in the mouse embryo. Physiol. Zool. *20*, 248–266.

Rea, S., Eisenhaber, F., O'Carroll, D., Strahl, B.D., Sun, Z.W., Schmid, M., Opravil, S., Mechtler, K., Ponting, C.P., Allis, C.D., et al. (2000). Regulation of chromatin structure by site-specific histone H3 methyltransferases. Nature *406*, 593–599.

Rebecca, V.W., Alicea, G.M., Paraiso, K.H.T., Lawrence, H., Gibney, G.T., and Smalley, K.S.M. (2014). Vertical inhibition of the MAPK pathway enhances therapeutic responses in NRAS-mutant melanoma. Pigment Cell & Melanoma Research *27*, 1154–1158.

Redmer, T., Welte, Y., Behrens, D., Fichtner, I., Przybilla, D., Wruck, W., Yaspo, M.-L., Lehrach, H., Schäfer, R., and Regenbrecht, C.R.A. (2014). The nerve growth factor receptor CD271 is crucial to maintain tumorigenicity and stem-like properties of melanoma cells. PLoS ONE *9*, e92596.

Reik, W. (2007). Stability and flexibility of epigenetic gene regulation in mammalian development. Nature *447*, 425–432.

Ren, J., Chen, Y., Song, H., Chen, L., and Wang, R. (2013). Inhibition of ZEB1 reverses EMT and chemoresistance in docetaxel-resistant human lung adenocarcinoma cell line. J. Cell. Biochem. *114*, 1395–1403.

Restifo, N.P., Marincola, F.M., Kawakami, Y., Taubenberger, J., Yannelli, J.R., and Rosenberg, S.A. (1996). Loss of functional beta 2-microglobulin in metastatic melanomas from five patients receiving immunotherapy. J. Natl. Cancer Inst. *88*, 100–108.

Restifo, N.P., Dudley, M.E., and Rosenberg, S.A. (2012). Adoptive immunotherapy for cancer: harnessing the T cell response. Nat. Rev. Immunol. *12*, 269–281.

Richmond, T.J., and Davey, C.A. (2003). The structure of DNA in the nucleosome core. Nature *423*, 145–150.

Ridolfi, R.L., Rosen, P.P., and Thaler, H. (1977). Nevus cell aggregates associated with lymph nodes: estimated frequency and clinical significance. Cancer *39*, 164–171.

Riising, E.M., Comet, I., Leblanc, B., Wu, X., Johansen, J.V., and Helin, K. (2014). Gene silencing triggers polycomb repressive complex 2 recruitment to CpG islands genome wide. Mol. Cell *55*, 347–360.

Ringrose, L., and Paro, R. (2007). Polycomb/Trithorax response elements and epigenetic memory of cell identity. Development *134*, 223–232.

Robert, C., Karaszewska, B., Schachter, J., Rutkowski, P., Mackiewicz, A., Stroiakovski, D., Lichinitser, M., Dummer, R., Grange, F., Mortier, L., et al. (2015a). Improved overall survival in melanoma with combined dabrafenib and trametinib. N. Engl. J. Med. *372*, 30–39.

Robert, C., Long, G.V., Brady, B., Dutriaux, C., Maio, M., Mortier, L., Hassel, J.C., Rutkowski, P., McNeil, C., Kalinka-Warzocha, E., et al. (2015b). Nivolumab in previously untreated melanoma without BRAF mutation. N. Engl. J. Med. *372*, 320–330.

Robert, C., Thomas, L., Bondarenko, I., O'Day, S., Weber, J., Garbe, C., Lebbe, C., Baurain, J.-F., Testori, A., Grob, J.-J., et al. (2011). Ipilimumab plus dacarbazine for previously untreated metastatic melanoma. N. Engl. J. Med. *364*, 2517–2526.

Roberts, P.J., Usary, J.E., Darr, D.B., Dillon, P.M., Pfefferle, A.D., Whittle, M.C., Duncan, J.S., Johnson, S.M., Combest, A.J., Jin, J., et al. (2012). Combined PI3K/mTOR and MEK inhibition provides broad antitumor activity in faithful murine cancer models. Clin. Cancer Res. *18*, 5290–5303.

Robinson, G., Parker, M., Kranenburg, T.A., Lu, C., Chen, X., Ding, L., Phoenix, T.N., Hedlund, E., Wei, L., Zhu, X., et al. (2012). Novel mutations target distinct subgroups of medulloblastoma. Nature *488*, 43–48.

Robinson, M.D., McCarthy, D.J., and Smyth, G.K. (2010). edgeR: a Bioconductor package for differential expression analysis of digital gene expression data. Bioinformatics *26*, 139–140.

Rodeck, U., Bossler, A., Graeven, U., Fox, F.E., Nowell, P.C., Knabbe, C., and Kari, C. (1994). Transforming growth factor beta production and responsiveness in normal human melanocytes and melanoma cells. Cancer Res. *54*, 575–581.

Rodeck, U., Nishiyama, T., and Mauviel, A. (1999). Independent regulation of growth and SMAD-mediated transcription by transforming growth factor beta in human melanoma cells. Cancer Res. *59*, 547–550.

Roderick, J.E., Tesell, J., Shultz, L.D., Brehm, M.A., Greiner, D.L., Harris, M.H., Silverman, L.B., Sallan, S.E., Gutierrez, A., Look, A.T., et al. (2014). c-Myc inhibition prevents leukemia initiation in mice and impairs the growth of relapsed and induction failure pediatric T-ALL cells. Blood *123*, 1040–1050.

Rodríguez-Paredes, M., and Esteller, M. (2011). Cancer epigenetics reaches mainstream oncology. Nat. Med. *17*, 330–339.

Roesch, A., Becker, B., Meyer, S., Wild, P., Hafner, C., Landthaler, M., and Vogt, T. (2005). Retinoblastoma-binding protein 2-homolog 1: a retinoblastoma-binding protein downregulated in malignant melanomas. Mod. Pathol. *18*, 1249–1257.

Roesch, A., Becker, B., Schneider-Brachert, W., Hagen, I., Landthaler, M., and Vogt, T. (2006). Re-expression of the retinoblastoma-binding protein 2-homolog 1 reveals tumor-suppressive functions in highly metastatic melanoma cells. J. Invest. Dermatol. *126*, 1850–1859.

Roesch, A., Fukunaga-Kalabis, M., Schmidt, E.C., Zabierowski, S.E., Brafford, P.A., Vultur, A., Basu, D., Gimotty, P., Vogt, T., and Herlyn, M. (2010). A Temporarily Distinct Subpopulation of Slow-Cycling Melanoma Cells Is Required for Continuous Tumor Growth. Cell *141*, 583–594.

Roesch, A., Mueller, A.M., Stempfl, T., Moehle, C., Landthaler, M., and Vogt, T. (2008). RBP2-H1/JARID1B is a transcriptional regulator with a tumor suppressive potential in melanoma cells. Int. J. Cancer *122*, 1047–1057.

Roesch, A., Vultur, A., Bogeski, I., Wang, H., Zimmermann, K.M., Speicher, D., Körbel, C., Laschke, M.W., Gimotty, P.A., Philipp, S.E., et al. (2013). Overcoming Intrinsic Multidrug Resistance in Melanoma by Blocking the Mitochondrial Respiratory Chain of Slow-Cycling JARID1B(high) Cells. Cancer Cell *23*, 811–825.

Rosato, R.R., Almenara, J.A., and Grant, S. (2003). The histone deacetylase inhibitor MS-275 promotes differentiation or apoptosis in human leukemia cells through a process regulated by generation of reactive oxygen species and induction of p21CIP1/WAF1 1. Cancer Res. *63*, 3637–3645.

Rosenberg, S.A., Yang, J.C., Sherry, R.M., Kammula, U.S., Hughes, M.S., Phan, G.Q., Citrin, D.E., Restifo, N.P., Robbins, P.F., Wunderlich, J.R., et al. (2011). Durable complete responses in heavily pretreated patients with metastatic melanoma using T-cell transfer immunotherapy. Clin. Cancer Res. *17*, 4550–4557.

Roy, D.M., Walsh, L.A., and Chan, T.A. (2014). Driver mutations of cancer epigenomes. Protein Cell *5*, 265–296.

Rudolph, P., Tronnier, M., Menzel, R., Möller, M., and Parwaresch, R. (1998). Enhanced expression of Ki-67, topoisomerase IIalpha, PCNA, p53 and p21WAF1/Cip1 reflecting proliferation and repair activity in UV-irradiated melanocytic nevi. Human Pathology *29*, 1480–1487.

Ryan, R.J.H., Nitta, M., Borger, D., Zukerberg, L.R., Ferry, J.A., Harris, N.L., Iafrate, A.J., Bernstein, B.E., Sohani, A.R., and Le, L.P. (2011). EZH2 codon 641 mutations are common in BCL2-rearranged germinal center B cell lymphomas. PLoS ONE *6*, e28585.

Saiki, Y., Yoshino, Y., Fujimura, H., Manabe, T., Kudo, Y., Shimada, M., Mano, N., Nakano, T., Lee, Y., Shimizu, S., et al. (2012). DCK is frequently inactivated in acquired gemcitabine-resistant human cancer cells. Biochem. Biophys. Res. Commun. *421*, 98–104.

Saint-Jeannet, J.P., He, X., Varmus, H.E., and Dawid, I.B. (1997). Regulation of dorsal fate in the neuraxis by Wnt-1 and Wnt-3a. Proc. Natl. Acad. Sci. USA *94*, 13713–13718.

Sala, E., Mologni, L., Truffa, S., Gaetano, C., Bollag, G.E., and Gambacorti-Passerini, C. (2008). BRAF silencing by short hairpin RNA or chemical blockade by PLX4032 leads to different responses in melanoma and thyroid carcinoma cells. Mol. Cancer Res. *6*, 751–759.

Sanchez-Laorden, B., Viros, A., Girotti, M.R., Pedersen, M., Saturno, G., Zambon, A., Niculescu-Duvaz, D., Turajlic, S., Hayes, A., Gore, M., et al. (2014). BRAF inhibitors induce metastasis in RAS mutant or inhibitor-resistant melanoma cells by reactivating MEK and ERK signaling. Sci. Signal. *7*, ra30.

Santini, R., Pietrobono, S., Pandolfi, S., Montagnani, V., D'Amico, M., Penachioni, J.Y., Vinci, M.C., Borgognoni, L., and Stecca, B. (2014). SOX2 regulates self-renewal and tumorigenicity of human melanoma-initiating cells. Oncogene *33*, 4697–4708.

Santini, R., Vinci, M.C., Pandolfi, S., Penachioni, J.Y., Montagnani, V., Olivito, B., Gattai, R., Pimpinelli, N., Gerlini, G., Borgognoni, L., et al. (2012). Hedgehog-GLI signaling drives self-renewal and tumorigenicity of human melanoma-initiating cells. Stem Cells *30*, 1808–1818.

Santoro, R. (2014). Analysis of chromatin composition of repetitive sequences: the ChIP-Chop assay. In Methods in Molecular Biology, (Clifton, NJ: Springer), pp. 319–328.

Sanulli, S., Justin, N., Teissandier, A., Ancelin, K., Portoso, M., Caron, M., Michaud, A., Lombard, B., da Rocha, S.T., Offer, J., et al. (2015). Jarid2 Methylation via the PRC2 Complex Regulates H3K27me3 Deposition during Cell Differentiation. Mol. Cell 57, 769–783.

Sarker, D., Ang, J.E., Baird, R., Kristeleit, R., Shah, K., Moreno, V., Clarke, P.A., Raynaud, F.I., Levy, G., Ware, J.A., et al. (2015). First-in-Human Phase I Study of Pictilisib (GDC-0941), a Potent Pan-Class I Phosphatidylinositol-3-Kinase (PI3K) Inhibitor, in Patients with Advanced Solid Tumors. Clin. Cancer Res. *21*, 77–86.

Sauka-Spengler, T., and Bronner, M. (2010). Snapshot: neural crest. Cell *143*, 486–486.e1.

Sayegh, J., Cao, J., Zou, M.R., Morales, A., Blair, L.P., Norcia, M., Hoyer, D., Tackett, A.J., Merkel, J.S., and Yan, Q. (2013). Identification of small molecule inhibitors of Jumonji AT-rich interactive domain 1B (JARID1B) histone demethylase by a sensitive high throughput screen. J. Biol. Chem. *288*, 9408–9417.

Sáez-Ayala, M., Montenegro, M.F., Sánchez-Del-Campo, L., Fernández-Pérez, M.P., Chazarra, S., Freter, R., Middleton, M., Piñero-Madrona, A., Cabezas-Herrera, J., Goding, C.R., et al. (2013). Directed phenotype switching as an effective antimelanoma strategy. Cancer Cell *24*, 105–119.

Scambler, P.J., Carey, A.H., Wyse, R.K., Roach, S., Dumanski, J.P., Nordenskjold, M., and Williamson, R. (1991). Microdeletions within 22q11 associated with sporadic and familial DiGeorge syndrome. Genomics *10*, 201–206.

Schatton, T., Murphy, G.F., Frank, N.Y., Yamaura, K., Waaga-Gasser, A.M., Gasser, M., Zhan, Q., Jordan, S., Duncan, L.M., Weishaupt, C., et al. (2008). Identification of cells initiating human melanomas. Nature *451*, 345–349.

Schatton, T., Scolyer, R.A., Thompson, J.F., and Mihm, M.C. (2014). Tumor-infiltrating lymphocytes and their significance in melanoma prognosis. In Methods in Molecular Biology, (Clifton, NJ: Springer), pp. 287–324.

Schell, J.C., Olson, K.A., Jiang, L., Hawkins, A.J., Van Vranken, J.G., Xie, J., Egnatchik, R.A., Earl, E.G., DeBerardinis, R.J., and Rutter, J. (2014). A role for the mitochondrial pyruvate carrier as a repressor of the warburg effect and colon cancer cell growth. Mol. Cell *56*, 400–413.

Schinke, C., Mo, Y., Yu, Y., Amiri, K., Sosman, J., Greally, J., and Verma, A. (2010). Aberrant DNA methylation in malignant melanoma. Melanoma Res. *20*, 253–265.

Schlegel, N.C., Planta, von, A., Widmer, D.S., Dummer, R., and Christofori, G. (2015). PI3K signalling is required for a TGFβ-induced epithelial-mesenchymal-like transition (EMT-like) in human melanoma cells. Exp. Dermatol. *24*, 22–28.

Schmidts, M., Frank, V., Eisenberger, T., Turki, Al, S., Bizet, A.A., Antony, D., Rix, S., Decker, C., Bachmann, N., Bald, M., et al. (2013). Combined NGS approaches identify mutations in the intraflagellar transport gene IFT140 in skeletal ciliopathies with early progressive kidney Disease. Hum. Mutat. *34*, 714–724.

Schneider, P., Schön, M., Pletz, N., Seitz, C.S., Liu, N., Ziegelbauer, K., Zachmann, K., Emmert, S., and Schön, M.P. (2014). The novel PI3 kinase inhibitor, BAY 80-6946, impairs melanoma growth in vivo and in vitro. Exp. Dermatol. *23*, 579–584.

Schwarz, D., Varum, S., Zemke, M., Schöler, A., Baggiolini, A., Draganova, K., Koseki, H., Schübeler, D., and Sommer, L. (2014). Ezh2 is required for neural crest-derived cartilage and bone formation. Development *141*, 867–877.

Scortegagna, M., Ruller, C., Feng, Y., Lazova, R., Kluger, H., Li, J.-L., De, S.K., Rickert, R., Pellecchia, M., Bosenberg, M., et al. (2014). Genetic inactivation or pharmacological inhibition of Pdk1 delays development and inhibits metastasis of Braf(V600E)::Pten(-/-) melanoma. Oncogene *33*, 4330–4339.

Scuoppo, C., Miething, C., Lindqvist, L., Reyes, J., Ruse, C., Appelmann, I., Yoon, S., Krasnitz, A., Teruya-Feldstein, J., Pappin, D., et al. (2012). A tumour suppressor network relying on the polyamine-hypusine axis. Nature *487*, 244–248.

Seftor, E.A., Seftor, R.E.B., Weldon, D.S., Kirsammer, G.T., Margaryan, N.V., Gilgur, A., and Hendrix, M.J.C. (2014). Melanoma tumor cell heterogeneity: a molecular approach to study subpopulations expressing the embryonic morphogen nodal. Semin. Oncol. *41*, 259–266.

Segura, M.F., Fontanals-Cirera, B., Gaziel-Sovran, A., Guijarro, M.V., Hanniford, D., Zhang, G., Gonzalez-Gomez, P., Morante, M., Jubierre, L., Zhang, W., et al. (2013). BRD4 Sustains Melanoma Proliferation and Represents a New Target for Epigenetic Therapy. Cancer Res. *73*, 6264–6276.

Senese, S., Zaragoza, K., Minardi, S., Muradore, I., Ronzoni, S., Passafaro, A., Bernard, L., Draetta, G.F., Alcalay, M., Seiser, C., et al. (2007). Role for histone deacetylase 1 in human tumor cell proliferation. Mol. Cell Biol. *27*, 4784–4795.

Sensi, M., Catani, M., Castellano, G., Nicolini, G., Alciato, F., Tragni, G., De Santis, G., Bersani, I., Avanzi, G., Tomassetti, A., et al. (2011). Human cutaneous melanomas lacking MITF and melanocyte differentiation antigens express a functional Axl receptor kinase. J. Invest. Dermatol. *131*, 2448–2457.

Serrano, M., Lee, H., Chin, L., Cordon-Cardo, C., Beach, D., and DePinho, R.A. (1996). Role of the INK4a locus in tumor suppression and cell mortality. Cell *85*, 27–37.

Serrano, M., Lin, A.W., McCurrach, M.E., Beach, D., and Lowe, S.W. (1997). Oncogenic ras provokes premature cell senescence associated with accumulation of p53 and p16INK4a. Cell *88*, 593–602.

Setia, N., Abbas, O., Sousa, Y., Garb, J.L., and Mahalingam, M. (2012). Profiling of ABC transporters ABCB5, ABCF2 and nestin-positive stem cells in nevi, in situ and invasive melanoma. Mod. Pathol. *25*, 1169–1175.

Setiadi, A.F., Omilusik, K., David, M.D., Seipp, R.P., Hartikainen, J., Gopaul, R., Choi, K.B., and Jefferies, W.A. (2008). Epigenetic enhancement of antigen processing and presentation promotes immune recognition of tumors. Cancer Res. *68*, 9601–9607.

Shah, N.M., Groves, A.K., and Anderson, D.J. (1996). Alternative neural crest cell fates are instructively promoted by TGFbeta superfamily members. Cell *85*, 331–343.

Shakhova, O. (2014). Neural crest stem cells in melanoma development. Curr. Opin. Oncol. *26*, 215–221.

Shakhova, O., Cheng, P., Mishra, P.J., Zingg, D., Schaefer, S.M., Debbache, J., Häusel, J., Matter, C., Guo, T., Davis, S., et al. (2015). Antagonistic Cross-Regulation between Sox9 and Sox10 Controls an Anti-tumorigenic Program in Melanoma. PLoS Genet. *11*, e1004877.

Shakhova, O., and Sommer, L. (2010). Neural crest-derived stem cells. In StemBook, (Cambridge (MA): Harvard Stem Cell Institute), pp. 1–20.

Shakhova, O., Zingg, D., Schaefer, S.M., Hari, L., Civenni, G., Blunschi, J., Claudinot, S., Okoniewski, M., Beermann, F., Mihic-Probst, D., et al. (2012). Sox10 promotes the formation and maintenance of giant congenital naevi and melanoma. Nat. Cell Biol. *14*, 882–890.

Shao, Q., Kannan, A., Lin, Z., Stack, B.C., Suen, J.Y., and Gao, L. (2014). BET Protein Inhibitor JQ1 Attenuates Myc-Amplified MCC Tumor Growth In Vivo. Cancer Res. *74*, 7090–7102.

Sharma, S.V., Lee, D.Y., Li, B., Quinlan, M.P., Takahashi, F., Maheswaran, S., McDermott, U., Azizian, N., Zou, L., Fischbach, M.A., et al. (2010). A chromatin-mediated reversible drug-tolerant state in cancer cell subpopulations. Cell *141*, 69–80.

Sharov, A., Tobin, D.J., Sharova, T.Y., Atoyan, R., and Botchkarev, V.A. (2005). Changes in different melanocyte populations during hair follicle involution (catagen). J. Invest. Dermatol. *125*, 1259–1267.

Sharpless, E., and Chin, L. (2003). The INK4a/ARF locus and melanoma. Oncogene *22*, 3092–3098.

Shaul, Y.D., Freinkman, E., Comb, W.C., Cantor, J.R., Tam, W.L., Thiru, P., Kim, D., Kanarek, N., Pacold, M.E., Chen, W.W., et al. (2014). Dihydropyrimidine accumulation is required for the epithelial-mesenchymal transition. Cell *158*, 1094–1109.

Shen, X., Liu, Y., Hsu, Y.-J., Fujiwara, Y., Kim, J., Mao, X., Yuan, G.-C., and Orkin, S.H. (2008). EZH1 mediates methylation on histone H3 lysine 27 and complements EZH2 in maintaining stem cell identity and executing pluripotency. Mol. Cell *32*, 491–502.

Shenoy, B.V., Fort, L., and Benjamin, S.P. (1987). Malignant melanoma primary in lymph node. The case of the missing link. Am. J. Surg. Pathol. *11*, 140–146.

Sher, F., Boddeke, E., Olah, M., and Copray, S. (2012). Dynamic Changes in Ezh2 Gene Occupancy Underlie Its Involvement in Neural Stem Cell Self-Renewal and Differentiation towards Oligodendrocytes. PLoS ONE *7*, e40399.

Sher, F., Rössler, R., Brouwer, N., Balasubramaniyan, V., Boddeke, E., and Copray, S. (2008). Differentiation of neural stem cells into oligodendrocytes: involvement of the polycomb group protein Ezh2. Stem Cells *26*, 2875–2883.

Shi, B., Liang, J., Yang, X., Wang, Y., Zhao, Y., Wu, H., Sun, L., Zhang, Y., Chen, Y., Li, R., et al. (2007). Integration of estrogen and Wnt signaling circuits by the polycomb group protein EZH2 in breast cancer cells. Mol. Cell Biol. *27*, 5105–5119.

Shi, H., Hugo, W., Kong, X., Hong, A., Koya, R.C., Moriceau, G., Chodon, T., Guo, R., Johnson, D.B., Dahlman, K.B., et al. (2014). Acquired resistance and clonal evolution in melanoma during BRAF inhibitor therapy. Cancer Discovery *4*, 80–93.

Shi, H., Kong, X., Ribas, A., and Lo, R.S. (2011). Combinatorial treatments that overcome PDGFRβ-driven resistance of melanoma cells to V600EB-RAF inhibition. Cancer Res. *71*, 5067–5074.

Shi, H., Moriceau, G., Kong, X., Koya, R.C., Nazarian, R., Pupo, G.M., Bacchiocchi, A., Dahlman, K.B., Chmielowski, B., Sosman, J.A., et al. (2012a). Preexisting MEK1 exon 3 mutations in V600E/KBRAF melanomas do not confer resistance to BRAF inhibitors. Cancer Discovery *2*, 414–424.

Shi, H., Moriceau, G., Kong, X., Lee, M.-K., Lee, H., Koya, R.C., Ng, C., Chodon, T., Scolyer, R.A., Dahlman, K.B., et al. (2012b). Melanoma whole-exome sequencing identifies (V600E)B-RAF amplification-mediated acquired B-RAF inhibitor resistance. Nat. Commun. *3*, 724.

Shi, J., Wang, E., Zuber, J., Rappaport, A., Taylor, M., Johns, C., Lowe, S.W., and Vakoc, C.R. (2013). The Polycomb complex PRC2 supports aberrant self-renewal in a mouse model of MLL-AF9;Nras(G12D) acute myeloid leukemia. Oncogene *32*, 930–938.

Shimamura, T., Chen, Z., Soucheray, M., Carretero, J., Kikuchi, E., Tchaicha, J.H., Gao, Y., Cheng, K.A., Cohoon, T.J., Qi, J., et al. (2013). Efficacy of BET Bromodomain Inhibition in Kras-Mutant Non-Small Cell Lung Cancer. Clin. Cancer Res. *19*, 6183–6192.

Shin, J., Vincent, J.G., Cuda, J.D., Xu, H., Kang, S., Kim, J., and Taube, J.M. (2012). Sox10 is expressed in primary melanocytic neoplasms of various histologies but not in fibrohistiocytic proliferations and histiocytoses. J. Am. Acad. Dermatol. *67*, 717–726.

Sieber-Blum, M., and Cohen, A.M. (1980). Clonal analysis of quail neural crest cells: they are pluripotent and differentiate in vitro in the absence of noncrest cells. Dev. Biol. *80*, 96–106.

Sieber-Blum, M., Grim, M., Hu, Y.F., and Szeder, V. (2004). Pluripotent neural crest stem cells in the adult hair follicle. Dev. Dyn. *231*, 258–269.

Sieber-Blum, M., Schnell, L., Grim, M., Hu, Y.F., Schneider, R., and Schwab, M.E. (2006). Characterization of epidermal neural crest stem cell (EPI-NCSC) grafts in the lesioned spinal cord. Mol. Cell. Neurosci. *32*, 67–81.

Siebzehnrubl, F.A., Silver, D.J., Tugertimur, B., Deleyrolle, L.P., Siebzehnrubl, D., Sarkisian, M.R., Devers, K.G., Yachnis, A.T., Kupper, M.D., Neal, D., et al. (2013). The ZEB1 pathway links glioblastoma initiation, invasion and chemoresistance. EMBO Mol. Med. *5*, 1196–1212.

Siegel, R., Naishadham, D., and Jemal, A. (2013). Cancer statistics, 2013. CA Cancer J. Clin. *63*, 11–30.

Sigalotti, L., Fratta, E., Coral, S., and Maio, M. (2014). Epigenetic drugs as immunomodulators for combination therapies in solid tumors. Pharmacol. Ther. *142*, 339–350.

Simon, C., Chagraoui, J., Krosl, J., Gendron, P., Wilhelm, B., Lemieux, S., Boucher, G., Chagnon, P., Drouin, S., Lambert, R., et al. (2012). A key role for EZH2 and associated genes in mouse and human adult T-cell acute leukemia. Genes Dev. *26*, 651–656.

Simon, J.A., and Kingston, R.E. (2009). Mechanisms of polycomb gene silencing: knowns and unknowns. Nat. Rev. Mol. Cell. Biol. *10*, 697–708.

Singh, N., Trivedi, C.M., Lu, M., Mullican, S.E., Lazar, M.A., and Epstein, J.A. (2011). Histone deacetylase 3 regulates smooth muscle differentiation in neural crest cells and development of the cardiac outflow tract. Circ. Res. *109*, 1240–1249.

Smyth, G.K. (2005). limma: Linear Models for Microarray Data. In Statistics for Biology and Health, (Clifton, NJ: Springer), pp. 397–420.

Snedecor, E.R., Sung, C., Moncayo, A., Rothstein, B.E., Mockler, D.C., Tonnesen, M.G., Jones, E.C., Fujita, M., Clark, R.A., Shroyer, K.R., et al. (2015). Loss of Primary Cilia in Melanoma Cells is Likely Independent of Proliferation and Cell Cycle Progression. J. Invest. Dermatol., doi:10.1038/jid.2015.22.

Sneeringer, C.J., Scott, M.P., Kuntz, K.W., Knutson, S.K., Pollock, R.M., Richon, V.M., and Copeland, R.A. (2010). Coordinated activities of wild-type plus mutant EZH2 drive tumor-associated hypertrimethylation of lysine 27 on histone H3 (H3K27) in human B-cell lymphomas. Proc. Natl. Acad. Sci. USA *107*, 20980–20985.

Sommer, L. (2011). Generation of melanocytes from neural crest cells. Pigment Cell & Melanoma Research *24*, 411–421.

Son, J., Shen, S.S., Margueron, R., and Reinberg, D. (2013). Nucleosome-binding activities within JARID2 and EZH1 regulate the function of PRC2 on chromatin. Genes Dev. *27*, 2663–2677.

Soriano, P. (1999). Generalized lacZ expression with the ROSA26 Cre reporter strain. Nat. Genet. *21*, 70–71.

Sosman, J.A., Kim, K.B., Schuchter, L., Gonzalez, R., Pavlick, A.C., Weber, J.S., McArthur, G.A., Hutson, T.E., Moschos, S.J., Flaherty, K.T., et al. (2012). Survival in BRAF V600-mutant advanced melanoma treated with vemurafenib. N. Engl. J. Med. *366*, 707–714.

Sosman, J.A., Moon, J., Tuthill, R.J., Warneke, J.A., Vetto, J.T., Redman, B.G., Liu, P.Y., Unger, J.M., Flaherty, L.E., and Sondak, V.K. (2011). A phase 2 trial of complete resection for stage IV melanoma: results of Southwest Oncology Group Clinical Trial S9430. Cancer *117*, 4740–4706.

Soudja, S.M., Wehbe, M., Mas, A., Chasson, L., de Tenbossche, C.P., Huijbers, I., Van den Eynde, B., and Schmitt-Verhulst, A.-M. (2010). Tumor-initiated inflammation overrides protective adaptive immunity in an induced melanoma model in mice. Cancer Res. *70*, 3515–3525.

Southard-Smith, E.M., Kos, L., and Pavan, W.J. (1998). Sox10 mutation disrupts neural crest development in Dom Hirschsprung mouse model. Nat. Genet. *18*, 60–64.

Sparmann, A., Xie, Y., Verhoeven, E., Vermeulen, M., Lancini, C., Gargiulo, G., Hulsman, D., Mann, M., Knoblich, J.A., and van Lohuizen, M. (2013). The chromodomain helicase Chd4 is required for Polycomb-mediated inhibition of astroglial differentiation. Embo J. *32*, 1598–1612.

Spasokoukotskaja, T., Arnér, E.S., Brosjö, O., Gunvén, P., Juliusson, G., Liliemark, J., and Eriksson, S. (1995). Expression of deoxycytidine kinase and phosphorylation of 2-chlorodeoxyadenosine in human normal and tumour cells and tissues. Eur. J. Cancer. *31A*, 202–208.

Stahl, J.M., Sharma, A., Cheung, M., Zimmerman, M., Cheng, J.Q., Bosenberg, M.W., Kester, M., Sandirasegarane, L., and Robertson, G.P. (2004). Deregulated Akt3 activity promotes development of malignant melanoma. Cancer Res. *64*, 7002–7010.

Staricco, R.G. (1963). Amelanotic melanocytes in the outer sheath of the human hair follicle and their role in the repigmentation of regenerated epidermis. Ann. NY Acad. Sci. *100*, 239–255.

Stark, M., and Hayward, N. (2007). Genome-wide loss of heterozygosity and copy number analysis in melanoma using high-density single-nucleotide polymorphism arrays. Cancer Res. *67*, 2632–2642.

Stegmann, A.P., Honders, M.W., Hagemeijer, A., Hoebee, B., Willemze, R., and Landegent, J.E. (1995). In vitro-induced resistance to the deoxycytidine analogues cytarabine (AraC) and 5-aza-2'-deoxycytidine (DAC) in a rat model for acute myeloid leukemia is mediated by mutations in the deoxycytidine kinase (dck) gene. Ann. Hematol. *71*, 41–47.

Steingrimsson, E., Copeland, N.G., and Jenkins, N.A. (2004). Melanocytes and the microphthalmia transcription factor network. Annu. Rev. Genet. *38*, 365–411.

Stemple, D.L., and Anderson, D.J. (1992). Isolation of a stem cell for neurons and glia from the mammalian neural crest. Cell *71*, 973–985.

Stoetzel, C., Weber, B., Bourgeois, P., Bolcato-Bellemin, A.L., and Perrin-Schmitt, F. (1995). Dorso-ventral and rostro-caudal sequential expression of M-twist in the postimplantation murine embryo. Mech. Dev. *51*, 251–263.

Straussman, R., Morikawa, T., Shee, K., Barzily-Rokni, M., Qian, Z.R., Du, J., Davis, A., Mongare, M.M., Gould, J., Frederick, D.T., et al. (2012). Tumour micro-environment elicits innate resistance to RAF inhibitors through HGF secretion. Nature *487*, 500–504.

Strobl-Mazzulla, P.H., and Bronner, M.E. (2012a). Epithelial to mesenchymal transition: new and old insights from the classical neural crest model. Semin. Cancer Biol. *22*, 411–416.

Strobl-Mazzulla, P.H., and Bronner, M.E. (2012b). A PHD12-Snail2 repressive complex epigenetically mediates neural crest epithelial-to-mesenchymal transition. J. Cell Biol. *198*, 999–1010.

Strobl-Mazzulla, P.H., Sauka-Spengler, T., and Bronner-Fraser, M. (2010). Histone demethylase JmjD2A regulates neural crest specification. Dev. Cell *19*, 460–468.

Su, I.-H., Basavaraj, A., Krutchinsky, A.N., Hobert, O., Ullrich, A., Chait, B.T., and Tarakhovsky, A. (2003). Ezh2 controls B cell development through histone H3 methylation and Igh rearrangement. Nat. Immunol. *4*, 124–131.

Sullivan, R.J., and Flaherty, K. (2013). MAP kinase signaling and inhibition in melanoma. Oncogene *32*, 2373–2379.

Sun, C., Wang, L., Huang, S., Heynen, G.J.J.E., Prahallad, A., Robert, C., Haanen, J., Blank, C., Wesseling, J., Willems, S.M., et al. (2014). Reversible and adaptive resistance to BRAF(V600E) inhibition in melanoma. Nature *508*, 118–122.

Suvà, M.-L., Riggi, N., Janiszewska, M., Radovanovic, I., Provero, P., Stehle, J.-C., Baumer, K., Le Bitoux, M.-A., Marino, D., Cironi, L., et al. (2009). EZH2 is essential for glioblastoma cancer stem cell maintenance. Cancer Res. *69*, 9211–9218.

Tai, K.-Y., Shieh, Y.-S., Lee, C.-S., Shiah, S.-G., and Wu, C.-W. (2008). Axl promotes cell invasion by inducing MMP-9 activity through activation of NF-kappaB and Brg-1. Oncogene *27*, 4044–4055.

Takahashi, K., and Yamanaka, S. (2006). Induction of pluripotent stem cells from mouse embryonic and adult fibroblast cultures by defined factors. Cell *126*, 663–676.

Takeda, K., Yasumoto, K., Takada, R., Takada, S., Watanabe, K., Udono, T., Saito, H., Takahashi, K., and Shibahara, S. (2000). Induction of melanocyte-specific microphthalmia-associated transcription factor by Wnt-3a. J. Biol. Chem. *275*, 14013–14016.

Tam, W.L., and Weinberg, R.A. (2013). The epigenetics of epithelial-mesenchymal plasticity in cancer. Nat. Med. *19*, 1438–1449.

Tanaka, S., Miyagi, S., Sashida, G., Chiba, T., Yuan, J., Mochizuki-Kashio, M., Suzuki, Y., Sugano, S., Nakaseko, C., Yokote, K., et al. (2012). Ezh2 augments leukemogenicity by reinforcing differentiation blockage in acute myeloid leukemia. Blood *120*, 1107–1117.

Tange, S., Oktyabri, D., Terashima, M., Ishimura, A., and Suzuki, T. (2014). JARID2 is involved in transforming growth factor-beta-induced epithelial-mesenchymal transition of lung and colon cancer cell lines. PLoS ONE *9*, e115684.

Tanimura, S., Tadokoro, Y., Inomata, K., Binh, N.T., Nishie, W., Yamazaki, S., Nakauchi, H., Tanaka, Y., McMillan, J.R., Sawamura, D., et al. (2011). Hair follicle stem cells provide a functional niche for melanocyte stem cells. Cell Stem Cell *8*, 177–187.

Taran, J.M., and Heenan, P.J. (2001). Clinical and histologic features of level 2 cutaneous malignant melanoma associated with metastasis. Cancer *91*, 1822–1825.

Tatton-Brown, K., Hanks, S., Ruark, E., Zachariou, A., Duarte, S.D.V., Ramsay, E., Snape, K., Murray, A., Perdeaux, E.R., Seal, S., et al. (2011). Germline mutations in the oncogene EZH2 cause Weaver syndrome and increased human height. Oncotarget *2*, 1127–1133.

Tatton-Brown, K., Murray, A., Hanks, S., Douglas, J., Armstrong, R., Banka, S., Bird, L.M., Clericuzio, C.L., Cormier-Daire, V., Cushing, T., et al. (2013). Weaver syndrome and EZH2 mutations: Clarifying the clinical phenotype. Am. J. Med. Genet. A. *161A*, 2972–2980.

Tatton-Brown, K., Seal, S., Ruark, E., Harmer, J., Ramsay, E., Del Vecchio Duarte, S., Zachariou, A., Hanks, S., O'Brien, E., Aksglaede, L., et al. (2014). Mutations in the DNA methyltransferase gene DNMT3A cause an overgrowth syndrome with intellectual disability. Nat. Genet. *46*, 385–388.

Teng, L., Mundell, N.A., Frist, A.Y., Wang, Q., and Labosky, P.A. (2008). Requirement for Foxd3 in the maintenance of neural crest progenitors. Development *135*, 1615–1624.

Terzian, T., Torchia, E.C., Dai, D., Robinson, S.E., Murao, K., Stiegmann, R.A., Gonzalez, V., Boyle, G.M., Powell, M.B., Pollock, P.M., et al. (2010). p53 prevents progression of nevi to melanoma predominantly through cell cycle regulation. Pigment Cell & Melanoma Research *23*, 781–794.

Testori, A., Rutkowski, P., Marsden, J., Bastholt, L., Chiarion-Sileni, V., Hauschild, A., and Eggermont, A.M.M. (2009). Surgery and radiotherapy in the treatment of cutaneous melanoma. Ann. Oncol. *20 Suppl. 6*, vi22–vi29.

Thakur, Das, M., Salangsang, F., Landman, A.S., Sellers, W.R., Pryer, N.K., Levesque, M.P., Dummer, R., McMahon, M., and Stuart, D.D. (2013). Modelling vemurafenib resistance in melanoma reveals a strategy to forestall drug resistance. Nature *494*, 251–255.

Theveneau, E., and Mayor, R. (2012). Neural crest delamination and migration: from epithelium-to-mesenchyme transition to collective cell migration. Dev. Biol. *366*, 34–54.

Tiacci, E., Trifonov, V., Schiavoni, G., Holmes, A., Kern, W., Martelli, M.P., Pucciarini, A., Bigerna, B., Pacini, R., Wells, V.A., et al. (2011). BRAF mutations in hairy-cell leukemia. N. Engl. J. Med. *364*, 2305–2315.

Tian, M., Neil, J.R., and Schiemann, W.P. (2011). Transforming growth factor-β and the hallmarks of cancer. Cell. Signal. *23*, 951–962.

Tien, C.-L., Jones, A., Wang, H., Gerigk, M., Nozell, S., and Chang, C. (2015). Snail2/Slug cooperates with Polycomb repressive complex 2 (PRC2) to regulate neural crest development. Development *142*, 722–731.

Tiffen, J., Gallagher, S.J., and Hersey, P. (2015). EZH2: an emerging role in melanoma biology and strategies for targeted therapy. Pigment Cell & Melanoma Research *28*, 21–30.

Tivol, E.A., Borriello, F., Schweitzer, A.N., Lynch, W.P., Bluestone, J.A., and Sharpe, A.H. (1995). Loss of CTLA-4 leads to massive lymphoproliferation and fatal multiorgan tissue destruction, revealing a critical negative regulatory role of CTLA-4. Immunity *3*, 541–547.

Tiwari, N., Tiwari, V.K., Waldmeier, L., Balwierz, P.J., Arnold, P., Pachkov, M., Meyer-Schaller, N., Schübeler, D., van Nimwegen, E., and Christofori, G. (2013). Sox4 is a master regulator of epithelial-mesenchymal transition by controlling ezh2 expression and epigenetic reprogramming. Cancer Cell *23*, 768–783.

Toh, B., Wang, X., Keeble, J., Sim, W.J., Khoo, K., Wong, W.-C., Kato, M., Prevost-Blondel, A., Thiery, J.P., and Abastado, J.-P. (2011). Mesenchymal transition and dissemination of cancer cells is driven by myeloid-derived suppressor cells infiltrating the primary tumor. PLoS Biol. *9*, e1001162.

Tolcher, A.W., Patnaik, A., Papadopoulos, K.P., Rasco, D.W., Becerra, C.R., Allred, A.J., Orford, K., Aktan, G., Ferron-Brady, G., Ibrahim, N., et al. (2015). Phase I study of the MEK inhibitor trametinib in combination with the AKT inhibitor afuresertib in patients with solid tumors and multiple myeloma. Cancer Chemother. Pharmacol. *75*, 183–189.

Tomita, Y., Matsumura, K., Wakamatsu, Y., Matsuzaki, Y., Shibuya, I., Kawaguchi, H., Ieda, M., Kanakubo, S., Shimazaki, T., Ogawa, S., et al. (2005). Cardiac neural crest cells contribute to the dormant multipotent stem cell in the mammalian heart. J. Cell Biol. *170*, 1135–1146.

Tong, Z.-T., Cai, M.-Y., Wang, X.-G., Kong, L.-L., Mai, S.-J., Liu, Y.-H., Zhang, H.-B., Liao, Y.-J., Zheng, F., Zhu, W., et al. (2012). EZH2 supports nasopharyngeal carcinoma cell aggressiveness by forming a co-repressor complex with HDAC1/HDAC2 and Snail to inhibit E-cadherin. Oncogene *31*, 583–594.

Topalian, S.L., Hodi, F.S., Brahmer, J.R., Gettinger, S.N., Smith, D.C., McDermott, D.F., Powderly, J.D., Carvajal, R.D., Sosman, J.A., Atkins, M.B., et al. (2012). Safety, activity, and immune correlates of anti-PD-1 antibody in cancer. N. Engl. J. Med. *366*, 2443–2454.

Topalian, S.L., Sznol, M., McDermott, D.F., Kluger, H.M., Carvajal, R.D., Sharfman, W.H., Brahmer, J.R., Lawrence, D.P., Atkins, M.B., Powderly, J.D., et al. (2014). Survival, durable tumor remission, and long-term safety in patients with advanced melanoma receiving nivolumab. J. Clin. Oncol. *32*, 1020–1030.

Topczewska, J.M., Postovit, L.-M., Margaryan, N.V., Sam, A., Hess, A.R., Wheaton, W.W., Nickoloff, B.J., Topczewski, J., and Hendrix, M.J.C. (2006). Embryonic and tumorigenic pathways converge via Nodal signaling: role in melanoma aggressiveness. Nat. Med. *12*, 925–932.

Trabucco, S.E., Gerstein, R.M., Evens, A.M., Bradner, J.E., Shultz, L.D., Greiner, D.L., and Zhang, H. (2015). Inhibition of Bromodomain Proteins for the Treatment of Human Diffuse Large B-cell Lymphoma. Clin. Cancer Res. *21*, 113–122.

Trochet, D., Bourdeaut, F., Janoueix-Lerosey, I., Deville, A., de Pontual, L., Schleiermacher, G., Coze, C., Philip, N., Frébourg, T., Munnich, A., et al. (2004). Germline mutations of the paired-like homeobox 2B (PHOX2B) gene in neuroblastoma. Am. J. Hum. Genet. *74*, 761–764.

Trochet, D., Hong, S.J., Lim, J.K., Brunet, J.-F., Munnich, A., Kim, K.-S., Lyonnet, S., Goridis, C., and Amiel, J. (2005). Molecular consequences of PHOX2B missense, frameshift and alanine expansion mutations leading to autonomic dysfunction. Hum. Mol. Genet. *14*, 3697–3708.

Tsao, H., Zhang, X., Benoit, E., and Haluska, F.G. (1998). Identification of PTEN/MMAC1 alterations in uncultured melanomas and melanoma cell lines. Oncogene *16*, 3397–3402.

Tsao, H., Zhang, X., Fowlkes, K., and Haluska, F.G. (2000). Relative reciprocity of NRAS and PTEN/MMAC1 alterations in cutaneous melanoma cell lines. Cancer Res. *60*, 1800–1804.

Tsao, H., Goel, V., Wu, H., Yang, G., and Haluska, F.G. (2004). Genetic interaction between NRAS and BRAF mutations and PTEN/MMAC1 inactivation in melanoma. J. Invest. Dermatol. *122*, 337–341.

Tsumura, A., Hayakawa, T., Kumaki, Y., Takebayashi, S.-I., Sakaue, M., Matsuoka, C., Shimotohno, K., Ishikawa, F., Li, E., Ueda, H.R., et al. (2006). Maintenance of self-renewal ability of mouse embryonic stem cells in the absence of DNA methyltransferases Dnmt1, Dnmt3a and Dnmt3b. Genes Cells *11*, 805–814.

Tumbar, T., Guasch, G., Greco, V., Blanpain, C., Lowry, W.E., Rendl, M., and Fuchs, E. (2004). Defining the epithelial stem cell niche in skin. Science *303*, 359–363.

Tumeh, P.C., Harview, C.L., Yearley, J.H., Shintaku, I.P., Taylor, E.J.M., Robert, L., Chmielowski, B., Spasic, M., Henry, G., Ciobanu, V., et al. (2014). PD-1 blockade induces responses by inhibiting adaptive immune resistance. Nature *515*, 568–571.

Tumes, D.J., Onodera, A., Suzuki, A., Shinoda, K., Endo, Y., Iwamura, C., Hosokawa, H., Koseki, H., Tokoyoda, K., Suzuki, Y., et al. (2013). The polycomb protein Ezh2 regulates differentiation and plasticity of CD4(+) T helper type 1 and type 2 cells. Immunity *39*, 819–832.

Ueda, Y., Okano, M., Williams, C., Chen, T., Georgopoulos, K., and Li, E. (2006). Roles for Dnmt3b in mammalian development: a mouse model for the ICF syndrome. Development *133*, 1183–1192.

Vacanti, N.M., Divakaruni, A.S., Green, C.R., Parker, S.J., Henry, R.R., Ciaraldi, T.P., Murphy, A.N., and Metallo, C.M. (2014). Regulation of substrate utilization by the mitochondrial pyruvate carrier. Mol. Cell *56*, 425–435.

Van Allen, E.M., Wagle, N., Sucker, A., Treacy, D.J., Johannessen, C.M., Goetz, E.M., Place, C.S., Taylor-Weiner, A., Whittaker, S., Kryukov, G.V., et al. (2014). The genetic landscape of clinical resistance to RAF inhibition in metastatic melanoma. Cancer Discovery *4*, 94–109.

Van den Broeck, W., Derore, A., and Simoens, P. (2006). Anatomy and nomenclature of murine lymph nodes: Descriptive study and nomenclatory standardization in BALB/cAnNCrl mice. J. Immunol. Methods *312*, 12–19.

Van der Meulen, J., Sanghvi, V., Mavrakis, K., Durinck, K., Fang, F., Matthijssens, F., Rondou, P., Rosen, M., Pieters, T., Vandenberghe, P., et al. (2015). The H3K27me3 demethylase UTX is a gender-specific tumor suppressor in T-cell acute lymphoblastic leukemia. Blood *125*, 13–21.

Van der Meulen, J., Speleman, F., and Van Vlierberghe, P. (2014). The H3K27me3 demethylase UTX in normal development and disease. Epigenetics *9*, 658–668.

van Haaften, G., Dalgliesh, G.L., Davies, H., Chen, L., Bignell, G., Greenman, C., Edkins, S., Hardy, C., O'Meara, S., Teague, J., et al. (2009). Somatic mutations of the histone H3K27 demethylase gene UTX in human cancer. Nat. Genet. *41*, 521–523.

van Limpt, V., Schramm, A., van Lakeman, A., Sluis, P., Chan, A., van Noesel, M., Baas, F., Caron, H., Eggert, A., and Versteeg, R. (2004). The Phox2B homeobox gene is mutated in sporadic neuroblastomas. Oncogene *23*, 9280–9288.

Van Raamsdonk, C.D., Bezrookove, V., Green, G., Bauer, J., Gaugler, L., O'Brien, J.M., Simpson, E.M., Barsh, G.S., and Bastian, B.C. (2009). Frequent somatic mutations of GNAQ in uveal melanoma and blue naevi. Nature *457*, 599–602.

Van Raamsdonk, C.D., Griewank, K.G., Crosby, M.B., Garrido, M.C., Vemula, S., Wiesner, T., Obenauf, A.C., Wackernagel, W., Green, G., Bouvier, N., et al. (2010). Mutations in GNA11 in uveal melanoma. N. Engl. J. Med. *363*, 2191–2199.

Varambally, S., Dhanasekaran, S.M., Zhou, M., Barrette, T.R., Kumar-Sinha, C., Sanda, M.G., Ghosh, D., Pienta, K.J., Sewalt, R.G.A.B., Otte, A.P., et al. (2002). The polycomb group protein EZH2 is involved in progression of prostate cancer. Nature *419*, 624–629.

Vardabasso, C., Hasson, D., Ratnakumar, K., Chung, C.-Y., Duarte, L.F., and Bernstein, E. (2014). Histone variants: emerging players in cancer biology. Cell. Mol. Life Sci. *71*, 379–404.

Vavvas, D., and Brodowska, K. (2009). Images in clinical medicine. Traumatic bleb. N. Engl. J. Med. *361*, e2.

Velichutina, I., Shaknovich, R., Geng, H., Johnson, N.A., Gascoyne, R.D., Melnick, A.M., and Elemento, O. (2010). EZH2-mediated epigenetic silencing in germinal center B cells contributes to proliferation and lymphomagenesis. Blood *116*, 5247–5255.

Venkataraman, S., Alimova, I., Balakrishnan, I., Harris, P., Birks, D.K., Griesinger, A., Amani, V., Cristiano, B., Remke, M., Taylor, M.D., et al. (2014). Inhibition of BRD4 attenuates tumor cell self-renewal and suppresses stem cell signaling in MYC driven medulloblastoma. Oncotarget *5*, 2355–2371.

Venza, M., Visalli, M., Biondo, C., Lentini, M., Catalano, T., Teti, D., and Venza, I. (2015). Epigenetic regulation of p14(ARF) and p16(INK4A) expression in cutaneous and uveal melanoma. Biochim. Biophys. Acta *1849*, 247–256.

Verma, S.K., Tian, X., LaFrance, L.V., Duquenne, C., Suarez, D.P., Newlander, K.A., Romeril, S.P., Burgess, J.L., Grant, S.W., Brackley, J.A., et al. (2012). Identification of Potent, Selective, Cell-Active Inhibitors of the Histone Lysine Methyltransferase EZH2. ACS Med. Chem. Lett. *3*, 1091–1096.

Vidwans, S.J., Flaherty, K.T., Fisher, D.E., Tenenbaum, J.M., Travers, M.D., and Shrager, J. (2011). A melanoma molecular disease model. PLoS ONE *6*, e18257.

Villanueva, J., Vultur, A., Lee, J.T., Somasundaram, R., Fukunaga-Kalabis, M., Cipolla, A.K., Wubbenhorst, B., Xu, X., Gimotty, P.A., Kee, D., et al. (2010). Acquired resistance to BRAF inhibitors mediated by a RAF kinase switch in melanoma can be overcome by cotargeting MEK and IGF-1R/PI3K. Cancer Cell *18*, 683–695.

Viros, A., Sanchez-Laorden, B., Pedersen, M., Furney, S.J., Rae, J., Hogan, K., Ejiama, S., Girotti, M.R., Cook, M., Dhomen, N., et al. (2014). Ultraviolet radiation accelerates BRAF-driven melanomagenesis by targeting TP53. Nature *511*, 478–482.

Viskochil, D., Buchberg, A.M., Xu, G., Cawthon, R.M., Stevens, J., Wolff, R.K., Culver, M., Carey, J.C., Copeland, N.G., and Jenkins, N.A. (1990). Deletions and a translocation interrupt a cloned gene at the neurofibromatosis type 1 locus. Cell *62*, 187–192.

Vogel, K.S., Klesse, L.J., Velasco-Miguel, S., Meyers, K., Rushing, E.J., and Parada, L.F. (1999). Mouse tumor model for neurofibromatosis type 1. Science *286*, 2176–2179.

Vousden, K.H., and Prives, C. (2009). Blinded by the Light: The Growing Complexity of p53. Cell *137*, 413–431.

Wagle, N., Emery, C., Berger, M.F., Davis, M.J., Sawyer, A., Pochanard, P., Kehoe, S.M., Johannessen, C.M., Macconaill, L.E., Hahn, W.C., et al. (2011). Dissecting therapeutic resistance to RAF inhibition in melanoma by tumor genomic profiling. J. Clin. Oncol. *29*, 3085–3096.

Wainwright, E.N., Svingen, T., Ng, E.T., Wicking, C., and Koopman, P. (2014). Primary cilia function regulates the length of the embryonic trunk axis and urogenital field in mice. Dev. Biol. *395*, 342–354.

Wallace, M.R., Marchuk, D.A., Andersen, L.B., Letcher, R., Odeh, H.M., Saulino, A.M., Fountain, J.W., Brereton, A., Nicholson, J., and Mitchell, A.L. (1990). Type 1 neurofibromatosis gene: identification of a large transcript disrupted in three NF1 patients. Science *249*, 181–186.

Wan, P.T.C., Garnett, M.J., Roe, S.M., Lee, S., Niculescu-Duvaz, D., Good, V.M., Jones, C.M., Marshall, C.J., Springer, C.J., Barford, D., et al. (2004). Mechanism of activation of the RAF-ERK signaling pathway by oncogenic mutations of B-RAF. Cell *116*, 855–867.

Wandel, A., Steigleder, G.K., and Bodeux, E. (1984). Primär-Zilien in Zellen der Epidermis und Dermis. Z. Hautkr. *59*, 389–392.

Wang, C., Thudium, K.B., Han, M., Wang, X.-T., Huang, H., Feingersh, D., Garcia, C., Wu, Y., Kuhne, M., Srinivasan, M., et al. (2014). In vitro characterization of the anti-PD-1 antibody nivolumab, BMS-936558, and in vivo toxicology in non-human primates. Cancer Immunol. Res. *2*, 846–856.

Wang, C., Liu, Z., Woo, C.-W., Li, Z., Wang, L., Wei, J.S., Marquez, V.E., Bates, S.E., Jin, Q., Khan, J., et al. (2012). EZH2 Mediates Epigenetic Silencing of Neuroblastoma Suppressor Genes CASZ1, CLU, RUNX3, and NGFR. Cancer Res. *72*, 315–324.

Wang, J., Zhang, M., Zhang, Y., Kou, Z., Han, Z., Chen, D.-Y., Sun, Q.-Y., and Gao, S. (2010a). The histone demethylase JMJD2C is stage-specifically expressed in preimplantation mouse embryos and is required for embryonic development. Biol. Reprod. *82*, 105–111.

Wang, J., Huang, S.K., Marzese, D.M., Hsu, S.C., Kawas, N.P., Chong, K.K., Long, G.V., Menzies, A.M., Scolyer, R.A., Izraely, S., et al. (2015). Epigenetic Changes of EGFR Have an Important Role in BRAF Inhibitor-Resistant Cutaneous Melanomas. J. Invest. Dermatol. *135*, 532–541.

Wang, K., Li, M., and Hakonarson, H. (2010b). ANNOVAR: functional annotation of genetic variants from high-throughput sequencing data. Nucleic Acids Res. *38*, e164.

Wang, L., Chang, J., Varghese, D., Dellinger, M., Kumar, S., Best, A.M., Ruiz, J., Bruick, R., Peña-Llopis, S., Xu, J., et al. (2013a). A small molecule modulates Jumonji histone demethylase activity and selectively inhibits cancer growth. Nat. Commun. *4*, 2035.

Wang, L.-X., Li, R., Yang, G., Lim, M., O'Hara, A., Chu, Y., Fox, B.A., Restifo, N.P., Urba, W.J., and Hu, H.-M. (2005). Interleukin-7-dependent expansion and persistence of melanoma-specific T cells in lymphodepleted mice lead to tumor regression and editing. Cancer Res. *65*, 10569–10577.

Wang, X., Dai, H., Wang, Q., Wang, Q., Xu, Y., Wang, Y., Sun, A., Ruan, J., Chen, S., and Wu, D. (2013b). EZH2 mutations are related to low blast percentage in bone marrow and -7/del(7q) in de novo acute myeloid leukemia. PLoS ONE *8*, e61341.

Warburg, O. (1956). On the origin of cancer cells. Science *123*, 309–314.

Warburg, O., Wind, F., and Negelein, E. (1927). The metabolism of tumors in the body. J. Gen. Physiol. *8*, 519–530.

Ward, P.S., Patel, J., Wise, D.R., Abdel-Wahab, O., Bennett, B.D., Coller, H.A., Cross, J.R., Fantin, V.R., Hedvat, C.V., Perl, A.E., et al. (2010). The common feature of leukemia-associated IDH1 and IDH2 mutations is a neomorphic enzyme activity converting alpha-ketoglutarate to 2-hydroxyglutarate. Cancer Cell *17*, 225–234.

Waterhouse, P., Penninger, J.M., Timms, E., Wakeham, A., Shahinian, A., Lee, K.P., Thompson, C.B., Griesser, H., and Mak, T.W. (1995). Lymphoproliferative disorders with early lethality in mice deficient in Ctla-4. Science *270*, 985–988.

Weber, M., Davies, J.J., Wittig, D., Oakeley, E.J., Haase, M., Lam, W.L., and Schübeler, D. (2005). Chromosome-wide and promoter-specific analyses identify sites of differential DNA methylation in normal and transformed human cells. Nat. Genet. *37*, 853–862.

Wehrle-Haller, B., and Weston, J.A. (1995). Soluble and cell-bound forms of steel factor activity play distinct roles in melanocyte precursor dispersal and survival on the lateral neural crest migration pathway. Development *121*, 731–742.

Wei, Q., Zhang, Y., Li, Y., Zhang, Q., Ling, K., and Hu, J. (2012). The BBSome controls IFT assembly and turnaround in cilia. Nat. Cell. Biol. *14*, 950–957.

Weiss, M.B., Abel, E.V., Mayberry, M.M., Basile, K.J., Berger, A.C., and Aplin, A.E. (2012). TWIST1 is an ERK1/2 effector that promotes invasion and regulates MMP-1 expression in human melanoma cells. Cancer Res. *72*, 6382–6392.

Wellbrock, C., Ogilvie, L., Hedley, D., Karasarides, M., Martin, J., Niculescu-Duvaz, D., Springer, C.J., and Marais, R. (2004). V599EB-RAF is an oncogene in melanocytes. Cancer Res. *64*, 2338–2342.

Whittaker, S.J., Demierre, M.-F., Kim, E.J., Rook, A.H., Lerner, A., Duvic, M., Scarisbrick, J., Reddy, S., Robak, T., Becker, J.C., et al. (2010). Final results from a multicenter, international, pivotal study of romidepsin in refractory cutaneous T-cell lymphoma. J. Clin. Oncol. *28*, 4485–4491.

Whittaker, S.R., Theurillat, J.-P., Van Allen, E., Wagle, N., Hsiao, J., Cowley, G.S., Schadendorf, D., Root, D.E., and Garraway, L.A. (2013). A genome-scale RNA interference screen implicates NF1 loss in resistance to RAF inhibition. Cancer Discovery *3*, 350–362.

Whitwam, T., Vanbrocklin, M.W., Russo, M.E., Haak, P.T., Bilgili, D., Resau, J.H., Koo, H.-M., and Holmen, S.L. (2007). Differential oncogenic potential of activated RAS isoforms in melanocytes. Oncogene *26*, 4563–4570.

Widlund, H.R., Horstmann, M.A., Price, E.R., Cui, J., Lessnick, S.L., Wu, M., He, X., and Fisher, D.E. (2002). Beta-catenin-induced melanoma growth requires the downstream target Microphthalmia-associated transcription factor. J. Cell Biol. *158*, 1079–1087.

Wigle, T.J., Knutson, S.K., Jin, L., Kuntz, K.W., Pollock, R.M., Richon, V.M., Copeland, R.A., and Scott, M.P. (2011). The Y641C mutation of EZH2 alters substrate specificity for histone H3 lysine 27 methylation states. FEBS Lett. *585*, 3011–3014.

Wilson, T.R., Fridlyand, J., Yan, Y., Penuel, E., Burton, L., Chan, E., Peng, J., Lin, E., Wang, Y., Sosman, J., et al. (2012). Widespread potential for growth-factor-driven resistance to anticancer kinase inhibitors. Nature *487*, 505–509.

Wilson, Y.M., Richards, K.L., Ford-Perriss, M.L., Panthier, J.-J., and Murphy, M. (2004). Neural crest cell lineage segregation in the mouse neural tube. Development *131*, 6153–6162.

Wong, C.E., Paratore, C., Dours-Zimmermann, M.T., Rochat, A., Pietri, T., Suter, U., Zimmermann, D.R., Dufour, S., Thiery, J.P., Meijer, D., et al. (2006). Neural crest-derived cells with stem cell features can be traced back to multiple lineages in the adult skin. J. Cell Biol. *175*, 1005–1015.

Wong, D.J.L., Robert, L., Atefi, M.S., Lassen, A., Avarappatt, G., Cerniglia, M., Avramis, E., Tsoi, J., Foulad, D., Graeber, T.G., et al. (2014). Antitumor activity of the ERK inhibitor SCH722984 against BRAF mutant, NRAS mutant and wild-type melanoma. Mol. Cancer *13*, 194.

Woods, D.M., Woan, K., Cheng, F., Wang, H., Perez-Villarroel, P., Lee, C., Lienlaf, M., Atadja, P., Seto, E., Weber, J., et al. (2013). The antimelanoma activity of the histone deacetylase inhibitor panobinostat (LBH589) is mediated by direct tumor cytotoxicity and increased tumor immunogenicity. Melanoma Res. *23*, 341–348.

Wrabetz, L., Feltri, M.L., Kim, H., Daston, M., Kamholz, J., Scherer, S.S., and Ratner, N. (1995). Regulation of neurofibromin expression in rat sciatic nerve and cultured Schwann cells. Glia *15*, 22–32.

Wrangle, J., Wang, W., Koch, A., Easwaran, H., Mohammad, H.P., Vendetti, F., Vancriekinge, W., Demeyer, T., Du, Z., Parsana, P., et al. (2013). Alterations of immune response of Non-Small Cell Lung Cancer with Azacytidine. Oncotarget *4*, 2067–2079.

Wu, H., Goel, V., and Haluska, F.G. (2003). PTEN signaling pathways in melanoma. Oncogene *22*, 3113–3122.

Wu, J., Williams, J.P., Rizvi, T.A., Kordich, J.J., Witte, D., Meijer, D., Stemmer-Rachamimov, A.O., Cancelas, J.A., and Ratner, N. (2008). Plexiform and dermal neurofibromas and pigmentation are caused by Nf1 loss in desert hedgehog-expressing cells. Cancer Cell *13*, 105–116.

Wu, T., Pinto, H.B., Kamikawa, Y.F., and Donohoe, M.E. (2015). The BET Family Member BRD4 Interacts with OCT4 and Regulates Pluripotency Gene Expression. Stem Cell Reports *4*, 390–403.

Wurdak, H., Ittner, L.M., and Sommer, L. (2006). DiGeorge syndrome and pharyngeal apparatus development. Bioessays *28*, 1078–1086.

Wurdak, H., Ittner, L.M., Lang, K.S., Leveen, P., Suter, U., Fischer, J.A., Karlsson, S., Born, W., and Sommer, L. (2005). Inactivation of TGFbeta signaling in neural crest stem cells leads to multiple defects reminiscent of DiGeorge syndrome. Genes Dev. *19*, 530–535.

Wyce, A., Degenhardt, Y., Bai, Y., Le, B., Korenchuk, S., Crouthame, M.-C., McHugh, C.F., Vessella, R., Creasy, C.L., Tummino, P.J., et al. (2013a). Inhibition of BET bromodomain proteins as a therapeutic approach in prostate cancer. Oncotarget *4*, 2419–2429.

Wyce, A., Ganji, G., Smitheman, K.N., Chung, C.-W., Korenchuk, S., Bai, Y., Barbash, O., Le, B., Craggs, P.D., McCabe, M.T., et al. (2013b). BET inhibition silences expression of MYCN and BCL2 and induces cytotoxicity in neuroblastoma tumor models. PLoS ONE *8*, e72967.

Xiao, W., Dong, W., Zhang, C., Saren, G., Geng, P., Zhao, H., Li, Q., Zhu, J., Li, G., Zhang, S., et al. (2013). Effects of the epigenetic drug MS-275 on the release and function of exosome-related immune molecules in hepatocellular carcinoma cells. Eur. J. Med. Res. *18*, 61.

Xie, W., Schultz, M.D., Lister, R., Hou, Z., Rajagopal, N., Ray, P., Whitaker, J.W., Tian, S., Hawkins, R.D., Leung, D., et al. (2013). Epigenomic analysis of multilineage differentiation of human embryonic stem cells. Cell *153*, 1134–1148.

Xing, F., Persaud, Y., Pratilas, C.A., Taylor, B.S., Janakiraman, M., She, Q.-B., Gallardo, H., Liu, C., Merghoub, T., Hefter, B., et al. (2012). Concurrent loss of the PTEN and RB1 tumor suppressors attenuates RAF dependence in melanomas harboring (V600E)BRAF. Oncogene *31*, 446–457.

Xu, B., On, D.M., Ma, A., Parton, T., Konze, K.D., Pattenden, S.G., Allison, D.F., Cai, L., Rockowitz, S., Liu, S., et al. (2015a). Selective inhibition of EZH2 and EZH1 enzymatic activity by a small molecule suppresses MLL-rearranged leukemia. Blood *125*, 346–357.

Xu, C., Bian, C., Yang, W., Galka, M., Ouyang, H., Chen, C., Qiu, W., Liu, H., Jones, A.E., MacKenzie, F., et al. (2010). Binding of different histone marks differentially regulates the activity and specificity of polycomb repressive complex 2 (PRC2). Proc. Natl. Acad. Sci. USA *107*, 19266–19271.

Xu, J., Acharya, S., Sahin, O., Zhang, Q., Saito, Y., Yao, J., Wang, H., Li, P., Zhang, L., Lowery, F.J., et al. (2015b). 14-3-3z Turns TGF-b's Function from Tumor Suppressor to Metastasis Promoter in Breast Cancer by Contextual Changes of Smad Partners from p53 to Gli2. Cancer Cell *27*, 177–192.

Xu, K., Wu, Z.J., Groner, A.C., He, H.H., Cai, C., Lis, R.T., Wu, X., Stack, E.C., Loda, M., Liu, T., et al. (2012). EZH2 Oncogenic Activity in Castration-Resistant Prostate Cancer Cells Is Polycomb-Independent. Science *338*, 1465–1469.

Xu, W., Yang, H., Liu, Y., Yang, Y., Wang, P., Kim, S.-H., Ito, S., Yang, C., Wang, P., Xiao, M.-T., et al. (2011). Oncometabolite 2-hydroxyglutarate is a competitive inhibitor of α-ketoglutarate-dependent dioxygenases. Cancer Cell *19*, 17–30.

Yadav, V., Burke, T.F., Huber, L., Van Horn, R.D., Zhang, Y., Buchanan, S.G., Chan, E.M., Starling, J.J., Beckmann, R.P., and Peng, S.-B. (2014). The CDK4/6 inhibitor LY2835219 overcomes vemurafenib resistance resulting from MAPK reactivation and cyclin D1 upregulation. Mol. Cancer. Ther. *13*, 2253–2263.

Yadav, V., Zhang, X., Liu, J., Estrem, S., Li, S., Gong, X.-Q., Buchanan, S., Henry, J.R., Starling, J.J., and Peng, S.-B. (2012). Reactivation of mitogen-activated protein kinase (MAPK) pathway by FGF receptor 3 (FGFR3)/Ras mediates resistance to vemurafenib in human B-RAF V600E mutant melanoma. J. Biol. Chem. *287*, 28087–28098.

Yamada, T., Hasegawa, S., Inoue, Y., Date, Y., Yamamoto, N., Mizutani, H., Nakata, S., Matsunaga, K., and Akamatsu, H. (2013). Wnt/β-catenin and kit signaling sequentially regulate melanocyte stem cell differentiation in UVB-induced epidermal pigmentation. J. Invest. Dermatol. *133*, 2753–2762.

Yamaguchi, H., and Hung, M.-C. (2014). Regulation and Role of EZH2 in Cancer. Cancer Res. Treat. *46*, 209–222.

Yamaguchi, T., Cubizolles, F., Zhang, Y., Reichert, N., Kohler, H., Seiser, C., and Matthias, P. (2010). Histone deacetylases 1 and 2 act in concert to promote the G1-to-S progression. Genes Dev. *24*, 455–469.

Yang, C., Ko, B., Hensley, C.T., Jiang, L., Wasti, A.T., Kim, J., Sudderth, J., Calvaruso, M.A., Lumata, L., Mitsche, M., et al. (2014a). Glutamine Oxidation Maintains the TCA Cycle and Cell Survival during Impaired Mitochondrial Pyruvate Transport. Mol. Cell *56*, 414–424.

Yang, H., Bueso-Ramos, C., DiNardo, C., Estecio, M.R., Davanlou, M., Geng, Q.-R., Fang, Z., Nguyen, M., Pierce, S., Wei, Y., et al. (2014b). Expression of PD-L1, PD-L2, PD-1 and CTLA4 in myelodysplastic syndromes is enhanced by treatment with hypomethylating agents. Leukemia *28*, 1280–1288.

Yang, H., Higgins, B., Kolinsky, K., Packman, K., Go, Z., Iyer, R., Kolis, S., Zhao, S., Lee, R., Grippo, J.F., et al. (2010). RG7204 (PLX4032), a selective BRAFV600E inhibitor, displays potent antitumor activity in preclinical melanoma models. Cancer Res. *70*, 5518–5527.

Yang, Z., Yik, J.H.N., Chen, R., He, N., Jang, M.K., Ozato, K., and Zhou, Q. (2005). Recruitment of P-TEFb for stimulation of transcriptional elongation by the bromodomain protein Brd4. Mol. Cell *19*, 535–545.

Yap, D.B., Chu, J., Berg, T., Schapira, M., Cheng, S.W.G., Moradian, A., Morin, R.D., Mungall, A.J., Meissner, B., Boyle, M., et al. (2011). Somatic mutations at EZH2 Y641 act dominantly through a mechanism of selectively altered PRC2 catalytic activity, to increase H3K27 trimethylation. Blood *117*, 2451–2459.

Yee, C., Thompson, J.A., Byrd, D., Riddell, S.R., Roche, P., Celis, E., and Greenberg, P.D. (2002). Adoptive T cell therapy using antigen-specific CD8+ T cell clones for the treatment of patients with metastatic melanoma: in vivo persistence, migration, and antitumor effect of transferred T cells. Proc. Natl. Acad. Sci. USA *99*, 16168–16173.

Yeh, I., Deimling, von, A., and Bastian, B.C. (2013). Clonal BRAF mutations in melanocytic nevi and initiating role of BRAF in melanocytic neoplasia. J. Natl. Cancer Inst. *105*, 917–919.

Yokoyama, S., Woods, S.L., Boyle, G.M., Aoude, L.G., MacGregor, S., Zismann, V., Gartside, M., Cust, A.E., Haq, R., Harland, M., et al. (2011). A novel recurrent mutation in MITF predisposes to familial and sporadic melanoma. Nature *480*, 99–103.

Yoshida, S., Shimmura, S., Nagoshi, N., Fukuda, K., Matsuzaki, Y., Okano, H., and Tsubota, K. (2006). Isolation of multipotent neural crest-derived stem cells from the adult mouse cornea. Stem Cells *24*, 2714–2722.

Young, L.C., and Hendzel, M.J. (2013). The oncogenic potential of Jumonji D2 (JMJD2/KDM4) histone demethylase overexpression. Biochem. Cell Biol. *91*, 369–377.

Yu, L., Harms, P.W., Pouryazdanparast, P., Kim, D.S., Ma, L., and Fullen, D.R. (2010). Expression of the embryonic morphogen Nodal in cutaneous melanocytic lesions. Mod. Pathol. *23*, 1209–1214.

Yuan, P., Ito, K., Perez-Lorenzo, R., Del Guzzo, C., Lee, J.-H., Shen, C.-H., Bosenberg, M.W., McMahon, M., Cantley, L.C., and Zheng, B. (2013). Phenformin enhances the therapeutic benefit of BRAF(V600E) inhibition in melanoma. Proc. Natl. Acad. Sci. USA *110*, 18226–18231.

Zhang, D., Zhao, T., Ang, H.S., Chong, P., Saiki, R., Igarashi, K., Yang, H., and Vardy, L.A. (2012a). AMD1 is essential for ESC self-renewal and is translationally down-regulated on differentiation to neural precursor cells. Genes Dev. *26*, 461–473.

Zhang, J., Ding, L., Holmfeldt, L., Wu, G., Heatley, S.L., Payne-Turner, D., Easton, J., Chen, X., Wang, J., Rusch, M., et al. (2012b). The genetic basis of early T-cell precursor acute lymphoblastic leukaemia. Nature *481*, 157–163.

Zhang, J., Ji, F., Liu, Y., Lei, X., Li, H., Ji, G., Yuan, Z., and Jiao, J. (2014a). Ezh2 regulates adult hippocampal neurogenesis and memory. J. Neurosci. *34*, 5184–5199.

Zhang, M., Wang, Y., Jones, S., Sausen, M., McMahon, K., Sharma, R., Wang, Q., Belzberg, A.J., Chaichana, K., Gallia, G.L., et al. (2014b). Somatic mutations of SUZ12 in malignant peripheral nerve sheath tumors. Nat. Genet. *46*, 1170–1172.

Zhao, T., Goh, K.J., Ng, H.H., and Vardy, L.A. (2012). A role for polyamine regulators in ESC self-renewal. Cell Cycle *11*, 4517–4523.

Zhou, X.P., Gimm, O., Hampel, H., Niemann, T., Walker, M.J., and Eng, C. (2000). Epigenetic PTEN silencing in malignant melanomas without PTEN mutation. Am. J. Pathol. *157*, 1123–1128.

Zimmer, L., Hillen, U., Livingstone, E., Lacouture, M.E., Busam, K., Carvajal, R.D., Egberts, F., Hauschild, A., Kashani-Sabet, M., Goldinger, S.M., et al. (2012). Atypical melanocytic proliferations and new primary melanomas in patients with advanced melanoma undergoing selective BRAF inhibition. J. Clin. Oncol. *30*, 2375–2383.

Zingg, D., Debbache, J., Schaefer, S.M., Tuncer, E., Frommel, S.C., Cheng, P., Arenas-Ramirez, N., Haeusel, J., Zhang, Y., Bonalli, M., et al. (2015). The epigenetic modifier EZH2 controls melanoma growth and metastasis through silencing of distinct tumour suppressors. Nat. Commun. *6*, 6051.

Zipser, M.C., Eichhoff, O.M., Widmer, D.S., Schlegel, N.C., Schoenewolf, N.L., Stuart, D., Liu, W., Gardner, H., Smith, P.D., Nuciforo, P., et al. (2011). A proliferative melanoma cell phenotype is responsive to RAF/MEK inhibition independent of BRAF mutation status. Pigment Cell & Melanoma Research *24*, 326–333.

8. Curriculum Vitae

CONTACT INFORMATION

Name	Daniel Kaspar ZINGG
Address	Zschokkestrasse 5 CH-8037 Zürich Switzerland
Mobile	+41 79 328 2508
E-mail	daniel.zingg@uzh.ch / zingg.daniel@gmail.com

PERSONAL INFORMATION

Date of Birth	January 1, 1985
Place of Birth	Zurich, Switzerland
Gender	Male
Citizenship	Switzerland

QUALIFICATION

Master of Science in Cell Biology
Date of graduation: October 2009, ETH Zurich, Zürich, Switzerland

Thesis: The p75 neurotrophin receptor is not associated with tumorigenic potential in the syngeneic *Tyr::N-Ras*^{Q61K} *Ink4a*$^{-/-}$ murine melanoma model.

Bachelor of Science in Biochemistry and Molecular Biology
Date of graduation: June 2006, University of Bern, Bern, Switzerland

Matura (high school diploma) with focus on Chemistry and Biology
Date of graduation: June 2003, Gymnasium Hofwil, Münchenbuchsee, Switzerland

EDUCATION

Feb 2010 – Apr 2015	**University of Zurich**, Switzerland PhD in Cancer Biology
Oct 2007 – Oct 2009	**ETH Zurich**, Zürch, Switzerland Major in Cell Biology
Oct 2003 – Jun 2006	**University of Bern**, Bern, Switzerland, Major in Biochemistry and Molecular Biology
Aug 2000 – Jun 2003	**high school**: Gymnasium Hofwil, Münchenbuchsee, Switzerland Main subjects in Chemistry and Biology

EXPERIENCE

Jul 2008 – Feb 2010	**Swissport International AG**, Zürich, Switzerland Aviation employee
Feb 2007 – Jul 2007	**Indiana University**, Bloomington, USA Internship in Microbiology and Biochemistry
Sep 2006 – Feb 2007	**Institute of Virology and Immunoprophylaxis**, Mittelhäusern, Switzerland Internship in Molecular Biology, Virology, and Immunology

PUBLICATIONS

Balmelli, C., Alves, M.P., Steiner, E., **Zingg**, **D.**, Peduto, N., Ruggli, N., Gerber, H., McCullough, K., and Summerfield, A. (2007). Responsiveness of fibrocytes to toll-like receptor danger signals. Immunobiology *212*, 693–699.

Gutu, A., Alvey, R.M., Bashour, S., **Zingg**, **D.**, and Kehoe, D.M. (2011). Sulfate-driven elemental sparing is regulated at the transcriptional and posttranscriptional levels in a filamentous cyanobacterium. J. Bacteriol. *193*, 1449–1460.

Shakhova, O., **Zingg**, **D.**, Schaefer, S.M., Hari, L., Civenni, G., Blunschi, J., Claudinot, S., Okoniewski, M., Beermann, F., Mihic-Probst, D., Moch, H., Wegner, M., Dummer, R., Barrandon, Y., Cinelli, P., and Sommer, L. (2012). Sox10 promotes the formation and maintenance of giant congenital naevi and melanoma. Nat. Cell. Biol. *14*, 882–890.

Zingg, **D.**, Debbache, J., Schaefer, S.M., Tuncer, E., Frommel, S.C., Cheng, P., Arenas-Ramirez, N., Haeusel, J., Zhang, Y., Bonalli, M., McCabe, M.T., Creasy, C.L., Levesque, M.P., Boyman, O., Santoro, R., Shakhova, O., Dummer, R., and Sommer, L. (2015). The epigenetic modifier EZH2 controls melanoma growth and metastasis through silencing of distinct tumour suppressors. Nat. Commun. *6*, 6051.

Shakhova, O., Cheng, P., Mishra, P.J., **Zingg**, **D.**, Schaefer, S.M., Debbache, J., Häusel, J., Matter, C., Guo, T., Davis, S., Meltzer, P., Mihic-Probst, D., Moch, H., Wegner, M., Merlino, G., Levesque, M.P., Dummer, R., Santoro, R., Cinelli, P., and Sommer, L. (2015). Antagonistic cross-regulation between Sox9 and Sox10 controls an anti-tumorigenic program in melanoma. PLoS Genet. *11*, e1004877.

Cheng, P.F., Shahkova, O., Widmer, D.S., Eichhoff, O.M., **Zingg**, **D.**, Frommel, S.C., Belloni, B., Raaijmakers, M.M., Goldinger, S.M., Santoro, R., Hemmi, S., Hoek, K.S., Sommer, L., Dummer, R., and Levesque, M.P. (2015). Methylation-dependent SOX9 expression mediates invasion in human melanoma cells and is a negative prognostic factor in advanced melanoma. Genome Biol. *16*, 3016.